



**HAL**  
open science

# Optimization of grade transition in polyethylene polymerization in a fluidized bed reactor

Sabrine Kardous

► **To cite this version:**

Sabrine Kardous. Optimization of grade transition in polyethylene polymerization in a fluidized bed reactor. Chemical engineering. Université de Lyon, 2021. English. NNT: 2021LYSE1064. tel-03827645

**HAL Id: tel-03827645**

**<https://theses.hal.science/tel-03827645>**

Submitted on 24 Oct 2022

**HAL** is a multi-disciplinary open access archive for the deposit and dissemination of scientific research documents, whether they are published or not. The documents may come from teaching and research institutions in France or abroad, or from public or private research centers.

L'archive ouverte pluridisciplinaire **HAL**, est destinée au dépôt et à la diffusion de documents scientifiques de niveau recherche, publiés ou non, émanant des établissements d'enseignement et de recherche français ou étrangers, des laboratoires publics ou privés.



N°d'ordre NNT : 2021LYSE1064

## **THESE de DOCTORAT DE L'UNIVERSITE DE LYON**

Opérée au sein de  
**L'Université Claude Bernard Lyon 1**

**Ecole Doctorale N° ED 206**  
**ECOLE DOCTORALE DE CHIMIE**

**Spécialité de doctorat** : Génie des procédés  
**Discipline** : Génie des procédés

Soutenue publiquement le 31/03/2021, par :  
**Sabrina KARDOUS**

---

# **Optimization of Grade Transition in Polyethylene Polymerization in a Fluidized Bed Reactor**

**Optimisation de la Transition de Grade dans la Polymérisation de  
Polyéthylène dans un Réacteur à lit Fluidisé**

---

Devant le jury composé de :

FONGARLAND, Pascal, Professeur des Universités, Université de Lyon 1  
BENYAHIA, Brahim, Professeur Associé, Université Loughborough  
LATIFI, Abderrazak, Professeur des Universités, Université de Lorraine  
GUICHARDON, Pierrette, Professeure des Universités, Ecole Centrale de  
Marseille

Président du jury  
Rapporteur  
Rapporteur  
Examinatrice

SHEIBAT-OTHMAN, Nida, Directrice de Recherche CNRS, Université de Lyon 1  
MCKENNA, Timothy, Directeur de Recherche CNRS, Université de Lyon 1

Directrice de thèse  
Co-encadrant de thèse

# Université Claude Bernard – LYON 1

Administrateur provisoire de l'Université	Président du Conseil	M. Frédéric FLEURY
Académique	Vice-Président du Conseil d'Administration	M. Hamda BEN HADID
Vice-Président du Conseil des Etudes et de la Vie Universitaire		M. Didier REVEL
Vice-Président de la Commission de Recherche	Directeur	M. Philippe CHEVALLIER
Général des Services		M. Jean-François MORNEX
		M. Pierre ROLLAND

## COMPOSANTES SANTE

Département de Formation et Centre de Recherche en Biologie Humaine	Directrice : Mme Anne-Marie SCHOTT
Faculté d'Odontologie	Doyenne : Mme Dominique SEUX
Faculté de Médecine et Maïeutique Lyon Sud - Charles Mérieux	Doyenne : Mme Carole BURILLON
Faculté de Médecine Lyon-Est	Doyen : M. Gilles RODE
Institut des Sciences et Techniques de la Réadaptation (ISTR)	Directeur : M. Xavier PERROT
Institut des Sciences Pharmaceutiques et Biologiques (ISBP)	Directrice : Mme Christine VINCIGUERRA

## COMPOSANTES & DEPARTEMENTS DE SCIENCES & TECHNOLOGIE

Département Génie Electrique et des Procédés (GEP)	Directrice : Mme Rosaria FERRIGNO
Département Informatique	Directeur : M. Behzad SHARIAT
Département Mécanique	Directeur M. Marc BUFFAT
Ecole Supérieure de Chimie, Physique, Electronique (CPE Lyon)	Directeur : Gérard PIGNAULT
Institut de Science Financière et d'Assurances (ISFA)	Directeur : M. Nicolas LEBOISNE
Institut National du Professorat et de l'Education	Administrateur Provisoire : M. Pierre CHAREYRON
Institut Universitaire de Technologie de Lyon 1	Directeur : M. Christophe VITON
Observatoire de Lyon	Directrice : Mme Isabelle DANIEL
Polytechnique Lyon	Directeur : Emmanuel PERRIN
UFR Biosciences	Administratrice provisoire : Mme Kathrin GIESELER
UFR des Sciences et Techniques des Activités Physiques et Sportives (STAPS)	Directeur : M. Yannick VANPOULLE
UFR Faculté Sciences	Directeur : M. Bruno ANDRIOLETTI

“A question opens **a** mind. A statement closes **the** mind”

*-Robert Kiyosaki*

# List of Abbreviations

$S_p$	potential catalyst active sites, ( $\text{mol m}^{-3}$ )
$P_0$	activated vacant catalyst sites, ( $\text{mol m}^{-3}$ )
$P_*$	total active sites, (vacant $P_0$ and occupied by a polymer chain $P_{n,i}$ ), ( $\text{mol m}^{-3}$ )
$P_{n,i}$	living copolymer chains of length $n$ ending with monomer $i$ , ( $\text{mol m}^{-3}$ )
$D_n$	dead copolymer chains of length $n$ , ( $\text{mol m}^{-3}$ )
$C_d$	deactivated catalyst sites
$\lambda_k$	moment $k$ of living chains, ( $\text{mol m}^{-3}$ )
$\mu_k$	moment $k$ of dead chains, ( $\text{mol m}^{-3}$ )
$M_w$	the instantaneous polymer average molecular weight, ( $\text{g mol}^{-1}$ )
$E$	activation energy, ( $\text{J mol}^{-1}$ )
$k_0$	pre-exponential factor
$\varepsilon_{\text{bed}}$	porosity of the bed
$X_i ; X_i^{\text{in}}$	mass fractions of component $i$ in the recycle stream; and in the input stream
$h$	bed height, (m)
$V_{\text{bed}}$	bed volume, ( $\text{m}^3$ )
$A$	cross-sectional area of the bed, ( $\text{m}^2$ )
$Q_0$	bed outlet volumetric flow rate, ( $\text{m}^3 \text{s}^{-1}$ )
$F_z$	inlet flow rate of component $z$ , ( $\text{kg s}^{-1}$ )
$F_{\text{rec}}$	recycling flow rate, ( $\text{kg s}^{-1}$ )
$X_z$	mass fraction of component $z$ in the gas phase
$\rho_c$	the cumulative density of the polymer, ( $\text{kg m}^{-3}$ )
$\rho_{\text{cat}}$	the density of the catalyst ( <b>2800</b> $\text{kg m}^{-3}$ )

## Résumé de thèse

---

La variété des applications de polyéthylène (PE) nécessite des spécifications de grades différentes pour répondre à la demande du marché. La plupart des procédés utilisés pour fabriquer du polyéthylène linéaire à basse densité (LLDPE) sont les procédés en phase gaz. Ces procédés sont propres et moins consommateurs d'énergie, mais ils sont limités dans leur productivité par la nature exothermique de la réaction. Afin de surmonter ce problème, le « refroidissement en mode condensé » est fréquemment utilisé, où des composés de type alcane (ICA), sont injectés afin d'absorber une partie de la chaleur générée par la réaction. Cependant, il a été observé que la présence d'ICA influence l'absorption du monomère dans le polymère et par conséquent la vitesse de la réaction et les propriétés du polymère.

Dans ce travail, deux objectifs sont visés : a) développer une procédure d'optimisation dynamique hors ligne pour optimiser la transition entre les différents grades de LLDPE dans un réacteur à lit fluidisé. Comme ce type de réacteur fonctionne fréquemment en présence d'ICA, il est important de considérer l'effet de l'ICA dans le modèle. Ainsi, un modèle cinétique est combiné à un modèle thermodynamique pour décrire les transitions de grade. Les résultats mettent en évidence l'importance du modèle thermodynamique dans la transition de grade. b) employer ce modèle pour prédire la température de début de fusion des particules de polyéthylène. De cette manière, le modèle prend en compte les effets de la densité du polymère et du gonflement des particules par les différents pénétrants sur la température de fusion. Ce modèle est ensuite utilisé dans une stratégie d'optimisation pour contrôler la transition entre les différents grades de polymère tout en évitant le début de fusion de polymère.

**Mots clés :** Transition de grade, réacteur à lit fluidisé, refroidissement en mode condensé, thermodynamique, polyéthylène, température de fusion du polymère, optimisation dynamique hors ligne.

## Ph.D. Thesis abstract

---

The variety of PE applications requires different grade specifications to suit the market demand. Most processes used to make linear low density polyethylene (LLDPE) are gas phase processes. These processes are clean (solvent-free) and less energy consuming, but they are limited in their productivity by the high exothermicity of the reaction. In order to overcome this issue, “condensed mode cooling” is frequently employed, where induced condensing agents (ICAs) are injected in order to absorb part of the reaction heat. However, it was observed that the presence of ICA influences the absorption of monomer into the polymer and consequently the reaction rate and the polymer properties.

This work has two objectives: a) to develop an off-line dynamic optimization procedure in order to optimize the transition between different grades of LLDPE in a fluidized bed reactor. As this reactor is frequently operated under condensed mode, it is important to account for the ICA effect in the process model. Hence, a kinetic model is combined with a thermodynamic model to describe the grade transitions. The results highlight the importance of the thermodynamic model during grade transition. b) to use the developed model in predicting the melting onset temperature of polyethylene particles in a fluidized bed reactor. By this way, the model accounts for the effects of the polymer density and particle swelling by the different penetrants on the melting temperature. This model is then used within an optimization strategy to control the transition between different polymer grades while avoiding polymer melting.

**Key words:** Grade transition, fluidized bed reactor; condensed mode cooling; thermodynamics; polyethylene, polymer melting temperature, off-line dynamic optimization.

## Acknowledgments

---

Now, that I am given the right to consider myself a researcher, I feel delighted to have accomplished what seemed difficult starting my Ph.D studentship. This work is the result of three years of research efforts. Of course, most of such work would have not been possible without the contribution of many people that I wish to acknowledge in my last blank page!

First of all, I wish to address my sincere thanks to the members of my Ph.D defense committee for accepting to judge my work. I was honored to have Prof. Abderrazak LATIFI and Dr. Brahim BENYAHIA as reviewers of my thesis. Their constructive comments and remarks on the manuscript were very precious. Their reflections enriched the field of my perspectives, and their kind encouragements touched me deeply. I would like to thank Prof. Pascal FONGARLAND for accepting to be the president of the jury. I also extend my sincere knowledgements to Prof. Pierrette GUICHARDON for examining my work and for the discussion we had.

This Ph.D started when I was in my Master 2 internship, and I met Nida SHEIBAT-OTHMAN who later became my Ph.D supervisor. Nida, I still remember our first meeting in Solvay! Thank you for inviting me to this exciting journey into modeling and Polyolefins. Thank you for your advices, your time and for your help, but especially for your enthusiasm and encouragements, which without them this thesis would not have been possible. I will always remember our high-fives, joy and even hugs during meetings when discussing good results! This thesis is our first project in Polyolefins together! It has been a challenge for me. And you taught me how to handle challenges very well during these three years. But not only, I learned a lot from your multiple skills and knowledge. It was a pleasure to work with you.

I am grateful to my Ph.D co-supervisor Timothy MCKENNA, for his important contribution. I also thank all the member of his team within C2P2 lab for the enormous knowledge we have shared during Group meetings. Thank you Tim for transmitting a part of your immense knowledge on

Polyolefins through the discussions we had. You always managed to make difficult approaches look easy. Thanks for your interesting ideas and advices!

I also thank the *Agence Nationale de la Recherche* for funding this work under the Growth Project “ThermoPoly”.

This Ph.D was developed at the LAGEPP. I would like to thank the director Prof. Stéphanie BRIANCON for welcoming me in her lab twice, for my Ph.D and for my Post-Doc!

I wish to express my appreciation to all the staff members from LAGEPP. I especially thank Nadia CHAPEL, the never-ending source of help; Dr. Abdelhamid ELAISSARI, our everyday motivation source in the first floor! and Dr. Yves CHEVALLIER., who I countlessly thank for the fruitful discussions we had, when I was writing this manuscript. At each time I needed a break I found myself at his office. I also appreciated him joining us for the well-deserved Friday after works!

I wish especially to thank Noureddine LEBAZ for his friendship. I really enjoyed our interesting discussions about science, and his positive view on all aspects of life. Thank you Nour for your advices, your encouragements during the toughest times, with a very impressive sense of humor! I wish you the best in your academic career.

I would like to thank the technical staff in LAGEPP and especially, Olivier GARRIGUES, for his help during the lockdown by introducing me to the virtual machine. That was indeed the best saving time way in a critical period of teleworking!

I am most grateful to Dr. Claudia COGNE, for offering me a great Post-Doc opportunity in this exceptional year of COVID. Thank you Claudia for your trust and to the really nice project in which you introduced me. It was a real pleasure to work with you in a new field “Freeze-drying” and the DEM simulations. I will never forget your support in a hard period, preparing my Ph.D. defense and working on my Post-Doc at the same time. This would not be possible without your encouragements.

A special acknowledgement goes to my office mate of many years; Manis. Fortunately, I have changed my office to yours! We started this journey almost at the same time, and we both learned

a lot of things together. I wish you all the best for future! And I also thank the other several office-mates coming and leaving from office G122; Geoffrey, Emilien, Pam, Georgio.

I would like to acknowledge my other friends at LAGEPP, the new family I had from all over the world. First and foremost, I would like to thank Nidhal & Haithem my compatriots (I was really spoiled during your time in LAGEPP!); Merymen the sweetest compatriot (thank you for your moral support); Maroua my jogging companion for a while! Maya my dear old student (thank you both! I will never forget your meaningful presence the day of my defense. I could not have my family present in such difficult situation. You were a family!); Mohamed1 (moitié de 1000 est 500!), Anna my PhD companion (I am grateful for your friendship and for Italian food parties); Laura my other PhD companion (I will never forget our funny story about PhD!). Also, I thank Fabrice my companion in teaching during three years; Camillo my companion in modeling with MATLAB. I also thank the forever friends Ben & Elena, Margaux & Francisco, and new arrivals Mohamed2, Aboubakar, and Jean.

A very special acknowledgment goes to my non-LAGEPP family, those who supported me the most since many years: Walid, Arbia, Fatma, Abir, Noura, Islem... Thank you guys for your presence, and for the long needed discussions we had.

I want to acknowledge the person who was my pillar during these past three years. Thank you Ahmed for being a good listener, for being an inexhaustible source of support & advices and for knowing how to lift me up.

Last but not least, I owe this achievement to my parents for always respecting my choices, believing in me, and unconditionally supporting me; to my two brothers and especially to my sister Mina, who had the opportunity to join me in Lyon. I am so grateful that we spent the difficult times of lockdown together. Thank you Mina for your patience during most difficult times when writing this thesis. But most of all, having cooked for me for almost the whole writing period!

**Sabrina KARDOUS**

# Contents

---

List of Abbreviations .....	4
<i>Résumé de thèse</i> .....	5
<i>Ph.D. Thesis abstract</i> .....	6
<i>Acknowledgments</i> .....	7
<i>General Introduction</i> .....	13
<b>Chapter 1 Context and Motivations</b> .....	<b>16</b>
<b>1. Polyolefins</b> .....	<b>16</b>
1.1. Types of Polyethylene.....	16
1.2. Polyolefin processes .....	18
1.3. Catalysts .....	21
1.4. Fluidized bed reactor.....	25
1.5. Condensed mode operation.....	27
1.6. Effects of ICA on thermodynamics and polymer properties.....	30
1.7. Polymer melting and temperature control .....	32
<b>2. Modelling and optimization</b> .....	<b>35</b>
2.1. Multi-scale phenomena .....	35
2.2. Importance of the thermodynamic model.....	36
2.3. Optimization of grade transitions.....	37
<b>3. Objectives</b> .....	<b>39</b>
<b>Chapter 2 Thermodynamic Modelling</b> .....	<b>49</b>
<b>1. Introduction</b> .....	<b>49</b>
<b>2. Thermodynamic Models</b> .....	<b>50</b>
2.1. Henry's law .....	51
2.2. Thermodynamic equations of state.....	54
<b>3. Binary Systems</b> .....	<b>60</b>
3.1. Parameters impacting the $k_{ij}$ .....	61
3.2. Application of the SL EoS.....	63

<b>4. Ternary Systems.....</b>	<b>65</b>
4.1. Procedure of identification of <i>kij</i> parameters.....	66
4.2. <i>kij</i> of the ternary system ethylene/ <i>n</i> -hexane/LLDPE .....	68
4.3. <i>kij</i> of the ternary system ethylene/ 1-butene/LLDPE .....	70
4.4. <i>kij</i> of the Ternary System ethylene/ 1-hexene/LLDPE .....	72
<b>5. Pseudo-quaternary systems .....</b>	<b>72</b>
5.1. Polyethylene in presence of ethylene, 1-hexene and <i>n</i> -hexane.....	73
5.2. Polyethylene in presence of ethylene, 1-butene and the iso-butane .....	75
<b>6. Simplified thermodynamic models.....</b>	<b>78</b>
6.1. Sorption of reactive penetrants.....	78
6.1.1. Ternary systems .....	79
6.1.2. Pseudo-quaternary systems.....	80
6.2. Sorption of diluents .....	81
6.3. Crystallinity.....	82
<b>7. Conclusions.....</b>	<b>83</b>
 <b>Chapter 3      <i>Kinetics and Reactor Models</i>.....</b>	 <b>93</b>
<b>1. Introduction .....</b>	<b>93</b>
<b>2. An overview: Modelling of Olefin Polymerization in FBRs.....</b>	<b>94</b>
<b>3. Model development .....</b>	<b>97</b>
3.1. Kinetic model.....	97
3.2. Mass and heat balances.....	101
3.3. Correlations of key properties.....	104
3.4. Simulation examples.....	107
<b>4. Conclusions.....</b>	<b>113</b>
 <b>Chapter 4      <i>Optimization of PE Grade Transitions in FBR</i>.....</b>	 <b>119</b>
<b>1. Introduction .....</b>	<b>119</b>
<b>2. Grade transition of Polyethylene .....</b>	<b>120</b>
2.1. Key properties during transition .....	120
2.2. Overview of grade transition strategies .....	122
2.3. Grade transition .....	125

2.3.1	<i>Formulation of the optimization problem</i> .....	125
2.3.2	<i>Objective function</i> .....	126
2.3.3	<i>Degree of freedom of the inputs</i> .....	127
<b>3.</b>	<b>Simulation results and discussion</b> .....	<b>128</b>
	<i>Copolymerization of ethylene and 1-hexene in presence of n-hexane as ICA</i> .....	129
	<i>Copolymerization of ethylene and 1-butene in presence of iso-butane as ICA</i> .....	134
	<i>Impact of the thermodynamic model</i> .....	137
<b>4.</b>	<b>Conclusions</b> .....	<b>140</b>
<b>Chapter 5</b>	<b><i>Optimization of PE Grade Transitions with constraints on the polymer sticking temperature</i></b> .....	<b>145</b>
<b>1.</b>	<b>Introduction</b> .....	<b>145</b>
<b>2.</b>	<b>Particle sticking in gas-phase PE production</b> .....	<b>146</b>
<b>3.</b>	<b>Defining the sticking temperature</b> .....	<b>147</b>
3.1.	<i>T<sub>m,0</sub> and MIT<sub>0</sub> of dry polymer</i> .....	148
3.2.	<i>T<sub>m</sub> of swollen polymer</i> .....	150
<b>4.</b>	<b>Dynamic off-line optimization and temperature control</b> .....	<b>152</b>
<b>5.</b>	<b>Simulation results and discussion</b> .....	<b>154</b>
	<i>Copolymerization of ethylene with 1-butene</i> .....	154
	<i>Copolymerization of ethylene with 1-hexene</i> .....	157
	<i>Copolymerization of ethylene with 1-hexene in presence of n-hexane</i> .....	159
<b>6.</b>	<b>Conclusion</b> .....	<b>161</b>
	<b><i>General Conclusions-Perspectives</i></b> .....	<b>166</b>
	<b><i>Appendixes</i></b> .....	<b>172</b>

# General Introduction

---

This thesis is a part of the research project “Experimental and modelling study of ethylene polymerization in gas phase reactors: impact of thermodynamics” (**THERMOPOLY**) which is financed by the **Agence Nationale de la Recherche (ANR)** in France. The research program involves three partners: ETH Zurich in Switzerland, LAGEPP and C2P2 research laboratories from University Claude Bernard (UCBL) in Lyon. In this program two PhD students were recruited at the UCBL (one for single particle modelling and the generation of experimental solubility data; and one on grade transition optimization) and a Post Doc fellowship at ETH (on modelling fluidized bed reactors (FBRs) by compartmentalization and computational fluid dynamics). The aim of these projects is to develop a fundamental understanding of the different phenomena observed during condensed mode cooling of ethylene polymerization in FBRs, and translate this knowledge into a complete polymerization model able to predict the gas phase reactor performance.

The PhD work presented in this thesis, carried out at the LAGEPP, focuses on optimizing the grade transitions of polyethylene in a fluidized bed reactor, to satisfy the rapidly evolving demands of market. More particularly, in the production of linear-low density polyethylene produced under condensed mode cooling, there is a need for thermodynamic models to predict the impact of the gas phase composition on the reaction rate and the end-use properties of the polymer. This work is also concerned with the industrial safety of polymerization during grade transitions by avoiding the risk of the particle sticking and aggregation while ensuring precise polymer quality control.

This thesis is organized in five chapters:

In Chapter 1, **Context and Motivations**, we present the general context and motivations of the study and we give a brief overview of the FBR gas phase polymerization process of polyethylene, comprising the condensed mode cooling. We also explain the need for the development of the combined kinetic and thermodynamic model. A detailed literature review will be presented in each

other chapters for a better organization. At the end of Chapter 1, the main objectives of this thesis are detailed.

In Chapter 2, **Thermodynamic Modeling**, the different thermodynamic models used for systems including a polymer component are discussed, and the Sanchez-Lacombe Equation of State (SL EoS) model chosen for this study is presented. This model uses interaction parameters, and when not available in the literature some assumptions about their evaluation need to be made. Simplified polynomial correlations were then identified in order to allow fast calculation of the solubility as a function of the operating conditions (pressure and temperature) for two ternary and quaternary systems. Approximations were also considered to extend the predictions to quaternary systems. This chapter highlights the importance of the co-solubility and anti-solubility effects when different penetrants are used.

In Chapter 3, **Kinetics and Reactor Models**, the major parts of the model of ethylene polymerization in a fluidized bed reactor are presented. A kinetic model of copolymerization of ethylene is used to estimate the reaction rate and the polymer properties. This model is combined with a reactor model (energy and mass balances), in which the bed is assumed to behave as a continuous stirred tank reactor. The different correlations describing the polymer main properties, namely the polymer density and melt index, are also presented.

In Chapter 4, **Optimization of PE Grade Transitions in FBR**, the dynamic model developed in chapter 3 combined with the thermodynamic model from chapter 2 are used to implement an off-line dynamic optimization of the LLDPE grade transitions. In this strategy, the controlled properties are the polymer density and melt index, and the manipulated variables are the flow rates of hydrogen and comonomer. It includes constraints on the inputs (flow rates) and in one scenario, constraints on the outputs are considered. This strategy demonstrates the importance of accounting for the effect of the comonomer or induced condensing agent in the model used for grade transition optimization, as it has a direct effect on the polymer properties and the reaction rate.

In Chapter 5, **Optimization of PE Grade Transitions with constraints on the polymer sticking temperature**, a measure of the risk of polymer fusion and particle sticking is included and a constraint is added in the optimization to avoid it. Polymer melting depends on a number of factors, including the bed temperature, the polymer properties (density, molecular weight), and the polymer swelling by solvents. A correlation based on data from patents is developed to predict the polymer melting initial temperature (MIT) as a function of the polymer density. Flory-Huggins theory is then used to estimate the polymer swelling by the different diluents and the change in the MIT. This model is combined to the kinetic and thermodynamic models and used within the off-line optimization strategy in order to control the polymer properties during grade transitions. In order to avoid polymer sticking, the bed temperature is also controlled.

An **appendix** is presented at the end of this thesis. It provides the equations of the SL EoS for binary and ternary systems.

"I am inclined to think that the development of polymerization is perhaps the biggest thing chemistry has done, where it has had the biggest effect on everyday life"

-Lord Todd (1907-1997)

President of the Royal Society, Chemistry Nobel Prize 1957

## 1. Polyolefins

The use of polymers is essential nowadays, because in many applications they cannot be replaced by another product of equivalent properties and at equivalent cost, such as for example the combination between mechanical properties, light weight, and non-flammability necessary in the aircraft constructions to minimize energy consumption while ensuring their safety.

Among all polymers, polyolefins are by far the most significant in terms of production volume worldwide (more than 60% of the total polymer production in 2019).[1] They include polyethylene (PE), polypropylene (PP) and their copolymers with  $\alpha$ -olefins. Polyethylene production is considered in this work.

### 1.1. Types of Polyethylene

Polyethylene (PE) homopolymer is a macromolecule consisting of a simple and repeating monomer (ethylene -C<sub>2</sub>H<sub>4</sub>). Random copolymers of ethylene are a combination of ethylene with small amounts of different  $\alpha$ -olefins (comonomers). PE is a semi-crystalline polymer composed of a combination of an amorphous phase and a crystalline phase.[2] Despite the very simple structure (composed only of carbon and hydrogen), PE is the most important polymer worldwide in terms of production volume, due to its significant capability to replace other more expensive and less environmentally friendly thermoplastics. In 2012, the global demand for this polymer was around

78 million tons (mmt); and increased to reach around 100 mmt in 2018 (27% of the Europe plastic production).[3]–[5] Its demand continues to rise, thanks to its versatility, ease of processing, low cost and recyclability. PE has also properties of waterproofing, moisture barrier, rigidity and clarity. It is expected to continue increasing worldwide for the foreseeable future.[4]

Polyethylene can be divided into three main types:

- Low density polyethylene (LDPE): this polymer was the first discovered industrially by Imperial Chemical Industries Laboratories in the UK in 1933. It is produced by free radical polymerization (FRP), at high temperature and pressure (120-300 MPa, 130-350 ° C).[6] It has a low density (0.915-0.935 g cm<sup>-3</sup>) due to the fact that its molar structure is highly branched. It is mainly used for packaging.
- High density polyethylene (HDPE): this polymer is produced by coordination chemistry at lower temperature (80-100 °C), and a pressure (<30 bars in most cases), either in a solution, gas phase or slurry process. It is linear and contains almost no branches thanks to the catalysts used (see Figure 1.1) It has a high density (0.96-0.97 g cm<sup>-3</sup>) and is also semi-crystalline (60 % crystallinity). It is used for making bottles, food containers, toys, piping and gas tanks. Being less flexible than LLDPE or LDPE, it cannot be used in applications such as food packaging.
- Linear low density polyethylene (LLDPE) or very low density polyethylene (VLDPE):[7] this polymer is also produced by coordination catalysis at low temperature and pressure. Unlike HDPE, LLDPE is produced almost exclusively in the gas phase because it is much more amorphous and is therefore very soluble in diluents such as iso-butane or hexane, which are used in slurry processes. This more amorphous nature is due to the fact that LLDPE (0.915-0.940 g cm<sup>-3</sup>)[6] contains short branches caused by the incorporation of significant amounts of  $\alpha$ -olefin type comonomer (for example 1-butene, or 1-hexene).

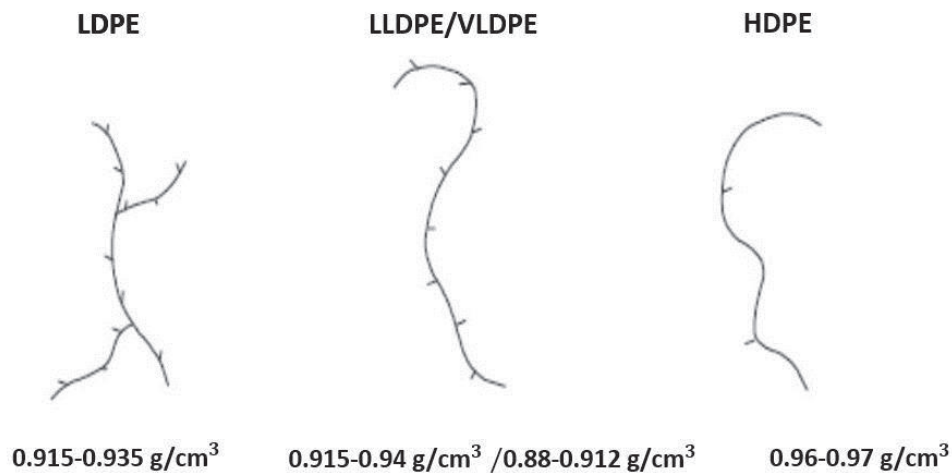


Figure 1.1. Classification of polyethylene into three groups according to the density and the branching.[8]

The market demand for LLDPE alone is 23 % of the polymer demand worldwide in 2019[9]. Besides, the market for LLDPE is expected to increase with a compound annual growth rate of 5.5 % between 2017 and 2022.[10] For instance, in 2018 LLDPE occupied an important position with around 30 % of the global PE production worldwide.[11] In this study we will focus on LLDPE not only for its global extensive utility, but also its properties are easily adjusted by modifying the amount, type and distribution of comonomer incorporated in the main chain of the polymer.[12]

## 1.2. Polyolefin processes

In industry, LDPE is produced by free radical polymerization, so will not be discussed in this thesis.[13] LLDPE and HDPE are produced by catalytic polymerization. Depending on the continuous medium in which the polymerization occurs, there are three different families of catalytic PE production processes: solution, slurry and gas phase, using several types of reactors.[8], [14]

**In solution processes**, as the name implies, the polymerization takes place in a liquid reaction medium (solvent such as cyclohexane), where both polymer and catalyst are soluble. Unsupported (molecular) catalysts such as homogenous vanadium-based Ziegler-Natta (ZN) or metallocenes can be used here. In order to keep the polymer in solution, the polymerization is performed at high temperatures (100-250°C), and pressures (40-100 bars) to keep the ethylene in solution. These operating conditions accelerate the reaction and reduce the residence time (1-20 minutes).[15] Stirred tank reactors (CSTR), tubular or loop reactors (3-15 m<sup>3</sup> volume range) and mostly autoclaves can be used in solution processes.[8]

**In slurry process**, the polymer and the supported catalyst particles are dispersed in a continuous alkane diluent such as iso-butane or n-hexane. Reaction temperatures are typically 80-110°C with a pressure range of 5-40 bar, depending on the chosen diluent and reactor.[15] The residence time (usually 45 minutes to 5 hours) is also affected by the type of the diluent and the operating reactor. Slurry processes are frequently carried in loop reactors for their good heat transfer conditions, and so a high space time yield. Among the different loop reactor technologies used for slurry processes (Chevron Phillips, LyondeBasell, Borealis, Mitsu and INEOS), Chevron Phillips loop reactor occupies the first position in terms of use for PE production.[16]

**The gas phase processes** are the latest processes developed to produce polyolefins. However, today they occupy the most significant position for producing LLDPE worldwide. The polymer particles are dispersed inside the reactor by a fluidizing gas flow.[14] Polymers with a wide range of final properties, such as high melt index (*MI*) (indicative of the flow rate of a specific molten polymer through a rheometer orifice, under a specific load condition), and important comonomer contents, can be produced in gas phase but not in slurry. Indeed, the solubility of hydrogen and monomers limitation in the slurry reaction medium, and the dissolution of the amorphous polymer in a diluent are avoided in gas phase processes.[17] However, the most critical issue of gas processes, compared to slurry and solution processes, is the poor heat removal because of the limited heat transfer properties of gaseous medium. This issue is related mostly to the production

rate, as the hotter the reactor of PE, the faster the polymerization can go and the more economic gain can be achieved. The reactor must however be maintained at a specific temperature to maintain the quality of the polymer and avoid overheating and polymer melting. Indeed, most of the polymer properties (e.g. molecular weight, chemical composition) and the kinetics of the polymerization are affected by the operating temperature. Moreover, overheating can also affect the process safety, as polymer softening or fusion may occur, thus causing particle agglomeration or the creation of some sheets in the walls of the reactor, which may in extreme cases lead to the reactor shutdown.[18]–[20] Operating temperature control is then needed, and adjusting the gas composition (ethylene, comonomer, hydrogen) can solve this problem.[21] More details about this issue are given in chapter 5.

In gas phase, polyolefins may be produced in FBRs or in horizontal or vertical stirred reactors.[19] However, except one Hyperzone process, that will come on line in 2021, which uses a multizone circulating reactor to make HDPE, virtually all gas phase PE processes use FBRs for their best heat removal capacity comparing to the other gas phase reactors.[18], [19] In industry, several gas phase technologies using FBRs are licensed. The most used are the Unipol PE from Univation Technologies[22] that produces around 48 million tons per year, and the Innovene G from INEOS Technologies[23] that produces 5 to 8 mmt per year.

To conclude, slurry and gas phase polymerization processes present a range of advantages and limitations and both are employed industrially. Nevertheless, gas phase polymerization allows to produce a wide range of different grades (e.g. LLDPE) and they are less expensive than slurry processes, if good heat evacuation is considered. Indeed, slurry processes require large amounts of liquid solvents with a huge environmental impact. Another important advantage of gas phase processes is the relative ease in recovering the final polymer when the monomer is in gas phase.

As the focus of this work is the production of LLDPE, only gas phase processes, and more particularly FBRs, will be discussed. Indeed, making LLDPE in slurry is very challenging, as the amorphous material can dissolve.

### 1.3. Catalysts

The catalytic synthesis of PE in the modern industry including LLDPE, is performed by coordination catalysis in the presence of a transition metal compounds. Ethylene polymerization takes place on the pores surface of the catalyst particles (at the active sites), into the fluidized main zone of the FBR. The active sites are installed on interior of a highly porous solid (the support), which is typically  $MgCl_2$  for Ziegler-Natta catalysts and silica for metallocenes. Upon Introducing the catalyst particle into the reactor, the molecules of ethylene start the diffusion from the bulk phase of the reactor, through the particle pores until reaching the active sites.

As the polymerization progresses, the polymer starts accumulating in the pores, creating a local stress. As soon as the stress exceeds a certain level, the initial catalyst particle undergoes a fragmentation process. Hence, the initial porous structure of the support breaks-up into small fragments. However, the particle maintains its integrity due to the entangled network of the polymer. Alizadeh et al.,[24] summarized the evolution of the catalyst particle during gas phase polymerization process with the schematic 3D-cut presentation in Figure 1.2.

Following the step of fragmentation, the active sites occupying the fragments of initial support of the catalyst are totally surrounded by semi-crystalline PE. The latter forms the continuous phase with the fragments of the support dispersed therein. The reaction continues as the monomer species diffuse through the particle pores, and then be sorbed from the gas phase into the polymer phase until reaching the surface of the catalyst fragment; exactly the active centers where the reaction takes place. The continuous evolution of polymer results in the increase of the size of the particles which turn into granules of 15-20 times the initial size of the catalyst.[15] The reader is referred to references[14], [25], [26] for further details about the steps of the polymer growth during polymerization (the transformation of a solid catalyst particle into a particle polymer). Since the polymer layer covering the active sites consist mostly of an amorphous material, the

polymerization rate will be determined by the concentration of monomers in the amorphous phase of the semi-crystalline polyethylene.

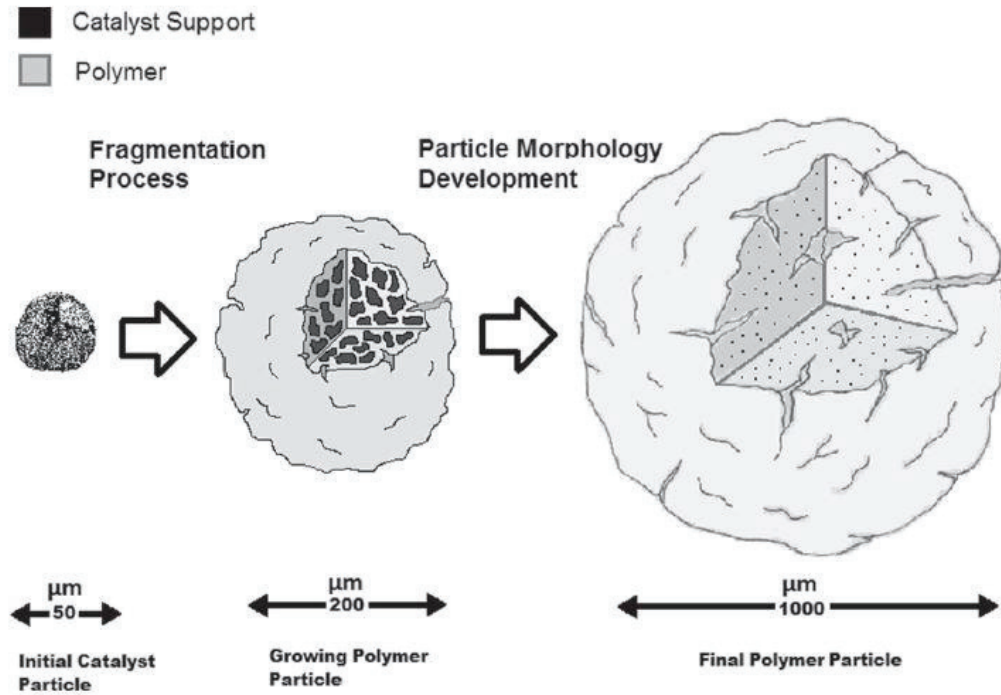


Figure 1.2. catalyst particle evolution during gas phase ethylene polymerization with the characteristic diameter at each step.[24]

There are three main types of catalysts used commercially for the polymerization of ethylene:

- i) Phillips (or Chromium Cr) catalysts were first discovered in 1951 by researchers at Phillips Petroleum Company, thus making the first breakthroughs occurring in the field of olefin catalytic polymerization.[27] Phillips catalysts are made of chromium oxide ( $\text{CrO}_x$ ) or vanadium oxide ( $\text{VO}_x$ ) and permeated on a silica support ( $\text{SiO}_2$ ); [28] then calcinated under vacuum by high thermal treatment (200-900°C).[29] Unlike Ziegler-Natta catalysts, these catalysts do not need a co-catalyst for their activation, which is performed directly *in situ* by ethylene. These catalysts produce PE with very wide molecular weight distributions (*MWD*), and are used to make around one third of the HDPE production worldwide, the other two-thirds are made with Ziegler-Natta

catalysts.[28] However, they cannot be used for instance to produce LLDPE, as they have a low incorporation of  $\alpha$ -olefin.

- ii) The discovery of Ziegler-Natta (ZN) presented the second major revolution for plastics industry due to a combination between the work of Ziegler who developed an organometallic catalyst, and the work of Natta who used Ziegler's catalyst (titanium trichloride/triethylaluminum) in the stereoselective polymerization of propylene. This marked numerous significant advances in the polyolefin field.[27], [30] The highly significant impact of the Ziegler-Natta catalyst in olefin polymerization domain was awarded in 1963 by the Nobel Prize in Chemistry. Ziegler-Natta is generally composed of a transition metal salt (mainly  $\text{TiCl}_4$ ) belonging to group IV-VIII and a metal alkyl (mainly alkyl aluminium compound such as triethylaluminum (TEA) or tributylaluminum (TIBA)) belonging to group I-II. The metal alkyls are known as the activators or the cocatalysts, as they are required in the activation of the catalyst in a two-step process of alkylation. The mechanism of activation starts with monomer coordination to the vacant site in the metal. [31], [32] This step results in the activation of the C-C double bond that enters into the Ti-C bond, which induces the polymer chain augmentation by one unit. Following the insertion step, the metal vacant site can be accessible for another insertion step and the polymer chain continues growing.

Ziegler- Natta catalysts are present in two forms: homogenous (molecular) and heterogeneous (supported). The molecular form is used in solution processes. However, Z-N catalysts are often used in supported form. The latter form is used in slurry or gas phase polymerization. In this study, the focus will be given to the heterogeneous form of these catalysts, since it is the most widely used in industry to produce LLDPE or HDPE.

Z-N catalysts are generally presented as multi-site catalysts-meaning they have different types of active sites that can be affected sterically and electronically by their surroundings. This slight effect

stands out in the monomer-coordination-insertion step, which results in a variation in the properties of the final produced polymer from each active site on the same supported catalyst particle.

Z-N catalysts are commonly used in the industrial polyolefin industry for their high activity and selectivity. These catalysts provide a wide range of different polymers in terms of microstructural properties (*MWD*) and macrostructural properties (morphology, porosity and the size distribution of the particle). These important properties allow them to be present in a wide range of applications, especially due to their economic profitability (lower cost compared to metallocene catalysts).[33], [34] Hence, these catalysts have not stopped evolving over the past sixty years and their productivity increased from around 2 kg polymer/g catalyst for their first generation to 100 kg polymer/g catalyst for their fifth generation.[35]

- iii) Metallocenes, or the so called “sandwich compounds”, are organometallic compounds consisting of a central transition metal (titanium, zirconium or hafnium) bounded to at least one aromatic ring of the cyclopentadienyl or substituted cyclopentadienyl rings.[30], [36] They perform in both molecular (unsupported) and heterogeneous (supported) form. In the molecular form, these catalysts are referred to as single site catalysts, as all the active sites are identical. Likewise, metallocenes, in the supported form, can be considered as single site catalysts, as there is no interaction between the support (usually silica) and the active site, unlike supported ZN catalysts. This helps if one needs a very precise control over comonomer incorporation, or over the *MWD*. [15] Generally, metallocenes need an activator such as methylaluminoxane (MAO); but recently they could be used without MAO due to the continuous progress in this field.[30], [36] Metallocenes present an attractive option for industrial applications, whether in supported or unsupported form as they are able to produce polymers with considerably more uniform properties than Phillips or ZN catalysts. Nevertheless, using metallocenes is much costlier.

In the copolymerization of ethylene with  $\alpha$ -olefins model, supported Ziegler-Natta catalysts are considered, which are commonly used to produce LLDPE.

## 1.4. Fluidized bed reactor

Figure 1.3 shows a typical polymerization FBR configuration with the different length scales from the micro-scale to the macro-scale of the reactor.

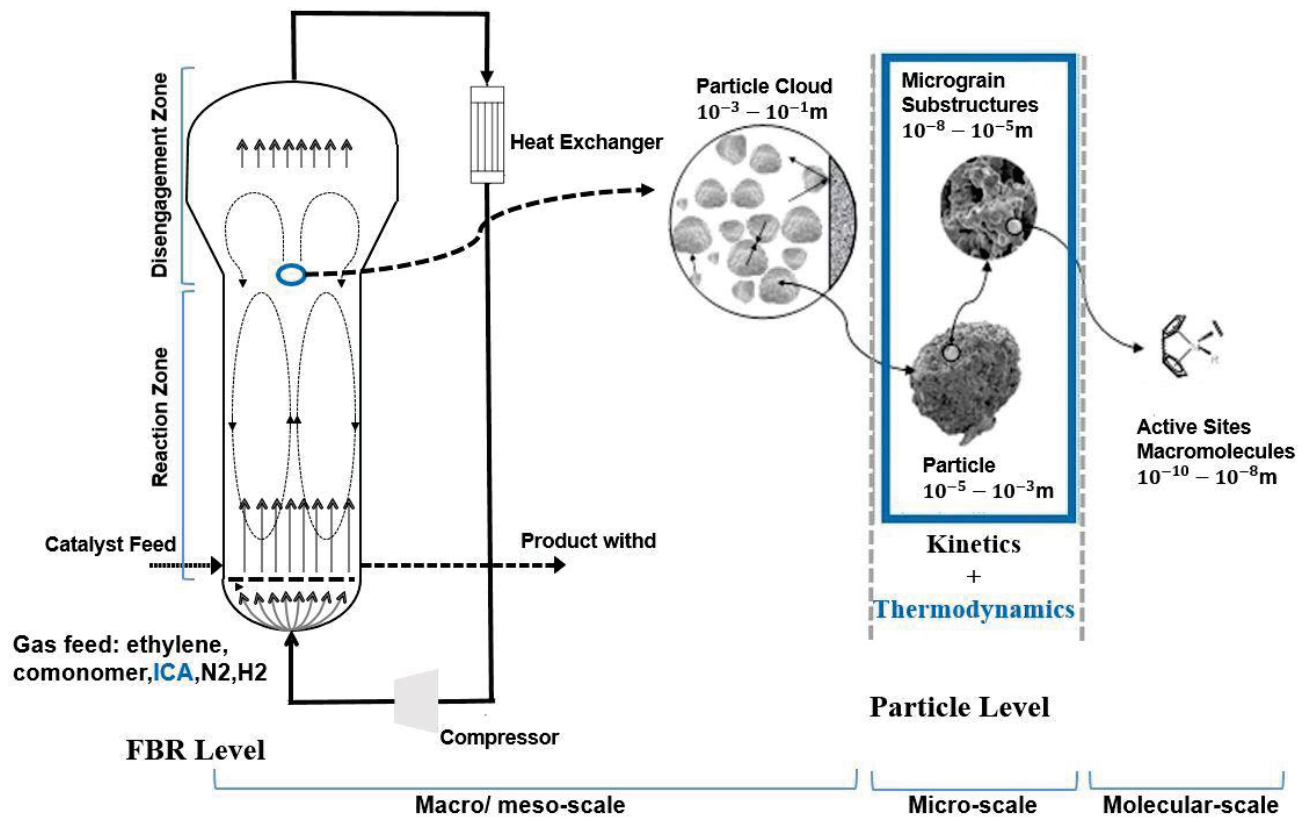


Figure 1.3 A typical fluidized bed reactor of catalytic olefin polymerization showing the interaction between the different length scales: the micro-scale level (the particle) with the polymerization active sites, and the macroscopic level (the reactor); and through which the kinetics and thermodynamics are connected. Adapted from Ref.[37]

Regarding the FBR level (the macro-scale), the reactor is an empty cylinder with two zones: the top zone (disengagement zone) is wider compared to the main zone (reaction zone). The cylinder of the main zone has a diameter on the order of 2-6 m and a height of 10-20 m.[18] The diameter of the upper zone is at least twice that of the main zone, and even larger ranges can be applied if the production capacity and the residence time require it.[21], [38] The purpose of the dome (the top zone) is the drop of the linear velocity of the reacting gas species (about 0.25 times that of the bed when the diameter is doubled), in order to defluidize the finest particles blown out of the bed and send them back to the main zone.

Typical industrial polyolefin FBRs operate at temperatures ranging from 75-110°C and pressures of 20-40 bar.[39] , [40] Due to the large scale of production, the FBRs are operated continuously. The reactor operates in a bubbling regime (i.e., at 3 to 8 times the minimum fluidization velocity), where there is a central upward flow which includes the circulation and mixing of the particles. This means that the bed will include three phases (assuming no condensed material): an emulsion phase (mixture of particles and vapor), a bubble phase (vapor only) and a wake phase (well-mixed phase of particles (lower amount than in the emulsion phase) and vapor).[8] The raw feed gas: monomer, comonomer hydrogen and inert materials (nitrogen and induced condensing agents (ICAs)), is introduced to the reactor through the distributor plate at the bottom of the reactor. This piece of equipment has an important role in properly distributing the flow of gas inside the reactor, in order to achieve a good fluidization.[41] The superficial gas velocity inside the reactor ranges between 50  $\text{cm} \cdot \text{s}^{-1}$  to 70  $\text{cm} \cdot \text{s}^{-1}$ . The single-pass monomer conversion is of the order of 2% -5%, while the total monomer conversion can reach 98%, since the majority of the unreacted monomer species are recompressed, cooled then recycled to the bottom of the reactor.[42] The relative gas-particle velocities are higher for FBRs comparing to other (stirred bed or recirculating) reactors, which means that FBRs provide the best heat removal capacity among gas phase reactors.[8] Note that the fluidization is affected by the size of particles. The gas rises similarly to

a plug flow movement through the bed. While moving up, the gas helps the mixing of the solid particles (fresh catalysts or prepolymers with growing polymer particles) in the bed.

The fluidization of the powder bed is not a simple task. One can consider that solid phase of the bed has a residence time distribution similar to that of a CSTR, which means that the particle size distribution (PSD) can be very broad (from several tens of microns if fresh catalysts are injected into the bed up to several hundreds of microns for the final powder).[18] Besides, the minimum fluidization velocity in a fluidized bed reactor is proportional to the square of the particle diameter, which requires a robust control of the gas flow rates and a proper design of the catalyst particles. Hence, the catalyst particles are often prepolymerized before their continuous injection into the reactor. Prepolymerization (producing small amounts of polymer on a fresh catalyst particle under less aggressive conditions in a reactor placed just beside of the main reactor) can help to reduce the presence of fine particles and to reduce the width of the particle size distribution in the fluidized bed. While the catalysts are fed into the reactor from a port above the gas species distributor, fresh monomers, hydrogen, nitrogen and other inert gases (ICAs) which constitutes the fluidizing reaction medium are injected at a point at the bottom under the distribution plate.

Particle level of the process model and the remaining length scales of the reactor; and how bridging them will be detailed below in section 2.

## 1.5. Condensed mode operation

The polymerization process is highly exothermic, and the reactor can generate an enormous heat rate of the order of 50-60 megawatts.[8] Most of the heat generated by the reaction is usually removed via the gas phase as it flows over the polymer particles inside the reactor. Therefore, the feed stream and the recycling stream temperatures allow controlling the bed temperature. This way of heat removal is called “dry mode” (DM), meaning that only gases are injected to the bed (ethylene, vaporized comonomer, hydrogen and nitrogen). In DM, it is also possible to inject a

specific quantity of alkanes, acting as induced condensing agents (ICAs), under their gaseous form (e.g. ethane, propane or butane).[18] The total flow rate of the gas through the reactor also influences the heat removal, but it is generally controlled in a way to ensure a good fluidization of the bed without flowing an important quantity of particles out of the reactor.[43]

If an ICA is added to the feed stream of the reactor, the operating mode is usually referred to as “super-dry mode” or SDM). This mode is similar to DM, but with a specific gas-phase alkane (of 4 to 6 carbons) in the feed stream. [18] This reactor operating mode helps improving the heat removal due to the enhanced heat capacity compared to nitrogen (the main inert gas in the DM). For higher heat removal, heavier alkanes can be injected, but then the feed stream can only be cooled to a particular point without condensation.[37], [43]

The most popular and appropriate method to increase the amount of heat removed from FBRs is operating under what is commonly referred to as condensed mode cooling (CM).[44] It consists of injecting the chemical inert compounds (ICAs) to the reactor. These species have much higher heat capacities than the other typical gaseous components, such as ethylene and nitrogen, so adding those increases the heat removal of the reactor, thereby allowing more heat to be removed and the polymerization to be faster. This technology was first defined in the patents of Jenkins III [21], [38], [45] since 1980 to cool down gas phase reactors. It consists of cooling the recycle stream to a temperature below its dew point, and feeding the partially liquefied mixture to the reactor (Figure 1.3). Condensable materials are usually C3-C6 alkanes often referred to as induced condensing agents (ICA) and comonomers (1-hexene or heavier  $\alpha$ -olefins).

Adding these species helps to cool the reactor by two ways. First, the feed stream is partially liquefied in a heat exchanger (see Figure 1.3) due to the cooling below the dew point of the heavier species (comonomers and inerts like alkanes), which is below the reactor temperature.[21], [46] Upon entering the reactor, the injected gas can vaporize and the latent heat of vaporization inside the reactor absorbs a significant amount of the reaction heat. Second, these species have much higher heat capacities than the other typical gaseous components such as ethylene and nitrogen.

Therefore, even under their gaseous form they will increase the heat removal of the reactor, thereby allowing the polymerization to be faster.[15]

Condensable materials are usually C3-C6 alkanes, but comonomers (1-hexene or heavier  $\alpha$ -olefins) can be also condensed and then evaporated during polymerization, which helps to remove the heat as well. In this work, comonomers and inert ICAs; despite their similar role; will be differentiated. Note that ICAs, even if sent to the reactor in vapor form, they are called induced condensing agents and they still improve the heat removal in the reaction medium. Actually, it is common to operate a fluidized bed reactor under conditions in which non-liquefied alkanes with high heat capacities (e.g. propane) are injected, to enhance the heat capacity of the gas stream; hence more heat can be removed.[43]

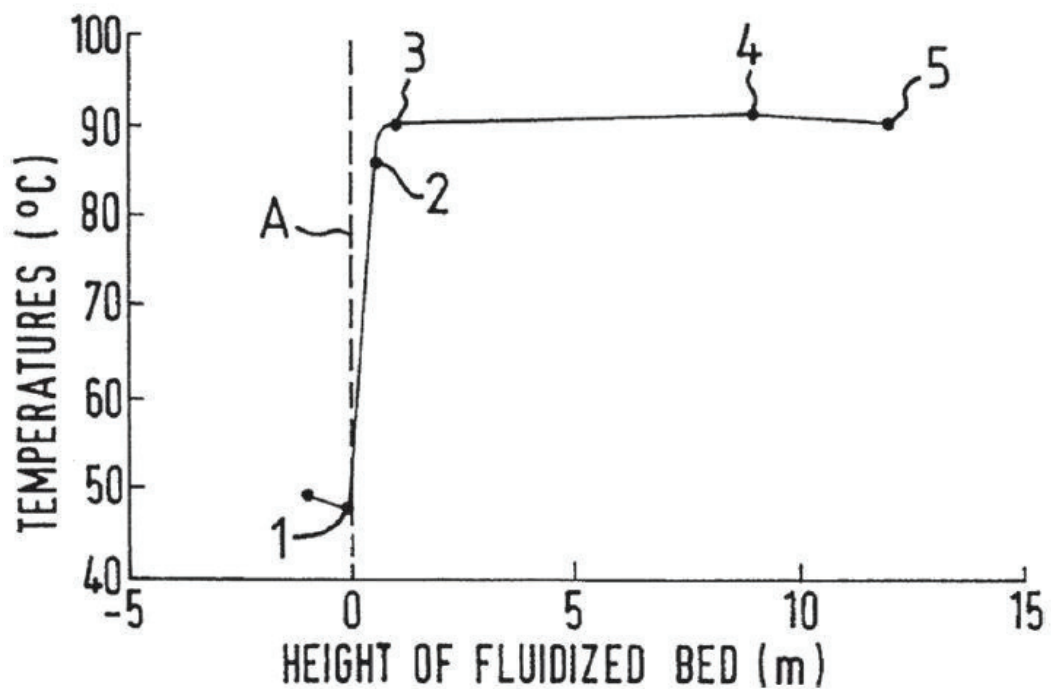


Figure 1.4 A fluidize-bed reactor temperature profile while introducing a partially liquefied feed stream.[46]

It should also be noted that in the condensed mode operation, the injected liquids are quickly evaporated in the reactor.[47] Indeed, the evaporation takes place in the first meter of the bed

below the distributor plate, for moderate liquid feed levels.[48] Generally, the more liquid one feeds into the reactor, the longer it will take to heat up and evaporate, and so the more extended the temperature profile in the bed will become. Figure 1.4 shows the temperature gradient over the height of the bed between position 1 and 3 while the liquid is evaporating. [46] If one increases the amount of liquid injected into the bed, position 3 will be move to a much higher up position in the bed. Eventually, the lifetime of a reasonably sized droplet of ICA in gas-phase is typically much higher than it would be in the liquid phase.[48] Thus, the comonomers and ICA will mostly be present in the reactor in the vapor phase, even if they are liquefied before entering to the reactor. The heat of vaporization allows an improved evacuation of heat compared to the DM. In CM, less than 20% by weight in the feed stream is liquid. If the feed stream contains more than 20% by weight liquid the reactor operating mode turns into “supercondensed mode” (SCM).[18] In the remaining discussion, we will consider only vaporized ICAs; and the proposed model in this work is only valid in the super-dry upper compartment of the FBR. The section of the bed containing liquid is neglected in the grade transition model (see chapter 4).

## 1.6. Effects of ICA on thermodynamics and polymer properties

Despite the wide-spread use of condensed mode cooling in the olefin industry, described in numerous patents in this field, e.g. [21], [38], [46], [49]–[51] the impact of induced condensing agents (ICAs) on the reaction rate, molecular weight distribution, particle morphology and particle agglomeration is still not completely understood. However, it has recently been showed that the ICAs can strongly impact the solubility of all species in the growing polymer particles, and since they also act as plasticizers they can also impact the physical properties of the particles.[24] As the rate of ethylene polymerization (affected by ICAs if present) depends on the ethylene concentration at the active sites, surrounding the catalyst fragment, its concentration is expected to impact the

properties of the final product such as its molecular weight and density.[52] It is then clear that the sorption of mixtures including ICA is complex: the amount and type of each species will have a significant effect on the solubility of the other species (monomer, comonomer) in PE and so on: the comonomer incorporation, the molecular weight and the other related properties.[15]

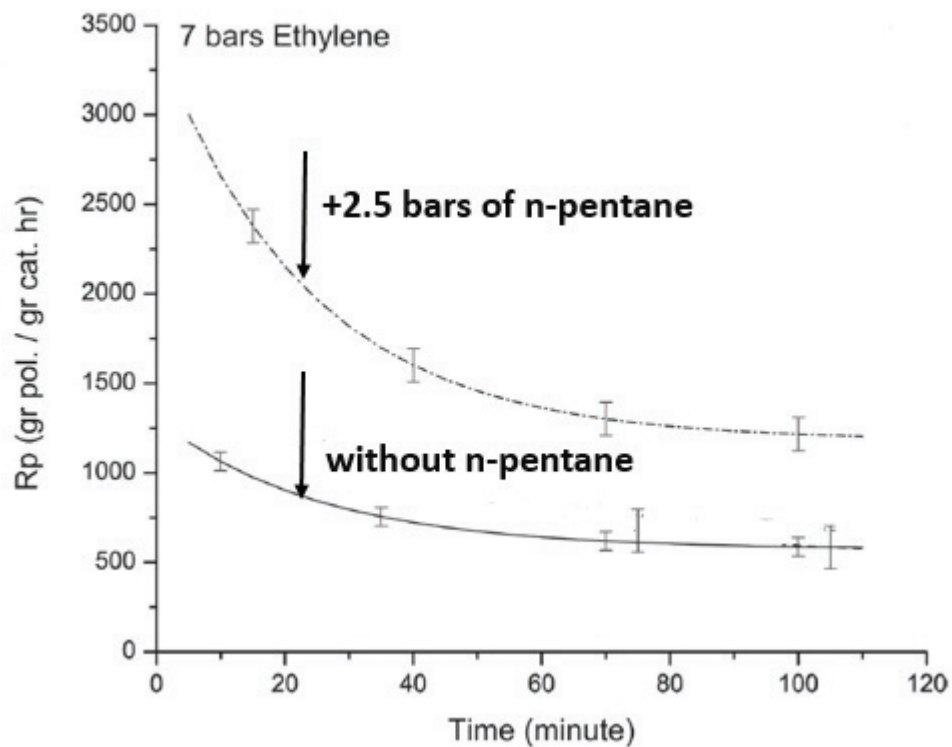


Figure 1.5 Relative rate of ethylene polymerization following the addition of 2.5 bars of ICA (here n-pentane) to 7 bars of ethylene (at 7 bars ethylene and 80°C). The relative rate ( $R_p$ ) refers to the polymerization rate of ethylene in the presence of ICA divided by the polymerization rate of only ethylene under identical conditions and with the same catalyst. Adapted from Ref.[24]

Indeed, the presence of chemically inert ICAs influences the thermodynamic equilibrium in the polymer (but does not impact the chemical nature of active sites). Several authors found that in the case of the sorption of two penetrants (ethylene+ comonomer or ICA) in the same polymer, the heavier sorbed species raise the sorption of the lighter species, which is referred to as the co-solubility effect.[21],[46],[53],[54] Therefore, when the growing polymer particle is swollen by an

alkane or an alkene, a significant change in the polymerization rate can be noticed.[24],[55],[56] For instance, Alizadeh and coworkers,[24] showed that including 2.5 bars of n-pentane in a reactor filled with 7 bars of ethylene at 80°C results in an increase of the reaction rate with a factor of 2, due to the co-solubility effect, which is a manifestation of non-ideal thermodynamics inherent to polymerization systems. (See Figure 1.5)

In other words, the heavier species (ICA) enhances the solubility of lighter species (ethylene) in the amorphous polymer, which results in increasing the concentration of ethylene in the amorphous phase of the polymer surrounding the active sites. **Consequently, the effect of condensed mode operation is not just limited to removing the heat from the reactor, but it also impacts the concentration of the different components in the polymer particles and thus at the active sites.**

Experimental studies on binary systems (one penetrant-PE) are frequent in the open literature.[57]–[60]. However, only few experimental studies concern the multicomponent systems (ternary or more), which represents most of the real conditions of PE in industry.[61] Therefore, it is important to account for these effects in the process model, especially in model-based optimization or control strategies, the objective of this study.

## 1.7. Polymer melting and temperature control

In a recent review by McKenna[18], it was shown that adding ICAs to the PE reactor is much more complex than increasing the heat removal by modifying the heat transfer. Polymer melting depends on a number of factors, including the bed temperature, the polymer properties (density, molecular weight), and the polymer swelling by solvents (e.g. ICAs). Hari et al. [62] related the melt initiation temperature (*MIT*) of polyethylene particles evaluated by differential scanning calorimetry to the sticking temperature experiments done in a stirred autoclave. They developed an empirical linear correlation of the sticking temperature as a function of an effective isopentane mass fraction in the

gas phase. The decrease in the sticking temperature could reach 10°C when doubling the fraction of isopentane in some situations. As a result, the more the polymer was amorphous (so less dense, but also able to swell with more ICA or comonomer), the faster the stickiness limit was reached.[63] This notion of using the melt onset, or melt initiation temperature as an indication of the temperature at which a polymer will begin to melt and to stick has been discussed in several patents. However, Large sets of experimental data would be required to develop an empirical correlation accounting for the different effects of temperature, polymer density, comonomer type and the swelling of the polymer by comonomers and induced condensing agents.

The concept can be shown in Figure 1.6 where 2 hypothetical melting thermograms are pictured, one for a dry polymer and one for a polymer swollen by one or more penetrants. When the dry polymer is heated, the polymer chains start losing their rigidity, become deformable then start to melt.[64] The *MIT* can be defined as the point where the tangent to the baseline and the tangent going through the inflection point in the rising part of the melt curve intersect, while the temperature at the peak of the curve is usually identified as the melting temperature ( $T_m$ ).

If the bed temperature gets close to the melting initiation temperature of the polymer, the particles may get sticky and start agglomeration. This can cause dramatic operability problems in the reactor such as particle agglomeration which may change the fluidization conditions and loss of bed stability, sheet formation and even the reactor shut down.

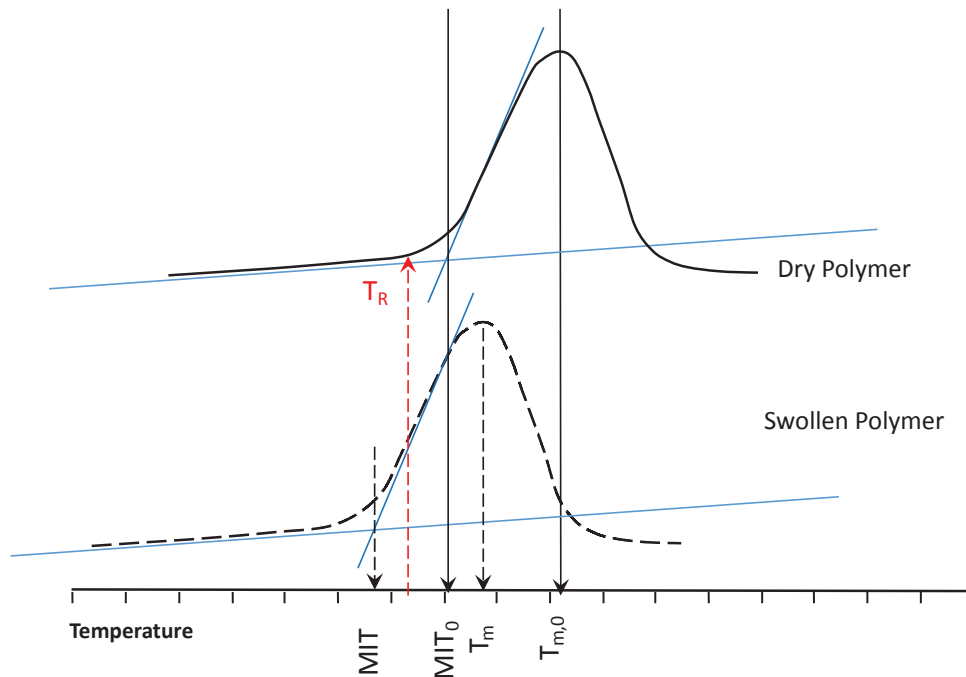


Figure 1.6 Scheme of the definition of the melt initiation temperature ( $MIT$ ), and the changes incurred in the values of the  $MIT$  and melting temperature of a dry polymer when it is swollen with a mixture of penetrants.

Again, the ICAs have a significant impact here. Indeed, besides the polymer density and molecular weight, its swelling with heavy components may affect the  $MIT$ . ICAs have been observed to contribute in the softening and the increase in stickiness of the particles.[65], [66] Indeed, the addition of ICAs, as well as comonomers affects the degree of the polymer swelling, which changes the nature of the amorphous phase.[67] The stickiness of the polymer increases as the amorphous fraction increases, and becomes more and more rubbery knowing that only crystals can melt.

This subject was reported by some patents as a serious issue in the determination of the safe operating temperature of FBRs.[68], [69] For the particular case of the fluidized bed reactors, the control of temperature is a composite task as they are generally susceptible to temperature oscillations.[70] Besides, FBRs are recommended to operate at high temperature in order to maximize the productivity, but lower than the polymer melting temperature.[71] Therefore, it is essential to include a model to predict particle sticking, especially in optimization and control strategies. This topic will be treated with more details in chapter 5.

## 2. Modelling and optimization

A process model is a mathematical representation of the real process. Process modeling have been extensively employed whether in industry or in academia, as it helps improving the process performance in different ways. For instance, the model may be used to predict and used to improve the product quality and the process efficiency and safety. The model should describe the various physical phenomena occurring in the system and the chemical reaction mechanisms.

### 2.1. Multi-scale phenomena

Modeling of the behavior of the FBR requires accounting for the full phenomena and their possible interconnections, which is not an easy task (see Figure 1.3). First, at the reactor level (macro-scale), studying the hydrodynamic aspects would help to ensure the bed stability, and the quality of mixing (fluidization of particles). Second, modelling the meso-scale (or the intermediate scale) would help to describe the interactions between the polymer particles. Third, the micro-scale represents the single particle level that states as a filter between macroscopic level and the polymerization active sites. This level should describe the phenomena related to the sorption of ethylene and other species from the gas phase and their diffusion through the polymer phase until reaching the active sites of the catalyst, where the polymerization reaction takes place. Thus, a robust predictive model has to account for the important phenomena at different length scales that occur in the polymerization process: e.g. reaction kinetics, thermodynamics, physical and transport phenomena, reactor outline and properties, etc.[72] For more information about research in the field of polymer reaction engineering modeling, the reader is referred to the interesting review made by Mueller et al [73]. In chapter 3, we discuss in detail the used kinetics and process model.

## 2.2. Importance of the thermodynamic model

We should take a quick look to the particle formation in a gas phase in order to better understand the importance of the thermodynamic model in this system. At the single particle level, the polymerization reaction is basically performed on the supported catalysts (e.g. ZN catalysts). The active sites located on the initial fragments of these supported catalysts are surrounded by the semi-crystalline produced polymer.[47] Consequently, the polymerization rate will depend mainly on the concentration of monomer (and comonomer if present) in the amorphous phase of semi-crystalline PE,[25] which clearly demonstrates the importance of considering the sorption process. In order to evaluate the effect of ICAs on the sorption of the other gases present in the bed, a valid thermodynamic model is needed. This model is to be connected at the micro-scale level with the reaction kinetics, in order to evaluate the effect of condensed mode on the gas phase composition, the concentrations of the different species, the reaction rate and so the quality of the polymer. (see chapter 3) In this context, and because of the strong non-ideality of thermodynamics in a system of penetrants-polymer, simple thermodynamic models such the case of Henry's law are not recommended, as it will be explained with further details in chapter 2 of this work. The most suitable thermodynamic model to quantify the speculated co-sorption phenomenon under equilibrium gas phase polymerization conditions that we have chosen for this study is Sanchez-Lacombe equation of state (SL EoS).

The SL EoS has been used frequently to predict the thermodynamic behavior in binary and ternary systems (polymer plus one or two penetrants respectively).[47], [73] The SL EoS provides a reliable evaluation of the solubility of solutes in the polymer. However, one must bear in mind that we have a multicomponent system and the model should allow predicting the concentration of all reactive components in the polymer. Indeed, the FBR contains numerous and different species such as  $\alpha$ -olefins (1-butene; 1-hexene), hydrogen and saturated alkanes like iso-butane or n-hexane

(see Figure 1.3). The used thermodynamic models, for ternary and quaternary systems, are detailed in chapter 2.

## 2.3. Optimization of grade transitions

The size of the market of PE and the increasing demand means that producers need to increase the production capacity by either improving existing processes, or building newer, more efficient processes. Optimization of polymerization processes might help at different levels:

- reduce energy consumption during the production (e.g. minimize reaction time, temperature, pressure);
- reduce risks for the operators and for the environment (e.g. choose a process without volatile organic solvent, raw materials of renewable origin);
- ensure the desired product quality based on the targeted application (e.g. density, melt index (*MI*), molecular architecture)
- make the raw materials profitable (e.g. ethylene constitutes a residue during refining process and would be burned if it is not exploited as plastic materials);
- reduce the waste and large amounts of off-spec products, especially using FBRs (long residence times)[8];

More particularly, in most industrial plants, frequent grade transitions are realized in order to satisfy the large market needs and the variety of polyethylene products and applications.[74], [75] Indeed, it is quite common to produce several tens of different grades in the same process, in order to obtain a polyethylene with different melt index (means the difference in the ease of processability),[76] molecular weights or densities. These derivation of these main polymer properties is based on physical interpretations. For instance, the melt index is highly correlated to the polymer molecular weight distribution and branching characteristics.[77] To simplify, the

instantaneous melt index is usually correlated to the instantaneous average polymer molecular weight  $M_w$ . The molecular weight is in turn affected by the temperature, the type of comonomer and catalyst, and the concentration of monomer, comonomer and hydrogen. Indeed, hydrogen plays the role of a chain transfer agent in catalytic ethylene reactions, thus allowing to reduce the polymer molecular weight.[78] It constitutes therefore a primary manipulated variable during grade transitions.

Concerning the polymer density, it is strongly affected by the length and the number of short chain branches. Hence, it is mainly governed by the fraction of reacted comonomer in the co-polymer ( $C_x$ ) (see chapter 3: Table 3-8).[79] By creating short chain branches on the polymer, the comonomer allows reducing the polymer density. As a consequence the crystallinity of the polymer also decreases.[15] The comonomer constitutes the second important manipulated variable during grade transition.

Due to the high cost of inventory and the changing market demand, frequent transitions are required. These transitions are challenging because it is necessary to optimize the economic yield and the product quality while ensuring the safety of the operations. Yet, these transitions are sometimes based only on the expertise of the operator, and when operating under condensed mode, the transitions might be more complex since the sorption/desorption dynamics of the different species in the reactor can change the behavior of the system according to the composition of the reaction medium. Given the large growing PE market, and the economic and safety challenges of this process, it is necessary to develop a methodology to improve the transition between grades of PE, while minimizing the off-specification product and/or transition time as well as ensuring the safety of the process.

Among gas phase processes, FBRs are able to produce a wide range of PE grades in the same unit. However, it may result in a huge waste of transition time and products, due to the long residence time. Consequently, an appropriate transition control methodology is needed to ensure the polymer

quality and the process safety at reduced cost.[80] In this work, off-line dynamic optimization will be employed to optimize grade transitions (in chapters 4 and 5).

### 3. Objectives

Based on the detailed context presented above, the objectives of this project can be defined. In this work we consider ethylene polymerization in gas phase, and more particularly the production of LLDPE in fluidized bed reactors.

As presented above, at the industrial scale, PE is produced in gas phase only in fluidized bed reactors (FBRs) (up to a volume of 200 m<sup>3</sup>, at temperatures in the range of 70-110°C and pressures typically on the order of 20-40 bar [39]), where the polymer is grown in the form of particles suspended in a fluidized flowing gas stream. Indeed, FBRs are the only reactors that can remove enough heat in the gas phase and thus allow the production of large amounts of polymer.[8] In order to further enhance heat transfer and increase productivity, condensed mode cooling is frequently employed, where induced condensing agents (ICAs, which are typically alkanes such propane or isomers of butane, pentane or hexane) are injected in either liquid or vapor form.[38], [61] Basically, for copolymerization systems, the comonomer also can be condensable just like ICAs. The heat of vaporization and/or increase in the heat capacity of the vapor phase in the reactor absorb a significant amount of the reaction heat. However, it has also been observed that when the polymer particles are swollen by an alkane or an alkene, the reaction rate can change significantly due to the so-called co-solubility (or co-solvent) effect (non-ideal sorption thermodynamics). Indeed, the presence of condensable species influences the thermodynamic equilibrium in the reactor: The presence of a hydrocarbon heavier than ethylene enhances the solubility of ethylene in the amorphous phase of the polymer, thereby contributing to a higher rate of polymerization, while the lighter hydrocarbons play the role of anti-solvent (anti-solubility) for the heavier ones.[24], [55] Therefore, the presence of ICA increases the ethylene concentration in

the polymer, leading to a higher reaction rate, while ethylene is expected to act as an anti-solvent for the ICAs (and eventually for comonomers like 1-butene or 1-hexene). The development of a process model that takes into account the effect of condensable compounds on the rate of polymerization constitutes the first objective of this project. The modelling part is presented in chapters 2 and 3, for two ternary and quaternary copolymerization systems.

The second objective of this work concerns the optimization of grade transitions. We will propose a model-based off-line dynamic optimization procedure to optimize the transition between grades of PE based on a process model including an accurate thermodynamic description. The thermodynamic model (based on SL EoS) is combined with the reactor model. The first control variable is the flowrate of hydrogen, which plays the role of a chain transfer agent and thus allows controlling the polymer molecular weight and melt index. The second control variable is the comonomer flowrate, which influences the polymer molecular weight as well, but has as a main role the creation of irregularities in the chain and so reduces the crystallinity and polymer density. The control objectives are the MI and polymer density. The development steps of the optimization methodology as well as the literature review of the available grade transition methodologies are provided in chapter 4.

The third objective of this work is to study the impact of inert alkanes on the sticking temperature of the polymer particles during grade transitions, which may generate disturbances in the bed stability. Indeed, increasing the amount of a diluent (ICAs and comonomer) might be needed to reach some desired properties of PE grades. It is necessary then to understand the impact of increasing diluents on the melting onset temperature of the polymer and thus on the particle stickiness. The bed temperature should absolutely remain lower than the polymer melting point (to avoid agglomeration of the particles), but high enough to ensure an acceptable productivity. Rahimpour et al.[70] also indicated that the bed temperature should be remained higher than the gas dew point, in order to avoid condensing the gas. In order to ensure the process safety, a new control variable is considered, which is the bed temperature that is controlled to remain lower than

the polymer melt initiation temperature. This later is obtained by a model combining data from patents and swelling models. This strategy provides a good control of the polymer final properties while keeping the temperature stability of the FBR. This topic is presented in chapter 5.

To avoid any confusion, the following notations of the different species are to be kept in mind:

- Monomer: Only ethylene is considered as monomer in this work.
- Comonomers: Either 1-butene or 1-hexene will be used. A comonomer is reactive, and is inserted in the polymer chain. It generally increases the amount of branches and reduces the crystallinity and the density of the polymer.
- Induced condensing agents (ICAs): Either n-hexane or iso-butane will be used. They are inert chemically.

As systems, we consider:

- Binary system: A binary system involves polymer and ethylene as gaseous penetrants. They are discussed briefly in chapter 2, just as a primary step towards the development of more advanced thermodynamic models.
- Ternary systems: A ternary system involves polymer (here LLDPE), and two gaseous penetrants. The first penetrant is always ethylene. The second is one of the comonomers or one of the ICAs.
- Pseudo-quaternary systems: They involve the polymer and three gaseous penetrants. Here, these gases are chosen to be ethylene, one comonomer and one ICA.

# References

- [1] S. Abedi et M. Abdouss, « A review of clay-supported Ziegler–Natta catalysts for production of polyolefin/clay nanocomposites through in situ polymerization », *Appl. Catal. Gen.*, vol. 475, p. 386–409, 2014.
- [2] S. Bensason, J. Minick, A. Moet, S. Chum, A. Hiltner, et E. Baer', « Classification of homogeneous ethylene-octene copolymers based on comonomer content », p. 15.
- [3] C. Opportunities *et al.*, « World Polyethylene », *The Freedonia Group*. <https://www.freedoniagroup.com/industry-study/world-polyethylene-3210.htm> (consulté le nov. 27, 2020).
- [4] E. Sagel, « Polyethylene Global Overview Today' s », *Foro Pemex*, 2012.
- [5] S. Senet, « Plastic production on the rise worldwide but slowing in Europe », *www.euractiv.com*, juin 05, 2019. <https://www.euractiv.com/section/energy-environment/news/while-global-plastic-production-is-increasing-worldwide-it-is-slowin-down-in-europe/> (consulté le déc. 23, 2020).
- [6] P. V. Hemmingsen, « Phase Equilibria in Polyethylene Systems », p. 180.
- [7] « Introduction to Polyolefins », in *Polyolefin Reaction Engineering*, John Wiley & Sons, Ltd, 2012, p. 1-13.
- [8] J. B. P. Soares, T. F. L. McKenna, *Polyolefin Reaction Engineering*, Wiley-VCH, Mannheim, Germany **2012**.
- [9] Pune, I.- January 16, et 2019 /MarketersMedia, « Industrial Films Market Report 2019, Top Companies, Pricing Trend, Growth Opportunity, Global Status, Driving Factor Analysis and Competition Outlook 2023 « MarketersMEDIA – Press Release Distribution Services – News Release Distribution Services ». <https://marketersmedia.com/industrial-films-market-report-2019-top-companies-pricing-trend-growth-opportunity-global-status-driving-factor-analysis-and-competition-outlook-2023/471418> (consulté le déc. 26, 2020).
- [10] « Linear Low Density Polyethylene (LLDPE) Market By Growth Opportunities and Regional Forecast 2024 », *MarketWatch*. <https://www.marketwatch.com/press-release/linear-low-density-polyethylene-lldpe-market-by-growth-opportunities-and-regional-forecast-2024-2019-02-28> (consulté le sept. 26, 2019).
- [11] T. J. Hutley et M. Ouederni, « Polyolefins—The History and Economic Impact », in *Polyolefin Compounds and Materials*, M. Al-Ali AlMa'adeed et I. Krupa, Éd. Cham: Springer International Publishing, 2016, p. 13-50.

- [12] M. M. de Camargo Forte, F. O. V. da Cunha, J. H. Z. dos Santos, et J. J. Zacca, « Ethylene and 1-butene copolymerization catalyzed by a Ziegler–Natta/Metallocene hybrid catalyst through a 23 factorial experimental design », *Polymer*, vol. 44, n° 5, p. 1377-1384, mars 2003, doi: 10.1016/S0032-3861(02)00874-1.
- [13] J. C. Woodbrey et P. Ehrlich, « The Free Radical, High Pressure Polymerization of Ethylene. II. The Evidence for Side Reactions from Polymer Structure and Number Average Molecular Weights », *J. Am. Chem. Soc.*, vol. 85, n° 11, p. 1580-1584, 1963.
- [14] T. F. McKenna et J. B. P. Soares, « Single particle modelling for olefin polymerization on supported catalysts: A review and proposals for future developments », *Chem. Eng. Sci.*, vol. 56, n° 13, p. 3931-3949, juill. 2001, doi: 10.1016/S0009-2509(01)00069-0.
- [15] F. Nascimento de Andrade, « Effect of condensable materials during the gas phase polymerization of ethylene on supported catalysts », Université Claude Bernard Lyon 1, 2019.
- [16] M. A. Bashir, « Impact of Physical Properties of Silica on the Reaction Kinetics of Silica Supported Metallocenes and Polyethylene Morphology », Ph.D. Thesis, Université de Lyon, 2016.
- [17] M. Daftaribesheli, « Comparison of catalytic ethylene polymerization in slurry and gas phase », *IEEE Trans. Instrum. Meas. - IEEE TRANS INSTRUM MEAS*, janv. 2009.
- [18] T. F. L. McKenna, « Condensed Mode Cooling of Ethylene Polymerization in Fluidized Bed Reactors », *Macromol. React. Eng.*, vol. 13, n° 2, p. 1800026, 2019, doi: 10.1002/mren.201800026.
- [19] « Polyolefin Reactors and Processes », in *Polyolefin Reaction Engineering*, John Wiley & Sons, Ltd, 2012, p. 87-129.
- [20] D. B. Fischbuch, R. O. Hagerty, S. C. Hinds, D. R. Holroyd, A. V. Ng, et D. Singh, « Low molecular weight induced condensing agents », US7696289B2, avr. 13, 2010.
- [21] J. M. J. III, R. L. Jones, et T. M. Jones, « Fluidized bed reaction systems », US4543399A, sept. 24, 1985.
- [22] « UNIPOL™ PE Process ». <https://www.prod.univation.com/en-us/unipol/process.html> (consulté le déc. 02, 2020).
- [23] D. F. Siberdt, « Innovene™ G & S technologies Recent advances and global positioning », p. 26.
- [24] A. Alizadeh, M. Namkajorn, E. Somsook, et T. F. L. McKenna, « Condensed Mode Cooling for Ethylene Polymerization: Part I. The Effect of Different Induced Condensing Agents on Polymerization Rate », *Macromol. Chem. Phys.*, vol. 216, n° 8, p. 903-913, avr. 2015, doi: 10.1002/macp.201400600.

- [25] T. F. L. McKenna, A. D. Martino, G. Weickert, et J. B. P. Soares, « Particle Growth During the Polymerisation of Olefins on Supported Catalysts, 1 – Nascent Polymer Structures », *Macromol. React. Eng.*, vol. 4, n° 1, p. 40-64, 2010, doi: 10.1002/mren.200900025.
- [26] A. Alizadeh et T. F. McKenna, « Particle growth during the polymerization of olefins on supported catalysts. Part 2: Current experimental understanding and modeling progresses on particle fragmentation, growth, and morphology development », *Macromol. React. Eng.*, vol. 12, n° 1, p. 1700027, 2018.
- [27] D. W. Sauter, M. Taoufik, et C. Boisson, « Polyolefins, a success story », *Polymers*, vol. 9, n° 6, p. 185, 2017.
- [28] P. C. Thüne, J. Loos, A. M. De Jong, P. J. Lemstra, et J. W. Niemantsverdriet, « Planar model system for olefin polymerization: the Phillips CrO<sub>x</sub>/SiO<sub>2</sub> catalyst », *Top. Catal.*, vol. 13, n° 1-2, p. 67-74, 2000.
- [29] « Polymerization Catalysis and Mechanism », in *Polyolefin Reaction Engineering*, John Wiley & Sons, Ltd, 2012, p. 53-86.
- [30] R. Mülhaupt, « Catalytic polymerization and post polymerization catalysis fifty years after the discovery of Ziegler's catalysts », *Macromol. Chem. Phys.*, vol. 204, n° 2, p. 289-327, 2003.
- [31] L. L. Böhm, « The Ethylene Polymerization with Ziegler Catalysts: Fifty Years after the Discovery », *Angew. Chem. Int. Ed.*, vol. 42, n° 41, p. 5010-5030, 2003, doi: <https://doi.org/10.1002/anie.200300580>.
- [32] P. Cossee, « Ziegler-Natta catalysis I. Mechanism of polymerization of  $\alpha$ -olefins with Ziegler-Natta catalysts », *J. Catal.*, vol. 3, n° 1, p. 80-88, févr. 1964, doi: 10.1016/0021-9517(64)90095-8.
- [33] J. K. and G. James Mark, Kia Ngai, William Graessley, Leo Mandelkern, Edward Samulski, *PHYSICAL PROPERTIES OF POLYMERS*, Third. 2003.
- [34] P. C. Painter et M. M. Coleman, *Fundamentals of polymer science : an introductory text*. Technomic Pub. Co, 1997.
- [35] E. Albizzati et M. Galimberti, « Catalysts for olefins polymerization », *Catal. Today*, vol. 41, n° 1, p. 159-168, mai 1998, doi: 10.1016/S0920-5861(98)00046-7.
- [36] G. G. Hlatky, « Heterogeneous single-site catalysts for olefin polymerization », *Chem. Rev.*, vol. 100, n° 4, p. 1347-1376, 2000.
- [37] J. B. P. Soares et T. F. L. McKenna, « Polyolefin Reaction Engineering », p. 345.
- [38] J. M. Jenkins III, R. L. Jones, T. M. Jones, et S. Beret, *Method for fluidized bed polymerization*. Google Patents, 1986.

- [39] T. Xie, K. B. McAuley, J. C. C. Hsu, et D. W. Bacon, « Gas Phase Ethylene Polymerization: Production Processes, Polymer Properties, and Reactor Modeling », *Ind. Eng. Chem. Res.*, vol. 33, n° 3, p. 449-479, mars 1994, doi: 10.1021/ie00027a001.
- [40] M. R. Abbasi, A. Shamiri, et M. A. Hussain, « A review on modeling and control of olefin polymerization in fluidized-bed reactors », *Rev. Chem. Eng.*, vol. 35, n° 3, p. 311-333, 2019.
- [41] S. Ohtani, S. Abe, et H. Nishida, « Process for producing olefinic polymer », US6858681B2, févr. 22, 2005.
- [42] K. B. McAuley, J. P. Talbot, et T. J. Harris, « A comparison of two-phase and well-mixed models for fluidized-bed polyethylene reactors », *Chem. Eng. Sci.*, vol. 49, n° 13, p. 2035-2045, juill. 1994, doi: 10.1016/0009-2509(94)E0030-T.
- [43] A. L. D. Braganca, A. L. R. de C. Morschbacker, E. Rubbo, C. N. Miro, T. Barlem, et A. Mukherjee, « Process for the gas phase polymerization and copolymerization of olefin monomers », US6864332B2, mars 08, 2005.
- [44] J. B. P. Soares et T. F. L. McKenna, *Polyolefin Reaction Engineering*. Weinheim, Germany: Wiley-VCH Verlag GmbH & Co. KGaA, 2012.
- [45] J. M. J. Iii, R. L. Jones, T. M. Jones, et S. Beret, « A method for controlling the temperature of a fluidized bed especially a process for producing polymers », EP0241947A2, oct. 21, 1987.
- [46] J.-C. Chinh, M. C. H. Filippelli, D. Newton, et M. B. Power, « Polymerization process », US5541270A, juill. 30, 1996.
- [47] A. Alizadeh, Study of sorption, heat and mass transfer during condensed mode operation of gas phase ethylene polymerization on supported catalyst, Ph.D. Thesis, Queen's University **2014**.
- [48] A. Alizadeh et T. F. L. McKenna, « Condensed Mode Cooling in Ethylene Polymerisation: Droplet Evaporation », *Macromol. Symp.*, vol. 333, n° 1, p. 242-247, nov. 2013, doi: 10.1002/masy.201300092.
- [49] G. Penzo, G. Mei, et G. Meier, « Gas-phase olefin polymerization process », US7482411B2, janv. 27, 2009.
- [50] M. L. DeChellis, Houston, J. R. Griffin, et Baytown, « Process for polymerizing monomers in fluidized beds », 5,352,749.
- [51] S. J. Rhee et L. L. Simpson, « Fluidized bed polymerization reactors », US4933149A, juin 12, 1990.
- [52] S. Floyd, K. Y. Choi, T. W. Taylor, et W. H. Ray, « Polymerization of olefins through heterogeneous catalysis. III. Polymer particle modelling with an analysis of intraparticle heat and mass transfer effects », *J. Appl. Polym. Sci.*, vol. 32, n° 1, p. 2935-2960, juill. 1986, doi: 10.1002/app.1986.070320108.

- [53] J.-S. Yoon, C.-Y. Chung, et I.-H. Lee, « Solubility and diffusion coefficient of gaseous ethylene and  $\alpha$ -olefin in ethylene/ $\alpha$ -olefin random copolymers », *Eur. Polym. J.*, vol. 30, n° 11, p. 1209-1214, nov. 1994, doi: 10.1016/0014-3057(94)90128-7.
- [54] L. M. Robeson et T. G. Smith, « The desorption of ethane-butane mixtures from polyethylene », *J. Appl. Polym. Sci.*, vol. 11, n° 10, p. 2007-2019, 1967, doi: 10.1002/app.1967.070111017.
- [55] A. Alizadeh, M. Namkajorn, E. Somsook, et T. F. L. McKenna, « Condensed Mode Cooling for Ethylene Polymerization: Part II. The Effect of Different Condensable Comonomers and Hydrogen on Polymerization Rate », *Macromol. Chem. Phys.*, vol. 216, n° 9, p. 985-995, mai 2015, doi: 10.1002/macp.201500023.
- [56] M. Namkajorn, A. Alizadeh, D. Romano, S. Rastogi, et T. F. L. McKenna, « Condensed Mode Cooling for Ethylene Polymerization: Part III. The Impact of Induced Condensing Agents on Particle Morphology and Polymer Properties », *Macromol. Chem. Phys.*, vol. 217, n° 13, p. 1521-1528, juill. 2016, doi: 10.1002/macp.201600107.
- [57] W. M. R. Parrish, « Solubility of isobutane in two high-density polyethylene polymer fluffs », *J. Appl. Polym. Sci.*, vol. 26, n° 7, p. 2279-2291, juill. 1981, doi: 10.1002/app.1981.070260715.
- [58] S. J. Moore et S. E. Wanke, « Solubility of ethylene, 1-butene and 1-hexene in polyethylenes », *Chem. Eng. Sci.*, vol. 56, n° 13, p. 4121-4129, juill. 2001, doi: 10.1016/S0009-2509(01)00082-3.
- [59] C. Kiparissides, V. Dimos, T. Boulouka, A. Anastasiadis, et A. Chasiotis, « Experimental and theoretical investigation of solubility and diffusion of ethylene in semicrystalline PE at elevated pressures and temperatures », *J. Appl. Polym. Sci.*, vol. 87, n° 6, p. 953-966, 2003, doi: 10.1002/app.11394.
- [60] J. Chmelař, K. Haškovcová, M. Podivinská, et J. Kosek, « Equilibrium Sorption of Propane and 1-Hexene in Polyethylene: Experiments and Perturbed-Chain Statistical Associating Fluid Theory Simulations », *Ind. Eng. Chem. Res.*, vol. 56, n° 23, p. 6820-6826, juin 2017, doi: 10.1021/acs.iecr.7b00572.
- [61] T. F. L. McKenna, « Condensed Mode Cooling of Ethylene Polymerization in Fluidized Bed Reactors », *Macromol. React. Eng.*, vol. 13, n° 2, p. 1800026, avr. 2019, doi: 10.1002/mren.201800026.
- [62] A. S. Hari, B. J. Savatzky, D. M. Glowczwski, et X. Cao, « Controlling a polyolefin reaction », US 9,718,896 B2, 2015.

- [63] M. G. Goode, M. W. Blood, et W. G. Sheard, « High condensing mode polyolefin production under turbulent conditions in a fluidized bed », US6391985B1, mai 21, 2002.
- [64] J. Chmelar, P. Matuska, T. Gregor, M. Bobak, F. Fantinel, et J. Kosek, « Softening of polyethylene powders at reactor conditions », *Chem. Eng. J.*, vol. 228, p. 907-916, juill. 2013, doi: 10.1016/j.cej.2013.05.069.
- [65] D. Singh, S. Hinds, B. Fischbuch, et N. A. Vey, « Gas-phase process », US20050182207A1, août 18, 2005.
- [66] G. G. Hendrickson, « Method for operating a gas phase polymerization reactor », US7531606B2, mai 12, 2009.
- [67] B. J. Banaszak *et al.*, « Ethylene and 1-Hexene Sorption in LLDPE under Typical Gas Phase Reactor Conditions: A Priori Simulation and Modeling for Prediction of Experimental Observations », *Macromolecules*, vol. 37, n° 24, p. 9139-9150, nov. 2004, doi: 10.1021/ma0491107.
- [68] R. O. Hagerty, K. B. Stavens, M. L. DeChellis, D. B. Fischbuch, et J. M. Farley, « Polymerization process », US7300987B2, nov. 27, 2007.
- [69] D. N. T. JR et E. J. Markel, « Polymerization reaction monitoring with determination of induced condensing agent concentration for preventing discontinuity events », US7754830B2, juill. 13, 2010.
- [70] M. R. Rahimpour, J. Fathikalajahi, B. Moghtaderi, et A. N. Farahani, « A Grade Transition Strategy for the Prevention of Melting and Agglomeration of Particles in an Ethylene Polymerization Reactor », *Chem. Eng. Technol.*, vol. 28, n° 7, p. 831-841, juill. 2005, doi: 10.1002/ceat.200500055.
- [71] C. Chatzidoukas, « Control and Dynamic Optimisation of Polymerization Reaction Processes », University of London, London, 2004.
- [72] A. Krallis, P. Pladis, V. Kanellopoulos, V. Saliakas, V. Touloupides, et C. Kiparissides, « Design, Simulation and optimization of polymerization processes using advanced open architecture software tools », in *Computer Aided Chemical Engineering*, vol. 28, Elsevier, 2010, p. 955-960.
- [73] P. A. Mueller, J. R. Richards, et J. P. Congalidis, « Polymerization Reactor Modeling in Industry », *Macromol. React. Eng.*, vol. 5, n° 7-8, p. 261-277, août 2011, doi: 10.1002/mren.201100011.
- [74] D. Bonvin, L. Bodizs, et B. Srinivasan, « Optimal Grade Transition for Polyethylene Reactors via NCO Tracking », *Chem. Eng. Res. Des.*, vol. 83, n° 6, p. 692-697, juin 2005, doi: 10.1205/cherd.04367.

- [75] Z. Liao, P. Wang, J. Wang, et Y. Yang, « A heuristic approach to grade transition strategy of the HDPE slurry process in different operation modes », *Clean Technol. Environ. Policy*, vol. 15, n° 5, p. 833-849, oct. 2013, doi: 10.1007/s10098-012-0574-2.
- [76] D20 Committee, « Test Method for Melt Flow Rates of Thermoplastics by Extrusion Plastometer », ASTM International. doi: 10.1520/D1238-20.
- [77] M. S. Abbas-Abadi, M. N. Haghighi, et H. Yeganeh, « Effect of the melt flow index and melt flow rate on the thermal degradation kinetics of commercial polyolefins », *J. Appl. Polym. Sci.*, vol. 126, n° 5, p. 1739-1745, déc. 2012, doi: 10.1002/app.36775.
- [78] V. Touloupides, V. Kanellopoulos, P. Pladis, C. Kiparissides, D. Mignon, et P. Van-Grambezen, « Modeling and simulation of an industrial slurry-phase catalytic olefin polymerization reactor series », *Chem. Eng. Sci.*, vol. 65, n° 10, p. 3208-3222, mai 2010, doi: 10.1016/j.ces.2010.02.014.
- [79] J. Shi, L. T. Biegler, et I. Hamdan, « Optimization of grade transitions in polyethylene solution polymerization processes », *AIChE J.*, vol. 62, n° 4, p. 1126-1142, avr. 2016, doi: 10.1002/aic.15113.
- [80] C. Chatzidoukas, J. D. Perkins, E. N. Pistikopoulos, et C. Kiparissides, « Optimal grade transition and selection of closed-loop controllers in a gas-phase olefin polymerization fluidized bed reactor », *Chem. Eng. Sci.*, vol. 58, n° 16, p. 3643-3658, août 2003, doi: 10.1016/S0009-2509(03)00223-9.

"The purpose of science is not to analyze or describe, but to make useful models of the world. A model is useful if it allows us to get use out of it"

- Edward de Bono (1933)

### 1. Introduction

The aim of this work is to develop a fundamental understanding of the impact of condensed mode cooling on ethylene polymerization, and to translate this knowledge into a model able to predict the quality of the polymer produced during grade transition. In the first chapter, we showed that induced condensed agents (ICAs), such as iso-butane or n-hexane, affect the thermodynamics, besides their primary goal, which is enhancing heat transfer. Accordingly, the addition of these species to the feed stream of the reactor can influence significantly the solubility of the different species of the system (monomers, comonomers etc.) in the growing polymer particles. As discussed earlier, this is referred to as the “co-solubility effect, where the presence of ICA increases the ethylene concentration but decreases the comonomer concentration in the amorphous polymer phase. Also, the polymer particles are swollen by an alkane or an alkene, which results in a change of the reaction rate. Consequently, and since ICAs also act as plasticizers, they can impact the physical properties of the particles. An appropriate thermodynamic model is then required to quantify the effect of the process operating conditions on the reaction rate of polymerization and especially on the polymer quality control.

In the current chapter, we give a description of the thermodynamic model developed in this thesis, which is based on the Sanchez-Lacombe equation of state (SL EoS). This model can be used to

model the solubility of different species and to evaluate the effect of different types of ICA on the concentration of reactive species in the amorphous phase of polyethylene (PE). This includes different cases of binary and ternary systems, then the extension of the model to pseudo-quaternary systems based on some assumptions. The required model parameters, such as the binary interaction parameters, are identified using the Matlab® global optimization toolbox by fitting the predicted solubility data with experimental values from the open literature. Then, in order to simplify the model and reduce the computational time, linear correlations are employed based on the SL EoS predictions or experimental data depending on the case. This allows for a faster implementation of the model into an optimization loop.

## 2. Thermodynamic Models

Advances in phase equilibria calculations and the improvement of the modelling capability, especially for polymer reaction engineering, have allowed the expansion of studies treating the equations of state for a polymerization mixture.[1] For instance, exploring polyolefin thermodynamics while using the equations of state is continuing to be subject to substantial improvements.

In this study, we would like to estimate the impact of adding ICA and/or comonomer on the rate of polymerization and the polymer properties. Since 1959, Roger et al.[2] showed that the crystalline phase of polyethylene is inaccessible by any penetrating species, therefore, only the amorphous phase is subject to sorption. They realized sorption experiments for thirteen common organic vapors in three different types of polyethylene (i.e. different crystallinity and density), using a quartz helix microbalance, at a temperature range of 0-25°C. Michaels and Bixler[3] also indicated that the solubility of gas species in the polyethylene is proportional to the volume fraction of only the amorphous phase, the only phase that can be penetrated by the solute species. However, despite the impermeability of the crystalline phase to diffusing molecules, it has been shown that the degree of crystallinity of PE affects the diffusion process.[4] In other words, the more the crystallinity

degree of a polymer increases the lower the diffusion and permeability constants become. In this work, we focus particularly on LLDPE, and so the degree of crystallinity is almost the same. Hence, in the thermodynamic model used in this work, we define the crystallinity of the polymer and we take into account only the amorphous region for evaluating the solubility/concentration. This point is important to mention as it concerns all the parts of the current study.

## 2.1. Henry's law

Henry's law is often used to evaluate the solubility of a single light solute in a polymer, at low pressures.[5] In case Henry's law is applicable, a vapor single penetrant solubility  $[M_1]^*$ , can be expressed as a function of its partial pressure ( $P_1$ ) above the polymer, following this form:

$$[M_1]^* = k^* P_1 \quad (2.1)$$

Where,  $k^*$  is the Henry's law constant, which is independent of both the volume fraction and the vapor solute pressure. Henry's equation can be considered as a simplified case of Flory-Huggins theory,[6] from which several many correlations can be derived. Among these correlations, is the correlation developed by Stern et al.[7] to express Henry's law based on their experimental observations, in which  $k^*$  increases whenever the critical temperature ( $T_c$ ) of the penetrant increases, and decreases inversely to the temperature of the system ( $T$ ). The following equation is the resulting correlation of  $\log(k^*)$  as a function of  $(T_c/T)$ : [6]

$$\log(k^*) = -2.38 + 1.08 \left( \frac{T_c}{T} \right)^2 \quad (2.2)$$

Equation (2.2) was found to fit very well a large set of literature data that was reported by Hutchinson et al.[6] for different penetrants in polyethylene, such as ethylene. But, the binary of constants (-2.38; 1.08) can be updated for other different solute species with different conditions such as the operating temperature.[6]

However, at higher pressure of penetrating species, even for pure components, the solubility increases and deviates from Henry's law.[8] Li and Long,[9] for instance showed that the solubility of ethylene in polyethylene obeyed Henry's law only up to the critical pressure of ethylene at 25°C. They reported the solubility of different gas species in polyolefin films at elevated pressures (up to 100 bars). Afterwards, they showed an exponential increase of ethylene solubility with increased pressure. At pressure higher than the critical pressure of the solute gas, they concluded a significant deviation from Henry's law. Stern et al.[7] analyzed experimental data reported by different research groups and concluded that when reaching the limit of Henry's law, an increase of the critical temperature led to an increase of the solute solubility; and an increase in the critical temperature, led to a decrease of the pressure at which the deviation from Henry's law becomes pronounced. Henry's law is also not applicable for evaluating the solubility of heavier hydrocarbon vapors since they tend to swell the polymer to a larger degree and act as plasticizers.[6] The Henry's law is not adequate as well for multicomponent systems, such as a copolymerization system. Indeed Yoon et al.[10] showed, while using a quartz spring balance for their experiments, that Henry's constant exhibited no change with the copolymer composition for ethylene/propylene or ethylene/1-butene copolymers.

Stern et al.[7] also suggested a correlation predicting the solute pressure ( $P_S$ ), when its deviation from Henry's law becomes significant (around 5% of deviation), due to the high plasticizing effect of penetrants. In this following equation,  $P_c$  is the critical pressure of the solute molecule:

$$\log\left(\frac{P_S}{P_c}\right) = 3.025 - 3.5\left(\frac{T_c}{T}\right) \quad (2.3)$$

As in this work we will be treating systems with several penetrants in PE, Henry's law seems to not be adequate for our case of study. In this context, several thermodynamic approaches with different degrees of complexity are developed in the open literature, in order to predict the phase equilibria and the partitioning of a polymerization mixture. Other than molecular simulation (i.e. Monte Carlo methods) and activity coefficient relations (e.g. Flory Huggins approach, etc.), there are two major categories of equations of state which have been used extensively in the polymer industry:[11] (a) perturbation theory models, such as the perturbed-chain statistical associating fluid theory (PC-SAFT), which is its most recent version and is widely applied in polymer industry;[12],[13] and (b) lattice theory model, such as the Sanchez-Lacombe equation of state (SL EoS) which is its most extensively used version.[14] The equations of state are preferred to present the phase diagrams of solvent-polymer systems,[15, p. 2] thanks to their high capability in capturing the dependency of phase volume on pressure, which is crucial for estimating the swelling degree of the polymer during the polymerization process, as well as other important thermodynamic properties (e.g. the density, the heat capacity, etc.).[16]

In this work, Henry's law[17] is adequate to evaluate the sorption of hydrogen in the amorphous phase of the polymer for the different studied systems., The hydrogen concentration in the polymer can be calculated as follows:

$$[H_2^p] = [H_2^{p,am}] = S_{H_2} \frac{\rho_{p,am}}{M_{w,H_2}} \quad (2.4)$$

with  $S_{H_2}=10^{-9}P_{H_2}$  in g  $H_2$  per g of amorphous polymer,  $\rho_{p,am}$  is the amorphous polymer density,  $M_{w,H_2}$  the hydrogen molecular weight,  $x_i$  the polymer crystallinity (calculated in section 6), and  $P_{H_2}$  its pressure.

## 2.2. Thermodynamic equations of state

There are two major classes of thermodynamic equations of state widely used in the polymer industry due to their excellent predictive capability. First, The Perturbed Chain SAFT (PC-SAFT) equation of state was derived from the Statistical Associating Fluid Theory (SAFT) for chain mixtures. In the structure of PC-SAFT, it is assumed that molecules can be represented by chains of spherical segments freely jointed and presenting attractive forces between them.[13] In **1989**, Chapman et al.[18] described for the first time the development of the SAFT equation of state based on Wertheim's perturbation theory of first order. This was the precursor of many other research studies, improving the SAFT EoS, including the modification proposed by Huang and Radosz (**1990-1991**)[12], [19], which is the most successful version of SAFT. It was obtained by extending the structure to mixtures of different types of molecules (small, large), at whether high or low pressures, and using rigorous parameters and association terms. Among the several modifications made on SAFT over the years, the PC-SAFT remains the most widely applied model of this family, which was particularly focused on the systems with polymeric components.[13], [20] Besides, the PC-SAFT indicates a higher predictive capability in describing the pure-component behavior compared to the SAFT. The robustness of this equation of state was tested by significantly describing the phase diagrams in polymer-solvent systems, which is particularly important in the polyolefin sector, namely for solution and slurry polymerization processes.[20]–[23] For gas phase systems, the PC-SAFT was also adapted to predict the solubility of not only a single solute but two different species (e.g. 1-hexene and ethylene) in LLDPE.[24] The discussion of the developmental details concerning the equations of the PC-SAFT model is outside the scope of this thesis. Such information about this perturbation theory-based model and its different versions can be found in References[1], [25] as well as the relevant thesis of Chmelar [27].

Second, The SL EoS[28]–[30], like other lattice models, considers molecules to have one or several segments, and the partition can be calculated by counting the number of different possible

configurations when these segments are filled in hypothetical cells, which seems like crystal lattice of a solid. The SL EoS assumes compressible networks.[28]–[30] Moreover, the penetrant molecules are assumed to incorporate randomly the polymer chains. These latter are considered as interacting beads inside each lattice, like in Flory-Huggins model.[31], [32] In this context, the SL EoS can be considered basically as an improved version of Flory-Huggins model. The major improvement here consists of the presence of empty sites or holes in the lattice, which allows the variation in compressibility and so both the volume and density change. [28]–[30]

SL EoS has been used frequently to study the phase diagrams of polymer-solvent systems,[15], [32] and also to predict the thermodynamic behavior in binary and ternary systems (polymer plus one or two penetrants respectively).[3], [13] As one of the most widely applied thermodynamic models in polymer industry, the SL EoS has been used for several years to solve different research problems.[15], [33]–[37] On the other side, the SAFT family of models remains somewhat complex algebraically.[38] They are mostly recommended for ethylene homopolymerization systems especially at high temperature, as they have superior predictive capability of the ethylene solubility in HDPE, compared to Sanchez-Lacombe equation of state.[11]

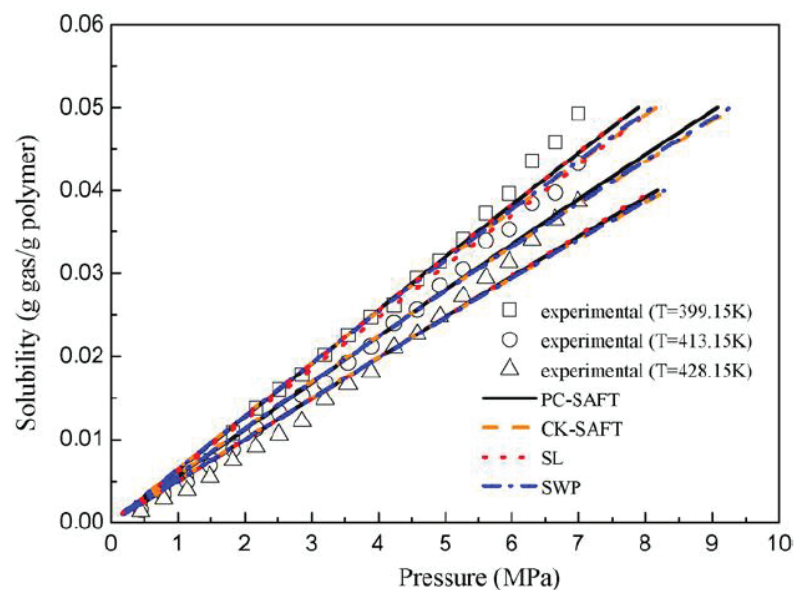


Figure 2.1 Solubility of ethylene in LDPE (binary system) (data from Cheng et al.[39]) [40]

Chen et al.[40] compared the capability of different equations of state in modelling the solubility of several subcritical and supercritical fluids using experimental data from the open literature. They found that both PC-SAFT and SL EoS provide pretty much the same satisfactory results for the case of the solubility of ethylene in LDPE based on the experimental data obtained from the relevant work of Cheng et al.[39] using a piezoelectric sorption device performing at high pressure up to 69 atm at different temperatures(see Figure 2.1). However, the authors mentioned that the results tend to be less satisfying for the case of sorption in semi-crystalline polymers when using PC-SAFT compared with SL EoS. Furthermore, according to Krallis et al.[11] SL EoS provides better prediction for monomers solubilities in polyolefin and so for ethylene copolymerization compared to PC-SAFT that shows poorer performance when the molecular size of comonomer increases. The SL EoS major advantage is its relative simplicity while keeping its excellent predictive capability for multicomponent systems. This could be the major reason why, in this study, the choice was made on SL EoS.

Following the original formulation of Sanchez and Lacombe, the SL EoS can be written as:

$$\bar{\rho}^2 + \bar{P} + \bar{T} \left[ \ln(1 - \bar{\rho}) + \left(1 - \frac{1}{r}\right) \bar{\rho} \right] = 0 \quad (2.5)$$

Where  $\bar{T} = T/T^*$ ,  $\bar{P} = P/P^*$ ,  $\bar{\rho} = \rho/\rho^* = 1/\bar{V} = V^*/V$  are the respective reduced temperature ( $T$ ), pressure ( $P$ ), density ( $\rho$ ) and volume ( $V$ ) of the pure components in the system, while  $T^*$ ,  $P^*$  and  $\rho^*$  represent their characteristic parameters. These characteristic parameters are needed in the model for the different penetrant species and the polymer in order to predict the solubility of each component in the amorphous polymer. The characteristic density,  $\rho^*$ , represents the mass density in the close-packed state, the characteristic pressure,  $P^*$ , represents the cohesive energy density in the close-packed state, and characteristic temperature,  $T^*$ , is linked to the depth of the potential

energy.[41] They can be evaluated experimentally by fitting the model with the available experimental  $PVT$  (pressure-volume-temperature) data, or estimated as did Kanellopoulos et al.[42] using a molecular dynamic simulation method. For each polymer chain, these parameters are defined as follows:[28].[43]

$$T^* = \varepsilon^*/R_g; P^* = \varepsilon^*/v^*; V^* = N(rv^*); \rho^* = M_w/(rv^*) \quad (2.6)$$

And

$$r = M_w P^* / R T^* \rho^* \quad (2.7)$$

where  $\varepsilon^*$  is the mer-mer interaction energy,  $v^*$ , is the closed packed molar volume of a mer (site),  $M_w$  is the molecular weight,  $N$  is number of molecules,  $r$  is the number of mers a molecule occupies in the lattice, and  $R$  is the universal gas constant. The parameters  $\varepsilon^*$ ,  $v^*$ , and  $r$  are the lattice variables on which depends the parameters  $T^*$ ,  $P^*$ , and  $\rho^*$ .

For a mixture of components such as in binary or higher order systems, combining rules have to be introduced in order to estimate the lattice properties of a mixture ( $\varepsilon^*_{\text{mix}}$ ,  $v^*_{\text{mix}}$ , and  $r_{\text{mix}}$ ) required by the equation of state. In this study, we chose to use the “van der Waals” mixing rule in the calculation of the different mixing parameters.

The characteristic closed-packed molar volume of one “mer” of the mixture is calculated, as follows:

$$v^*_{\text{mix}} = \sum_i \sum_j \phi_i \phi_j v^*_{ij} \quad (2.8)$$

In which;

$$v^*_{ij} = v^*_{ii} + v^*_{jj}(1 - n_{ij})/2 \quad (2.9)$$

Where  $n_{ij}$  refers to the correction of the arithmetic mean deviation and subscripts  $i$  and  $j$  represent the components in the system. In the remaining discussion, we shall assume  $n_{ij}$  to be equal to zero, as agreed for Sanchez-Lacombe model. In addition, the closed-packed volume fraction,  $\phi_i$  or  $\phi_j$  depending on the component used at incompressible state, is defined as:

$$\phi_i = \frac{\omega_i}{\rho_i^* v_i^*} / \sum_j \left( \frac{\omega_j}{\rho_j^* v_j^*} \right) \quad (2.10)$$

In which  $\omega_i$  and  $\omega_j$  represent the mass fraction of the component  $i$  and  $j$ , respectively.

Likewise, the “van der Waals” mixing rule on the characteristic interaction energy for the mixture is expressed as:

$$\varepsilon_{\text{mix}}^* = \frac{1}{v_{\text{mix}}^*} \sum_i \sum_j \phi_i \phi_j \varepsilon_{ij}^* v_{ij}^* \quad (2.11)$$

In which:

$$\varepsilon_{ij}^* = (\varepsilon_{ii}^* \varepsilon_{jj}^*)^{0.5} (1 - k_{ij}) \quad (2.12)$$

Where  $\varepsilon_{ii}^*$  and  $\varepsilon_{jj}^*$  represent the characteristic interaction energies between mers of components  $i$  and  $j$ , and  $k_{ij}$  is the binary interaction parameter between components  $i$  and  $j$  to be adjusted while fitting the model with the mixture experimental solubility data. It is the only binary interaction parameter used when applying the Sanchez-Lacombe model. However,  $n_{ij}$  will be assumed to as equal to zero for all the related calculations in this work. In the remaining discussion and for the different studied systems, we assume that the interaction between molecules of olefins and/or ICA are ideal.[44] Thus, in a quaternary system (the highest order systems to be treated in this study),

of three penetrating gaseous species, ethylene (1), ICA (2) and comonomer (3), in the polymer (4),  $k_{12}$ ,  $k_{13}$  and  $k_{23}$  are equal to zero.

Following the same route of computation,  $r_{\text{mix}}$  which denotes the number of mers occupied by a molecule of the mixture, is defined as:

$$\frac{1}{r_{\text{mix}}} = \sum_j \frac{\phi_j}{r_j} \quad (2.13)$$

in which  $r_j$  denotes the number of mers occupied by component  $j$  in the lattice.

Finally, the chemical potential of component  $i$  in a multicomponent system that is required to calculate the sorption equilibrium for polymer-solvent system, can be expressed as following in the SL EoS model:[45]

$$\begin{aligned} \mu_i = R_g T \left[ \ln \phi_i + \left( 1 - \frac{r_i}{r} \right) \right] + r_i \left\{ -\bar{\rho} \left[ \frac{2}{v^*} (\sum_j \phi_j v_{ij}^* \varepsilon_{ij}^* - \varepsilon^* \sum_j \phi_j v_{ij}^*) + \varepsilon^* \right] + \right. \\ \left. \frac{R_g T}{\bar{\rho}} \left[ (1 - \bar{\rho}) \ln(1 - \bar{\rho}) + \frac{\bar{\rho}}{r_i} \ln \bar{\rho} \right] + \frac{P}{\bar{\rho}} (2 \sum_j \phi_j v_{ij}^* - v^*) \right\} \end{aligned} \quad (2.14)$$

For the sake of accuracy, one should make the difference between two confusing terms “component” and “phase”. As a simple example to outline the difference, let’s consider a ternary system constituted of two phases; a polymer “phase” in equilibrium with a “gas” phase. The “gas” phase is constituted of two different volatiles “components” or solutes; while the “polymer” phase is gathering both the polymer and the sorbed “components”.

Unless indicated otherwise, in the remaining discussion, we shall use the following notations: to denote the phase of property, the superscript is used; while the subscript is used to refer to the component in that specific phase like for the chemical potential  $\mu_i^{\text{pol}}$  (i.e., calculating the potential chemical related to the  $i^{\text{th}}$  component in the polymer phase). More information about SL EoS can be found in **Appendix A** and in the relevant thesis of Alizadeh[5].

It should be noted that this thermodynamic model is only adapted to describe the sorption and the effect of inert condensing agents at the equilibrium state, without considering the diffusion of species phenomenon; i.e. concentration gradients from the particle's surface until its core and the mass transfer resistance inside the polymer particle during the polymerization. Thus, in this project we will assume equilibrium conditions, for simplification. In other words, the diffusion of gas species into the polymer is assumed to be fast. Of course, this is not the reality, but considering the diffusion phenomenon requires a particle model, which would lead to an increase in the number of unknown parameters, model complexity and an increase in the computation time. Extending the model to a more realistic state can be made by using a single particle model like Polymer Flow Model[5] as well as an experimental study, which is not the subject of this work. Another important assumption on which the thermodynamic model is based is that, only the global degree of crystallinity of the polymer is accounted for in the thermodynamic model. Strictly speaking, also tie molecules linking the crystalline lamellae can influence the solubility of different species in the amorphous phase.[46]

### 3. Binary Systems

As a first step, we consider the identification of the optimal  $k_{ij}$  required by the SL EoS model to represent the behavior of a binary system. Generally, reliable binary sorption experimental data of gas solute species, like ethylene in PE, are available in the literature.[5] This facilitates the estimation of the  $k_{ij}$ .

Chen [47] throughout his PhD thesis, used the Heuer-Schotte equation of state to predict the solubility of sorbed hydrocarbon vapors in the amorphous phase of polyethylene. Sarti and Doghieri[48] showed a satisfactory adequacy between the predicted solubilities of CO<sub>2</sub>, N<sub>2</sub>, CH<sub>4</sub> and C<sub>2</sub>H<sub>4</sub> in polycarbonate and polystyrene as polymer matrixes with experimentally available set of data of sorption. For the data prediction, they used their no equilibrium lattice fluid (NELF)

model [49] that is based on the Sanchez-Lacombe equation of state. In a later publication,[50] they used the same model to estimate the solubility of several gas species in glassy polymers for a variety pressure phase behavior of industrially relevant systems of ethylene/PE and 1-butene/polybutene. They showed the importance of the temperature-dependent binary interaction parameters for obtaining satisfactory results. Orbey et al.[51] also insisted on the SL EoS need for relevant binary interaction parameters of each pair of pure components, in order to get an accurate representation of the VLE (vapor liquid equilibrium) behavior of binary ethylene/low density PE systems. In their study, the binary interaction parameters were obtained by fitting the VLE data, using the Polymers Plus simulation software. Kiparissides et al.[52] employed the SL EoS to derive the equilibrium concentration of ethylene in amorphous PE at elevated pressures and temperatures, which showed a good agreement with experimental solubility measurements.

### 3.1. Parameters impacting the $k_{ij}$

The binary interaction parameters  $k_{ij}$  were observed in literature to be temperature-dependent.[14] Indeed, these parameters show a slight exponential decrease with the temperature as shown by Kanellopoulos et al.[42], for ethylene/LLDPE binary system. (see Figure 2.2- a) However, Figure 2.2- b) shows that a linear approximation can fit the change in the  $k_{i,j}$  for the binary system (1-hexene/LLDPE) with the temperature. Touloupides et al.[53] indicated that the presence of the comonomer (e.g. 1-hexene) in the polymer is the reason behind the strong dependence of the binary interaction parameters on the temperature.

The interaction parameters depend also on the type of the polymer grade, for instance the interaction of ethylene with the copolymer LLDPE-1-hexene is slightly different to that with the copolymer LLDPE-1-butene.[42] Likewise, the presence of comonomer in copolymer chains leads to different properties than a pure HDPE.[42]

Finally, the figure shows that the value of  $k_{ij}$  is close to zero at high temperature such as for  $T > 65^\circ\text{C}$ , so the mixture tends to behave like an ideal mixture, with no deviation from Lorentz-Berthelot combining rules. The decrease with temperature becomes slightly less pronounced at higher polymerization temperature, as shown in Figure 2.2- a).

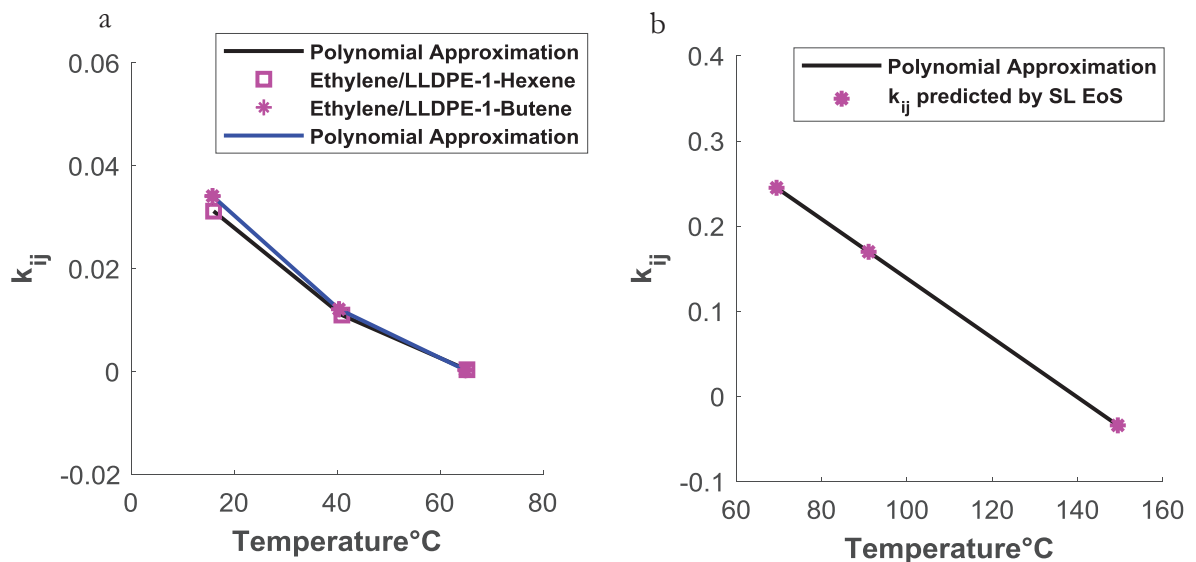


Figure 2.2 The binary interaction parameter is a temperature dependent parameter in: a) ethylene/LLDPE binary systems, adapted from Kanellopoulos et al.[42], and b) 1-Hexene/LLDPE, adapted from Touloupides et al.[53]

The software Plot Digitizer was employed to extract the experimental data from the figures in the literature as a function of their respective pressure in the gas phase, and readings were repeated twice. This data was used for the prediction of the binary interaction parameters,  $k_{ij}$ .

The model, while developed on a specific range of experimental thermodynamic data, is useful to predict the solubility on a wider range. In this context Kirby and McHugh[54] mentioned that the equation of state “*can be used to correlate data and with caution they can be used to simulate other experimental conditions not explicitly measured*”. But, as appears from the literature review, the interaction parameters depend on temperature, and therefore correlations with temperature are required. The identified values are also valid only over the range of pressure over which they were identified. Finally, they depend on the polymer type and properties.

## 3.2. Application of the SL EoS

The calculation of the sorption equilibrium of the polymer can be done by solving the chemical potential of the gas component in the polymer using equation (2.14). This equation is solved simultaneously with the Sanchez-Lacombe EoS (2.5) in order to obtain the reduced density of the polymer,  $\bar{\rho}^{\text{pol}}$  and the closed-packed volume fraction of solute molecules in the polymer,  $\phi_1^{\text{pol}}$ . When it is necessary to identify the interaction parameters, we used Matlab® global optimization Toolbox's Multistart solver combined with fmincon/least square nonlinear solver (lsqnonlin) function, to make sure we get the global solution.

In SL EoS, care must be taken when choosing the characteristic parameters ( $T^*$ ,  $P^*$  and  $\rho^*$ ) used for the pure components, as different sets of these parameters appear in the literature, as shown by Table 2-1, taken from two different references[33], [52] for the same system, ethylene (the penetrating monomer) in LLDPE.[55] Bashir and co-workers,[41] investigated the effect of the pure component characteristic parameter on the SL EoS predictive capabilities and found that the sensitivity of the model is more affected by changes of the characteristic parameters of the monomer, compared with the characteristic parameters of the polymer. Moreover, the characteristic temperature of the monomer has a higher significant effect than its characteristic density.

Figure 2.3 shows the solubility predictions with the SL EoS for the experimental data of J. Moore and E. Wanke of ethylene (the penetrating monomer) in LLDPE at 27.6°C.[56] The sorption of ethylene in LDPE was modeled by Henry's law (equation (2.2)). The results show that Henry's law can satisfactorily describe the solubility and pressure of ethylene dependency in a binary system. This is an expected result, since Henry's law is generally applicable for the evaluation of single solute sorption in polymer, and especially at a low temperature and a pressure up to 40 bars, which is the case of the system treated in this paragraph.

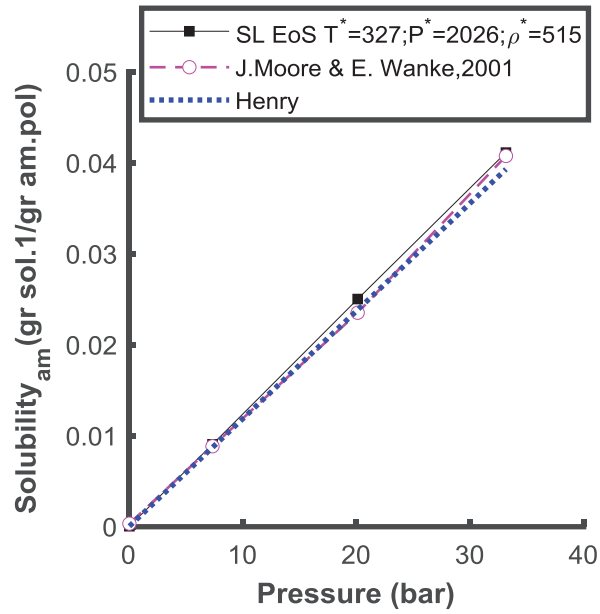


Figure 2.3. Comparing SL EoS solubility predictions in ethylene/LDPE binary system at 27.6°C from J. Moore and E. Wanke [56] and Henry's law, using characteristic parameters of Ethylene from Koak et al.[33] and estimated  $k_{ij} = 0.005$

Figure 2.4 shows the simulation of the SL EoS model for two binary systems (1-butene/HDPE)[56] and (iso-butane/HDPE)[57] with identification of  $k_{ij}$ . A good agreement of the model with the experimental data can be observed thanks to the global optimization and the binary interaction parameter best fitting.

Table 2-1. Characteristic parameters used for the binary system (Ethylene/LDPE)

Component	$T^*(K)$	$P^*(bar)$	$\rho^*(bar)$	Ref
Ethylene	327	2026	515	[33]
Ethylene	294	3396	682	[52]
LDPE	887	3543	887	[58]

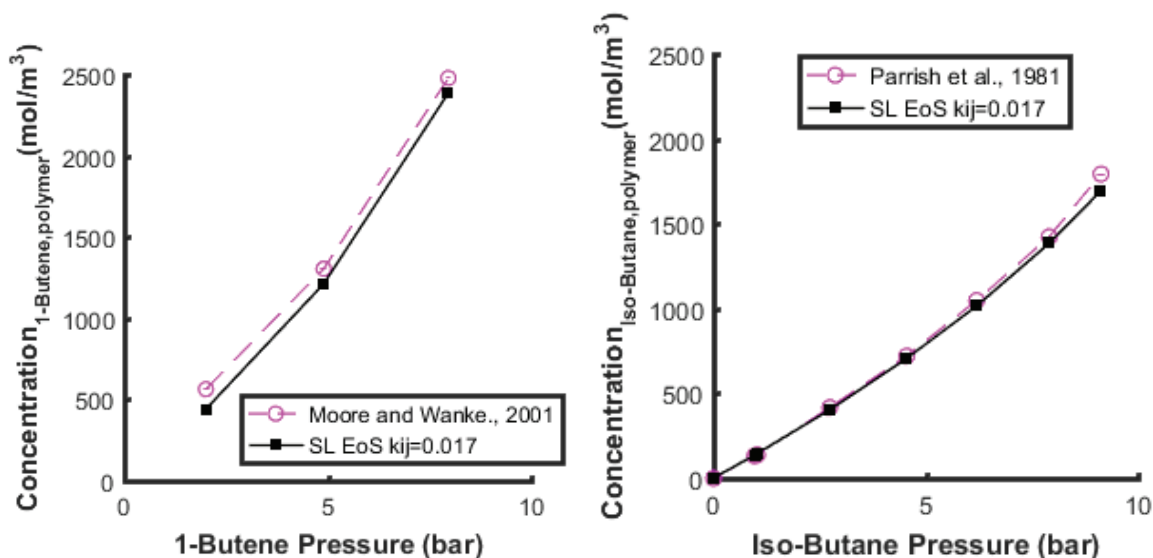


Figure 2.4. SL EoS and compared to experimental binary solubility data in HDPE of a) comonomer 1-butene at 68.9°C, and b) ICA iso-butane at 65.6°C.

## 4. Ternary Systems

The SL EoS was first extended from a binary to a ternary system by Bashir et al.[44], who validated its high capability in estimating the co-solubility phenomenon for the different systems that they analyzed.

Experimental solubility data for multicomponent systems (ternary or more) are scarce in the open literature. In order to remedy to the lack of data, Alves et al.,[59] for instance, recently used the binary experimental solubility data of (ethylene/LLDPE)[24] and (iso-butane/LLDPE)[57] to estimate the concentrations of the different penetrating species to simulate the ternary system (ethylene (1)/ iso-butane (2)/ LLDPE (3)). But, the interactions (co-solubility and anti-solubility effects) between the different species usually do not allow to use binary parameters in a ternary system and vice versa.

Among experimental ternary sorption data present in the open literature we may cite[24], [42], [56], [60]–[66]. Among these studies, the experimental data provided by the group of Yang using the

pressure decay method [60] were used by Alizadeh[5] to explore the effect of n-hexane on the concentration of ethylene in the amorphous phase of LLDPE.

Yao et al,[60] studied the effect of the partial pressure of different alkanes (i.e. n-hexane, iso-butane and iso-pentane) on the ternary system ethylene, alkane (ICA) and PE. They found that solubility of ethylene is higher in a ternary system than in a binary system. Likewise, the solubility of ethylene increases in presence of a comonomer in a ternary system.[17], [24], [67] Chmelar et al.[62] measured the sorption of ethylene and 1-hexene in PE and showed the co-solvent effect of 1-hexene on ethylene and the anti-solvent effect of ethylene, which consists of a decrease of the solubility of 1-hexene. The co-solubility effect due to the presence of ICA in a ternary gas-phase system has been extensively studied in the C2P2 research group.[68], [69] Alizadeh et al. [68] showed an important increase of the rate of polymerization when adding an ICA to the system, due to the co-solubility effect.

#### 4.1. Procedure of identification of kij parameters

In the following, the components (1) and (2) refer to the solute species and (3) represent the polymer. The characteristic temperature  $T^*$ , characteristic pressure  $P^*$  and characteristic density  $\rho^*$  of the different solute species and the polymer required by the SL EoS for the different systems studied in this work are given in Table 2-2.

Table 2-2. Characteristic parameters of pure components required by the SL EoS in the different ternary and pseudo-quaternary systems

Component	$T^*$ (K)	$P^*$ (bar)	$\rho^*$ (kg m <sup>-3</sup> )	Ref
Ethylene	283	3395	680	[42]
n-hexane	476	2979.1	775	[28]
LLDPE				[42]
(LLDPE-1-hexene)	653	4360	903	
1-butene	410	3350	770	[11]
1-hexene	450	3252	814	[41]
LLDPE-1-butene	667	4370	900	[42]

For the prediction of  $k_{ij}$ , the model is solved using the same methodology used for binary systems and the predictions are compared to the experimental data until getting more accurate estimations according to the procedure illustrated schematically in Figure 2.5.

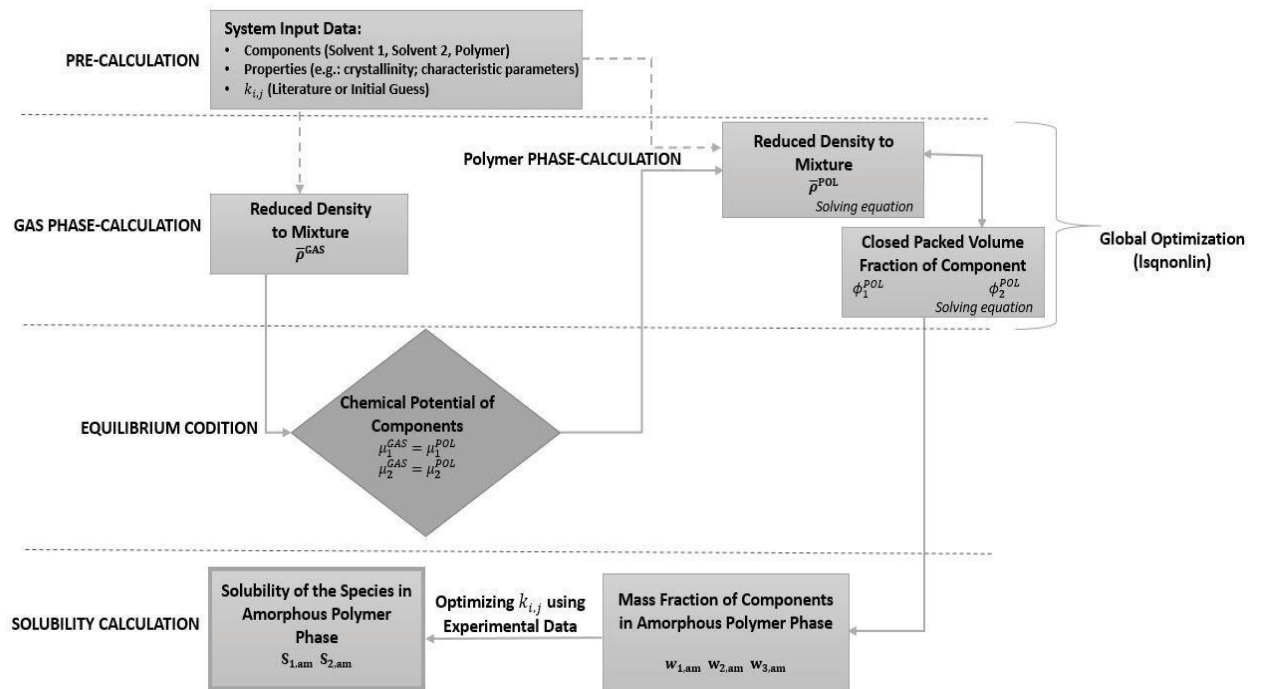


Figure 2.5. Schematic representation of the subroutines of the thermodynamic model to evaluate the solubility of solutes in a ternary system.

## 4.2. $k_{ij}$ of the ternary system ethylene/n-hexane/LLDPE

The ternary system ethylene (1)/n-hexane (2)/LLDPE (3) was experimentally investigated and its ternary data are available in the work of the group of Yang.[60] Therefore, the  $k_{ij}$  parameters can be estimated for this ternary system, as done by Alizadeh et al.[70]. The interaction between the small species, ethylene/n-hexane, is assumed ideal, therefore  $k_{12} = 0$ ,

Figure 2.6 and Figure 2.7 show the predictions by the SL EoS of the concentrations of ethylene in the amorphous polymer phase at 80°C and 90°C, chosen from the set of experimental data of the ternary system ethylene/n-hexane/LLDPE presented by Yao et al.,[60], as they match with the temperature range usually used for an industrial PE polymerization reactor.[71] The figures show a good agreement of the model with the experimental data at both temperatures. This is not the case of Henry's law model, which does not give an accurate representation of the experimental data, as expected since we have a multicomponent system. A clear co-solubility effect of n-hexane on ethylene can be observed, as we notice an increased ethylene solubility in the amorphous polymer phase when the pressure of ICA increases. In the other side, and since the sorption measurements are performed at a constant gas phase pressure of (ethylene+n-hexane), the higher the partial pressure of ethylene, in turn, results in a slighter decrease of ethylene solubility due to the decrease of the partial pressure of n-hexane. Also, we notice that increasing temperature decreases the sorption of both gases.

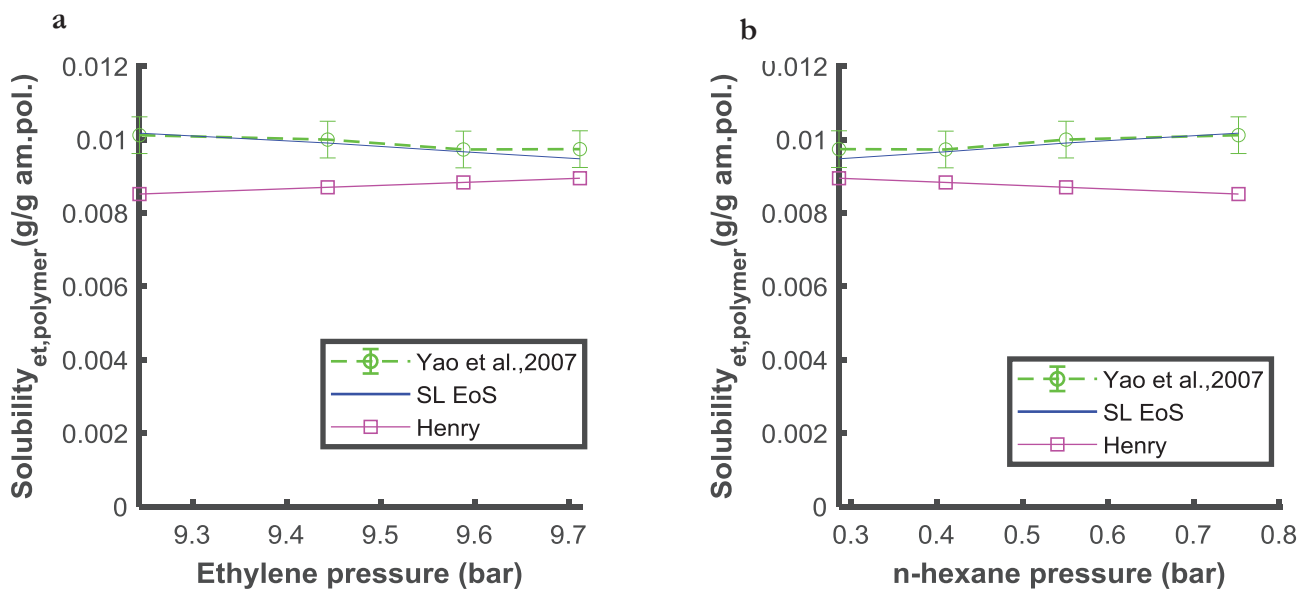


Figure 2.6. Application of the SL EoS in the ternary system ethylene/n-hexane/LLDPE at 80°C a) Solubility of ethylene obtained from fitted SL EoS, and b) Effect of n-hexane on the solubility of ethylene in the amorphous phase of the polymer.

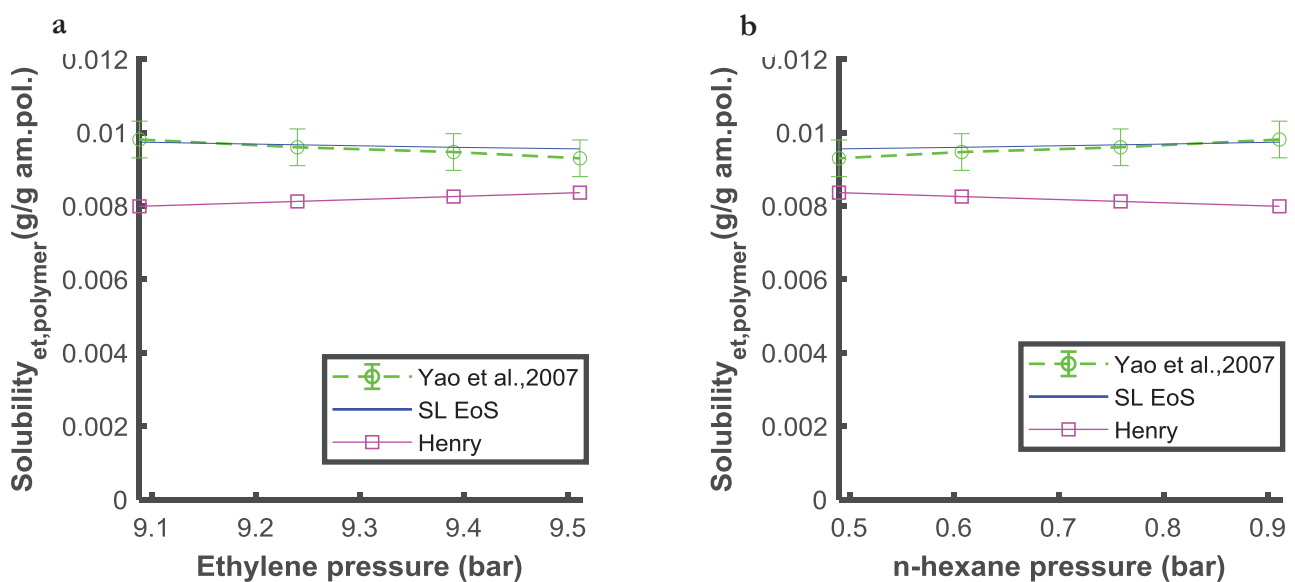


Figure 2.7. Application of the SL EoS in the ternary system ethylene/n-hexane/LLDPE at 90°C a) Solubility of ethylene obtained from fitted SL EoS, and b) Effect of n-hexane on the solubility of ethylene in the amorphous phase of the polymer.

### 4.3. $k_{ij}$ of the ternary system ethylene/1-butene/LLDPE

In this ternary system, ethylene is used as monomer (component 1), 1-butene as comonomer (2) and LLDPE (3) is the polymer. Again, the interaction between small molecules is assumed to be ideal, so  $k_{12}=0$ . The other parameters, i.e. the interaction parameter of ethylene with polymer,  $k_{13}$ , and 1-butene with polymer,  $k_{23}$ , need to be identified based on ternary data, as it is not possible to use binary data due to the co-solubility (i.e. the presence of 1-butene increases the solubility of ethylene compared to a binary system) and anti-solvent effects (i.e. the presence of ethylene reduces the solubility of 1-butene). Ternary data for this system are available at 70°C within a total pressure of monomer plus comonomer in the range of 2.5-4 bar, for which the interaction parameters  $k_{ij}$  were identified (Table 2-3).[72] It is required to extrapolate these parameters to 90°C and to a wider range of pressure. For this extension, few assumptions were made, but the estimations can be improved once ternary data become available at 90°C and under the real operating pressure. First of all,  $k_{ij}$  are assumed to vary linearly with the temperature, as discussed in the section of binary systems.[53][42] Binary data of 1-butene in LLDPE-1-butene are available at different temperatures between 30-88°C over the pressure range of 0-15 bar.[73] From this binary data, the slope of variation of the binary interaction parameters with temperature can be determined and employed in the ternary system.[74] Using the identified  $k_{ij}$  parameters within SL EoS, the solubility can be estimated at 70 and 90°C and over a wider monomer and comonomer pressure ranges ( $P_1=7$  bar,  $P_2=1.55-10$  bar).

Table 2-3. Binary interaction parameters of the ternary system ethylene/1-butene/LLDPE, P1=7bar, P2=0-10 bar ( $k_{12}=0$  ethylene/1-butene).

Temperature	Ethylene/LLDPE	1-butene/LLDPE
	$k_{13}$	$k_{23}$
70°C[72]	-0.09495	0.04618
90°C	-0.1089	0.0302
$T=[70-90]^{\circ}\text{C}$	$k_{13} = -6.98 \cdot 10^{-4} T(\text{K}) + 0.144$	$k_{23} = -7.99 \cdot 10^{-4} T(\text{K}) + 0.32$

Figure 2.8 shows the results of the SL EoS (as well as the linear correlations, identified in section 6) predicting the concentrations of ethylene and 1-butene in the amorphous polymer. A slight co-solubility effect of 1-butene on ethylene can be observed, while a more significant anti-solvent effect of ethylene on 1-butene appears when comparing to binary data in LLDPE-1-butene.

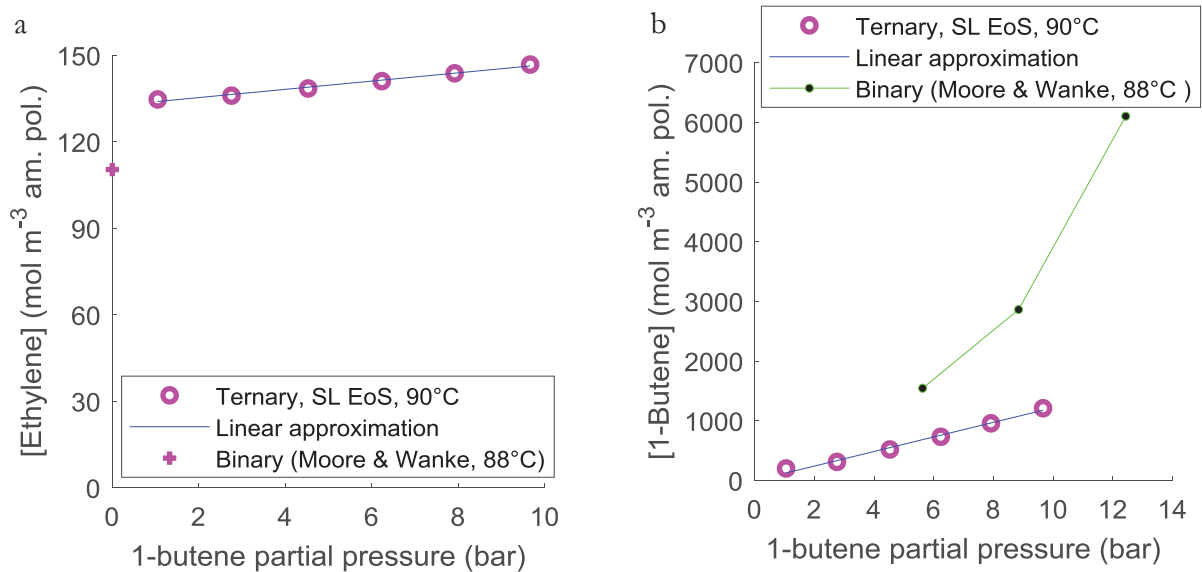


Figure 2.8. Estimated concentrations in LLDPE amorphous phase using SL EoS for the ternary system ethylene/1-butene/LLDPE, at 90°C and 7 bar of ethylene: a) ethylene and b) 1-butene.

Comparison with binary data.[73]

#### 4.4. $k_{ij}$ of the Ternary System ethylene/1-hexene/LLDPE

The ternary system here consists of the monomer ethylene, comonomer 1-hexene and polymer LLDPE. As there are no available thermodynamic data for this system, it is assumed that 1-hexene behaves like n-hexane for which solubility data are available (Yao et al.[60]), as suggested by Alizadeh et al.[5] This approximation is reasonable as 1-hexene and n-hexane have similar binary solubility data in PE and they are comparable in structure. Therefore, the available ternary solubility data for the system ethylene/n-hexane/LLDPE[60] are used to estimate the  $k_{ij}$  for the current system (see Table 2-4).[5] The identified parameters are valid for a comonomer pressure range of 0-1 bar and 10 bar ethylene. It is to be noted that 1-hexene has a much higher solubility in the polymer than 1-butene.[73]

Table 2-4. Binary interaction parameters of the ternary system ethylene/1-hexene/LLDPE (based on assumptions and optimization), P1=10 bar, P2=0-1 bar ( $k_{12}=0$  Ethylene/1-hexene).

Temperature	Ethylene/LLDPE	1-hexene/LLDPE
	$k_{13}$ [5]	$k_{23}$
80°C	-0.022	0.0145
90°C	-0.032	0.021
$T=[80-90]^{\circ}\text{C}$	$k_{13} = -10^{-3} T(\text{K}) + 0.331$	$k_{23} = -6 \cdot 10^{-4} T(\text{K}) - 0.2149$

### 5. Pseudo-quaternary systems

A simple examination of the recent patent literature of PE gas phase reactors clearly shows that the vapor phase can contain numerous condensable species (up to even 8 species),[75] thus creating a serious complexity in modelling the sorption. Therefore, in the absence of a reliable data set, in this section, we will propose a simplified model accounting for 3 penetrants (i.e. quaternary system) in an LLDPE plant. Two systems are considered, at 90°C, which are frequently employed in industry, as mentioned earlier:

1. Copolymerization of ethylene and 1-hexene in presence of n-hexane as ICA
2. Copolymerization of ethylene and 1-butene in presence of iso-butane as ICA

Due to the lack of solubility data, the quaternary system is approximated by a ternary system: ethylene/ (ICA+comonomer)/ LLDPE, as suggested by Alves et al.[59] (*Additive effect*). Thus, a “pseudo component”, representing the mixture of ICA plus comonomer, is defined for which the thermodynamic parameters are identified. In this assumption, no interaction between ICA and comonomer is considered, which means that these species behave independently from each other as if they were present in a ternary system (PE, ethylene and either ICA or comonomer). This is not unreasonable if the comonomer and ICA are similar in structure. This assumption is thus applicable for the two systems studied in this work, i.e the comonomer 1-hexene and n-hexane as ICA, as well as the comonomer 1-butene and iso-butane as ICA. In addition, it has been shown that comonomers and alkanes swell the polyethylene the same way,[76] which would give the same co-solubility effects, and therefore the same productivities. However, this assumption does not mean that the ICA and the comonomer have the same solubility or co-solubility effect, as discussed in the following two sections.

## 5.1. Polyethylene in presence of ethylene, 1-hexene and n-hexane

For the first system, the comonomer 1-hexene and the ICA n-hexane, both the comonomer and the ICA were found to have comparable solubilities in a binary system, especially at low pressure, as shown by Figure 2.10 (Yao et al.[60] and Jin et al.[77]). Therefore, Alizadeh et al.[5] assumed it safe to consider that they have similar solubility in LLDPE in a ternary or quaternary system. A similar observation was found for other 3 and 6 carbon pairs, such as the isomers propene and propane, where the difference in their solubility constant of Henry's law was 10 % at 25 °C, as reported by Michaels et al.[3] This can be explained by the fact that 1-hexene and n-hexane have

similar shapes and same number of carbons, so almost the same size, therefore, they have similar tendency to condense (i.e., same volatility). Besides, they have similar nature of interaction with LLDPE segments (i.e., same nature of van der Waals forces).[5] Therefore, in a quaternary system, the ratio of solubility of 1-hexene in LLDPE to n-hexane is assumed  $r = \frac{S_{1\text{-hexene}}}{S_{\text{n-hexane}}} = 1$ .

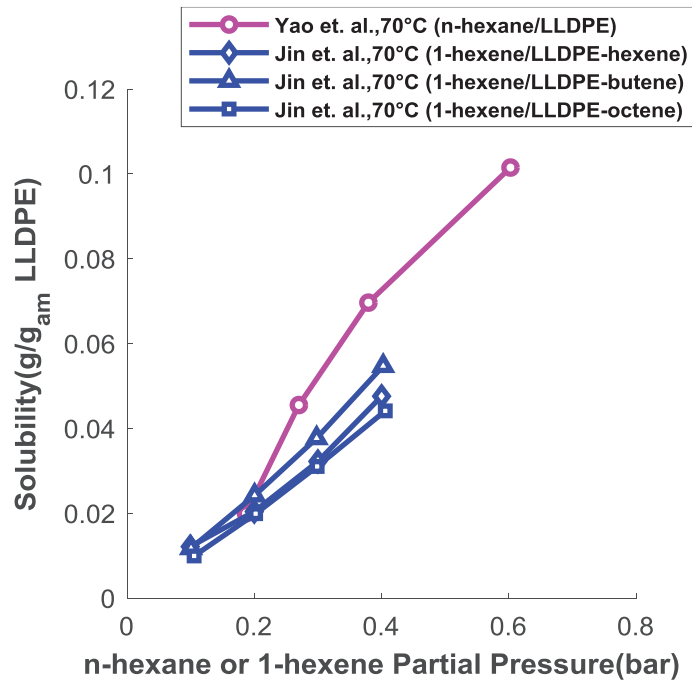


Figure 2.10. Solubility of n-hexane and 1-hexene in LLDPE (binary systems) at 70°C (data from Yao et al.[63] and Jin et al. [77])

Based on this approximation and using the solubility data available for the ternary system ethylene/n-hexane/PE at 10 bar ethylene[63] (Figure 2.11), the *Additive effect* assumption[5] is applied to predict data in a quaternary system. Note that when increasing temperature (Figure 2.11; Table 2-7), the sorption is decreased, and the slope of the concentration of n-hexane with its partial pressure decreases (from  $C \sim 624$  to  $506 \text{ mol m}^{-3} \text{ bar}^{-2}$ ), while the slope of the concentration of ethylene increases (from  $A \sim 26$  to  $34 \text{ mol m}^{-3} \text{ bar}^{-1}$ ). Increasing the temperature thus increases slightly the impact of ICA on ethylene absorption, but it remains very low. Besides, the figure shows that the concentration of n-hexane in amorphous PE increases only slightly in a binary

system compared to a ternary system, due to the anti-solvent effect of ethylene on ICA in a ternary system.[24], [69] Note that the concentration plots were calculated by converting solubility data found in the open literature (in  $\text{g g}^{-1}$  amorphous polymer) into  $\text{mol m}^{-3}$  using the amorphous polymer densities (i.e., the values of the swollen polymer density with different ICAs) estimated by SL EoS.

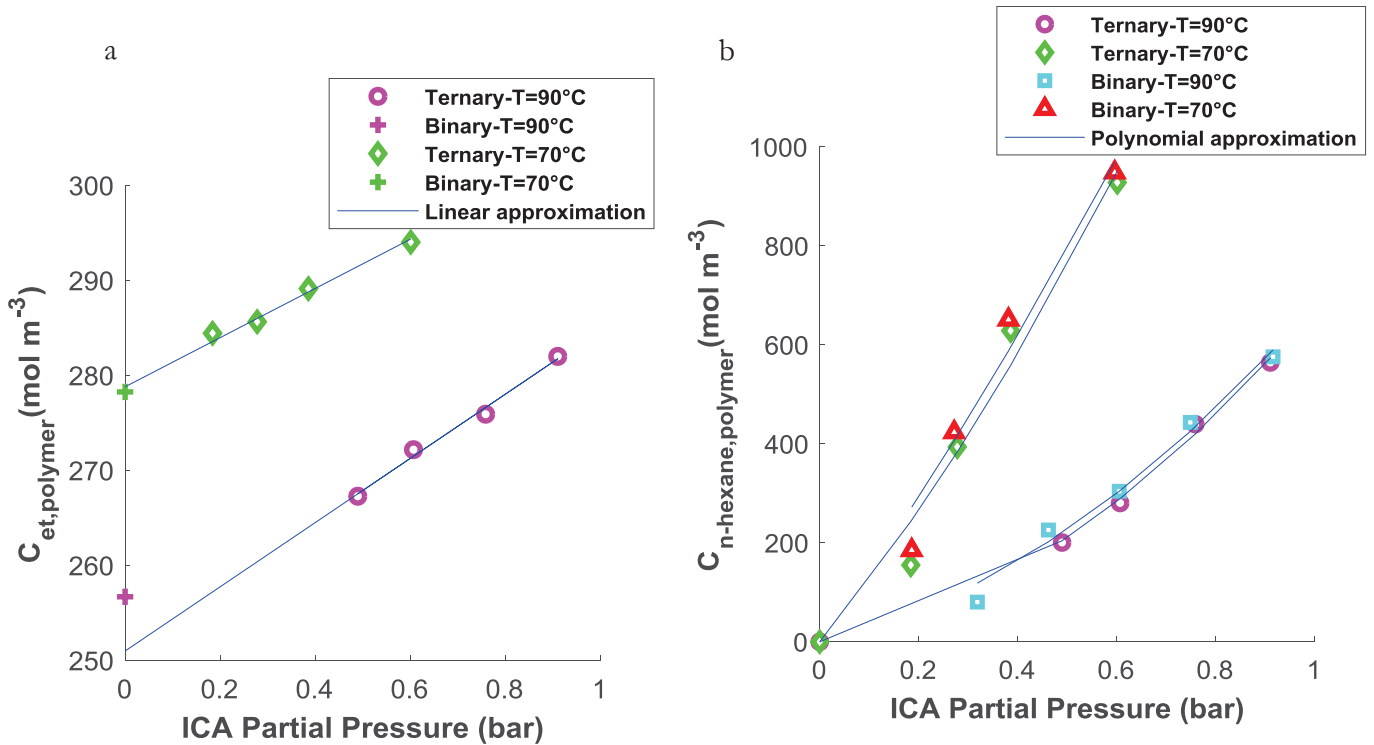


Figure 2.11. Ternary solubility data ethylene/n-hexane/LLDPE at 90°C and 70°C at 10 bar of ethylene (experimental data are taken for ternary systems from Yao et al.[60] and for binary systems from Yao et al.[63]): a) Concentration of ethylene in amorphous LLDPE as a function of the partial pressure of n-hexane, b) Concentration of n-hexane as a function of its partial pressure.

## 5.2. Polyethylene in presence of ethylene, 1-butene and the iso-butane

For the copolymerization of ethylene with 1-butene in presence of iso-butane as ICA, ternary data are not available for either ethylene/iso-butane/LLDPE or for ethylene/1-butene/LLDPE.

Moreover, the available binary sorption data (Figure 2.4)[56], [57] indicates that 1-butene and iso-butane have different solubilities in the polymer and cannot be assumed to be similar, as could be done for 1-butene/n-butane and 1-hexene/n-hexane. Indeed, the solubility of 1-butene in HDPE is higher than that of iso-butane by almost a factor of  $r = \frac{S_{1\text{-butene}}}{S_{\text{iso-butane}}} = 1.78$ , at nearly the same temperature.

Due to this lack of data, the following assumptions are made only for this system:

- The ratio of sorption of 1-butene to iso-butane,  $r$  (Figure 2.4), identified in a binary system, was assumed to remain unchanged in a ternary system, and to remain unchanged within a temperature range of 65-90 °C. This means that they are assumed to have the same co-solubility effect on ethylene.
- The  $k_{ij}$  parameters are assumed to vary linearly with temperature. So, as solubility data are not available, an extrapolation of  $k_{ij}$  is done to predict them at 90°C.
- The solubility of iso-butane in the amorphous fractions of HDPE and LLDPE is assumed to be the same, as only solubility data in HDPE are available (in a binary system)[57]. Of course, we are aware that in the amorphous phase of HDPE and LLDPE will be slightly different, but actually we have no means of correcting for this.

Again, the *Additive effect* assumption is also applied to this system: The comonomer and ICA were assumed to have an additive effect in a quaternary system. Alves et al.[56] validated this assumption for propane and iso-butane based on reaction data from patents. This means that propane and iso-butane do not affect the solubility of each other (i.e. there is no co-solubility effect), which is reasonable in view of their similarities. A similar assumption can be done regarding 1-butene and iso-butane in our system. Based on this assumption, Alves et al.[59] estimated the binary interaction parameters  $k_{ij}$  for the ternary system ethylene/iso-butane/LLDPE by fitting to experimental solubility data of the binary systems ethylene/LLDPE and iso-butane/HDPE at 70°C (Table 2-5).[57] In order to identify the parameters of the equations used to calculate the concentrations in

the pseudo-quaternary system, SL EOS is first used in the ternary system ethylene/iso-butane/LLDPE (with  $k_{ij}$  identified using binary solubility data[56]) to identify the solubility of ethylene and iso-butane at different pressures of iso-butane. Then, the  $k_{ij}$  parameters were extrapolated over temperature to have values at 90°C (Figure 2.12, Table 2-5). The concentration of 1-butene is then calculated using  $S_{1\text{-butene}} = r S_{\text{iso-butane}}$ . From the obtained data points, polynomials of order 1 were identified for both ternary systems.

As in the first system, it can be noted that the concentration of ethylene only varies slightly as a function of the partial pressure of the pseudo-component “iso-butane+1-butene”, while the concentration of comonomer 1-butene is very sensitive to its partial pressure (Figure 2.12).

Table 2-5. Binary interaction parameters of the ternary system ethylene/iso-butane/LLDPE (based on binary thermodynamic data).

Temperature (°C)	Ethylene/iso-butane ( $k_{12}$ )	Ethylene/LLDPE ( $k_{13}$ ) [5]	Iso-butane/LLDPE ( $k_{23}$ )
70°C	0	-0.014	0.025 (74°C) [59]
80°C	0	-0.022	0.022 (82°C) [59]
90°C	0	-0.032	$-3.75 \cdot 10^{-4} T(\text{K}) + 0.1551$

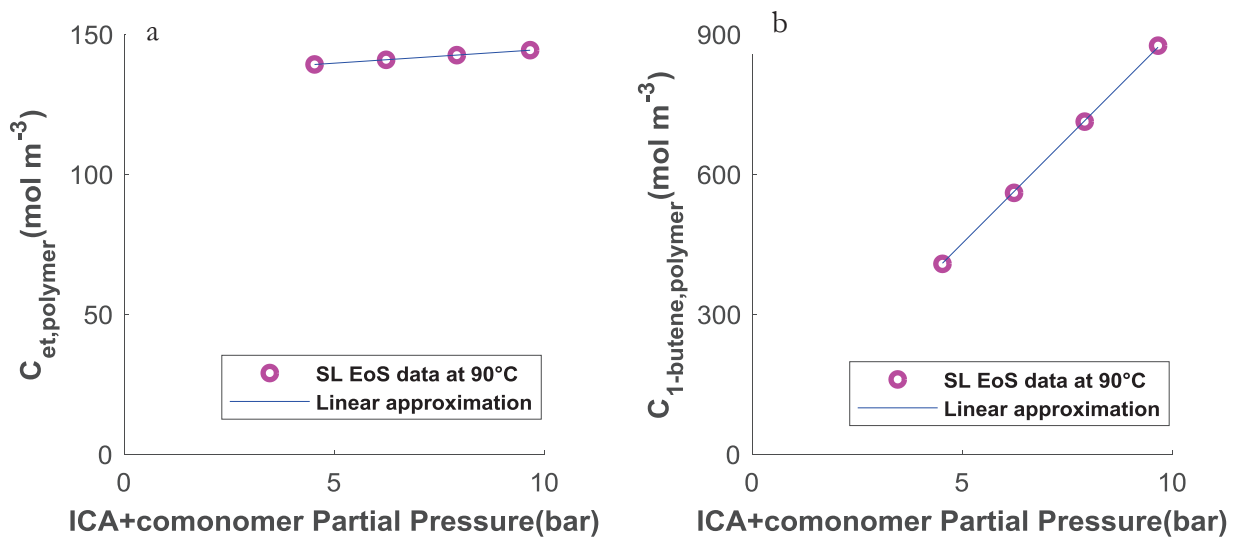


Figure 2.12. Concentrations in amorphous LLDPE obtained using SL EoS and simplified correlations. Pseudo-quaternary system ethylene/(ICA+comonomer)/HDPE, at **90°C** (after extrapolation of  $k_{ij}$ ) and 7 bar of ethylene: a) ethylene and b) comonomer 1-butene and ICA iso-butane.

## 6. Simplified thermodynamic models

Simplified thermodynamic correlations can be very useful to reduce the computation time that is encountered with the SL EoS, especially as we need to employ an optimization strategy. Such correlations were proposed by Alves. [59] They can be linear or polynomial correlations relating the concentration in the amorphous phase with the partial pressures. Also, as the temperature can vary in the bed, it is useful to predict a thermodynamic model that varies automatically with temperature.

### 6.1. Sorption of reactive penetrants

Based on SL EoS, the  $k_{ij}$  parameters can be identified for different temperatures (as indicated in the previous sections for the different systems) and a linear or polynomial correlation can be

identified to relate the concentrations of reactive penetrants (monomer and comonomer) in the amorphous polymer to the partial pressure of diluent (comonomer or ICA). These concentrations are required in the mass and heat balances in order to calculate the reaction rate and predict the polymer properties.

### 6.1.1. Ternary systems

For the ternary system, the concentrations of ethylene in the polymer particles (total, amorphous and crystalline parts),  $[M_1^p]$ , and comonomer (1-butene or 1-hexene),  $[M_2^p]$ , are given by:

$$[M_1^p] = [M_1^{p,am}] = [AP_2 + B] \quad (2.15)$$

$$[M_2^p] = [M_2^{p,am}] = [CP_2^2 + DP_2] \quad (2.16)$$

where  $A$ ,  $B$ ,  $C$  and  $D$  are temperature-dependent model parameters (Table 2-6) and  $[M_i^{p,am}]$  is the concentration of monomer  $i$  in the amorphous polymer. Note that the crystalline chains form far the active sites. Therefore, the catalyst active sites are supposed to be exposed to the amorphous polymer. So, we need to use the concentration of monomer in the amorphous polymer to calculate the reaction rate (without correcting for crystallinity). Ternary systems were investigated at variable temperature in chapter 5. Note for instance that  $B$  is the concentration of ethylene in the amorphous phase when no comonomer (or ICA) is used.

Table 2-6. Coefficients of the correlations of the ternary systems ethylene/1-butene/LLDPE and ethylene/1-hexene/LLDPE.

Relation \ Validity domain	1-butene		1-hexene		Units
	$P_1=7$ bar $P_2=[1.55-10]$ bar $T=[70-90]$ °C		$P_1=10$ bar $P_2=[0-1]$ bar $T=[80-90]$ °C		
$[M_1^{\text{p,am}}] = [AP_2 + B]$ $A = A_1T + A_2$ $B = B_1T + B_2$	$A_1$	-0.019	-2.24		$\text{mol m}^{-3} \text{bar}^{-2} \text{K}^{-1}$
	$A_2$	8.29	819		$\text{mol m}^{-3} \text{bar}^{-2}$
	$B_1$	0.018	-1.75		$\text{mol m}^{-3} \text{bar}^{-1} \text{K}^{-1}$
	$B_2$	125.8	906		$\text{mol m}^{-3} \text{bar}^{-1}$
$[M_2^{\text{p,am}}] = [CP_2^2 + DP_2]$ $C = C_1T + C_2$ $D = D_1T + D_2$	$C_1$	0	-16.85		$\text{mol m}^{-3} \text{K}^{-1}$
	$C_2$	0	6162		$\text{mol m}^{-3}$
	$D_1$	-1.35	-30.2		$\text{mol m}^{-3} \text{bar}^{-2} \text{K}^{-1}$
	$D_2$	612.44	11539		$\text{mol m}^{-3} \text{bar}^{-2}$
$\phi_d = EP_2^2 + FP_2$ $E = E_1T + E_2$ $F = F_1T + F_2$	$E_1$	0	-0.001		$\text{bar}^{-2} \text{K}^{-1}$
	$E_2$	0	0.37		$\text{bar}^{-2}$
	$F_1$	-0.0001	-0.0038		$\text{bar}^{-1} \text{K}^{-1}$
	$F_2$	0.053	1.44		$\text{bar}^{-1}$
$x_i = x_{i,1} \rho_p - x_{i,2}$	$x_{i1}$	0.007			$\text{m}^3 \text{kg}^{-1}$
	$x_{i2}$	-5.84			-

### 6.1.2. Pseudo-quaternary systems

For the pseudo quaternary systems, one should keep in mind that the pseudo species is composed of ICA plus comonomer, so  $P_2$  is to be replaced by  $P_{\text{ICA}} + P_2$ . Moreover, the ratio of solubility of comonomer to ICA ( $r$ ) is to be accounted for when calculating the concentration of comonomer, which gives:

$$[M_1^{\text{p,am}}] = A(P_{\text{ICA}} + P_2) + B \quad (2.17)$$

$$[M_2^{\text{p,am}}] = r \frac{P_2}{P_{\text{ICA}} + P_2} [C(P_{\text{ICA}} + P_2)^2 + D(P_{\text{ICA}} + P_2)] \quad (2.18)$$

The pseudo-quaternary systems were considered in chapter 4 at constant bed temperature, and the parameters are given in Table 2-7. One case study is also considered in chapter 5 at variable temperature.

Table 2-7. Coefficients of the correlations allowing to estimate the concentrations in amorphous LLDPE

	ethylene and 1-hexene <sup>1</sup>		ethylene and 1-butene <sup>2</sup>	units
	Value at 90°C	Value at 70°C	Value at 90°C	
<i>A</i>	33.8	25.9	0.992	mol m <sup>-3</sup> bar <sup>-1</sup>
<i>B</i>	251	278.8	134.73	mol m <sup>-3</sup>
<i>C</i>	505.8	623.9	0	mol m <sup>-3</sup> bar <sup>-2</sup>
<i>D</i>	169.2	1206.3	90.209	mol m <sup>-3</sup> bar <sup>-1</sup>
<i>r</i>		1	1.78	-

<sup>1</sup> valid at ethylene pressure of 10 bar and pseudo-component pressure on the range 0-1 bar

<sup>2</sup> valid at ethylene pressure of 7 bar and pseudo-component pressure on the range 5-10 bar

## 6.2. Sorption of diluents

Another parameter that we extract from SL EoS and that will be necessary in this work, is the volume fraction of diluent,  $\phi_d$ , (comonomer and ICA). Indeed, swelling by diluents can impact the effective melting temperature of the polymer in the reactor, following Flory theory.[78],[79] Regarding lighter compounds such as ethylene and hydrogen, it is likely that they do not need to be considered as sticking promoters due to their lower solubility in the amorphous polymer.[80] This estimation is then used in the Flory-Huggins equation in order to calculate the melting temperature of swollen polymer  $T_m$  (see chapter 5). Simplified correlations were therefore to predict the volume fraction of diluent in the polymer, as follows:

$$\phi_d = EP_2^2 + FP_2 \quad (2.19)$$

where  $E$  and  $F$  are temperature-dependent model parameters (Table 2-6).  $P_2$  is to be replaced by  $P_2 + P_{ICA}$  in the quaternary system involving comonomer and ICA.

For instance, Figure 2.9 shows the variation of the volume fraction of the comonomer 1-butene, in the ternary system LLDPE/Ethylene/1-butene, as calculated by SL EoS from which the linear correlation could be identified at different temperatures.

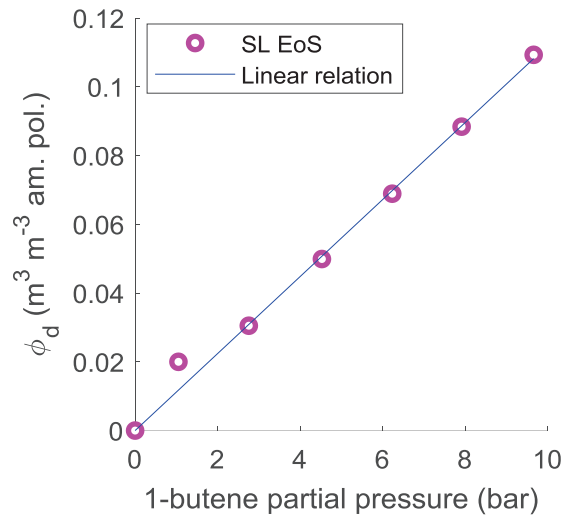


Figure 2.9. Volume fraction of the comonomer 1-butene in the amorphous polymer as a function of its partial pressure (90°C, 7 bar of ethylene).

### 6.3. Crystallinity

It is also required to evaluate the variation of the polymer crystallinity with time,  $x_i$ , especially if the polymer density is varied. Indeed, the crystallinity is known to vary with the comonomer content in the polymer chains.[81]. Chmelar et al.[82] indicated that the polymer crystallinity varies linearly with the polymer density ( $\rho_p$ ), from which the following relation can be identified:

$$x_i = x_{i,1} \rho_p - x_{i,2} \quad (2.20)$$

The parameters  $x_{i,1}$  and  $x_{i,2}$  are given in Table 2-6.

## 7. Conclusions

In this chapter, we introduced the chosen thermodynamic model for this work. This model is based on Sanchez-Lacombe EoS, but then simplified correlations were used to reduce the calculation time. This thermodynamic model was used in binary system, for the estimation of the solubility of a single solute in the polymer. Then, it was used in ternary systems, in order to estimate the concentrations of both ethylene and the induced condensing agent in the amorphous polymer, at both a constant or a variable temperature of the FBR. We showed the high predictive capability of this model in evaluating the effect of ICAs (heavier penetrants) on enhancing the solubility of ethylene (lighter components) or the so-called co-solubility effect. We described the proposed subroutines and the used tools for the thermodynamic model to get the best fit with experimental data, by optimizing the binary interaction parameters,  $k_{i,j}$ . Furthermore, we compared the results found with SL EoS to that obtained with Henry's law model. As a result, the latter model was found as inadequate to account for the ICA effect in ternary systems, despite the fact that it gave good agreement with experimental data for binary systems. The thermodynamic model is adapted over a wide range of temperature.

Moving on to the pseudo-quaternary systems, the thermodynamic model was used in order to account for the co-solubility effects of the different gas species. Two quaternary systems of PE copolymerization were considered, the copolymerization of ethylene with 1-hexene in presence of n-hexane as ICA and the copolymerization of ethylene with 1-butene in presence of iso-butane. Some assumptions were made, mainly due to the lack of thermodynamic data in the literature, to allow the prediction of the solubility of the different species in PE in quaternary systems.

This model represents an essential part of the global process model. It will allow ensuring a better estimation of the rate of ethylene polymerization, and consequently ensuring a better safety of the reactor in the optimization strategies developed in this work.

# References

- [1] Y. S. Wei et R. J. Sadus, « Equations of state for the calculation of fluid-phase equilibria », *AIChE J.*, vol. 46, n° 1, p. 169-196, 2000, doi: 10.1002/aic.690460119.
- [2] C. E. Rogers, V. Stannett, et M. Szwarc, « The Sorption of Organic Vapors by Polyethylene », *J. Phys. Chem.*, vol. 63, n° 9, p. 1406-1413, sept. 1959, doi: 10.1021/j150579a017.
- [3] A. S. Michaels et H. J. Bixler, « Solubility of gases in polyethylene », *J. Polym. Sci.*, vol. 50, n° 154, p. 393-412, 1961, doi: 10.1002/pol.1961.1205015411.
- [4] « Flow of gases through polyethylene - Michaels - 1961 - Journal of Polymer Science - Wiley Online Library ». <https://onlinelibrary.wiley.com/doi/abs/10.1002/pol.1961.1205015412> (consulté le janv. 25, 2021).
- [5] A. Alizadeh, « Study of sorption, heat and mass transfer during condensed mode operation of gas phase ethylene polymerization on supported catalyst », Queen's University, Kingston, Ontario, Canada, 2014.
- [6] R. A. Hutchinson et W. H. Ray, « Polymerization of olefins through heterogeneous catalysis. VIII. Monomer sorption effects », *J. Appl. Polym. Sci.*, vol. 41, n° 1-2, p. 51-81, 1990, doi: 10.1002/app.1990.070410106.
- [7] S. A. Stern, J. T. Mullhaupt, et P. J. Gareis, « The effect of pressure on the permeation of gases and vapors through polyethylene. Usefulness of the corresponding states principle », *AIChE J.*, vol. 15, n° 1, p. 64-73, janv. 1969, doi: 10.1002/aic.690150117.
- [8] C. E. Rogers, V. Stannett, et M. Szwarc, « The sorption, diffusion, and permeation of organic vapors in polyethylene », *J. Polym. Sci.*, vol. 45, n° 145, p. 61-82, 1960, doi: 10.1002/pol.1960.1204514506.
- [9] N. N. Li et R. B. Long, « Permeation through plastic films », *AIChE J.*, vol. 15, n° 1, p. 73-80, 1969, doi: 10.1002/aic.690150118.
- [10] J.-S. Yoon, C.-Y. Chung, et I.-H. Lee, « Solubility and diffusion coefficient of gaseous ethylene and  $\alpha$ -olefin in ethylene/ $\alpha$ -olefin random copolymers », *Eur. Polym. J.*, vol. 30, n° 11, p. 1209-1214, nov. 1994, doi: 10.1016/0014-3057(94)90128-7.
- [11] A. Krallis et V. Kanellopoulos, « Application of Sanchez-Lacombe and Perturbed-Chain Statistical Associating Fluid Theory Equation of State Models in Catalytic Olefins (Co)polymerization Industrial Applications », *Ind. Eng. Chem. Res.*, vol. 52, n° 26, p. 9060-9068, juill. 2013, doi: 10.1021/ie401056j.

- [12] S. H. Huang et M. Radosz, « Equation of state for small, large, polydisperse, and associating molecules: extension to fluid mixtures », *Ind. Eng. Chem. Res.*, vol. 30, n° 8, p. 1994-2005, août 1991, doi: 10.1021/ie00056a050.
- [13] J. Gross et G. Sadowski, « Modeling Polymer Systems Using the Perturbed-Chain Statistical Associating Fluid Theory Equation of State », *Ind. Eng. Chem. Res.*, vol. 41, n° 5, p. 1084-1093, mars 2002, doi: 10.1021/ie010449g.
- [14] P. A. Mueller, J. R. Richards, et J. P. Congalidis, « Polymerization Reactor Modeling in Industry », *Macromol. React. Eng.*, vol. 5, n° 7-8, p. 261-277, août 2011, doi: 10.1002/mren.201100011.
- [15] H. Inomata, Y. Honma, M. Imahori, et K. Arai, « Fundamental study of de-solventing polymer solutions with supercritical CO<sub>2</sub> », *Fluid Phase Equilibria*, vol. 158-160, p. 857-867, juin 1999, doi: 10.1016/S0378-3812(99)00148-X.
- [16] Z. Lei, B. Chen, C. Li, et H. Liu, « Predictive Molecular Thermodynamic Models for Liquid Solvents, Solid Salts, Polymers, and Ionic Liquids », *Chem. Rev.*, vol. 108, n° 4, p. 1419-1455, avr. 2008, doi: 10.1021/cr068441+.
- [17] J. Sun *et al.*, « Solubility measurement of hydrogen, ethylene, and 1-hexene in polyethylene films through an intelligent gravimetric analyzer », *J. Appl. Polym. Sci.*, vol. 134, n° 8, 2017, doi: 10.1002/app.44507.
- [18] W. G. Chapman, K. E. Gubbins, G. Jackson, et M. Radosz, « SAFT: Equation-of-state solution model for associating fluids », *Fluid Phase Equilibria*, vol. 52, p. 31-38, 1989.
- [19] S. H. Huang et M. Radosz, « Equation of state for small, large, polydisperse, and associating molecules », *Ind. Eng. Chem. Res.*, vol. 29, n° 11, p. 2284-2294, nov. 1990, doi: 10.1021/ie00107a014.
- [20] F. Tumakaka, J. Gross, et G. Sadowski, « Modeling of polymer phase equilibria using Perturbed-Chain SAFT », *Fluid Phase Equilibria*, vol. 194-197, p. 541-551, mars 2002, doi: 10.1016/S0378-3812(01)00785-3.
- [21] A. K. Chun Chan et M. Radosz, « Fluid-Liquid and Fluid-Solid Phase Behavior of Poly(ethylene-co-hexene-1) Solutions in Sub- and Supercritical Propane, Ethylene, and Ethylene + Hexene-1 », *Macromolecules*, vol. 33, n° 18, p. 6800-6807, sept. 2000, doi: 10.1021/ma991994k.
- [22] A. Ghosh et W. G. Chapman, « SAFT Modeling of the Effect of Various Carriers on the Operating Range of Slurry Reactors », *Ind. Eng. Chem. Res.*, vol. 41, n° 22, p. 5529-5533, oct. 2002, doi: 10.1021/ie020320m.
- [23] C. McCabe, A. Galindo, M. N. García-Lisbona, et G. Jackson, « Examining the Adsorption (Vapor-Liquid Equilibria) of Short-Chain Hydrocarbons in Low-Density Polyethylene with the

- SAFT-VR Approach », *Ind. Eng. Chem. Res.*, vol. 40, n° 17, p. 3835-3842, août 2001, doi: 10.1021/ie0101386.
- [24] A. Novak *et al.*, « Ethylene and 1-hexene sorption in LLDPE under typical gas-phase reactor conditions: Experiments », *J. Appl. Polym. Sci.*, vol. 100, n° 2, p. 1124-1136, avr. 2006, doi: 10.1002/app.23508.
- [25] G. Sadowski, « Modeling of Polymer Phase Equilibria Using Equations of State », in *Polymer Thermodynamics: Liquid Polymer-Containing Mixtures*, B. A. Wolf et S. Enders, Éd. Berlin, Heidelberg: Springer, 2011, p. 389-418.
- [26] J. Gross et G. Sadowski, « Perturbed-Chain SAFT: An Equation of State Based on a Perturbation Theory for Chain Molecules », *Ind. Eng. Chem. Res.*, vol. 40, n° 4, p. 1244-1260, févr. 2001, doi: 10.1021/ie0003887.
- [27] J. Chmelař, « Sorption Processes in Amorphous and Semi-Crystalline Polymers », University of Chemistry and Technology, Czech Republic, 2015.
- [28] I. C. Sanchez et R. H. Lacombe, « An elementary molecular theory of classical fluids. Pure fluids », *J. Phys. Chem.*, vol. 80, n° 21, p. 2352-2362, oct. 1976, doi: 10.1021/j100562a008.
- [29] R. H. Lacombe et I. C. Sanchez, « Statistical thermodynamics of fluid mixtures », *J. Phys. Chem.*, vol. 80, n° 23, p. 2568-2580, nov. 1976, doi: 10.1021/j100564a009.
- [30] I. C. Sanchez et R. H. Lacombe, « Statistical Thermodynamics of Polymer Solutions », *Macromolecules*, vol. 11, n° 6, p. 1145-1156, nov. 1978, doi: 10.1021/ma60066a017.
- [31] P. J. Flory, « Thermodynamics of High Polymer Solutions », *J. Chem. Phys.*, vol. 10, n° 1, p. 51-61, janv. 1942, doi: 10.1063/1.1723621.
- [32] M. L. Huggins, « Solutions of Long Chain Compounds », *J. Chem. Phys.*, vol. 9, n° 5, p. 440-440, mai 1941, doi: 10.1063/1.1750930.
- [33] N. Koak, R. M. Visser, et T. W. de Loos, « High-pressure phase behavior of the systems polyethylene+ethylene and polybutene+1-butene », *Fluid Phase Equilibria*, vol. 158-160, p. 835-846, juin 1999, doi: 10.1016/S0378-3812(99)00123-5.
- [34] K. Gauter et R. A. Heidemann, « Modeling polyethylene-solvent mixtures with the Sanchez-Lacombe equation », *Fluid Phase Equilibria*, vol. 183-184, p. 87-97, juill. 2001, doi: 10.1016/S0378-3812(01)00423-X.
- [35] I. Nagy, T. W. Loos, R. A. Krenz, et R. Heidemann, « High pressure phase equilibria in the systems linear low density polyethylene + n-hexane and linear low density polyethylene + n-hexane + ethylene: Experimental results and modelling with the Sanchez-Lacombe equation of state », *J. Supercrit. Fluids*, vol. 37, p. 115-124, févr. 2006, doi: 10.1016/j.supflu.2005.08.004.

- [36] M. Haruki, S. Mano, Y. Koga, S. Kihara, et S. Takishima, « Phase behaviors for the supercritical ethylene+1-hexene+hexane+polyethylene systems at elevated temperatures and pressures », *Fluid Phase Equilibria*, vol. 295, n° 1, p. 137-147, août 2010, doi: 10.1016/j.fluid.2010.04.014.
- [37] X. Chen, K. Yasuda, Y. Sato, S. Takishima, et H. Masuoka, « Measurement and correlation of phase equilibria of ethylene + n-hexane + metallocene polyethylene at temperatures between 373 and 473K and at pressures up to 20MPa », *Fluid Phase Equilibria*, vol. 215, n° 1, p. 105-115, janv. 2004, doi: 10.1016/j.fluid.2003.07.004.
- [38] N. Koak et R. A. Heidemann, « Polymer–Solvent Phase Behavior near the Solvent Vapor Pressure », *Ind. Eng. Chem. Res.*, vol. 35, n° 11, p. 4301-4309, janv. 1996, doi: 10.1021/ie950684x.
- [39] Y. L. Cheng et D. C. Bonner, « Solubility of ethylene in liquid, low-density polyethylene to 69 atmospheres », *J. Polym. Sci. Polym. Phys. Ed.*, vol. 15, n° 4, p. 593-603, 1977, doi: 10.1002/pol.1977.180150401.
- [40] Z. Chen, K. Cao, Z. Yao, et Z. Huang, « Modeling solubilities of subcritical and supercritical fluids in polymers with cubic and non-cubic equations of state », *J. Supercrit. Fluids*, vol. 49, n° 2, p. 143-153, juin 2009, doi: 10.1016/j.supflu.2008.12.013.
- [41] M. A. Bashir, M. A. Ali, V. Kanellopoulos, J. Seppälä, E. Kokko, et S. Vijay, « The Effect of Pure Component Characteristic Parameters on Sanchez–Lacombe Equation-of-State Predictive Capabilities », *Macromol. React. Eng.*, vol. 7, n° 5, p. 193-204, 2013, doi: 10.1002/mren.201200054.
- [42] V. Kanellopoulos, D. Mouratides, P. Pladis, et C. Kiparissides, « Prediction of Solubility of  $\alpha$ -Olefins in Polyolefins Using a Combined Equation of StateMolecular Dynamics Approach », *Ind. Eng. Chem. Res.*, vol. 45, n° 17, p. 5870-5878, août 2006, doi: 10.1021/ie060137j.
- [43] C. Panayiotou et I. C. Sanchez, « Statistical thermodynamics of associated polymer solutions », *Macromolecules*, vol. 24, n° 23, p. 6231-6237, 1991.
- [44] M. A. Bashir, M. Al-haj Ali, V. Kanellopoulos, et J. Seppälä, « Modelling of multicomponent olefins solubility in polyolefins using Sanchez–Lacombe equation of state », *Fluid Phase Equilibria*, vol. 358, p. 83-90, nov. 2013, doi: 10.1016/j.fluid.2013.08.009.
- [45] M. McHugh et V. Krukoniš, *Supercritical Fluid Extraction: Principles and Practice*. Elsevier, 2013.
- [46] F. Nascimento de Andrade, « Effect of condensable materials during the gas phase polymerization of ethylene on supported catalysts », Université Claude Bernard Lyon 1, 2019.
- [47] C. M. Chen, « Gas Phase Olefin Copolymerization with Ziegler-Natta Catalysts », Ph.D. Thesis, University of Wisconsin-Madison, Madison, Wisconsin, 1991.

- [48] G. C. Sarti et F. Doghieri, « Predictions of the solubility of gases in glassy polymers based on the NELF model », *Chem. Eng. Sci.*, vol. 53, n° 19, p. 3435-3447, oct. 1998, doi: 10.1016/S0009-2509(98)00143-2.
- [49] F. Doghieri et G. C. Sarti, « Nonequilibrium Lattice Fluids: A Predictive Model for the Solubility in Glassy Polymers », *Macromolecules*, vol. 29, n° 24, p. 7885-7896, janv. 1996, doi: 10.1021/ma951366c.
- [50] F. Doghieri et G. C. Sarti, « Predicting the low pressure solubility of gases and vapors in glassy polymers by the NELF model », *J. Membr. Sci.*, vol. 147, n° 1, p. 73-86, août 1998, doi: 10.1016/S0376-7388(98)00123-9.
- [51] H. Orbey, C. P. Bokis, et C.-C. Chen, « Equation of State Modeling of Phase Equilibrium in the Low-Density Polyethylene Process: The Sanchez–Lacombe, Statistical Associating Fluid Theory, and Polymer-Soave–Redlich–Kwong Equations of State », *Ind. Eng. Chem. Res.*, vol. 37, n° 11, p. 4481-4491, nov. 1998, doi: 10.1021/ie980220+.
- [52] C. Kiparissides, V. Dimos, T. Boulouka, A. Anastasiadis, et A. Chasiotis, « Experimental and theoretical investigation of solubility and diffusion of ethylene in semicrystalline PE at elevated pressures and temperatures », *J. Appl. Polym. Sci.*, vol. 87, n° 6, p. 953-966, 2003, doi: 10.1002/app.11394.
- [53] V. Touloupides, V. Kanellopoulos, P. Pladis, C. Kiparissides, D. Mignon, et P. Van-Grambezen, « Modeling and simulation of an industrial slurry-phase catalytic olefin polymerization reactor series », *Chem. Eng. Sci.*, vol. 65, n° 10, p. 3208-3222, mai 2010, doi: 10.1016/j.ces.2010.02.014.
- [54] C. F. Kirby et M. A. McHugh, « Phase behavior of polymers in supercritical fluid solvents », *Chem. Rev.*, vol. 99, n° 2, p. 565-602, 1999.
- [55] M. A. Bashir, V. Monteil, V. Kanellopoulos, M. Al-haj Ali, et T. F. L. McKenna, « An Equation of State-Based Modeling Approach for Estimating the Partial Molar Volume of Penetrants and Polymers in Binary Mixtures », *Ind. Eng. Chem. Res.*, vol. 52, n° 46, p. 16491-16505, nov. 2013, doi: 10.1021/ie4025193.
- [56] S. J. Moore et S. E. Wanke, « Solubility of ethylene, 1-butene and 1-hexene in polyethylenes », *Chem. Eng. Sci.*, vol. 56, n° 13, p. 4121-4129, juill. 2001, doi: 10.1016/S0009-2509(01)00082-3.
- [57] W. M. R. Parrish, « Solubility of isobutane in two high-density polyethylene polymer fluffs », *J. Appl. Polym. Sci.*, vol. 26, n° 7, p. 2279-2291, juill. 1981, doi: 10.1002/app.1981.070260715.

- [58] M. B. Kiszka, M. A. Meilchen, et M. A. McHugh, « Modeling high-pressure gas–polymer mixtures using the Sanchez-Lacombe equation of state », *J. Appl. Polym. Sci.*, vol. 36, n° 3, p. 583-597, 1988, doi: 10.1002/app.1988.070360311.
- [59] R. Alves, M. A. Bashir, et T. F. L. McKenna, « Modeling Condensed Mode Cooling for Ethylene Polymerization: Part II. Impact of Induced Condensing Agents on Ethylene Polymerization in an FBR Operating in Super-Dry Mode », *Ind. Eng. Chem. Res.*, vol. 56, n° 46, p. 13582-13593, nov. 2017, doi: 10.1021/acs.iecr.7b02963.
- [60] W. Yao, X. Hu, et Y. Yang, « Modeling the solubility of ternary mixtures of ethylene, isopentane, n-hexane in semicrystalline polyethylene », *J. Appl. Polym. Sci.*, vol. 104, n° 6, p. 3654-3662, 2007, doi: 10.1002/app.26137.
- [61] T. F. McKenna, « Solubility and crystallinity data for ethylene/polyethylene systems », *Eur. Polym. J.*, vol. 34, n° 9, p. 1255-1260, sept. 1998, doi: 10.1016/S0014-3057(97)00251-6.
- [62] J. Chmelař, K. Haškovcová, M. Podivinská, et J. Kosek, « Equilibrium Sorption of Propane and 1-Hexene in Polyethylene: Experiments and Perturbed-Chain Statistical Associating Fluid Theory Simulations », *Ind. Eng. Chem. Res.*, vol. 56, n° 23, p. 6820-6826, juin 2017, doi: 10.1021/acs.iecr.7b00572.
- [63] W. Yao, X. Hu, et Y. Yang, « Modeling solubility of gases in semicrystalline polyethylene », *J. Appl. Polym. Sci.*, vol. 103, n° 3, p. 1737-1744, févr. 2007, doi: 10.1002/app.24969.
- [64] B. J. Savatsky, J. A. Moebus, et B. R. Greenhalgh, « Parameterization of Models for Vapor Solubility in Semicrystalline Polyethylene », *Macromol. React. Eng.*, vol. 13, n° 4, p. 1900003, 2019, doi: 10.1002/mren.201900003.
- [65] J.-S. Yoon, H.-S. Yoo, et K.-S. Kang, « Solubility of  $\alpha$ -olefins in linear low density polyethylenes », *Eur. Polym. J.*, vol. 32, n° 11, p. 1333-1336, nov. 1996, doi: 10.1016/S0014-3057(96)00090-0.
- [66] J. A. Moebus et B. R. Greenhalgh, « Modeling Vapor Solubility in Semicrystalline Polyethylene », *Macromol. React. Eng.*, vol. 12, n° 4, p. 1700072, 2018, doi: 10.1002/mren.201700072.
- [67] S. K. Nath, B. J. Banaszak, et J. J. de Pablo, « Simulation of Ternary Mixtures of Ethylene, 1-Hexene, and Polyethylene », *Macromolecules*, vol. 34, n° 22, p. 7841-7848, oct. 2001, doi: 10.1021/ma002197l.
- [68] A. Alizadeh, M. Namkajorn, E. Somsook, et T. F. L. McKenna, « Condensed Mode Cooling for Ethylene Polymerization: Part I. The Effect of Different Induced Condensing Agents on Polymerization Rate », *Macromol. Chem. Phys.*, vol. 216, n° 8, p. 903-913, avr. 2015, doi: 10.1002/macp.201400600.

- [69] M. A. Bashir, V. Monteil, V. Kanellopoulos, M. A.-H. Ali, et T. McKenna, « Partial Molar Volumes and Thermal Expansion Coefficients as an Explanation for Co-Solvent Effect of Penetrants in Multicomponent Polymer Mixtures », *Macromol. Chem. Phys.*, vol. 216, n° 21, p. 2129-2140, 2015, doi: 10.1002/macp.201500170.
- [70] A. Alizadeh, J. Chmelař, F. Sharif, M. Ebrahimi, J. Kosek, et T. F. L. McKenna, « Modeling Condensed Mode Operation for Ethylene Polymerization: Part I. Thermodynamics of Sorption », *Ind. Eng. Chem. Res.*, vol. 56, n° 5, p. 1168-1185, févr. 2017, doi: 10.1021/acs.iecr.6b04288.
- [71] T. Xie, K. B. McAuley, J. C. C. Hsu, et D. W. Bacon, « Gas Phase Ethylene Polymerization: Production Processes, Polymer Properties, and Reactor Modeling », *Ind. Eng. Chem. Res.*, vol. 33, n° 3, p. 449-479, mars 1994, doi: 10.1021/ie00027a001.
- [72] A. Ben Mrad, « Effect of Induced Condensing Agents on Ethylene Polymerization in Gas-Phase Reactors », University of Lyon, 2020.
- [73] S. J. Moore et S. E. Wanke, « Solubility of ethylene, 1-butene and 1-hexene in polyethylenes », *Chem. Eng. Sci.*, vol. 56, n° 13, p. 4121-4129, juill. 2001, doi: 10.1016/S0009-2509(01)00082-3.
- [74] S. Kardous, T. F. L. McKenna, et N. Sheibat-Othman, « Thermodynamic Effects on Grade Transition of Polyethylene Polymerization in Fluidized Bed Reactors », *Macromol. React. Eng.*, vol. n/a, n° n/a, p. 2000013, doi: 10.1002/mren.202000013.
- [75] A. L. D. Braganca, A. L. R. de C. Morschbacker, E. Rubbo, C. N. Miro, T. Barlem, et A. Mukherjee, « Process for the gas phase polymerization and copolymerization of olefin monomers », US6864332B2, mars 08, 2005.
- [76] B. J. Banaszak *et al.*, « Ethylene and 1-Hexene Sorption in LLDPE under Typical Gas Phase Reactor Conditions: A Priori Simulation and Modeling for Prediction of Experimental Observations », *Macromolecules*, vol. 37, n° 24, p. 9139-9150, nov. 2004, doi: 10.1021/ma0491107.
- [77] H.-J. Jin, S. Kim, et J.-S. Yoon, « Solubility of 1-hexene in LLDPE synthesized by (2-MeInd)<sub>2</sub>ZrCl<sub>2</sub>/MAO and by Mg(OEt)<sub>2</sub>/DIBP/TiCl<sub>4</sub>-TEA », *J. Appl. Polym. Sci.*, vol. 84, n° 8, p. 1566-1571, mai 2002, doi: 10.1002/app.10418.
- [78] D. Singh, S. Hinds, B. Fischbuch, et N. A. Vey, « Gas-phase process », US20050182207A1, août 18, 2005.
- [79] G. G. Hendrickson, « Method for operating a gas phase polymerization reactor », US7531606B2, mai 12, 2009.
- [80] R. O. Hagerty, K. B. Stavens, M. L. DeChellis, D. B. Fischbuch, et J. M. Farley, « Polymerization process », US7122607B2, oct. 17, 2006.

[81] M. M. de Camargo Forte, F. O. V. da Cunha, J. H. Z. dos Santos, et J. J. Zacca, « Ethylene and 1-butene copolymerization catalyzed by a Ziegler–Natta/Metallocene hybrid catalyst through a 23 factorial experimental design », *Polymer*, vol. 44, n° 5, p. 1377-1384, mars 2003, doi: 10.1016/S0032-3861(02)00874-1.

[82] J. Chmelar, P. Matuska, T. Gregor, M. Bobak, F. Fantinel, et J. Kosek, « Softening of polyethylene powders at reactor conditions », *Chem. Eng. J.*, vol. 228, p. 907-916, juill. 2013, doi: 10.1016/j.cej.2013.05.069.

"With thermodynamics, one can calculate almost everything crudely; with kinetic theory, one can calculate fewer things, but more accurately"  
-Eugene Wigner (1902-1995)

### 1. Introduction

In the previous chapter, the potential effect of the condensable species on the thermodynamic equilibrium was investigated, and the concentrations of the different species in the amorphous polymer phase were estimated using a thermodynamic-model based on the SL EoS or simplified correlations. In this chapter, a combined kinetic and reactor model is developed in order to evaluate the changes in the rate of the polymerization and polymer properties. Note that this model is to be combined with the thermodynamic model. It is then able to better evaluate the heat removal. This complete model of polymerization will be used in the next chapters to optimize the transition between different grades of LLDPE, in order to control the polymer morphological properties, such as the molecular weight and polymer density in the FBR.[1]

On an industrial scale, polyethylene in gas-phase, is produced only in fluidized bed reactors. In this work, the bed is approximated by a CSTR due to its high recycle ratio and low single pass conversion.[2] The reactor model thus includes mass balances of the different species and energy balances of the bed and the heat exchanger of the recycling gas. A classical kinetic model is used to describe the copolymerization of ethylene with  $\alpha$ -olefins (1-hexene or 1-butene) over a Ziegler-Natta catalyst; in presence or absence of an ICA. Indeed, ICA has no direct impact on the reactivity of the species at the active sites, nor on the behavior of the catalysts. Finally, correlations for the final properties of the polymer are provided.

This chapter is organized as follows: we first give an overview on modelling olefin polymerization in fluidized bed reactors, especially when operating under condensed mode by injecting the thermodynamic model. Second, we present the kinetic model for two different copolymerization systems. Third, we present the reactor model of the FBR (i.e. mass and energy balance equations) and the correlations used for the key properties of the polymer. The effect of ICA on the reaction rate and the polymer properties is investigated.

## 2. An overview: Modelling of Olefin Polymerization in FBRs

The complexity of the interactions between the different species in the polymerization system, as well as the complex structure of the bed and the interacted phenomena makes the development of a robust and comprehensive model absolutely necessary to operate and control the process effectively. A detailed FBR model can also be useful for a deep understanding of the interaction between the process and the chemistry to understand how to make the final product.

In this work, the process model will be useful at first to study the impact of the inert gases (or ICAs) on the reaction rate, and other properties such as the polymer molecular weight or the particle (agglomeration; stickiness...). The second use of the PE polymerization process model is to provide a detailed description of how the different parts of the model from the reaction mechanism (micro-scale) to the reactor type and the different operating conditions (macro-scale) participate in creating different quality polymer products, which is the major objective of the process.[3]

Ray[4], [5] suggested to organize the polymerization model into three different levels based on both, the time dimension and the relative scale: micro-scale, meso-scale, and macro-scale. This hierarchy was adopted by other researchers (Xie et al.[6]; Zacca [7]) in olefin polymerization. An accurate description should show a strong interaction between the levels, in the sense that no clear

boundaries should be distinguished. However, it is common to simplify the hierarchy by selecting only the levels of interest for a relative application.

Many models have been recommended in the open literature; so that one can understand how gas phase ethylene polymerization works in a real process application. The FBRs have been modeled as a single, two or three-phase reactors. McAuley et al. [2] and Xie et al.[6] proposed the reactor to behave like a single phase CSTR. They compared this approach and a simple-two phase steady state model, and noticed minor deviations when predicting the reactor temperature and the monomer concentration.[8] They indicated that the well-mixed CSTR assumption is accurate in case of small fluidization bubbles, negligible heat and mass transfer resistance between the polymer and the gas phase. This assumption becomes also possible based on the high circulation ratio and the low single pass conversion.[2] Furthermore, Chatzidoukas[9] focused on modelling the kinetics of a catalytic gas-phase copolymerization (ethylene-1 butene) process and considered the bed to be mixed uniformly as a CSTR. Therefore, this assumption is often made in optimization and control strategies of FBRs for simplicity.[10], [11] More complex models are also developed, for instance Choi and Ray[12] proposed to describe the reactor with a two-phase model, a bubble phase and a well-mixed emulsion phase. They showed in their work that the polymerization only takes place in the emulsion phase, while the bubbles are free of polymer. Fernandes and Lona[13] further proposed a three-phase heterogeneous model , consisting of emulsion, bubble and solid phases that work as a plug flow. The reactor was divided further into several solid-free well-mixed compartments in series in which emulsion and bubble phases are well mixed together according to the approach of Hatzantonis et al,[14].

In this study, the FBR is modeled as a single well-mixed phase (simplified CSTR bed model), as usually done in the literature for the optimization of grade transitions.[2], [11]

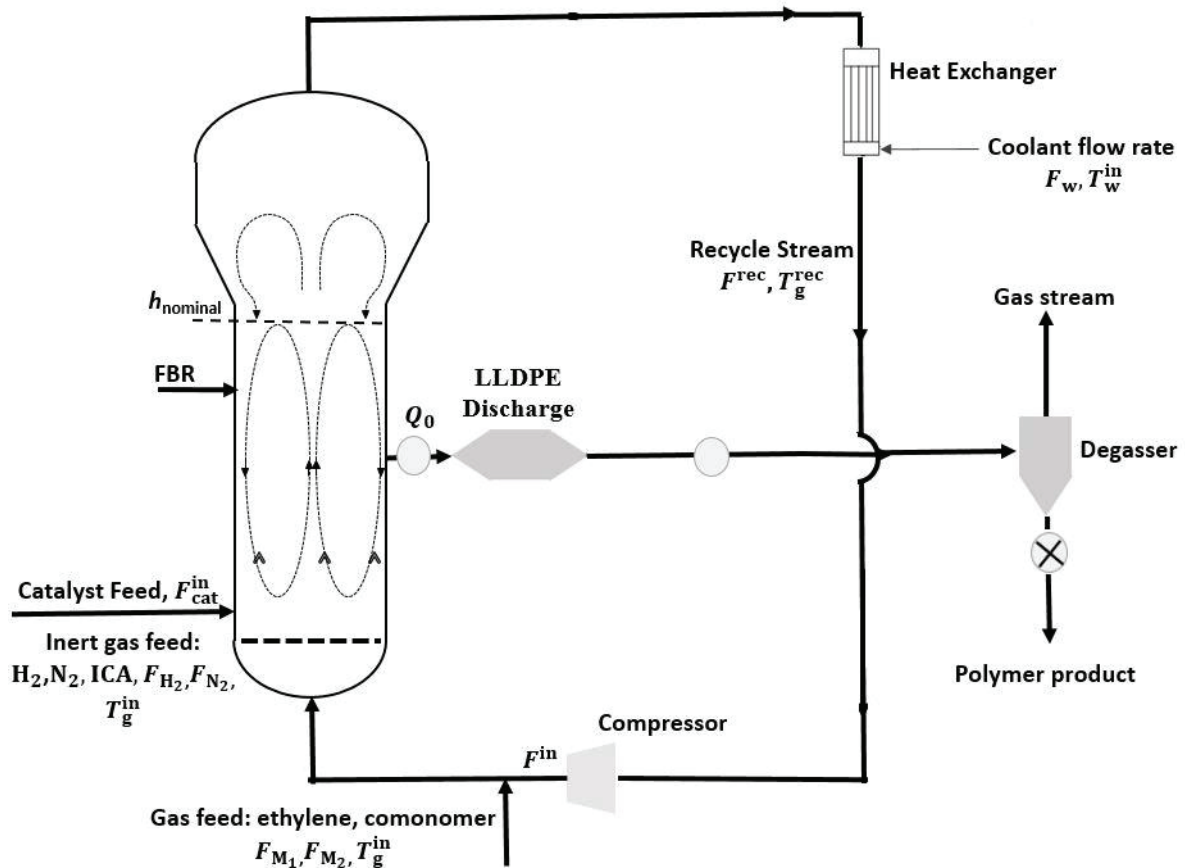


Figure 3.1. Schematic representation of the FBR polymerization reactor.

A good reactor model in our case, has to be adequate to deal with control problems. Figure 3.1 shows a typical gas-phase catalytic ethylene polymerization FBR. The polymerization takes place into the fluidized main zone of the FBR. The addition of the catalyst particles and the withdrawal of the polymer product are pulsed. The unreacted gases rise through the bed from the bottom to the top, where they are evacuated, compressed, cooled and recycled. They are afterwards mixed with fresh monomers, and eventually other reacting species before re-entering the bed. Due to the exothermic nature of ethylene polymerization, the temperature of the injected gases (fresh gas and the recycled gas) is controlled to keep the bed at the desired temperature. Therefore, the recycling stream is equipped with an exchanger to cool the recycled gas. Regarding the polymer powder, it generally rises through the center of the bed where the velocity is the highest, then falls back along the walls of the reactor with an internal recirculation time of the order of few minutes. The polymer product is continuously removed through a product discharge valve at a point slightly close to the

bottom of the reactor, and separated from unreacted monomers through a degassing tank, then pelletized. In these conditions of high solid recirculation rate with respect to the product withdrawal rate (residence time of the reactor on the order of few hours), and the per pass conversion of the gas phase on the order (2-5 %), one can approximate the residence time distribution of an FBR with that of a CSTR.[11], [15] The dynamic behavior of FBR in this work was then assumed to behave like a single-phase CSTR, as in the models of McAuley et al. [2] and Chatzidoukas et al.[11]. This assumption is sufficient to get an order of magnitude of estimate of the reactor behavior, which is subjected to different process variables such as the monomer concentrations (the effect of ICA) and the feed gas temperature.

The main assumptions considered in the model are therefore:

- The reactor is considered to operate in a super-dry mode, i.e. the injected ICAs or comonomers are assumed to evaporate instantaneously at the inlet of the bed;
- The reactor is approximated by a single-phase well-mixed reactor (the CSTR), i.e. the polymer and gas phases have the same temperature (temperature of particles ( $T_p$ ) = temperature of gas ( $T_{gas}$ )); And the partitioning of gaseous between the polymer and the gas phase is assumed at equilibrium, therefore the concentrations in the polymer can be taken from SL EoS;[2], [8]

## 3. Model development

### 3.1. Kinetic model

In this work, we are interested in the copolymerization of ethylene with  $\alpha$ -olefins. It is worth mentioning that PE can be formed with ethylene homopolymerization to produce HDPE (though usually with small amounts of comonomer), but we consider here the production of LLDPEs,

which are copolymers of ethylene with a comonomer (e.g. 1-butene, 1-pentene, 1-hexene, 1-octene).[16]

Kinetic studies of ethylene polymerization over conventional Ziegler-Natta catalysts were first performed by Edgecombe[17] and Lipman and Norrish[18] in 1963. The catalyst particle contains several reactive sites at which the reaction takes place. Generally, the reaction rates differ with respect to the type of sites. The polymerization reactions correspond to the production of *n*-type sites, the propagation, the transfer and the deactivation reactions on these. De Carvalho et al.[19] define the propagation site as an active site on which there is a monomer molecule or a growing polymer chain. They consider an active site without monomer molecule or growing chain as an initiation site. Finally, the number of active sites is the sum of the propagation sites and the initiation sites, which is equivalent to the surface area of the catalyst. Kinetic models that have been developed to account for the broad rate constants distribution, often consider only two different sites for simplification.[2], [11], [14] In the present study, we use a classical reaction scheme (Table 3-1) of copolymerization of ethylene in presence of a catalyst having one type of active sites, as suggested for instance by de Carvalho et al.[19], McAuley et al.[2], Chatzidoukas et al.[11]. Indeed, one type of active sites allows to reduce an additional complexity to the model by removing a large number of kinetic parameters useless for our case of study. After all, the only difference between the two copolymerization systems considered in this work, with the comonomer 1-hexene or with 1-butene, is the value of the rate coefficients. The reaction rate equations resulting from the proposed reaction scheme are given in Table 3-2. All concentrations are in ( $\text{mol m}^{-3}$ )

Table 3-1. Kinetic scheme of the copolymerization of ethylene with a catalyst of one site (without co-catalyst)

Designation	Reaction
Spontaneous activation	$S_p \xrightarrow{k_a} P_0$
Chain initiation	$P_0 + M_i \xrightarrow{k_{oi}} P_{1,i}$
Propagation	$P_{n,i} + M_j \xrightarrow{k_{pij}} P_{n+1,j}$
Spontaneous deactivation	$P_{n,i} \xrightarrow{k_{dsp}} C_d + D_n, P_0 \xrightarrow{k_{dsp}} C_d$
Spontaneous chain transfer	$P_{n,i} \xrightarrow{k_{tsp}} P_0 + D_n$
Chain transfer to hydrogen (H <sub>2</sub> )	$P_{n,i} + H_2 \xrightarrow{k_{tH}} P_0 + D_n$
Chain transfer to monomer M <sub>j</sub>	$P_{n,i} + M_j \xrightarrow{k_{tmij}} P_{1,j} + D_n$

Table 3-2. Reaction rates of the different species (mol m<sup>-3</sup> s<sup>-1</sup>)

$R_{S_p} = -k_a[S_p]$
$R_{P_0} = k_a[S_p] - k_{dsp}[P_0] - (k_{o1}[M_1^p] + k_{o2}[M_2^p])[P_0] + (k_{tsp} + k_{tH}[H_2^p])\lambda_0$
$R_{\lambda_0} = [P_0](k_{o1}[M_1^p] + k_{o2}[M_2^p]) - \lambda_0(k_{dsp} + k_{tsp} + k_{tH}[H_2^p])$
$R_{\lambda_1} = [P_0](k_{o1}[M_1^p] + k_{o2}[M_2^p]) + \lambda_0((k_{tm11}\phi_1 + k_{tm21}\phi_2 + k_{p11}\phi_1 + k_{p21}\phi_2)[M_1^p] + (k_{tm12}\phi_1 + k_{tm22}\phi_2 + k_{p12}\phi_1 + k_{p22}\phi_2)[M_2^p]) - \lambda_1(k_{dsp} + k_{tsp} + k_{tH}[H_2^p] + (k_{tm11}\phi_1 + k_{tm21}\phi_2)[M_1^p] + (k_{tm12}\phi_1 + k_{tm22}\phi_2)[M_2^p])$
$R_{\lambda_2} = [P_0](k_{o1}[M_1^p] + k_{o2}[M_2^p]) + \lambda_0((k_{tm11}\phi_1 + k_{tm21}\phi_2)[M_1^p] + (k_{tm12}\phi_1 + k_{tm22}\phi_2)[M_2^p]) + (\lambda_0 + 2\lambda_1)((k_{p11}\phi_1 + k_{p21}\phi_2)[M_1^p] + (k_{p12}\phi_1 + k_{p22}\phi_2)[M_2^p]) - \lambda_2(k_{dsp} + k_{tsp} + k_{tH}[H_2^p] + (k_{tm11}\phi_1 + k_{tm21}\phi_2)[M_1^p] + (k_{tm12}\phi_1 + k_{tm22}\phi_2)[M_2^p])$
$R_{\mu_0} = \lambda_0(k_{dsp} + k_{tsp} + k_{tH}[H_2^p] + (k_{tm11}\phi_1 + k_{tm21}\phi_2)[M_1^p] + (k_{tm12}\phi_1 + k_{tm22}\phi_2)[M_2^p])$
$R_{\mu_1} = \lambda_1(k_{dsp} + k_{tsp} + k_{tH}[H_2^p] + (k_{tm11}\phi_1 + k_{tm21}\phi_2)[M_1^p] + (k_{tm12}\phi_1 + k_{tm22}\phi_2)[M_2^p])$
$R_{\mu_2} = \lambda_2(k_{dsp} + k_{tsp} + k_{tH}[H_2^p] + (k_{tm11}\phi_1 + k_{tm21}\phi_2)[M_1^p] + (k_{tm12}\phi_1 + k_{tm22}\phi_2)[M_2^p])$
$R_{H_2} = k_{tH}[H_2^p]\lambda_0$
$R_{M_1} = (k_{o1}[P_0] + (k_{tm11}\phi_1 + k_{tm21}\phi_2 + k_{p11}\phi_1 + k_{p21}\phi_2)\lambda_0)[M_1^p]$
$R_{M_2} = (k_{o2}[P_0] + (k_{tm22}\phi_2 + k_{tm12}\phi_1 + k_{p22}\phi_2 + k_{p12}\phi_1)\lambda_0)[M_2^p]$
With $\phi_1 = \frac{k_{p21}[M_1^p]}{k_{p12}[M_2^p] + k_{p21}[M_1^p]}, \phi_2 = 1 - \phi_1,$
$[H_2^p]$ (mol m <sup>-3</sup> am. polymer) = $S_{H_2} \frac{\rho_{PE}}{MW_{H_2}} (1 - x_i), S_{H_2}$ (g H <sub>2</sub> g <sup>-1</sup> am. polymer) = $10^{-9} P_{H_2}$ [20]
$\lambda_k = \lambda_{k,1} + \lambda_{k,2} = \sum_{n=1}^{\infty} n^k [P_{n,1}] + \sum_{n=1}^{\infty} n^k [P_{n,2}],$
$\mu_k = \sum_{n=2}^{\infty} n^k [D_n]$

The values of the different kinetic rate constants are given in Tables 3.3 and 3.4. For the case of ethylene-co-1-butene, the parameters were taken from Chatzidoukas et al.[11] or Ghasem et al.[21]. For the system ethylene-co-1-hexene in gas-phase, fewer parameters are available. Chakravarti et al.[22] gave some kinetic parameters for this system using a metallocene catalyst. In order to keep both systems comparable in terms of catalyst activity, only the reactivity ratios were taken from Chakravarti et al.[22], and the other parameters and ratios were kept as for the first system. The identification of a specific kinetic model for a defined system is out of the scope of this work.

Table 3-3. Pre-exponential factors and activation energies of the kinetic parameters of co-polymerization of ethylene and a comonomer (common values for both systems) ( $k_i = k_{i,0}e^{-\frac{E_a}{RT}}$ )

Parameter	Value
Spontaneous activation [21]	
$k_{a,0}$ (s <sup>-1</sup> )	$7.2 \times 10^4$
$E_a$ (J mol <sup>-1</sup> )	33472
Spontaneous deactivation[11]	
$k_{dsp,0}$ (s <sup>-1</sup> )	7.2
$E_{dsp}$ (J mol <sup>-1</sup> )	33472
Initiation [21]	
$k_{0,1}$ (m <sup>3</sup> mol <sup>-1</sup> s <sup>-1</sup> )	$2.9 \times 10^2$
$E_{0,1}$ (J mol <sup>-1</sup> )	37656
Spontaneous chain transfer [11]	
$k_{tsp,0}$ (m <sup>3</sup> mol <sup>-1</sup> s <sup>-1</sup> )	7.2
$E_{tsp}$ (J mol <sup>-1</sup> )	33472
Transfer to hydrogen[21]	
$k_{tH,0}$ (m <sup>3</sup> mol <sup>-1</sup> s <sup>-1</sup> )	6.3
$E_{tH}$ (J mol <sup>-1</sup> )	33472
Transfer to monomer [21]	
$k_{tm11,0}$ (m <sup>3</sup> mol <sup>-1</sup> s <sup>-1</sup> )	0.15
$k_{tm12,0}$ (m <sup>3</sup> mol <sup>-1</sup> s <sup>-1</sup> )	0.43
$k_{tm21,0}$ (m <sup>3</sup> mol <sup>-1</sup> s <sup>-1</sup> )	0.15
$k_{tm22,0}$ (m <sup>3</sup> mol <sup>-1</sup> s <sup>-1</sup> )	0.43
$E_{tmij,0}$ (J mol <sup>-1</sup> )	33472
Activation energy of propagation [11]	
$E_{pij}$ (J mol <sup>-1</sup> )	37656

Table 3-4. Propagation rate coefficients of the co-polymerization of ethylene with a comonomer

	1-Butene	1-Hexene
Reactivity ratios (-):		
$r_1 = k_{p11}/k_{p12}$	42.5	18.94[22]
$r_2 = k_{p22}/k_{p21}$	0.023	0.04 [22]
Pre-exponential factor of propagation( $\text{m}^3 \text{mol}^{-1} \text{s}^{-1}$ ):		
$k_{p11,0}$	$2.48 \times 10^4$ [21]	$2.48 \times 10^4$
$k_{p12,0}$	$5.82 \times 10^2$ [21]	$k_{p11}/r_1 = 1.3 \times 10^3$
$k_{p21,0}$	$1.86 \times 10^4$ [21]	$k_{p22}/r_2 = 2.65 \times 10^3$
$k_{p22,0}$	$4.37 \times 10^2$	$1.06 \times 10^2$ [22]*
Comonomer initiation ( $\text{m}^3 \text{mol}^{-1} \text{s}^{-1}$ ):		
$k_{0,2}$	40.7[21]	$k_{0,1}k_{p22}/k_{p11} = 1.25$
$E_{0,2}$ ( $\text{J mol}^{-1}$ )	37656	37656

\* Calculated to respect the ratio  $k_{p11}/k_{p22}$  in reference [22].

In this model, the equilibrium sorption from the gas phase to the polymer is described by the thermodynamic correlations presented in chapter 2 (equations 2-17; 2-18), which are valid at equilibrium. The reaction rates are calculated based on these equilibrium concentrations in the polymer, which gives the consumption of moles of monomer per  $\text{m}^3$  bed (see Table 3-2). These reaction terms are required in the following section in the gas material balances (see Table 3-5).

## 3.2. Mass and heat balances

The FBR is modeled as a single-phase CSTR as indicated previously. Fresh catalyst particles, gas species (monomers,  $\text{N}_2$ ,  $\text{H}_2$ ) and condensed gas (ICA) are assumed to be fed continuously at the bottom of the reactor. Thus, the FBR can roughly be divided into two compartments: one super-dry compartment in the upper containing only gas and polymer, and one much smaller compartment in the bottom also containing condensed vapors. Only the upper compartment is considered in the present model, which represents most of the reactor volume. Indeed, when operating under condensed mode, the injected liquid species evaporate rapidly and the major part of the reactor only contains solid and gas species (i.e. super-dry mode).[23]

The mass balances of the different species in the FBR are given in Table 3-5.[11]

Table 3-5. Mass balances of the different species in the FBR

Monomer $i$	$\frac{d[M_i]}{dt} = \frac{(F_{M_i} + F^{\text{in}}X_{M_i}^{\text{in}} - F^{\text{rec}}X_{M_i}^{\text{rec}})/M_{w,i}}{\varepsilon_{\text{bed}}V_{\text{bed}}} - \frac{Q_0[M_i]}{V_{\text{bed}}} - \frac{(1 - \varepsilon_{\text{bed}})}{\varepsilon_{\text{bed}}}R_{M_i} - \frac{[M_i]A}{V_{\text{bed}}}\frac{dh}{dt}$
	With: $M_i: M_1, M_2$ (considering no bleed stream: $F^{\text{in}} = F^{\text{rec}}$ )
Hydrogen	$\frac{d[H_2]}{dt} = \frac{(F_{H_2} + F^{\text{in}}X_{H_2}^{\text{in}} - F^{\text{rec}}X_{H_2}^{\text{rec}})/M_{w,H_2}}{\varepsilon_{\text{bed}}V_{\text{bed}}} - \frac{Q_0[H_2]}{V_{\text{bed}}} - \frac{(1 - \varepsilon_{\text{bed}})}{\varepsilon_{\text{bed}}}R_{H_2} - \frac{[H_2]A}{V_{\text{bed}}}\frac{dh}{dt}$
Nitrogen	$\frac{d[N_2]}{dt} = \frac{(F_{N_2} + F^{\text{in}}X_{N_2}^{\text{in}} - F^{\text{rec}}X_{N_2}^{\text{rec}})/M_{w,N_2}}{\varepsilon_{\text{bed}}V_{\text{bed}}} - \frac{Q_0[N_2]}{V_{\text{bed}}} - \frac{[N_2]A}{V_{\text{bed}}}\frac{dh}{dt}$
ICA	$\frac{d[\text{ICA}]}{dt} = \frac{(F_{\text{ICA}} + F^{\text{in}}X_{\text{ICA}}^{\text{in}} - F^{\text{rec}}X_{\text{ICA}}^{\text{rec}})/M_{w,\text{ICA}}}{\varepsilon_{\text{bed}}V_{\text{bed}}} - \frac{Q_0[\text{ICA}]}{V_{\text{bed}}} - \frac{[\text{ICA}]A}{V_{\text{bed}}}\frac{dh}{dt}$
	With: $Z: M_i, H_2, N_2, \text{ICA}$ $X_Z = [Z]M_{w,Z} / \sum [Z]M_{w,Z}$
Potential catalyst sites $S_p$	$\frac{d[S_p]}{dt} = \frac{F_{\text{cat}}^{\text{in}}[S_p]^{\text{in}}}{\rho_{\text{cat}}(1 - \varepsilon_{\text{bed}})V_{\text{bed}}} - \frac{Q_0[S_p]}{V_{\text{bed}}} + R_{S_p} - \frac{[S_p]A}{V_{\text{bed}}}\frac{dh}{dt}$
$Y: P_0, \lambda_0, \lambda_1, \lambda_2, \mu_0, \mu_1, \mu_2$	$\frac{d[Y]}{dt} = R_Y - \frac{Q_0[Y]}{V_{\text{bed}}} - \frac{[Y]A}{V_{\text{bed}}}\frac{dh}{dt}$

The mass balance for the bed height is given by:

$$\frac{dh}{dt} = (R_{M_1}M_{w1} + R_{M_2}M_{w2})\frac{V_{\text{bed}}}{\rho_c A} + \frac{F_{\text{cat}}/\rho_{\text{cat}} - Q_0(1 - \varepsilon_{\text{bed}})}{(1 - \varepsilon_{\text{bed}})A} \quad (3.1)$$

And the steady state mass balance for the polymer in the bed is given by the following equation

(when  $h \geq h_{\text{nominal}}$ ):[11]

$$Q_0 = \frac{(R_{M_1}M_{w1} + R_{M_2}M_{w2})V_{\text{bed}}}{\rho_c} + \frac{F_{\text{cat}}}{\rho_{\text{cat}}(1 - \varepsilon_{\text{bed}})} \quad (3.2)$$

The dimensions of the bed are given in Table 3-6.

Table 3-6. Reactor dimensions

Parameter	Designation	Value
$D_{\text{bed}}$	Bed diameter	4.75 m
$\varepsilon_{\text{bed}}$	Bed voidage	0.7
$h$	Height of the bed	13.3 m

In the single-phase model, the gas and particles are assumed to have the same temperature ( $T$ ). The exchanger is considered to be a series of four small counter flow heat exchangers. Based on this, a heat balance of the bed and the exchanger was proposed by Chatzidoukas et al.:[11]

$$\frac{dT}{dt} = \frac{H_{\text{gas}}^{\text{in}} + H_{\text{gas}}^{\text{rec}} + H_{\text{p}}}{H_{\text{cum}}} - \frac{TA}{V_{\text{bed}}} \frac{dh}{dt} \quad (3.3)$$

$$\rho_{\text{gas}} V_j C_{p,\text{gas}} \frac{dT_j}{dt} = F^{\text{rec}} C_{p,\text{gas}} (T_{j-1} - T_j) - U_j A_j (T_j - T_w), j = 1:4 \quad (3.4)$$

$$m_w C_{p,w} \frac{dT_w}{dt} = F_w C_{p,w} (T_w^{\text{in}} - T_w) + \sum_{j=1}^4 U_j A_j (T_j - T_w) \quad (3.5)$$

where  $H_{\text{gas}}^{\text{in}}$ ,  $H_{\text{gas}}^{\text{rec}}$  and  $H_{\text{p}}$  define respectively the enthalpies ( $\text{J s}^{-1}$ ) of the gases in the input stream, the recycle stream, the recycle stream and the heat of polymerization.  $H_{\text{cum}}$  ( $\text{J K}^{-1}$ ) is the cumulated heat. (Table 3-7)  $T$ ,  $T_j$  and  $T_w$  are the temperatures of the bed, exchanger section  $j$  and coolant respectively.  $U_j$ ,  $A_j$  and  $V_j$  are respectively the heat transfer coefficient, the surface area and the volume of the exchanger section  $j$ .  $C_p$  is the specific heat capacity ( $\text{J kg}^{-1} \text{K}^{-1}$ ) and  $\Delta H_{r,i}$  ( $\text{J mol}^{-1}$ ) the enthalpy of polymerization.

Table 3-7. Enthalpies used in the energy balance of the FBR

---


$$H_p = -[R_{M_1} \Delta H_{r,1} + R_{M_2} \Delta H_{r,2}](1 - \varepsilon_{bed})V_{bed}$$

$$H_{cum} =$$

$$\left[ [M_1]C_{p,M_1}M_{w,1} + [M_2]C_{p,M_2}M_{w,2} + [N_2]C_{p,N_2}M_{w,N_2} + [H_2]C_{p,H_2}M_{w,H_2} + [ICA]C_{p,ICA}M_{w,ICA} \right] V_{bed} \varepsilon_{bed} +$$

$$\rho_p C_{p,p}(1 - \varepsilon_{bed})V_{bed}$$

$$H_{gas}^{in} = [F_{M_1}C_{p,M_1} + F_{M_2}C_{p,M_2} + F_{N_2}C_{p,N_2} + F_{H_2}C_{p,H_2}] (T_{gas}^{in} - T)$$

$$H_{gas}^{rec} = F^{rec}C_{p,gas} (T_{gas}^{rec} - T)$$

$$C_{p,gas} = X_{M_1} \frac{C_{p,M_1}}{M_{w,M_1}} + X_{M_2} \frac{C_{p,M_2}}{M_{w,M_2}} + X_{N_2} \frac{C_{p,N_2}}{M_{w,N_2}} + X_{H_2} \frac{C_{p,H_2}}{M_{w,H_2}} + X_{ICA} \frac{C_{p,ICA}}{M_{w,ICA}}$$


---

### 3.3. Correlations of key properties

The main properties to be controlled in the gas-phase copolymerization of ethylene are the polymer melt index (*MI*, or melt flow index *MFI*, g/10 min) and the polymer density ( $\rho_p$ ). Correlations are therefore needed to estimate these properties. *MI* or melt flow index (*MFI*) represents the flow rate of a molten polymer through a standard capillary in 10 minutes under the load of 2.16 kg at 190 °C (ASTM D1238).[24],[16] The available correlations in the literature can be divided into two categories:

- A. Correlations which relate the final properties to the individual monomer conversions in the reactor (i.e. to reacted species) (Table 3-8).[25] These correlations are universal and remain valid when varying the operating conditions.
- B. Correlations which relate the final properties to the operating conditions (i.e. *T*, *P*, or concentrations of unreacted species in the gas phase), such as: [25]

$$\ln MI_i = 3.5 \ln \left( k_0 + k_1 \frac{[M_2]}{[M_1]} + k_2 \frac{[M_3]}{[M_1]} + k_3 \frac{[H_2]}{[M_1]} \right) + k_4 \left( \frac{1}{T} - \frac{1}{T_0} \right)$$

$$\rho_i = \rho_0 + \rho_1 \ln MI_i - \left[ \rho_2 \frac{[M_2]}{[M_1]} + \rho_3 \frac{[M_3]}{[M_1]} \right]^{\rho_4}$$
(3-6)

Where  $k_{i(i=1-4)}$ ,  $\rho_{k(k=0-4)}$  are tuning parameters and  $M_2$  and  $M_3$  are comonomers. Other correlations also exist in the open literature.[26] [27]–[30] Such correlations are only valid for the set of operating conditions for which they were derived and cannot be used if the reaction conditions change; because the thermodynamic effects such as the co-solubility effect will not be accounted for. Therefore, such correlations are not valid during grade transition where the operating conditions change.

In this work, the correlations of the first category (developed by McAuley and MacGregor[25] for both MI and density ) will be employed (Table 3-8), as only such correlations would be able to account for the co-solubility effect for instance. (see Table 3-8).

Concerning the polymer density, the correlation proposed by McAuley and MacGregor [25] is based on patent data collected by Sinclair [31], and it relates the instantaneous polymer density to the comonomer incorporation in the polymer by including  $C_x$  (where  $C_x = \varphi_2 \times 100$ , and  $\varphi_2 =$

$$\frac{R_{M_2}}{R_{M_2} + R_{M_1}}, \text{ see Table 3-2).}$$

Table 3-8. Correlations of Category A for the properties of the polymer: MI and density

Ref	Melt index (g/10 min)	Density (g cm <sup>-3</sup> )	Data from
[25]	$M_w = 111525 MI_i^{-0.288}$ (or $MI = 3.35 \times 10^{17} M_w^{-3.47}$ )	$\rho_i = 0.966 - 0.02386 C_x^{0.514}$	Butene grades [31]
[32]	$MI = 2.7 \times 10^{19} M_w^{-3.92}$		[33]
[33]	$MI = 4.195 \times 10^{19} M_w^{-3.92}$		
[34]	$MI = 3 \times 10^{19} M_w^{-3.92}$	$\rho_i = -0.023 \ln C_x + 0.9192$	Octene grades [35]

The cumulative density  $\rho_c$  (of the polymer exiting the reactor) can be calculated from the instantaneous one (this being produced at time t) by integration over the residence time ( $\tau$ ). [36]

$$\frac{d(\rho_c^{-1})}{dt} = \frac{1}{\tau} \rho_i^{-1} - \frac{1}{\tau} \rho_c^{-1} \quad (3.7)$$

Regarding the melt index, both instantaneous  $MI_i$  and cumulative  $MI_c$  can be calculated using the correlations in Table 3-9.

Table 3-9 Model of the instantaneous and cumulative polymer molecular weight

	Relation
Instantaneous molecular weight[37]	$M_{w,i} = M_{w,m} \frac{\lambda_2}{\lambda_1}, M_{w,m} = \sum_{i=1}^2 \varphi_i M_{wi}$
Cumulative molecular weight (kg mol <sup>-1</sup> ) [38]	$M_{w,c} = \bar{M}_{w,m} \frac{\lambda_2 + \mu_2}{\lambda_1 + \mu_1}, \bar{M}_{w,m} = \sum_{i=1}^2 \Phi_i M_{wi}$
Instantaneous copolymer composition	$\varphi_i = \frac{R_{M_i}}{\sum_{i=1}^2 R_{M_i}}$
Cumulative copolymer composition	$\Phi_i = \frac{m_{p,i}/M_{w,i}}{\sum_j m_{p,j}/M_{w,j}}$
Mass of polymer per bed unit volume	$\frac{dm_{p,i}}{dt} = R_{M_i} M_{w,i} - \frac{Q_0 m_{p,i}}{V_{bed}} - \frac{m_{p,i} A}{V_{bed}} \frac{dh}{dt}$

### 3.4. Simulation examples

Through the combined kinetics, FBR and thermodynamic model, the effect of ICA on the different parameters of the polymerization process can be evaluated. It can be seen for instance in Figure 3.2 (at a temperature  $T=90^{\circ}\text{C}$ ), the presence of ICA, whether n-hexane for the system ethylene copolymerization with 1-hexene, or iso-butane for the system ethylene copolymerization with 1-butene, increases the PE production rate. This can be explained by the co-solubility effect as presented in chapter 2. In fact, the presence of n-hexane for example increases the concentration of ethylene in the amorphous phase of the polymer. Also, as the total pressure of comonomer and ICA increases, the concentration of comonomer in the amorphous phase also increases (as it depends nonlinearly on the pressure; Figure 2.10). This explains the increase of the rate of polymerization. n-hexane has a more pronounced effect than iso-butene, since the heavier the added ICA to the system, the greater is its effect. This increases the solubility, which leads to an increase in the monomers concentrations in the growing particles, and therefore to a much higher reaction rate.

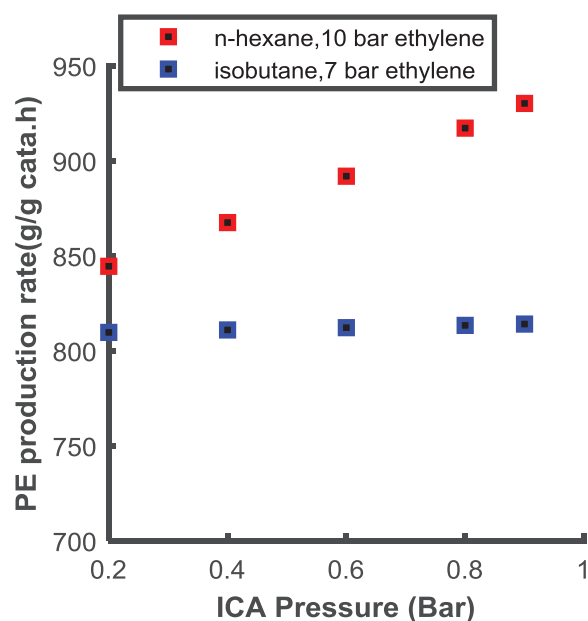


Figure 3.2. Influence of ICAs (n-hexane or iso-butene) on PE production rate in gas-phase ethylene-comonomer (1-hexene or 1-butene) copolymerization at 90°C.

Figure 3.3 shows the effect of the concentration of ICA, whether n-hexane in the quaternary system ethylene/1-hexene/n-hexane/LLDPE or iso-butane in the quaternary system ethylene/1-butene/iso-butane/LLDPE on the cumulative melt index and the cumulative density estimated by the correlations from Table 3-8 and equation (3.7), respectively.

Figure 3.3-a shows that increasing the ICA, leads to an increase in the density. Indeed, since the comonomer and ICA are assumed to be a pseudo-species, adding more ICA forces the decrease of the comonomer flow rate in the case of the (ethylene/1-hexene/ n-hexane/LLDPE), as the total pressure of pseudo-species should not exceed 1 bar for this system. The small decrease in the comonomer flow rate explains the slight increase of the polymer density for this system. This effect is very small (almost invisible) for the system (ethylene/1-butene/iso-butane/LLDPE) under the given pressure and temperature conditions. Hence, the effect of ICA is more pronounced on the molecular weight and so the melt index.

Figure 3.3-b shows that the higher the ICA pressure, the lower the cumulative melt index of the polymer under same temperature. This is due to the fact that the concentration of ethylene

increases with the partial pressure of the pseudo-species ICA and comonomer, which leads to an increase in the polymer molecular weight.

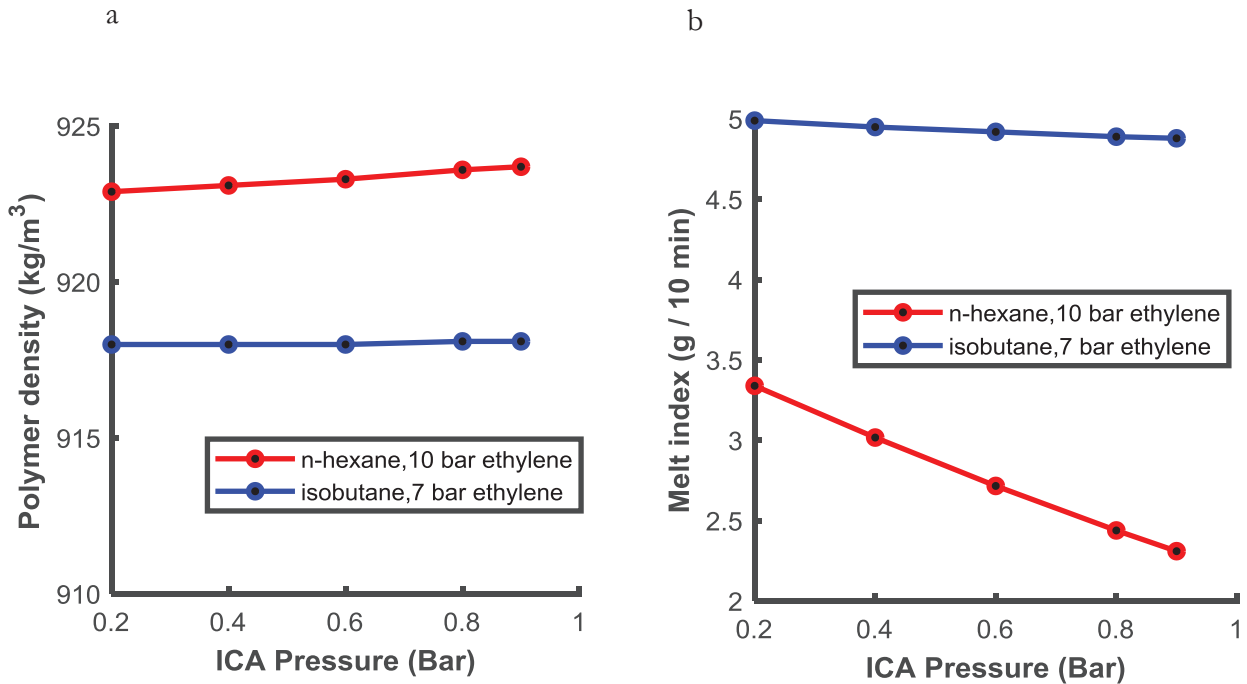


Figure 3.3. ICA effect on: a) the cumulative density and b) the cumulative melt index at 90°C for different quaternary systems (ethylene/1-hexene/ n-hexane/LLDPE) and (ethylene/1-butene/isobutane/LLDPE).

The effect of the temperature variation of the reactor on the concentrations of the different species is also investigated. Figure 3.4-a, shows that the increase in the reactor temperature reduces the concentrations of the reactive species (ethylene and 1-hexene) in the ternary system ethylene/1-hexene/LLDPE (without ICA). This leads to a lower total concentration of (ethylene+1-hexene) in the amorphous phase of the polymer. However, an increase in the temperature leads to an increase of the PE production rate as shown in Figure 3.4-b. Indeed, the temperature affects both thermodynamics (reduces the concentrations in the polymer particle) and polymerization kinetics (increase of the kinetics parameters). The latter governs the production rate behavior in this case.

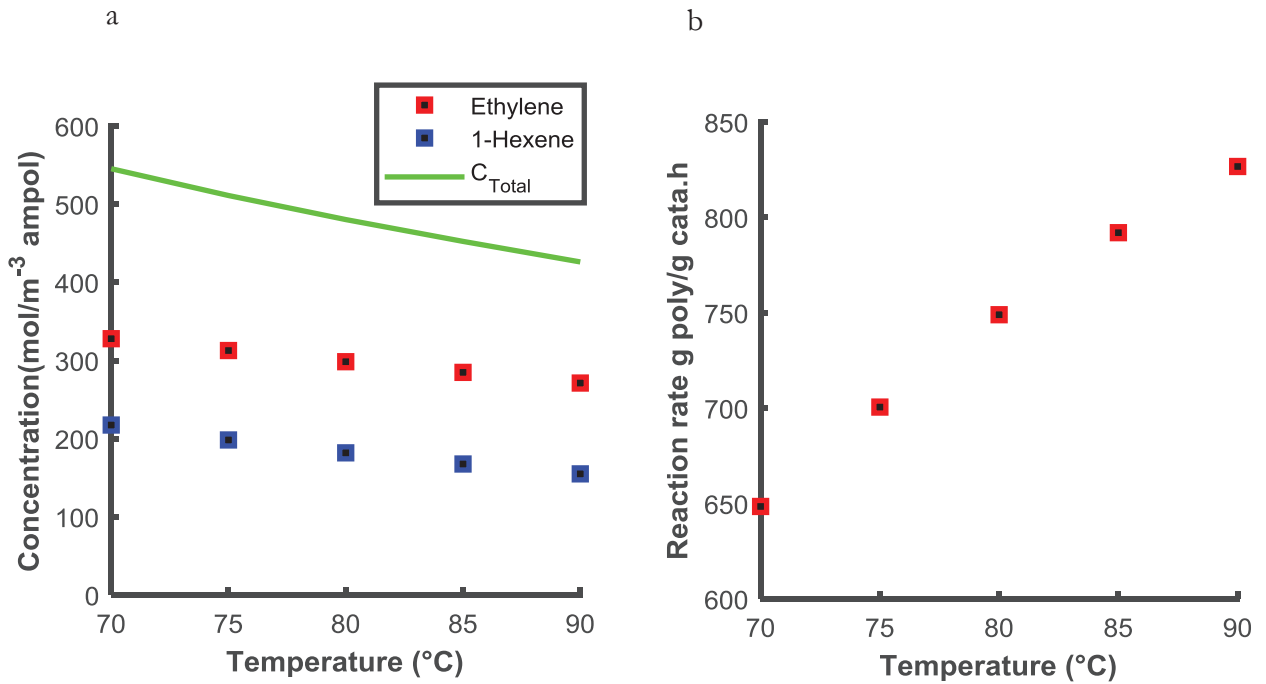


Figure 3.4. Influence of the temperature variation on: a) the concentrations of monomer and comonomer in the amorphous phase of the polymer and b) the PE production rate in a ternary system of (ethylene/1-Hexene/LLDPE).

The temperature also affects the polymer properties. The increase of the density with temperature (Figure 3.5-a), can be explained by the decrease of the comonomer fraction in the polymer presented in Figure 3.4-a. The decrease of the melt index at higher temperature (see Figure 3.5-b) can be explained by the increase of the polymer molecular weight, due to the increased kinetic parameters, activation energies and the temperature effect on the different concentrations of the system.

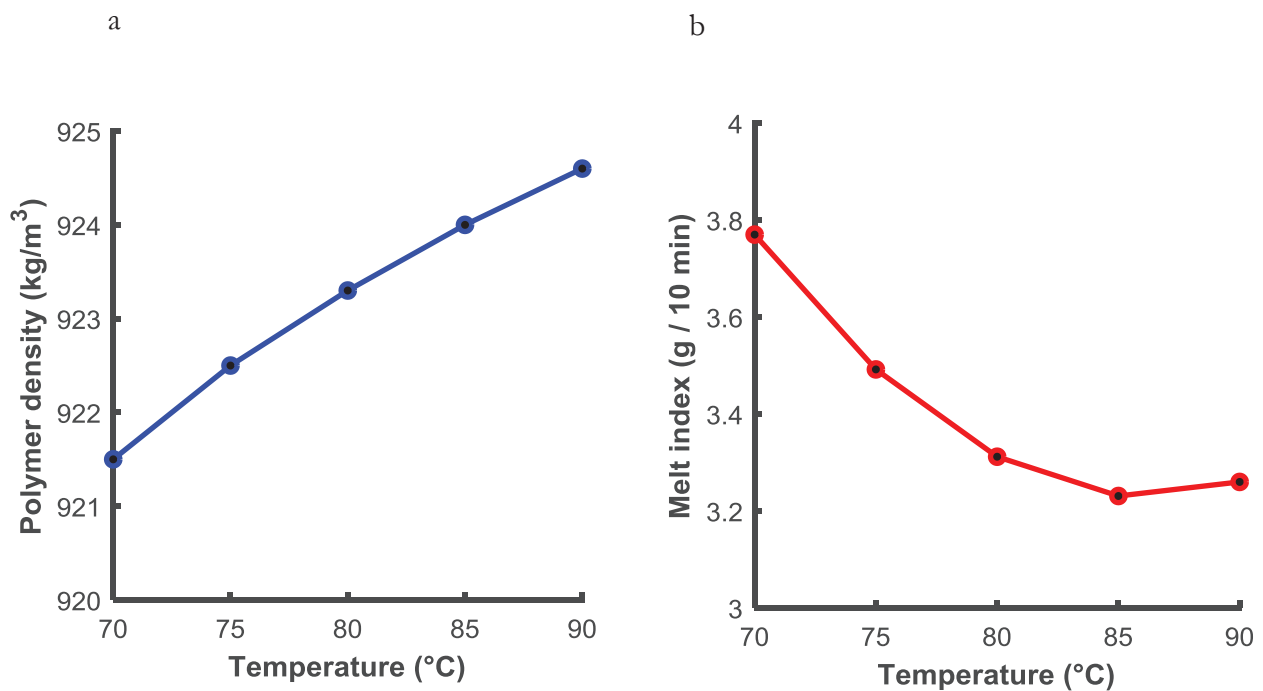


Figure 3.5. Temperature effect on: a) the cumulative density and b) the cumulative melt index at 90°C for the ternary system of (ethylene/1-Hexene/LLDPE).

Figure 3.6 and Figure 3.7 show the effect of changing the flowrates of hydrogen and comonomer on the main polymer properties, i.e. the melt index and density. First (Figure 3.6), only the flowrate of comonomer was changed from 0.105 to 0.07 kg s<sup>-1</sup>, and the hydrogen flow rate was kept at 1.2 10<sup>-3</sup> kg s<sup>-1</sup>. It can be seen that a change in the comonomer flow rate influences both the MI and the polymer density. The inverse is not true, as changing the flow rate of hydrogen does not impact the polymer density. This highlights the coupling between the control variables and the outputs.

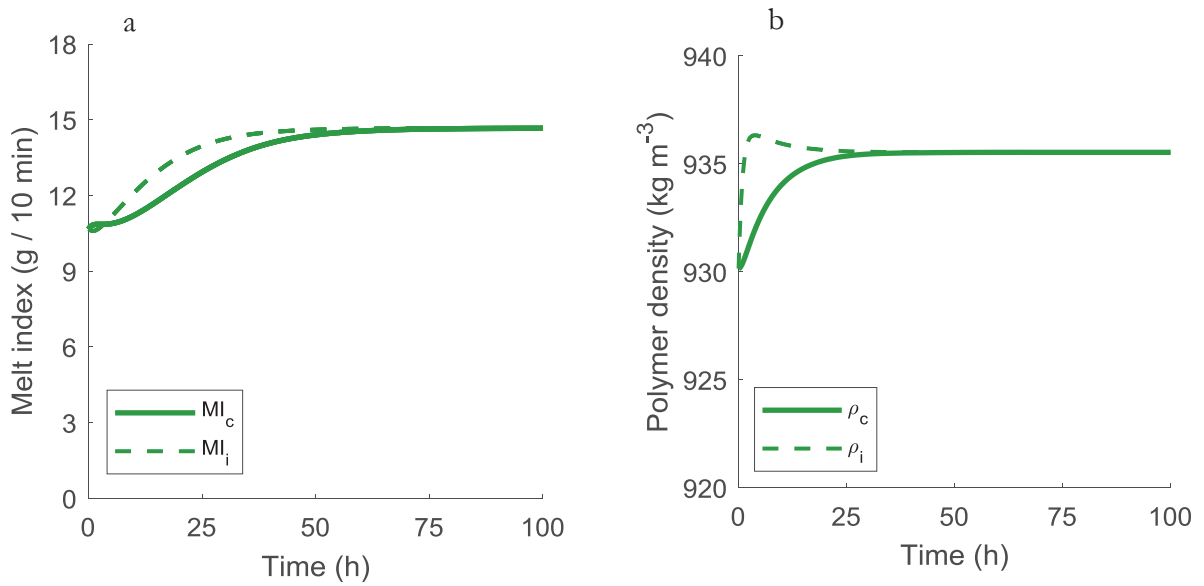


Figure 3.6. Open loop simulation of the system ethylene/1-hexene/LLDPE indicating the change in the MI and density (flow rate of comonomer changed from 0.105 to 0.07 kg s<sup>-1</sup>)

In Figure 3.7, the flowrate of hydrogen was changed from  $1.2 \times 10^{-3}$  to  $1 \times 10^{-3}$  kg s<sup>-1</sup> and the flowrate of comonomer from 0.105 to 0.07 kg s<sup>-1</sup>. As a consequence, the MI decreased from 10.6 to 8.1, and the density increased from 930 to 935.7 kg m<sup>-3</sup>. Indeed, usually in grade specifications, when a product with improved mechanical properties is desired, this means a higher molecular weight (i.e. lower MI) and a higher density. So, in grade transitions, when the density is increased, usually the MI is decreased.

The figures show that the instantaneous properties reach faster the steady state than the cumulative. However, due to the long residence time of the bed, the convergences of both cumulative properties takes about 30 hours in this case (the duration depends on the amplitude of the realized change). The residence time of this system, under the considered operating conditions (initial grade in the figures), is 8.3 hours. Therefore, an optimization is required to accelerate the convergence during grade transitions.

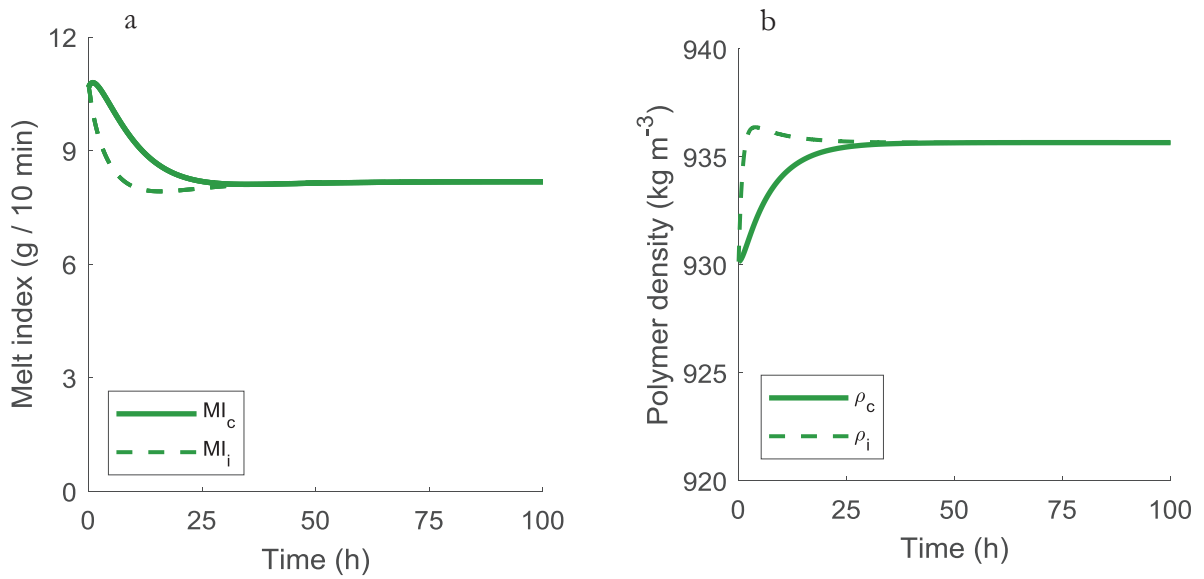


Figure 3.7. Open loop simulation of the system ethylene/1-hexene/LLDPE indicating the change in the MI and density (flowrates of hydrogen changed from  $1.2 \times 10^{-3}$  to  $1 \times 10^{-3}$  kg s<sup>-1</sup> and of comonomer from 0.105 to 0.07 kg s<sup>-1</sup>)

## 4. Conclusions

In this chapter, we presented the different models, other than the thermodynamic models, necessary in this work, as well as the relation between each.

The dynamic model includes the kinetics of copolymerization coupled with the FBR model (the mass and energy balances of a CSTR) and the correlations of the polymer key properties. However, this model does not include a detailed description of all levels (hydrodynamics of the bed and heterogeneity (of species and temperature), diffusion of penetrants within the particle, differences in temperature between the particles and the gas or within the particle, the particle size distribution, multiple site catalysts) and is not dedicated to a specific catalyst so the used kinetics parameters are only indicative. The CSTR bed model can be extended to a multi-compartment model; and the kinetic model can be extended to multiple site catalysts. Also, a particle model would be useful in order to consider the dynamics of diffusion within the particle rather than assuming equilibrium in

terms of thermodynamics. Such improvements are useful and represent important perspectives of this work.

In the next two chapters we study:

- The optimization of PE grade transitions in a fluidized bed reactor taking into consideration the effect of thermodynamics (chapter 4)
- Improving the optimization by adding a constraint on the bed temperature to avoid polymer particle sticking and agglomeration, and ensure the process safety (chapter 5)

# References

- [1] A. Krallis et V. Kanellopoulos, « Application of Sanchez–Lacombe and Perturbed-Chain Statistical Associating Fluid Theory Equation of State Models in Catalytic Olefins (Co)polymerization Industrial Applications », *Ind. Eng. Chem. Res.*, vol. 52, n° 26, p. 9060–9068, juill. 2013, doi: 10.1021/ie401056j.
- [2] K. B. McAuley, J. F. MacGregor, et A. E. Hamielec, « A kinetic model for industrial gas-phase ethylene copolymerization », *AIChE J.*, vol. 36, n° 6, p. 837–850, juin 1990, doi: 10.1002/aic.690360605.
- [3] C. Kiparissides, « Polymerization reactor modeling: A review of recent developments and future directions », *Chem. Eng. Sci.*, vol. 51, n° 10, p. 1637–1659, mai 1996, doi: 10.1016/0009-2509(96)00024-3.
- [4] W. H. Ray, « Modelling of Polymerization Phenomena », *Berichte Bunsenges. Für Phys. Chem.*, vol. 90, n° 11, p. 947–955, 1986, doi: 10.1002/bbpc.19860901106.
- [5] W. H. Ray, « Modelling of addition polymerization processes — Free radical, ionic, group transfer, and ziegler–natta kinetics », *Can. J. Chem. Eng.*, vol. 69, n° 3, p. 626–629, 1991, doi: 10.1002/cjce.5450690304.
- [6] T. Xie, K. B. McAuley, J. C. C. Hsu, et D. W. Bacon, « Gas Phase Ethylene Polymerization: Production Processes, Polymer Properties, and Reactor Modeling », *Ind. Eng. Chem. Res.*, vol. 33, n° 3, p. 449–479, mars 1994, doi: 10.1021/ie00027a001.
- [7] J. J. Zacca, « Distributed parameter modelling of the polymerization of olefins in chemical reactors. », p. 1, 1997.
- [8] K. B. McAuley, J. P. Talbot, et T. J. Harris, « A comparison of two-phase and well-mixed models for fluidized-bed polyethylene reactors », *Chem. Eng. Sci.*, vol. 49, n° 13, p. 2035–2045, juill. 1994, doi: 10.1016/0009-2509(94)E0030-T.
- [9] C. Chatzidoukas, « Control and Dynamic Optimisation of Polymerization Reaction Processes », University of London, London, 2004.
- [10] R. Alves, M. A. Bashir, et T. F. L. McKenna, « Modeling Condensed Mode Cooling for Ethylene Polymerization: Part II. Impact of Induced Condensing Agents on Ethylene Polymerization in an FBR Operating in Super-Dry Mode », *Ind. Eng. Chem. Res.*, vol. 56, n° 46, p. 13582–13593, nov. 2017, doi: 10.1021/acs.iecr.7b02963.

- [11] C. Chatzidoukas, J. D. Perkins, E. N. Pistikopoulos, et C. Kiparissides, « Optimal grade transition and selection of closed-loop controllers in a gas-phase olefin polymerization fluidized bed reactor », *Chem. Eng. Sci.*, vol. 58, n° 16, p. 3643–3658, août 2003, doi: 10.1016/S0009-2509(03)00223-9.
- [12] K.-Y. Choi et W. Harmon Ray, « The dynamic behaviour of fluidized bed reactors for solid catalysed gas phase olefin polymerization », *Chem. Eng. Sci.*, vol. 40, n° 12, p. 2261–2279, janv. 1985, doi: 10.1016/0009-2509(85)85128-9.
- [13] F. A. N. Fernandes et L. M. F. Lona, « The fluidized bed reactor with a prepolymerization system and its influence on polymer physicochemical characteristics », *Braz. J. Chem. Eng.*, vol. 20, n° 2, p. 171–179, juin 2003, doi: 10.1590/S0104-66322003000200011.
- [14] H. Hatzantonis, H. Yiannoulakis, A. Yiagopoulos, et C. Kiparissides, « Recent developments in modeling gas-phase catalyzed olefin polymerization fluidized-bed reactors: The effect of bubble size variation on the reactor's performance », *Chem. Eng. Sci.*, vol. 55, n° 16, p. 3237–3259, août 2000, doi: 10.1016/S0009-2509(99)00565-5.
- [15] D. Kunii et O. Levenspiel, « Bubbling Bed Model. Model for Flow of Gas through a Fluidized Bed », *Ind. Eng. Chem. Fundam.*, vol. 7, n° 3, p. 446–452, août 1968, doi: 10.1021/i160027a016.
- [16] F. Nascimento de Andrade, « Effect of condensable materials during the gas phase polymerization of ethylene on supported catalysts », Université Claude Bernard Lyon 1, 2019.
- [17] F. H. C. Edgecombe, « The Vapor Phase Polymerization of Ethylene on an Organotitanium Catalytic Surface », *Can. J. Chem.*, vol. 41, n° 5, p. 1265–1275, 1963.
- [18] R. D. A. Lipman et R. G. W. Norrish, « Kinetic studies with a Ziegler catalyst system in the gaseous phase », *Proc. R. Soc. Lond. Ser. Math. Phys. Sci.*, vol. 275, n° 1362, p. 310–337, 1963.
- [19] A. B. de Carvalho, P. E. Gloor, et A. E. Hamielec, « A kinetic mathematical model for heterogeneous Ziegler-Natta copolymerization », *Polymer*, vol. 30, n° 2, p. 280–296, févr. 1989, doi: 10.1016/0032-3861(89)90118-3.
- [20] J. Sun *et al.*, « Solubility measurement of hydrogen, ethylene, and 1-hexene in polyethylene films through an intelligent gravimetric analyzer », *J. Appl. Polym. Sci.*, vol. 134, n° 8, 2017, doi: 10.1002/app.44507.

- [21] N. M. Ghasem, W. L. Ang, et M. A. Hussain, « Dynamics and stability of ethylene polymerization in multizone circulating reactors », *Korean J. Chem. Eng.*, vol. 26, n° 3, p. 603–611, mai 2009, doi: 10.1007/s11814-009-0102-1.
- [22] S. Chakravarti et W. H. Ray, « Kinetic study of olefin polymerization with a supported metallocene catalyst. II. Ethylene/1-hexene copolymerization in gas phase », *J. Appl. Polym. Sci.*, vol. 80, n° 8, p. 1096–1119, mai 2001, doi: 10.1002/app.1194.
- [23] A. Alizadeh et T. F. L. McKenna, « Condensed Mode Cooling in Ethylene Polymerisation: Droplet Evaporation », *Macromol. Symp.*, vol. 333, n° 1, p. 242–247, nov. 2013, doi: 10.1002/masy.201300092.
- [24] M. F. Bergstra, G. Weickert, et G. B. Meier, « Metallocene-Catalyzed Gas-Phase Ethylene Copolymerization: Kinetics and Polymer Properties », *Macromol. React. Eng.*, vol. 3, n° 8, p. 433–447, oct. 2009, doi: 10.1002/mren.200900019.
- [25] K. B. McAuley, « Modelling, Estimation and Control of Product Properties in a Gas Phase Polyethylene Reactor », A Thesis, McMaster University, Hamilton, Ontario, 1991.
- [26] H.-S. Yi, J. H. Kim, C. Han, J. Lee, et S.-S. Na, « Plantwide Optimal Grade Transition for an Industrial High-Density Polyethylene Plant », *Ind. Eng. Chem. Res.*, vol. 42, n° 1, p. 91–98, janv. 2003, doi: 10.1021/ie0202221.
- [27] P.-O. Larsson, J. Akesson, et N. Andersson, « Cost function design for economically optimal grade changes for a polyethylene gas phase reactor », in *IEEE Conference on Decision and Control and European Control Conference*, Orlando, FL, USA, déc. 2011, p. 6590–6595, doi: 10.1109/CDC.2011.6160620.
- [28] M. Ogawa, M. Ohshima, K. Morinaga, et F. Watanabe, « Quality inferential control of an industrial high density polyethylene process », *J. Process Control*, vol. 9, n° 1, p. 51–59, févr. 1999, doi: 10.1016/S0959-1524(98)00029-8.
- [29] A. Gisas, B. Srinivasan, et D. Bonvin, « Optimal grade transitions for polyethylene reactors », in *Computer Aided Chemical Engineering*, vol. 15, Elsevier, 2003, p. 463–468.
- [30] A. Kiashemshaki, N. Mostoufi, R. Sotudeh-Gharebagh, et S. Pourmahdian, « Reactor Modeling of Gas-Phase Polymerization of Ethylene », *Chem. Eng. Technol.*, vol. 27, n° 11, p. 1227–1232, nov. 2004, doi: 10.1002/ceat.200401964.
- [31] K. B. Sinclair, « Characteristics of Linear LPPE and Description of UCC Gas Phase Process », 1983.
- [32] K. C. Seavey, Y. A. Liu, N. P. Khare, T. Bremner, et C.-C. Chen, « Quantifying Relationships among the Molecular Weight Distribution, Non-Newtonian Shear

- Viscosity, and Melt Index for Linear Polymers », *Ind. Eng. Chem. Res.*, vol. 42, n° 21, p. 5354–5362, oct. 2003, doi: 10.1021/ie021003i.
- [33] T. Bremner, A. Rudin, et D. G. Cook, « Melt flow index values and molecular weight distributions of commercial thermoplastics », *J. Appl. Polym. Sci.*, vol. 41, n° 7–8, p. 1617–1627, 1990, doi: 10.1002/app.1990.070410721.
- [34] J. Shi, L. T. Biegler, et I. Hamdan, « Optimization of grade transitions in polyethylene solution polymerization processes », *AIChE J.*, vol. 62, n° 4, p. 1126–1142, avr. 2016, doi: 10.1002/aic.15113.
- [35] A. J. Peacock, « Handbook of Polyethylene », p. 54.
- [36] M. R. Rahimpour, J. Fathikalajahi, B. Moghtaderi, et A. N. Farahani, « A Grade Transition Strategy for the Prevention of Melting and Agglomeration of Particles in an Ethylene Polymerization Reactor », *Chem. Eng. Technol.*, vol. 28, n° 7, p. 831–841, 2005, doi: 10.1002/ceat.200500055.
- [37] W. H. Ray, « On the mathematical modeling of polymerization reactors », *J. Macromol. Sci. Macromol. Chem.*, vol. 8, n° 1, p. 1–56, 1972.
- [38] T. Xie et A. E. Hamielec, « Modelling free-radical copolymerization kinetics—evaluation of the pseudo-kinetic rate constant method, 1. Molecular weight calculations for linear copolymers », *Macromol. Theory Simul.*, vol. 2, n° 3, p. 421–454, 1993.

# Chapter 4 Optimization of PE Grade Transitions in FBR

---

Results in this chapter have been published in *Macromolecular Reaction Engineering* journal:

S. Kardous, T. F. L. McKenna, N. Sheibat-Othman, “Thermodynamic effects on grade transition of polyethylene polymerization in fluidized bed reactors”, 2000013, 14 (2020) *Macromolecular Reaction Engineering*, DOI: 10.1002/mren.202000013

## 1. Introduction

Gas-phase processes are adequate for multipurpose production of a wide range of Polyethylene grades. The variety of PE applications requires different grade specifications to suit the market demand. As has been seen in the first chapter, most processes used to make linear low density polyethylene (LLDPE) are gas phase processes to avoid problems linked to the solubility of amorphous polymers in liquid hydrocarbons. These processes are clean, solvent-free and less energy consuming than free radical processes (lower temperature and pressure), but their productivity is limited by the capacity of heat evacuation. This type of reactors is then frequently operated under condensed mode, which consists of injecting induced condensing agents (ICAs) to absorb part of the reaction heat. However, the presence of ICA affects the solubility of monomers in the polymer as was shown previously, so it is important to account for this effect in a grade transition optimization strategy.

In this chapter, the grade transition of PE copolymers in a gas-phase FBR operating under condensed mode is considered. The system therefore includes the polymer, the monomer ethylene, a comonomer and ICA (i.e. three penetrants, so a quaternary system). First, a literature review of grade transition policies proposed in the literature is presented. Then, the findings from chapter 2 concerning the effect of ICA (n-hexane or iso-butane) on the absorption of monomer (ethylene)

and comonomer (1-butene or 1-hexene) using a model based on the Sanchez-Lacombe equation of state (SL EoS) and experimental data from literature, will be used in this chapter.[1],[2] Since no sufficient experimental data are available in the open literature for quaternary systems (i.e. a copolymerization in presence of an ICA), the simplifying thermodynamic correlations proposed in the same chapter are used to calculate the equilibrium solubility for two copolymerization systems of ethylene with  $\alpha$ -olefins; and so to allow for fast prediction of the co-solubility effects in a quaternary system.[2] The thermodynamic model is then combined to the kinetic and process model presented in chapter 3, and used to optimize the transitions between different grades of LLDPE. This is the first time to the best of our knowledge, a multicomponent thermodynamic model has been used for the optimization of grade transition of polyethylene. Finally, the simulation results are discussed to highlight the importance of thermodynamic model during grade transitions.

## 2. Grade transition of Polyethylene

### 2.1. Key properties during transition

It is essential to be able to produce in the same plant different types of polyethylene via frequent grade transition policies, to meet the market needs as well as the broad range of polyolefin applications, such as wire coatings and films. This trend has appeared in the polyolefin industry since few decades such as the case of the Philips Plant which is able to produce few dozens of polymer grades.[3] Therefore, the polymer industry was forced to move away from the classical continuous production of the single polymer grade to a more flexible production strategy.[4], [5] The grade transition problem examined in this chapter is the catalytic gas phase polymerization process of polyolefin in a fluidized-bed reactor. The key parameters frequently used to describe the polymer product quality in a FBR are the melt index ( $MI$ ) and the polymer density ( $\rho_p$ ), because

they are easy to measure and they give quite important indications for polymer processing and use properties.[4], [6], [7] These two properties are linked to process operation (so they can be controlled online).[4]

On one hand, the melt index is related to the polymer viscosity which highly depends on the polymer molecular weight ( $M_w$ ) as well as its distribution that is governed both by the transfer to hydrogen and the comonomer fraction in the copolymer. It describes the facility with which the polymer can be processed after melting. The higher the molecular weight, the lower the polymer melt index becomes; and so the more viscous is the melted polymer (at a specific temperature) and so the more difficult it can be processed in an extruder, which requires higher energy.[6] The choice between high or low melt index polymers is decided according to the market demand/application, which may prefer the low MI polymers, despite the difficulty of production, as a polymer with a high  $M_w$  presents favorable rheological properties such as high stress, crack resistance and tensile strength.[8] Note that the polymer molecular weight distributions, branching and the type of comonomer may also affect the melt index, therefore the correlations describing the melt index are usually valid for a comonomer (and somehow catalyst) type.

On the other hand, the density is related to the polymer degree of branching related to the comonomer fraction in the copolymer and on the polymer crystallinity. The higher are the number of branches and the branch chain length, the lower the PE density becomes: the number of branches is generally lower than 10 branches per 1000 carbons for a high-density PE (HDPE;  $\rho > 0.94 \text{ kg/m}^3$ ); LLDPE ( $\rho \sim 0.915 - 0.93 \text{ kg/m}^3$ ) chains generally contain 10 to 35 branches per 1000 carbons, and a very low-density PE (VLDPE) has the lowest density, presents a high number of short-chain branches.[6] Likewise, an increase in the degree of crystallinity leads to a higher PE density, and thus a strong, stiff and tough material. However, information about the branch size, the branch frequency distribution and the crystallinity of the polymer is significant for the industrial processability, which radically differs from an LDPE to an LLDPE, although they might have

similar densities, which again makes the used correlations valid only to a specific comonomer type or range of operability.[4]

Consequently, the reactor' grade transition from one specific melt index and density to the next are required in order to adjust the polymer product quality. But, this is not a simple task in a polymerization plant.[9] The process variables that affect the most these properties and that are required to be manipulated online are the flow rates of hydrogen and comonomer.

## 2.2. Overview of grade transition strategies

Conducting polymer grade transition is affected by a set of diverse process aspects, including the reactor design, the residence time, the residence time distribution, the runtime per grade and especially the plant safety that may be affected by the properties of the polymer. All these aspects should be explicitly or implicitly considered. In a continuous polymer production, the grade transition can result in a large amount of transition product, which can partly be outside of the specifications (off-spec), and a long transition time that might exceed 10 hours or even some days depending on the required change and bed volume. The long transition time is mainly due to the long residence time of polymer in the bed.[10] This amount of transition products can be more amplified if we increase the frequency of the grade changes, which is determined by the market demand and the economic profitability (can be each couple days). Consequently, a significant loss of raw material, and production time as well as a waste of manpower and a contamination of the environment are some of the issues that can be encountered.[5]

The first method would be to shut down the reactor, empty it, and modify one or more of the operating conditions, and then restart to produce a new grade. However, this represents an expensive practice for polyolefin industry.[4] Debling et al.[11] studied the effect of different parameters on grade transition of solution, slurry, bulk and gas-phase polyolefin reactions in commonly used reactors, including horizontal or vertical stirred beds, loop and FBRs. They

indicated the residence time distribution of the different components to be a determining factor in the speed of grade transition and summarized the procedures employed to speed the transition in FBRs, such as de-inventorying the reactor content or venting/overshooting the gases at the beginning of the transition. However, they did not investigate the effect of ICA on the residence time of the reactor. Rahimpour et al.[12] also indicated that partial venting of the reactor, composing a new gas phase and reducing the bed level, reduce the quantity of transition product in PE FBRs. They highlighted that such so-called semi-continuous strategy was necessary in some situations in order to keep the reactor temperature between the gas dew point and the polymer melting point (to avoid agglomeration of the particles), which could not be achieved with the continuous strategy (i.e. by controlling only the flow rates). Note that the flow rates employed during the transition were those used for the final grade, which were calculated by solving the model equations under steady state conditions, and identifying the boundary conditions to be implemented for each new grade. However, numerous works indicated that the flow rates of the final grade do not necessarily ensure the best transition, and suggested the employment of dynamic optimization or control algorithms to ensure better transitions. [13],[14]

For the particular problem of grade transition in FBRs, most model-based works are based on offline optimization, rather than online control, due to the long calculation time and the complexity of problem formulation. McAuley et al.[7],[15] were the first to investigate dynamic optimization of grade transition of PE in gas-phase FBR. They provided a kinetic model for copolymerization, correlations for the final properties based on patent data (i.e. melt index and polymer density), and modelled the FBR as a continuous stirred tank reactor (CSTR) due to its high recycle ratio and low single pass conversion. The suggested control variables were the flow rates of hydrogen and comonomer (1-butene or 1-hexene), as they directly affect the polymer molecular weight and density. Afterwards, optimization strategies were proposed for different types of processes, for instance for slurry high density polyethylene (HDPE) processes composed of two loop reactors[16] or two CSTRs.[17]

Furthermore, different improvements in the optimization approaches were suggested. For instance, Chatzidoukas et al.[18] proposed a mixed integer dynamic optimization approach to realize a closed-loop control in a fluidized-bed reactor. Nystrom et al.[19] employed a comparable approach based on dynamic optimization combined to a mixed-integer linear problem related to the sequencing, and solved these decoupled problems by iteration. Bonvin et al.[20] proposed to employ a measurement-based approach by tracking the necessary conditions of optimality, for instance based on run-to-run basis, in order to correct for modelling mismatch in a homopolymerization process.

Regarding closed-loop control, it was usually considered using algorithms based on an optimization criterion, such as model predictive control (MPC). The closed-loop character of MPC makes it more robust to modelling errors than open-loop dynamic optimization. But, in order to allow its online implementation in FBRs, part of the optimization is usually solved offline. For instance, Wang et al.[21] combined an offline optimizer and a nonlinear MPC, where the optimal feed rates were calculated offline and the MPC allowed minimizing the modeling error and updating the feed rates. A shrinking horizon nonlinear model predictive control with expanding horizon least-squares estimation was also implemented to control the grade transition in FBRs. [22]

It should be noted that the high nonlinearity of the system and the interaction/coupling between the different inputs and outputs, as well as the high unstable behavior of the FBR (i.e. sensitivity of fluidization to the inputs and polymer properties, which adds some constraints) [10], [23]–[25] greatly complicates the reactor control. Among the cited works, in terms of methodology, it could be seen that dynamic optimization-based policies were the most widely used for gas-phase processes, and they will therefore be employed in this work. Indeed, the optimization criterion is flexible and can be tuned to optimize instantaneous or cumulative properties during transition, or the transition time. Dynamic optimization is usually opted when time-dependent (decision) variables are considered, like the majority of dynamic systems in chemical engineering, and the problem formulation includes differential equation constraints.[26].

In addition, the previous literature analysis highlights showed that the parameters that most affect the grade transition are the residence time (and its distribution) and the hydrogen and comonomer flow rates. However, the thermodynamic interactions that are due to the use of a condensing agent and/or comonomer were not considered in the presented literature. This work is focused particularly on condensed mode, and will use a more representative thermodynamic model that takes into account the interactions between the different species.

## 2.3. Grade transition

### 2.3.1 Formulation of the optimization problem

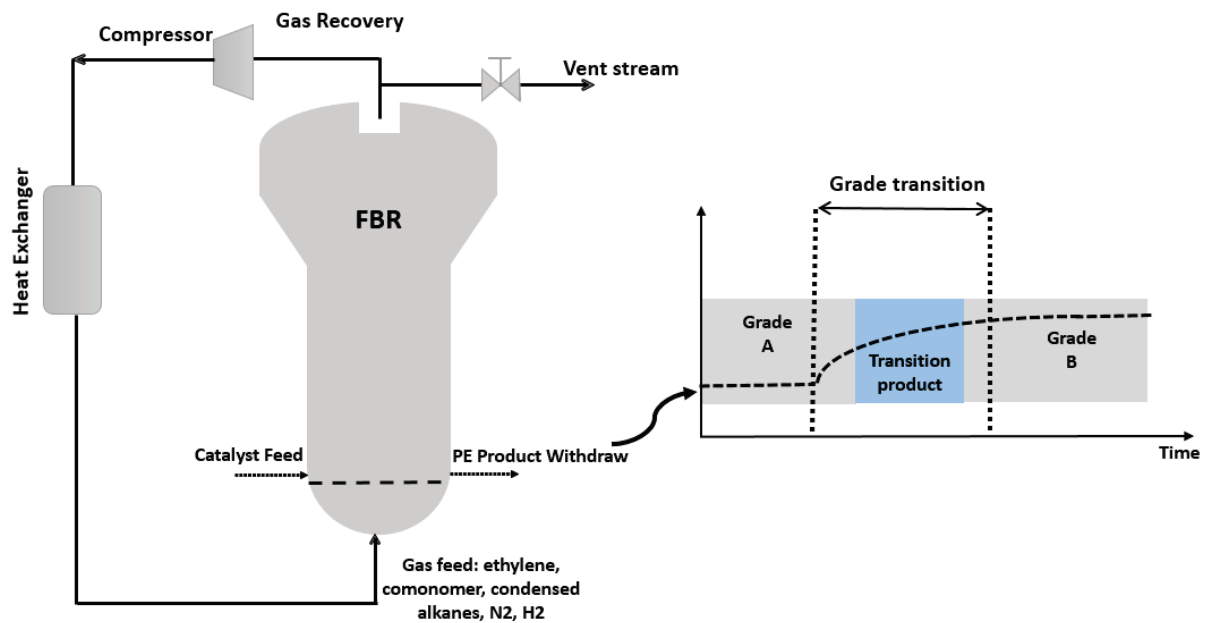


Figure 4.1. Grade transition strategy for PE gas-phase polymerization under condensed mode operating.

The manipulated variables are the flow rates of hydrogen and comonomer and the controlled outputs are the melt index and the polymer density. The hydrogen acts as a chain transfer agent which allows to control the molecular weight. The type as well as the amount of the comonomer

affect the architecture and end-use properties of PE in different ways; here we focus on the polymer density.[27]

The optimization problem can be written as follows:[15]

$$\min_{\mathbf{u}(t)} J(\mathbf{u}(t), \mathbf{x}(t)), t \in [t_0, t_f] \quad (4.1)$$

$$\mathbf{u}_{\min} \leq \mathbf{u}(t) \leq \mathbf{u}_{\max} \quad (4.2)$$

where  $J$  is the objective function,  $\mathbf{x}(t)$  is the vector of state variables (see Table 3-5) and  $\mathbf{u}(t)$  represents the vector of manipulated variables,  $\mathbf{u}(t) = [F_{H_2}, F_{com}]$ . The inequality constraints (4.2) indicate the available ranges of manipulated variables; here simply fixed at  $\mathbf{u}_{\min} = 0.1 \mathbf{u}_0(t)$  and  $\mathbf{u}_{\max} = 5 \mathbf{u}_0(t)$ , where  $\mathbf{u}_0(t)$  is the optimal input vector of the previous grade.

In Figure 4.1 we take a closer look at the optimal strategy used to handle the grade transition problem. The major focus of the grade transition is to reduce the transition product and/or the time of transition, knowing that the grade transition ends only when the required PE properties reach the desired specification.

### 2.3.2 Objective function

In this chapter, the considered objective function is the following:

$$J(\mathbf{u}) = \int_{t_0}^{t_f} w_1 \frac{|MI_i - MI_{sp}|}{MI_{sp}} + w_2 \frac{|MI_c - MI_{sp}|}{MI_{sp}} + w_3 \frac{|\rho_i - \rho_{sp}|}{\rho_{sp}} + w_4 \frac{|\rho_c - \rho_{sp}|}{\rho_{sp}} dt + w_5 \sum_{i=1}^2 \frac{\Delta u_i}{u_i(t_0)} \quad (4.3)$$

By considering both instantaneous and cumulative properties (of the melt index and polymer density), and by a good tuning the weighting factors  $w_i$  (with  $i = 1 - 5$ ), one may accelerate the convergence of cumulative properties while keeping the instantaneous properties within an acceptable range. The key properties used in the objective function ( $MI$  and  $\rho$ ) are estimated with the simplified correlation found in the open literature as suggested in chapter 3. The last term on

the right hand side of this equation is intended to minimize the variation of the input during the transition, in order to avoid oscillations (as in model predictive control). The normalization of the different terms (i.e. the division by the set-points of the *MI* and density) allows for an easier tuning of the weighting factors. The indices **i**, **c** and **sp** refer to the instantaneous, cumulative and set-point properties, respectively. The optimization is solved using the function `fmincon` of Matlab®. At a constant reaction rate, the proposed objective function allows reducing the quantity of transition product as well as the transition time, even though the time is not explicitly minimized in this function. If the reaction rate varies during the transition, then this objective function allows minimizing only the transition time. The minimization of the transition product would necessitate, in case of variable reaction rate, to multiply the criterion by the instantaneous reaction rate ( $R_p$ ), as done by McAuley and MacGregor[15] for instance. Takeda et al.[16] suggested that the choice between minimizing the transition product and the transition time should be based on the market demand: at high polymer sales and plant capacity production it is preferred to minimize the transition time; while at low polymer sales and reduced plant capacity it is preferred to minimize the transition production and authorize a longer transition time. A transition product can usually be sold, although at a discounted price.

### 2.3.3 *Degree of freedom of the inputs*

It is usually sufficient to assume the manipulated variables (here, the flow rates of hydrogen and comonomer) to vary by a series of ramps during the transition.[15] Based on the literature study and the residence time of the considered FBR (~7-10 hours in this study, depending on the operating conditions), the transition is divided into 5 intervals, where the final interval corresponds

to the steady state interval, to be maintained until the end of the production of the new grade. Thus, the optimization allows switching the flow rates every 2 hours during the first 8 hours, and the last ramp corresponds to the steady state flow rate of the new grade. The duration of each grade production is usually defined by the market demand, the specifications or the claims of the production. Here, an arbitrary duration of production of each grade of 30 hours is implemented in both systems. No particular change is required at the optimization level to change to shorter or longer production periods, only the final times need to be indicated. Therefore, the last optimized ramp is employed between 8 to 30 hours.

### 3. Simulation results and discussion

The proposed strategy is evaluated in grade transition starting from grade A, to grade B with higher or lower  $MI$  and  $\rho$ , then coming back to grade A, for both of the copolymerization systems (Table 4-1). These choices are based on LLDPE specifications, i.e.  $MI \in [0.01-100]$  g/10min [4] and  $\rho \in [915-935]$  kg m<sup>-3</sup> [6]. The initial steady state conditions, producing grade A, are given in Table 4-2.

The weighting factors were tuned as follows, except otherwise mentioned:  $w_1 = 0.4$ ,  $w_2 = 1$ ,  $w_3 = 7$ ,  $w_4 = 10$  and  $w_5 = 10^4$ . This choice was based on few simulation tests, in a way to ensure a compromise between fast convergence of the cumulative properties while reducing the overshoots of the instantaneous properties. Indeed, while allowing for big variations in the instantaneous properties lead to a faster convergence of the cumulative properties, some conditions of comonomer or hydrogen pressures might lead to polymer softening or sticking problems.[28] Excessive overshoots of the melt index or density also provoke uncontrollable effects on the overall polymer distribution properties in the reactor, hence they should be avoided.[4] In the

following simulations, temperature control is assumed to be perfectly controlled in the bed at the nominal working temperature.

Table 4-1. LLDPE grades considered in the grade transition policy

Grade	Melt index Target (g / 10 min)		Density Target (kg m <sup>-3</sup> )	
	1-hexene	1-butene	1-hexene	1-butene
A	2.7	4.5	923.3	918.4
B	4	2	916	922
A	2.7	4.5	923.3	918.4

Table 4-2. Initial conditions of the grade transition simulations (leading to grade A under steady state)

	1-hexene	1-butene
$T$ (°C)	90	90
$P_1$ (bar)	9.4	7
$P_2$ (bar)	0.35	1.55
$P_{ICA}$ (bar)	0.6	3.5
$P_{H_2}$ (bar)	2.2	2.2
$F_{H_2}$ (kg/s)	0.001	0.0013
$F_{com}$ (kg/s)	0.11	0.19

### *Copolymerization of ethylene and 1-hexene in presence of n-hexane as ICA*

The optimization strategy was evaluated using the parameters of the first system, i.e. the copolymerization of ethylene with 1-hexene in presence of n-hexane. Note that the thermodynamic model was developed for this system for ethylene pressure of 10 bar and pseudo-component (i.e.

comonomer plus ICA) pressure on the range of 0-1 bar. Therefore, the simulations (including the choices of the set-points) are conducted in a way to respect these ranges.

Figure 4.2 shows the results of the two grade transitions, from A to B, and from B back to A. This scenario was simulated using the following weighting factors:  $w_1 = 0.4$ ,  $w_2 = 1$ ,  $w_3 = 7$ ,  $w_4 = 10$  and  $w_5 = 0$ , therefore the instantaneous properties ( $MI_i$  and  $\rho_i$ ) go beyond the set-point (SP) during the transition in order to accelerate the convergence of the cumulative properties ( $MI_c$  and  $\rho_c$ ). This is related to the variations of the flow rates of hydrogen and 1-hexene, which are higher at the beginning of the grade transition and then they stabilize, as indicated by the increase in the pressure. The overshoots in the instantaneous properties can be reduced by decreasing the weighting factors multiplying the cumulative properties  $w_2$  and  $w_4$  compared to those of the instantaneous properties  $w_1$  and  $w_3$ , or by considering  $w_5 \neq 0$ , or by adding constraints on the outputs, as discussed in the following scenario. The  $MI$  is inversely proportional to the polymer molecular weight. Therefore, an increase in the hydrogen pressure during the transition, from grade A to B for instance, led to a decrease in the polymer molecular weight and thus to an increase in the melt index. Likewise, an increase in the comonomer pressure during the transition from grade A to B, led to an increase in the amount of short branches and thus to a decrease in the polymer density. The proposed strategy allows to move either to higher (grade A to grade B) or lower (B to A) values of  $MI$ , and vice versa for  $\rho$ .

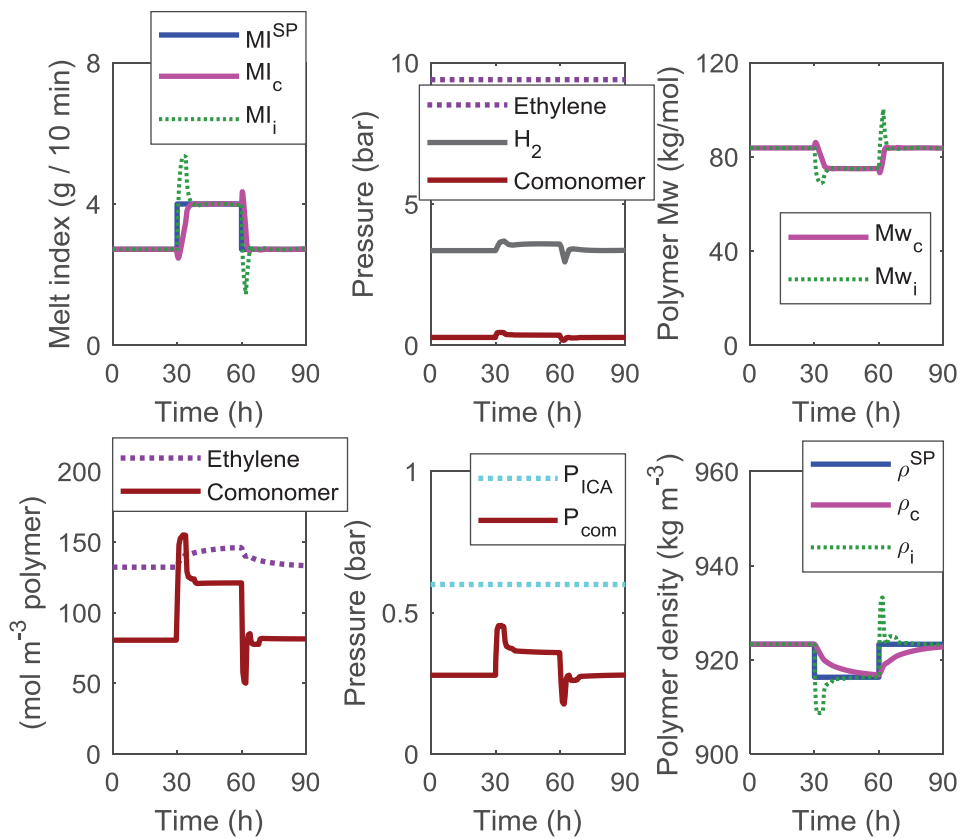


Figure 4.2. Grade transition in ethylene-1-hexene copolymerization in presence of n-hexane at  $90^{\circ}\text{C}$  ( $w_1 = 0.4$ ,  $w_2=1$ ;  $w_3=7$ ,  $w_4 = 10$ ,  $w_5 = 0$ ).

The figure shows that the concentration of ethylene in the polymer particles (which constitutes the site of the reaction) does not change significantly during the transition, where the comonomer flow rate is varied, so the co-solubility effect is low in this sense and under the realized changes in the comonomer pressure. Note that the ethylene pressure is maintained constant in all the grades. However, the concentration of comonomer in the polymer particles is highly affected by these changes, which demonstrates the necessity of using a good thermodynamic model. The impact of the thermodynamic model is investigated more deeply in the last section of this chapter. Note that the total pressure of comonomer and ICA reached 1.05 bar at the maximum in this simulation, but only for a short duration, and therefore the employed thermodynamic correlation remains valid during most of the time ( $P_{\text{ICA}}+P_{\text{com}}=0-1$  bar).

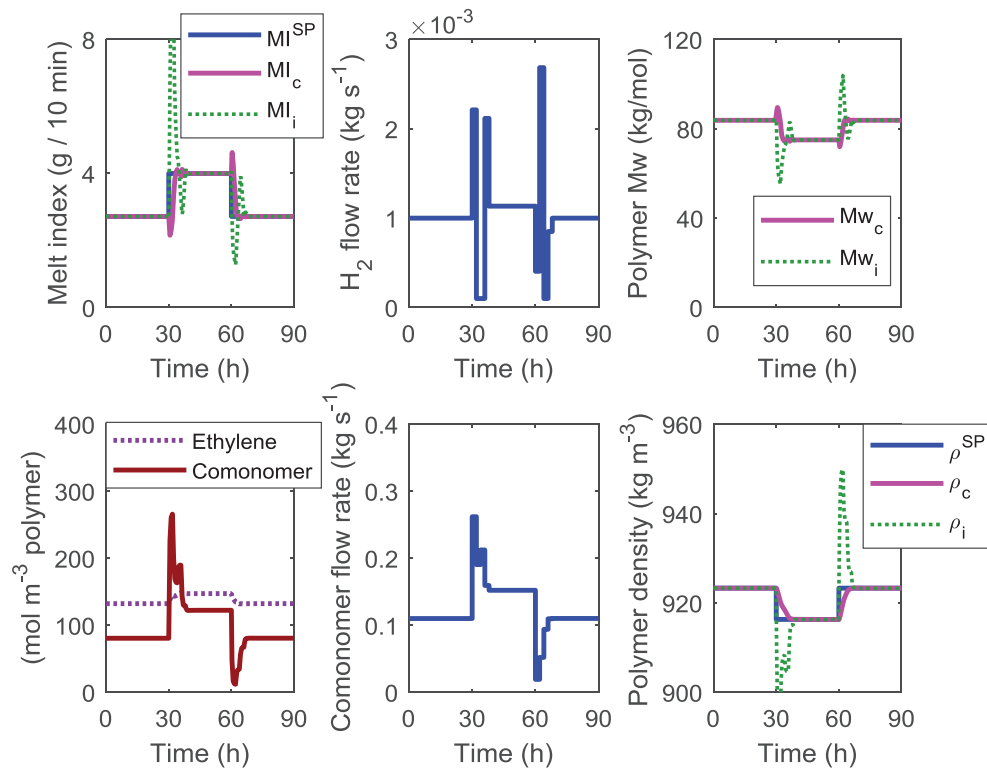


Figure 4.3. Grade transition in ethylene-1-hexene copolymerization in presence of n-hexane at  $90^{\circ}C$  ( $w_1 = 0$ ,  $w_2=1$ ;  $w_3=0$ ,  $w_4 = 10$ ,  $w_5 = 0$ ).

The same scenario presented in Figure 4.2 was simulated when setting the weighting factors of the instantaneous properties to zero, i.e.  $w_1 = w_3 = 0$ . This indicates that only the cumulative properties are tracked, while full freedom is given to the instantaneous properties. The results of this simulation are shown in Figure 4.3, in which it can be seen that the overshoots in the instantaneous properties ( $MI_i$  and  $\rho_i$ ) are more pronounced than in Figure 4.2 (where both the instantaneous and the cumulative properties were tracked, by adjusting the coefficients of the objective function). The objectives in these scenarios is to show that the strategy is capable to realize transition in both directions (increasing as well as decreasing the  $MI$  and the density). The speed of convergence in both directions is not the same, due to the residence time constraints. Of course, in real industrial production, there are transitions in both directions, with different production times (note that the production time of each grade was set to 30 hours in the presented simulations just as an example).

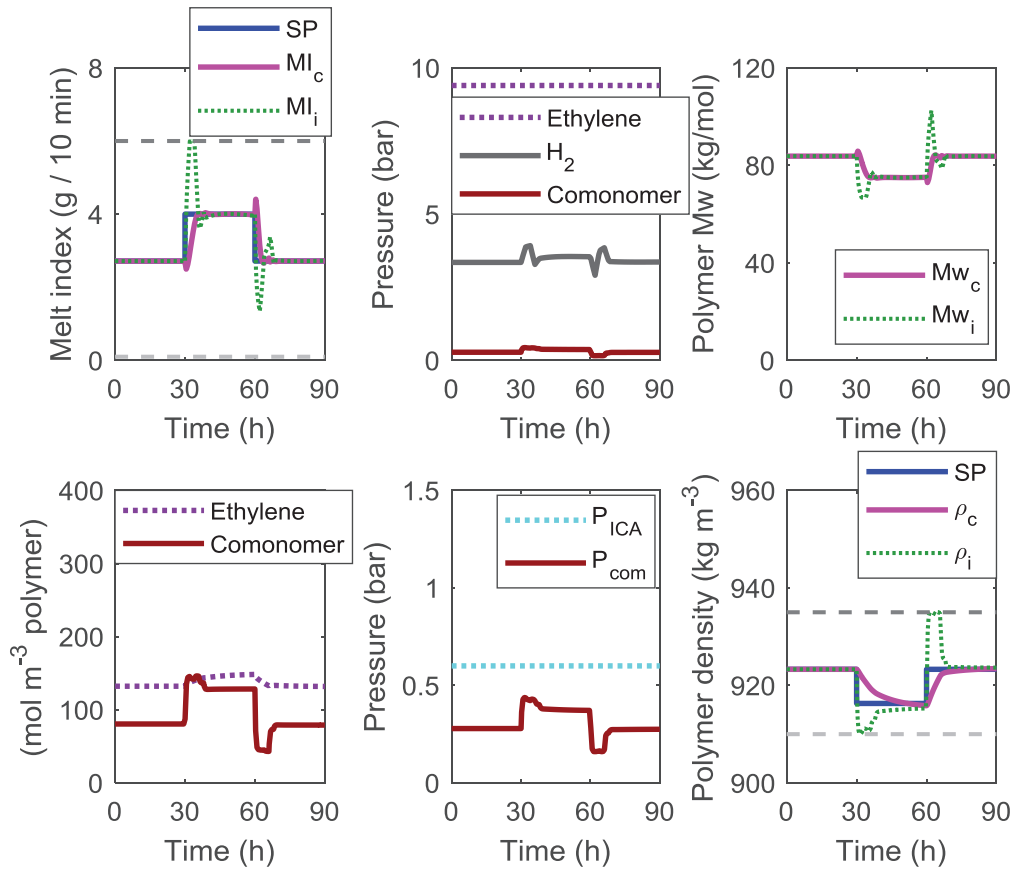


Figure 4.4. Grade transition in ethylene-1-hexene co-polymerization in presence of n-hexane: Tracking of the cumulative properties ( $w_1 = w_3 = w_5 = 0; w_2 = 1; w_4 = 4$ ), with constraints on the instantaneous properties ( $0.1 < MI_i < 6$  and  $910 < \rho_i < 935$ ).

The same scenario presented in Figure 4.2 was simulated again while tracking only the cumulative properties (i.e.  $w_1 = w_3 = 0$ ) but while considering constraints on the instantaneous properties, as follows:  $0.1 < MI_i < 6$  and  $910 < \rho_i < 935$  (Figure 4.4). It can be seen that the convergence of the cumulative properties is slowed down compared to Figure 4.2, but the overshoots in the instantaneous properties ( $MI_i$  and  $\rho_i$ ) are reduced and kept within the constraints. Adding hard constraints allows remaining within the acceptable range of properties, but it slows down the calculation. Another way to reduce the overshoots in the instantaneous properties, without considering constraints, consists of increasing the values of  $w_2$  and  $w_4$  with respect to  $w_1$  and  $w_3$  or by considering  $w_5 \neq 0$  (as shown in the next section).

## Copolymerization of ethylene and 1-butene in presence of iso-butane as ICA

The proposed grade transition optimization strategy was evaluated in the second pseudo-quaternary system: ethylene and 1-butene copolymerization in presence of iso-butane as ICA. Note that the thermodynamic model was developed for different conditions for this system: i.e. ethylene pressure of 7 bar and pseudo-component pressure on the range of 5-10 bars. The set-points of the melt index and polymer density of grades A and B were also set differently in this system, but still within LLDPE grades. The same weighting factors as the first system were considered.

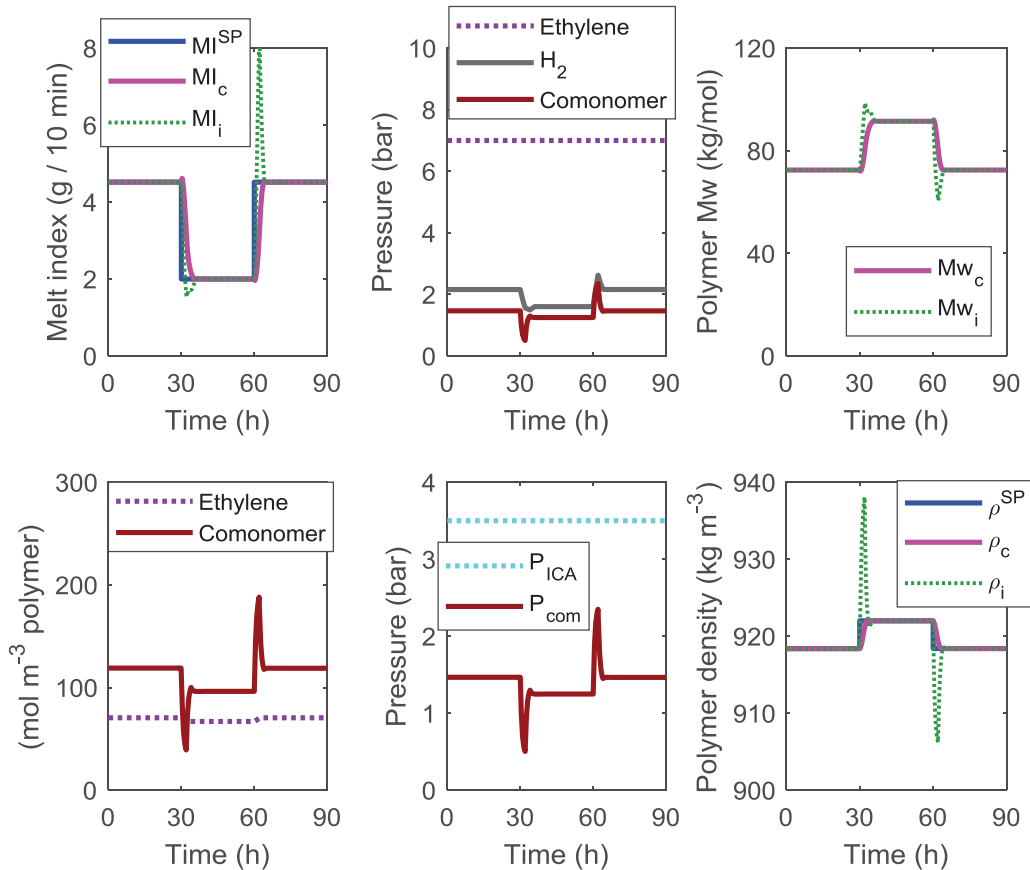


Figure 4.5. Grade transition in ethylene-1-butene co-polymerization in presence of iso-butane ( $w_1 = 0.4, w_2=1, w_3=7, w_4 = 10$  and  $w_5 = 0$ ).

Figure 4.5 shows the simulation results. The melt index converges in about 5 hours to the set-point, while the density converges to the set-point in 3 hours. The overshoots of the instantaneous

properties remain acceptable, but they can be reduced by either manipulating the weighting coefficients (as discussed in the following scenario) or by adding hard constraints on the outputs as discussed in the previous section. Note that the total pressure of comonomer and ICA is around 6 bar, therefore the employed thermodynamic correlation is valid ( $P_{ICA}+P_{com}=5-10$  bar).

The last term of the objective function ( $w_5 \sum_{i=1}^2 \frac{\Delta u_i}{u_i(t_0)}$ ) can allow minimizing the variation of the manipulated variables (flow rates of hydrogen and the comonomer), and thus to reduce the overshoots in the instantaneous properties. Indeed, injecting big amounts of hydrogen or comonomer rapidly increases the risk of polymer softening and stickiness.[28] As a consequence, adding this term is expected to reduce the overshoots in the instantaneous properties. Due to the low values of the variations of the flow rates, it was necessary to have a high weighting factor, ( $w_5 = 10^4$ ), to ensure an impact on the performance. Figure 4.6 shows the results when adding this term to the objective function, which is to be compared to Figure 4.5 done under the same conditions but without this term. The figure clearly shows that the pressures of hydrogen and comonomer undergo less changes. As a consequence, the instantaneous properties have lower overshoots. However, this delays a little the convergence of the cumulative properties to the set-points. A compromise is thus to be determined between fast convergence of the cumulative properties and less variation in the instantaneous properties.

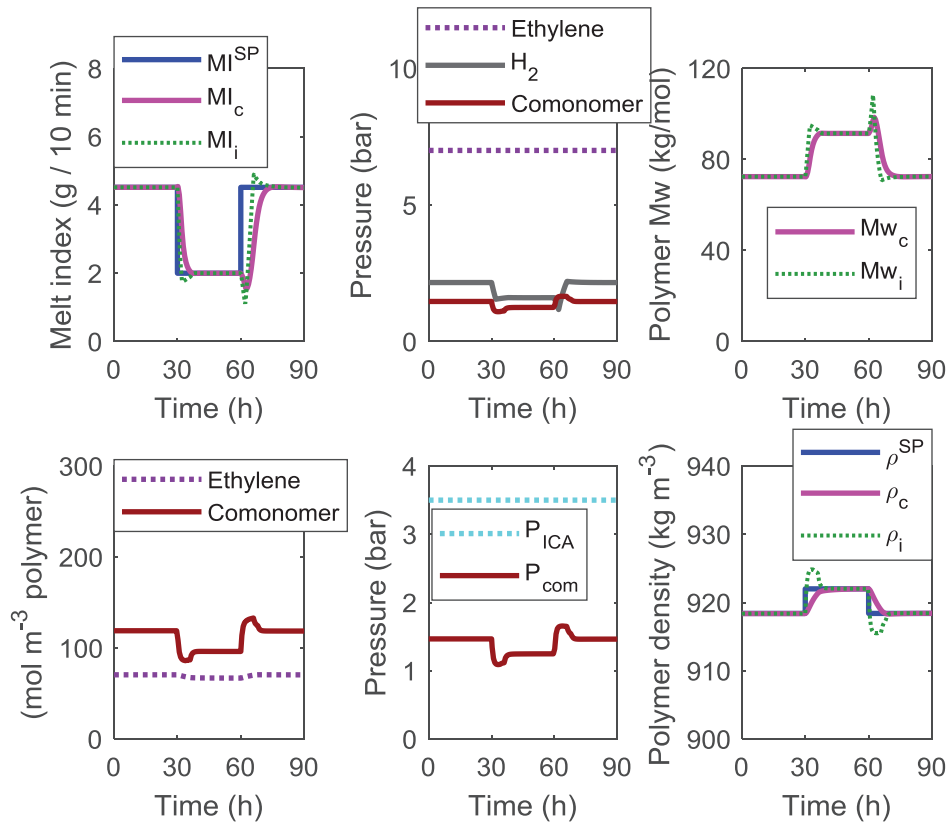


Figure 4.6. Grade transition in ethylene-1-butene: effect of the term  $w_5 \sum_{i=1}^2 \frac{\Delta u_i}{u_i(t_0)}$  in the objective function ( $w_1 = 0.4$ ,  $w_2=1$ ,  $w_3=7$ ,  $w_4 = 10$  and  $w_5 = 10^4$ )

In order to evaluate the gain realized by the optimization strategy, its performance was compared to the case of injecting the optimal feed rates of the final grade during the transition (here called the final steady-state, SS), as done for instance by Rahimpour et al.[12] (Figure 4.7). When employing a constant flow rate during the transition, the convergence time is that of the residence time of the reactor. It can be seen that employing the optimized varying flow rates during the transition allows reducing the convergence times of the cumulative melt index and the density.

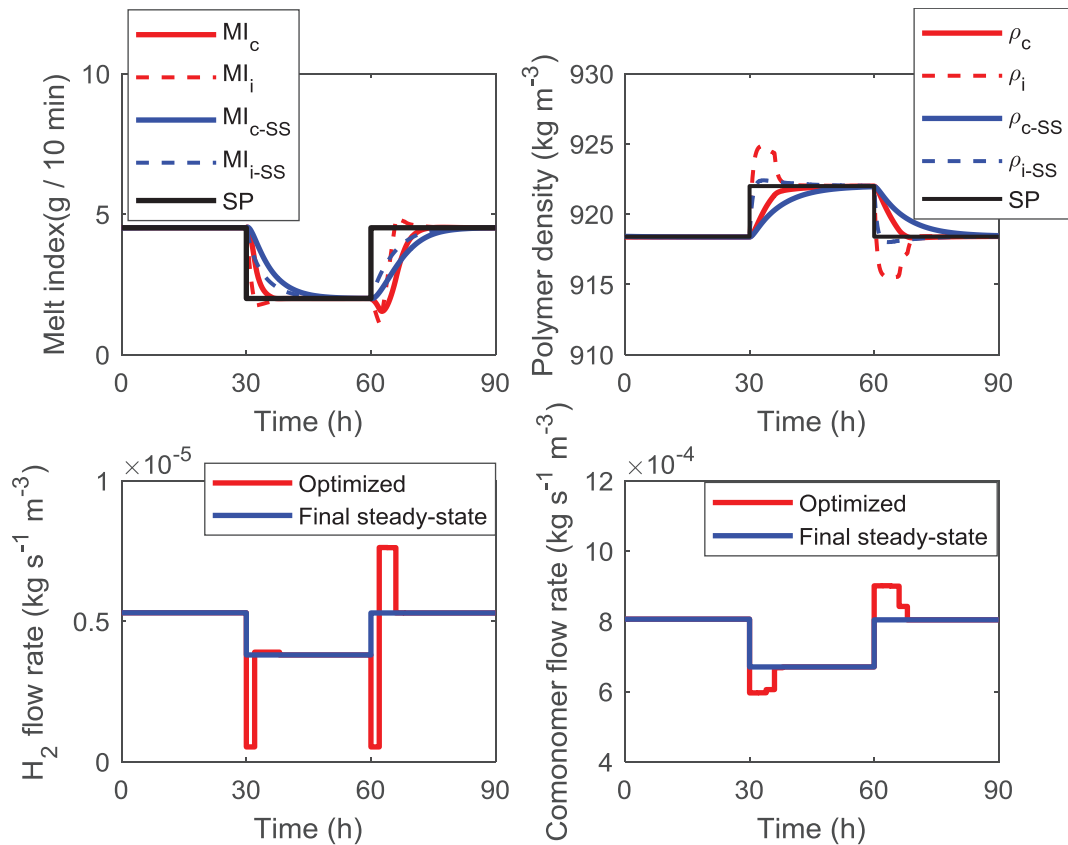


Figure 4.7. Grade transition in ethylene-1-butene copolymerization: comparison between the proposed grade transition strategy (leading to varying optimized flow rates during the transition) and injecting a constant flow rate during the transition (corresponding to the optimal flow rate of the final grade, under steady-state conditions)

### *Impact of the thermodynamic model*

In order to demonstrate the importance of employing a good thermodynamic model in the optimization strategy, two scenarios were simulated. The first scenario was performed by assuming an error in the parameters of the thermodynamic model. The second system was used for this purpose, i.e. ethylene-1-butene co-polymerization in presence of iso-butane as ICA.

In Figure 4.8, an error is assumed in the parameters  $A$  and  $D$  in equations 2-17 and 2-18, related to the calculation of ethylene and comonomer concentrations in polymer,  $[M_1^P]$  and  $[M_2^P]$ , respectively. It can be seen that the employed flow rates bring the process to different set-points

than the desired ones (lower  $MI$  and  $\rho$ , as the used parameters  $A$  and  $D$  were assumed to be underestimated). Indeed, using lower  $A$  and  $D$  parameters in the model gives lower  $[M_1^P]$  and  $[M_2^P]$  than the real ones. In order to correct ratios of monomer to hydrogen as well as to comonomer (to obtain the desired properties), the optimization strategy forces the decrease in the hydrogen flow rate, which leads to an increase in the polymer molecular weight, and a decrease in the  $MI$ . Similarly, the optimization forces the decrease in the comonomer flow rate, and as a result of errors in  $[M_1^P]$  and  $[M_2^P]$ , a decrease in the polymer density is observed in this case. Note that the optimization strategy continues to work adequately, but as it is based on a wrong model it does not converge to the correct optimal points, therefore the use of an adequate thermodynamic model is essential.

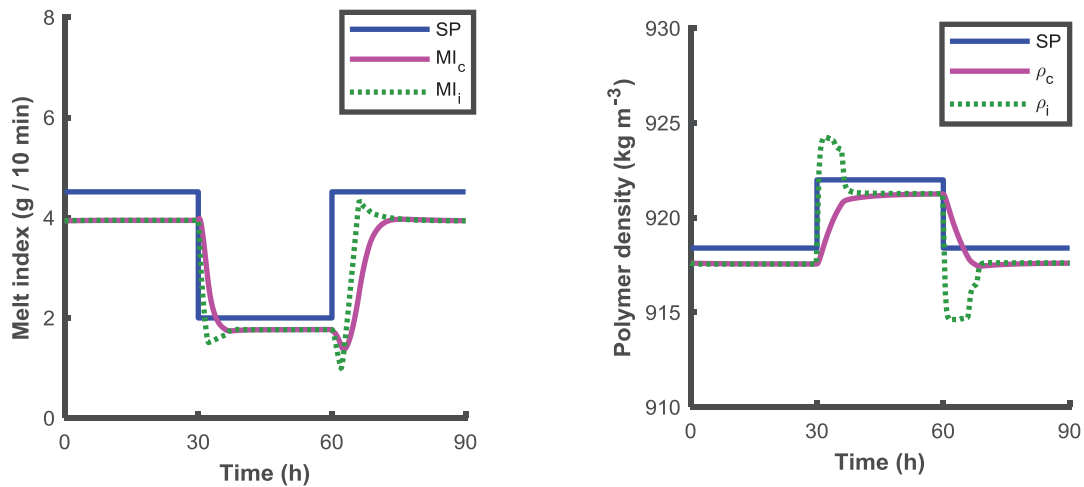


Figure 4.8. Influence of the thermodynamic model parameters on the process response, in ethylene and 1-butene copolymerization (Process parameters:  $A = 1.98 \text{ mol m}^{-3} \text{ bar}^{-1}$ ,  $D = 180 \text{ mol m}^{-3}$ , Model parameters used for optimization:  $A = 0.992 \text{ mol m}^{-3} \text{ bar}^{-1}$ ,  $D = 90.2 \text{ mol m}^{-3}$ )

The second scenario was performed by switching to a binary model to describe the solubility of the different species in the polymer (i.e. with no co-solubility effect). The system ethylene-1-hexene co-polymerization in presence of n-hexane as ICA was used for this simulation. In this case, the thermodynamic model leads to the calculation of an incorrect concentration of ethylene in the

amorphous phase of the polymer,  $[M_1^P]=121 \text{ mol m}^{-3}$  at 10 bar ethylene and  $90^\circ\text{C}$  (as it assumes a binary system)[29] instead of around  $133 \text{ mol m}^{-3}$  estimated in the pseudo-quaternary system. It also calculates an incorrect comonomer concentration in the polymer particle  $[M_2^P]$ . The concentration of 1-hexene in a binary system (1-hexene+LLDPE)[30] is expected to be higher compared to its concentration in a ternary system due to the anti-solvent effect of ethylene (as shown in Figure 2.11). However, combining ICA+comonomer in a pseudo-quaternary system leads to a global pressure which is much higher. As indicated by Figure 2.12, a small change in the pressure leads to a high change in the solubility of the pseudo-component, so the quaternary system leads to a much higher concentration of comonomer in the particles than in a binary system at the same pressure. Note however that the same flow rate is injected in the model and the process, but different reaction rates occur (due to the use of different thermodynamic models), therefore the comonomer pressure varies a lot between the two simulations, and therefore it is not straightforward to compare the concentration of comonomer in the model and the process in this simulation. In this simulation, when  $[M_2^P]= 80.6 \text{ mol m}^{-3}$  in the pseudo-quaternary system, it was  $[M_2^P]= 77.5 \text{ mol m}^{-3}$  in the binary model.

The simulation test was performed using the binary model for both the concentrations of ethylene and 1-hexene in the amorphous phase of the polymer (so the model and grade transition is simulated using the binary model while the process is simulated using the pseudo-quaternary model). Figure 4.9 shows that using a binary thermodynamic model and ignoring the co-solubility effect leads to a big drift of the properties from the set-points. Indeed, the model assumes a lower  $[M_1^P]$  (so a lower polymer molecular weight and a higher  $MI$ ). Therefore, the optimization strategy based on this model makes the decision to decrease the hydrogen flow rate. However, when implemented to the process (simulated using the pseudo-quaternary model, where the concentration of monomer is higher), this flow rate leads to a higher  $M_w$ , so to a lower  $MI$ . Following the same reasoning, a drift in the polymer density occurs due to errors in both  $[M_1^P]$  and

$[M_2^P]$ . This simulation demonstrates the importance of using an adequate thermodynamic model in the optimization strategy.

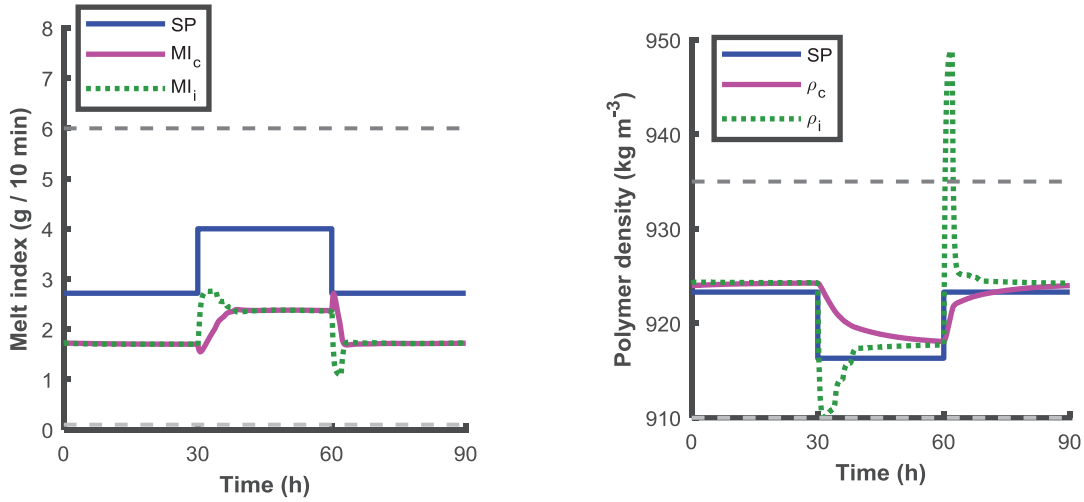


Figure 4.9. Influence of using binary thermodynamic model (not taking in account the co-solubility effect) on the process response. System ethylene-1-hexene copolymerization in presence of n-hexane at 90°C. ( $w_1 = 0.4$ ,  $w_2=1$ ;  $w_3=7$ ,  $w_4 = 10$ ,  $w_5 = 10^4$ )

## 4. Conclusions

In this chapter, off-line dynamic optimization was implemented to optimize the grade transitions in a fluidized bed reactor of polyethylene. This strategy was based on the combined kinetic and thermodynamic model previously developed (chapters 2 and 3), in order to account for the co-solubility effects of the different gas species. Two different quaternary systems were considered, the copolymerization of ethylene with 1-hexene in presence of n-hexane as ICA and the copolymerization of ethylene with 1-butene in presence of iso-butane.

The simulation results demonstrate the importance of the thermodynamic model in the optimization strategy. A good control of the polymer melt index and density could be realized by manipulating the flow rates of hydrogen and comonomer. Nevertheless, in both systems, the co-solubility effect of comonomer on ethylene was not observed, which is due to the low impact of the pseudo-component on the solubility of ethylene under the employed operating conditions

(pressure and temperature). The importance of the thermodynamic model was mainly related to evaluating the concentration of comonomer in the polymer during the transition, which highly impacts the polymer properties.

Both the instantaneous and the cumulative properties could be controlled, in a duration lower than the residence time of the reactor. The role of the weighting factors, in the minimization function, is determinant at this level, where it can either give more importance to controlling the instantaneous properties (thus eliminating any overshoot) or on the contrary allow a faster control of the cumulative properties in detriment of the instantaneous ones. A compromise between these two options is necessary in order to ensure a fast convergence of the cumulative properties to the set-points (thus reduce the transition product) while avoiding big variations in the flow rates or pressures of hydrogen and comonomer as they may increase the risk of polymer sticking or softening, that will be treated with more details in the chapter 5. To reach the same objective, constraints on the instantaneous properties can be considered, but this slows down the calculation. The proposed optimization tool should allow a more efficient operation and a better control of the polymer quality. Indeed, the optimization strategy can be easily updated in presence of any improvement of the simplified kinetics and polymerization models. Moreover, the availability of more thermodynamic data or the use of a particle model accounting for diffusion would allow to improve the precision of the outcome of the optimization strategy. The developed strategy can also be used for simple systems (e.g. ternary or binary systems) when using a classical kinetic model of homopolymerization.

Finally, the novelty in this work lies essentially in the use of more detailed thermodynamic considerations within the model in order to include the thermodynamic effect of induced condensed agents on the grade transitions of ethylene polymerization fluidized bed reactors, which was clearly described in this chapter.

# References

- [1] I. C. Sanchez et R. H. Lacombe, « Statistical Thermodynamics of Polymer Solutions », *Macromolecules*, vol. 11, n° 6, p. 1145-1156, nov. 1978, doi: 10.1021/ma60066a017.
- [2] R. Alves, M. A. Bashir, et T. F. L. McKenna, « Modeling Condensed Mode Cooling for Ethylene Polymerization: Part II. Impact of Induced Condensing Agents on Ethylene Polymerization in an FBR Operating in Super-Dry Mode », *Ind. Eng. Chem. Res.*, vol. 56, n° 46, p. 13582-13593, nov. 2017, doi: 10.1021/acs.iecr.7b02963.
- [3] M. P. McDaniel, « Controlling polymer properties with the Phillips chromium catalysts », *Ind. Eng. Chem. Res.*, vol. 27, n° 9, p. 1559-1564, 1988.
- [4] C. Chatzidoukas, « Control and Dynamic Optimisation of Polymerization Reaction Processes », University of London, London, 2004.
- [5] Z. Liao, P. Wang, J. Wang, et Y. Yang, « A heuristic approach to grade transition strategy of the HDPE slurry process in different operation modes », *Clean Technol. Environ. Policy*, vol. 15, n° 5, p. 833-849, oct. 2013, doi: 10.1007/s10098-012-0574-2.
- [6] D. P. Lo et W. H. Ray, « Dynamic Modeling of Polyethylene Grade Transitions in Fluidized Bed Reactors Employing Nickel-Diimine Catalysts », *Ind. Eng. Chem. Res.*, vol. 45, n° 3, p. 993-1008, févr. 2006, doi: 10.1021/ie0580598.
33. K. B. McAuley, Modelling, Estimation and Control of Product Properties in a Gas Phase Polyethylene Reactor, Ph.D. Thesis, McMaster University **1991**.
- [8] F. W. Billmeyer, *Textbook of Polymer Science*. John Wiley & Sons, 1984.
- [9] W. H. Ray, « Modelling of Polymerization Phenomena », *Berichte Bunsenges. Für Phys. Chem.*, vol. 90, n° 11, p. 947-955, 1986, doi: 10.1002/bbpc.19860901106.
- [10] K.-Y. Choi et W. Harmon Ray, « The dynamic behaviour of fluidized bed reactors for solid catalysed gas phase olefin polymerization », *Chem. Eng. Sci.*, vol. 40, n° 12, p. 2261-2279, janv. 1985, doi: 10.1016/0009-2509(85)85128-9.
- [11] J. A. Debling, G. C. Han, F. Kuijpers, J. Verburg, J. Zacca, et W. H. Ray, « Dynamic modeling of product grade transitions for olefin polymerization processes », *AIChE J.*, vol. 40, n° 3, p. 506-520, mars 1994, doi: 10.1002/aic.690400312.
- [12] M. R. Rahimpour, J. Fathikalajahi, B. Moghtaderi, et A. N. Farahani, « A Grade Transition Strategy for the Prevention of Melting and Agglomeration of Particles in an Ethylene

- Polymerization Reactor », *Chem. Eng. Technol.*, vol. 28, n° 7, p. 831-841, 2005, doi: 10.1002/ceat.200500055.
- [13] M. Ohshima, I. Hashimoto, T. Yoneyama, M. Takeda, et F. Gotoh, « Grade Transition Control for an Impact Copolymerization Reactor », *IFAC Proc. Vol.*, vol. 27, n° 2, p. 505-510, mai 1994, doi: 10.1016/S1474-6670(17)48200-0.
- [14] H. Seki, M. Ogawa, S. Ooyama, K. Akamatsu, M. Ohshima, et W. Yang, « Industrial application of a nonlinear model predictive control to polymerization reactors », *Control Eng. Pract.*, vol. 9, n° 8, p. 819-828, août 2001, doi: 10.1016/S0967-0661(01)00046-6.
- [15] K. B. McAuley et J. F. MacGregor, « Optimal grade transitions in a gas phase polyethylene reactor », *AIChE J.*, vol. 38, n° 10, p. 1564-1576, oct. 1992, doi: 10.1002/aic.690381008.
- [16] M. Takeda et W. H. Ray, « Optimal-grade transition strategies for multistage polyolefin reactors », *AIChE J.*, vol. 45, n° 8, p. 1776-1793, août 1999, doi: 10.1002/aic.690450813.
- [17] H.-S. Yi, J. H. Kim, C. Han, J. Lee, et S.-S. Na, « Plantwide Optimal Grade Transition for an Industrial High-Density Polyethylene Plant », *Ind. Eng. Chem. Res.*, vol. 42, n° 1, p. 91-98, janv. 2003, doi: 10.1021/ie0202221.
- [18] C. Chatzidoukas, J. D. Perkins, E. N. Pistikopoulos, et C. Kiparissides, « Optimal grade transition and selection of closed-loop controllers in a gas-phase olefin polymerization fluidized bed reactor », *Chem. Eng. Sci.*, vol. 58, n° 16, p. 3643-3658, août 2003, doi: 10.1016/S0009-2509(03)00223-9.
- [19] R. H. Nyström, R. Franke, I. Harjunkoski, et A. Kroll, « Production campaign planning including grade transition sequencing and dynamic optimization », *Comput. Chem. Eng.*, vol. 29, n° 10, p. 2163-2179, sept. 2005, doi: 10.1016/j.compchemeng.2005.07.006.
- [20] D. Bonvin, L. Bodizs, et B. Srinivasan, « Optimal Grade Transition for Polyethylene Reactors via NCO Tracking », *Chem. Eng. Res. Des.*, vol. 83, n° 6, p. 692-697, juin 2005, doi: 10.1205/cherd.04367.
- [21] Y. Wang, H. Seki, S. Ohyama, K. akamatsu, M. Ogawa, et M. Ohshima, « Optimal grade transition control for polymerization reactors », *Comput. Chem. Eng.*, vol. 24, n° 2-7, p. 1555-1561, juill. 2000, doi: 10.1016/S0098-1354(00)00550-0.
- [22] Y. Wang, G. S. Ostace, R. A. Majewski, et L. T. Biegler, « Optimal Grade Transitions in a Gas-phase Polymerization Fluidized Bed Reactor », *IFAC-Pap.*, vol. 52, n° 1, p. 448-453, 2019, doi: 10.1016/j.ifacol.2019.06.103.

- [23] K. B. McAuley et J. F. Macgregor, « Nonlinear product property control in industrial gas-phase polyethylene reactors », *AIChE J.*, vol. 39, n° 5, p. 855-866, 1993, doi: 10.1002/aic.690390514.
- [24] K. B. McAuley, D. A. Macdonald, et P. J. McLellan, « Effects of operating conditions on stability of gas-phase polyethylene reactors », *AIChE J.*, vol. 41, n° 4, p. 868-879, 1995, doi: 10.1002/aic.690410414.
- [25] E. M. Ali, A. E. Abasaheed, et S. M. Al-Zahrani, « Improved Regulatory Control of Industrial Gas-Phase Ethylene Polymerization Reactors », *Ind. Eng. Chem. Res.*, vol. 38, n° 6, p. 2383-2390, juin 1999, doi: 10.1021/ie980636n.
- [26] A. E. Bryson et Y. C. Ho, *Applied Optimal Control*. Hemisphere, Washington DC, 1975.
- [27] F. Nascimento de Andrade, « Effect of condensable materials during the gas phase polymerization of ethylene on supported catalysts », Université Claude Bernard Lyon 1, 2019.
- [28] T. F. L. McKenna, « Condensed Mode Cooling of Ethylene Polymerization in Fluidized Bed Reactors », *Macromol. React. Eng.*, vol. 0, n° 0, p. 1800026, doi: 10.1002/mren.201800026.
- [29] W. Yao, X. Hu, et Y. Yang, « Modeling solubility of gases in semicrystalline polyethylene », *J. Appl. Polym. Sci.*, vol. 103, n° 3, p. 1737-1744, févr. 2007, doi: 10.1002/app.24969.
- [30] A. Novak *et al.*, « Ethylene and 1-hexene sorption in LLDPE under typical gas-phase reactor conditions: Experiments », *J. Appl. Polym. Sci.*, vol. 100, n° 2, p. 1124-1136, avr. 2006, doi: 10.1002/app.23508.
- [31] H.-S. Yi, J. H. Kim, C. Han, J. Lee, et S.-S. Na, « Plantwide Optimal Grade Transition for an Industrial High-Density Polyethylene Plant », *Ind. Eng. Chem. Res.*, vol. 42, n° 1, p. 91-98, janv. 2003, doi: 10.1021/ie0202221.

# Chapter 5 Optimization of PE Grade Transitions with constraints on the polymer sticking temperature

---

Results in this chapter have been published in Industrial & Engineering Chemistry Research journal:

S. Kardous, T. F. L. McKenna, N. Sheibat-Othman, “Optimization of Polyethylene Grade Transitions in Fluidized Bed Reactors with Constraints on the Polymer Sticking Temperature”, Ind. Eng. Chem. Res., Janv. 2021,, , DOI: 10.1021/acs.iecr.0c05466

## 1. Introduction

In gas phase polyolefin processes, while ensuring the control of polymer properties in a reduced transition time, all the changes in the FBR should be done safely, in order to avoid serious problems, such as large process overshooting that may result in polymer sticking or even reactor runaway. Building on the developed grade transitions methodology presented in chapter 4, it is also important to estimate the sticking temperature (and the melt onset temperature) of particles, in order to maintain the control of the reactor temperature during the transition. In this chapter, we improve the optimization of transition between different polymer grades (defined by the polymer density and the melt index) in a fluidized bed reactor of polyethylene, to keep the reactor temperature lower than the polymer sticking point. A model based on data collected from the patent literature will be used to define a stickiness limit of the dry polymer. Then, using Flory-Huggins theory, the effect of swelling on the particle sticking temperature is calculated.

The other parts of the model were presented in the other chapters: in chapter 3 one may find the used kinetic copolymerization model in the bed; and in chapter 2 one may find the SL EoS and the simplified thermodynamic correlations required here. Three systems are considered:

copolymerization of ethylene with 1-butene, and copolymerization of ethylene with 1-hexene in the presence or not of the ICA (here; n-hexane).

## 2. Particle sticking in gas-phase PE production

It has been highlighted previously that diluents like ICA or comonomers play an important role in the thermodynamics, and should therefore be accounted for in the model. Another issue in gas phase reactions is related to particle sticking that may occur if the reaction temperature is close enough to the melting temperature of the polymer particles. If a fraction of the polymer in the growing particles begins to melt, this can cause the outer layers to become stickier, eventually leading to particle aggregation, which can influence the quality of fluidization, as well as to fouling or blocking of the distributor plate.[1],[2] It is therefore essential to maintain control of the reactor temperature at all times. Generally speaking, one wishes to keep it low enough that the particle does not stick, but maintain it high enough that the productivity of the system is not compromised.[3]–[7]

The melting temperature of particles is linked to the polymer density, which in turn depends on the amount of comonomer incorporated in the polyethylene (PE) chain. The rate of incorporation of comonomer depends on the amount of comonomer absorbed in the amorphous polymer (that requires an adapted thermodynamic model to be calculated) as well as the type of catalyst and its ability to incorporate comonomer.[8],[9] A second polymer property that may affect the particle melting temperature is the polymer molecular weight. Significant fractions of low molecular weight polymer, including the low molecular weight tail of a broad molecular weight distribution were found to promote particle sticking.[10] Besides, the type of catalyst has a significant role here. In addition to its influence on the comonomer incorporation and the average molecular weight, it may impact the molecular weight distribution and the polymer branches distribution. Finally, the swelling of a polymer by different penetrants will also have a strong influence on the melting temperature of polyethylene. ICAs such as n-pentane or n-hexane, or  $\alpha$ -olefin comonomers, all of

which are commonly found in a gas phase process can impact the effective melting temperature of the polymer in the reactor.[11],[12] However, it is likely that lighter compounds such as ethylene and hydrogen do not need to be considered as sticking promoters due to their lower solubility in the amorphous polymer.[10]

In the following section, the development of a model allowing the prediction of the sticking temperature is presented. Then, the optimization and control methodologies are presented.

### 3. Defining the sticking temperature

It is difficult to know how to calculate precisely when the polymer becomes too sticky, as this depends on a number of factors linked to a number of polymer properties, the temperature of the polymer particles, and to the reactor operating conditions. Experimental methods have been proposed to measure the melting temperatures of polymer as a function of the polymer density, molecular weight and comonomer type.[13] Also, the effect of the particle swelling by ICA on the melting temperature was evaluated. In general, the more the polymer is amorphous (so less dense, but also able to swell with more ICA or comonomer), the faster the stickiness limit is reached.[14] Swelling the polymer by one or more penetrants causes a depression in the melting temperature ( $T_m$ ), and will also reduce the *MIT*. The melt point depression ( $\Delta T_m$ ) and the reduction in the *MIT* ( $\Delta MIT$ ) can be defined as follows:

$$\begin{aligned}\Delta T_m &= T_{m,0} - T_m \\ \Delta MIT &= MIT_0 - MIT\end{aligned}\tag{5.1}$$

Where  $T_{m,0}$  and  $T_m$  refer to the melting temperatures of the unswollen (dry) and swollen polymer respectively. Similarly,  $MIT_0$  and  $MIT$  refer to the melt initiation temperatures of the dry and swollen polymer respectively.

The *MIT* appears to be the closest to the sticking temperature (see Figure 1.6); and will thus be adopted in this work.[15] Note that other works related the sticking to the softening of particles such the well-known Vicat softening temperature or the method suggested by Chmelar et al.[8]. However, while the softening temperature is most likely correlated with stickiness, as it determines when the polymer becomes deformable, the initiation of melting represents a better indication of when the polymer becomes dangerously sticky.

In general, one tries to operate the FBR at a temperature a few degrees lower than the *MIT*. This means that if the FBR is operated at a temperature  $T_{R,dry}$  as shown in Figure 1.6, then it should be possible to avoid a lot of sticking of the polymer. However, if one were to change the feed composition to bring the reactor to the swollen conditions shown in this same figure without changing the reactor temperature, then the reactor would be operating at a point higher than the *MIT* and we would run the risk of significant sticking of the polymer. Ideally one would like to be able to predict the impact of swelling directly on the *MIT*. In the following sections, we first discuss the estimation of the melting temperature of a dry polymer (here called  $T_{m,0}$ ), in the absence of swelling, then we investigate the influence of swelling on the swollen particle melting temperature (here called  $T_m$ ).

### 3.1. $T_{m,0}$ and $MIT_0$ of dry polymer

In the case of linear low density polyethylene (LLDPE), the melting temperature of a dry polymer first depends on the type and amount of  $\alpha$ -olefin comonomers incorporated into the LLDPE chain.[16] The most commonly used  $\alpha$ -olefin comonomers for producing LLDPE are 1-butene and 1-hexene. The melting temperature for several commercial grades of LLDPE is correlated with the polymer density in Figure 5.1.[13] The data shown here are for a mixture of 1-butene and 1-hexene-based copolymers, so it appears that the impact of the comonomer type on  $T_{m,0}$  is limited. Also, the values of the melt flow index (*MI*) at 2.16 kg are  $0.45 < MI < 20$ , suggesting that for this

range of values the molecular weight does not have a significant influence on the melting temperature. Similarly, Hari et al.[15] provided data on the  $MIT$  as a function of LLDPE density. Once again, a linear correlation between the  $MIT$  and polymer density appears to provide a good estimate of the value of this important temperature. We will use the correlation shown in this figure to calculate the dry  $MIT$  of the LLDPE as a function of its density. The influence of the  $MI$  or molecular weight on the  $MIT$  was not indicated, so we will suppose that the polymer molecular weight does not have a significant impact on the  $MIT$ , as observed on the same figure for  $T_{m,0}$ . The effect of the molecular weight on  $T_{m,0}$  was found in the literature to become negligible above 10 kg mol<sup>-1</sup>. [17]

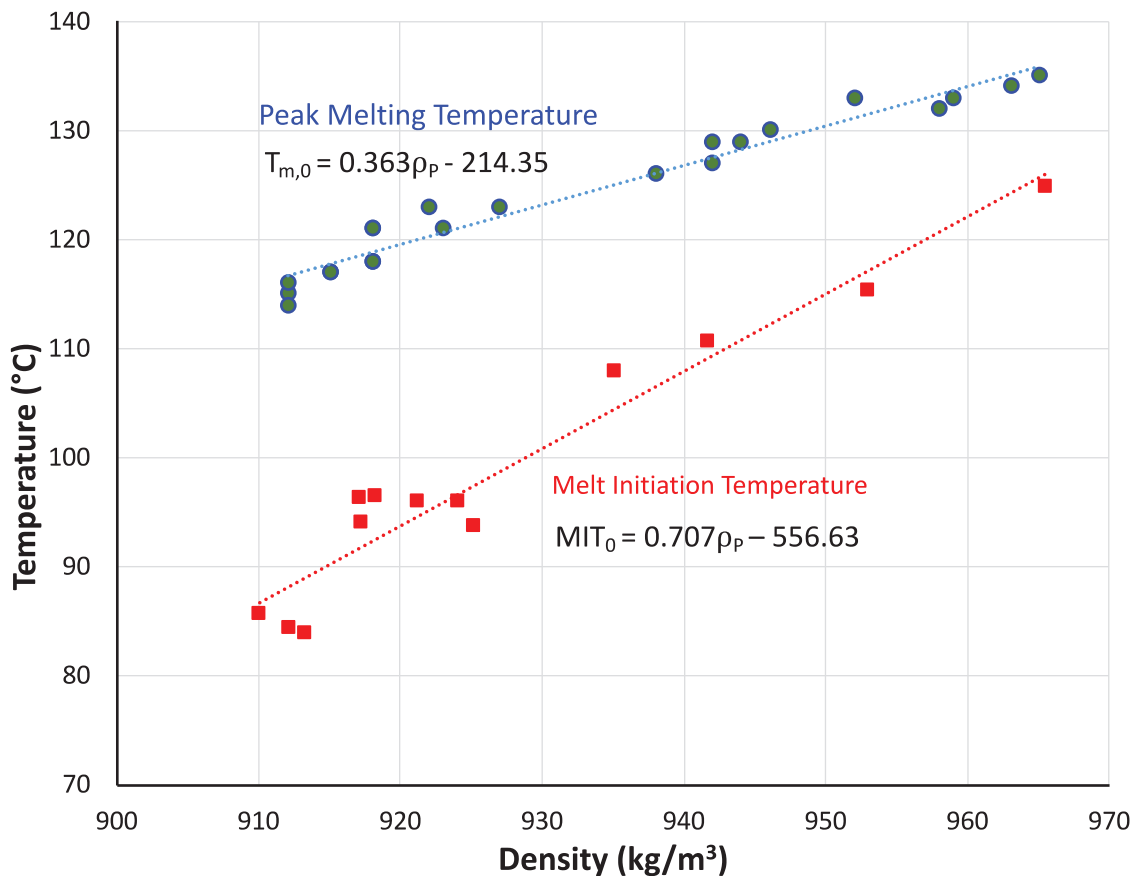


Figure 5.1. Peak melt temperatures ( $T_{m,0}$ ) for a range of commercial LLDPE and HDPE powders, and the  $MIT_0$ , also for a range of different commercial polymers. Both temperatures are shown as a function of the polymer density.

Note that also fundamental models were proposed to predict the melting temperature,  $T_{m,0}$  of polyethylene as a function of the polymer density, polymer molecular weight and comonomer type, such as the model of Kamal et al. based on Flory theory.[17] However, this model did not give good predictions of the data shown in Figure 5.1 regarding  $T_{m,0}$ , which highlights the complexity of the system and the impact of the distributions of branches and chain lengths which are difficult to account for in the model. Moreover, as indicated above, we prefer using the predictions of  $MIT_0$ , which is supposed to be more representative of the sticking temperature.

### 3.2. $T_m$ of swollen polymer

It is worth reminding here that not all the gases that dissolve in the amorphous phase of the polymer do act as sticking promoters. The penetrants which are known to act as sticking promoters are only ICAs and comonomers.

A model of the polymer melting temperature that accounts for the presence of diluents that swell the particle was suggested by Flory-Huggins theory:[18]

$$\frac{1}{T_m} - \frac{1}{T_{m,0}} = \frac{R}{\Delta H_u} \frac{V_u}{V_d} (\phi_d - \chi \phi_d^2) \quad (5.2)$$

Where  $T_m$  is the equilibrium melting temperatures of the polymer-diluent mixture and  $T_{m,0}$  is the melting temperature of dry polymer (here obtained by the correlation in Figure 5.1). The same equation will be applied for  $MIT$  instead of  $T_m$ .  $V_u$  is the volume of the repeat unit ( $38 \text{ \AA}^3$  for ethylene molecule), the comonomer impact being neglected here  $V_d$  the volume of the diluents that are assumed to act as sticking promoters ( $73 \text{ \AA}^3$  for 1-butene molecule and  $107.6$  for 1-hexene[19], can also be ICAs) and  $\phi_d$  is the volume fraction of the diluent (ICAs and comonomer).  $\chi$  is the temperature- and concentration-dependent Flory-Huggins interaction parameter for which

different measurement methods and models have been proposed.[20]·[21]·[22] It describes the miscibility of the diluent into the polymer:  $\chi > 0.55$  indicates that the diluent is immiscible,  $0.3 < \chi < 0.55$  indicates a moderate miscibility and  $\chi < 0.3$  indicates a good miscibility.[23] Note that the melting point depression in Flory-Huggins theory characterizes the decrease of the melting point of a polymer due to the mixing with another species (diluent) and occurs only if the two species (PE & diluent) are miscible or partially miscible.[24]

Simulations of the Flory-Huggins equation combined with the correlation of  $MIT$  presented in the previous section are shown in Figure 5.2. The diluent 1-butene is considered. It can be seen that the effect of density is very important as it may decrease  $MIT_0$  from 100°C to 90°C when decreasing the density from  $\rho_p = 930$  to  $915 \text{ kg m}^{-3}$ , in the absence of diluent. Swelling by the diluent by  $\phi_d = 10\%$  may decrease  $MIT_0$  by 6°C. Finally, the figure shows that in the region of coherent fractions of diluent in the polymer (i.e.  $\phi_d < 20\%$ ), the interaction parameter  $\chi$  has a negligible influence on  $MIT$ . Therefore,  $\chi$  can be fixed at 0.5 and there is no need for using a detailed model to compute it for the present application.

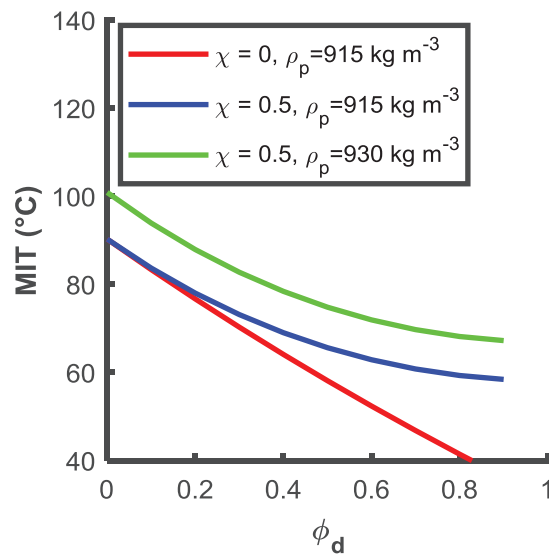


Figure 5.2. Effects of the polymer density  $\rho_p$  and volume fraction of diluent  $\phi_d$  on the melting initiation temperatures of the swollen or dry polymer.

This model will be used to calculate the melting point depression due to swelling, and we make the approximation that  $\Delta T_m \approx \Delta MIT$ , therefore  $MIT = MIT_0 - \Delta MIT$ . There is no guarantee that  $\Delta T_m \approx \Delta MIT$ , as these values will depend on a number of physical characteristics of the polymer. However, in the absence of concrete data it seems to be a reasonable assumption to equate the two. The reactor temperature for the swollen polymer must be less than or equal to this new value of  $MIT$ . Generally, one can add a “safety margin” to this  $MIT$  value, as a function of the catalyst and the type of the polymer between, 1-10°C.[25] In the current work, we will choose a value of 5°C.

## 4. Dynamic off-line optimization and temperature control

In order to ensure fast and safe transitions between different polymer grades, an offline optimization is employed as follows:[26]

$$\min_{\mathbf{u}(t)} J(\mathbf{u}(t), \mathbf{x}(t)), t \in [t_0, t_f] \quad (5.3)$$

$$0.1 \mathbf{u}_0 \leq \mathbf{u}(t) \leq 5 \mathbf{u}_0$$

where  $J$  is the objective function,  $\mathbf{x}(t)$  the vector of state variables and the manipulated variables of the optimization are the flow rates of hydrogen and comonomer,  $\mathbf{u}(t) = [F_{H_2}, F_{com}]$ . Inequality constraints are imposed to define the available ranges of manipulated variables based on the optimal input of the previous grade,  $\mathbf{u}_0$ .

This objective function enables the control of the polymer quality, melt index and density, by considering both the instantaneous and the cumulative properties, as in the previous chapter, with indices  $c$  and  $i$  respectively, as follows:

$$J(\mathbf{u}) = \int_{t_0}^{t_f} w_1 \frac{|MI_i - MI_{sp}|}{MI_{sp}} + w_2 \frac{|MI_c - MI_{sp}|}{MI_{sp}} + w_3 \frac{|\rho_i - \rho_{sp}|}{\rho_{sp}} + w_4 \frac{|\rho_c - \rho_{sp}|}{\rho_{sp}} dt \quad (5.4)$$

where  $w_i$  (with  $i = 1 - 4$ ) are tuning weights.

In order to ensure the reactor temperature to remain lower than the *MIT* with a safety margin of 5°C, the following algorithm is employed:

- From the desired polymer density, the  $MIT_0$  is predicted using the correlation presented in Figure 5.1.
- The optimization gives the optimal pressure of comonomer required to get the desired polymer density. This pressure is added to the ICA pressure if present, and the fraction of penetrants in the polymer particles is calculated (using the simplified thermodynamic correlation in section 6 chapter 2). Then, using Flory-Huggins theory, the *MIT* is calculated.
- If  $MIT - 5^\circ\text{C}$  is higher than the nominal bed temperature,  $90^\circ\text{C}$ , the bed temperature is kept at its nominal value and there is no risk of sticking.
- If  $MIT - 5^\circ\text{C}$  is lower than  $80^\circ\text{C}$ , this option is not realizable. So, one needs either to reduce the temperature more, or try to use less ICA if present, to produce the desired polymer density without a risk of sticking.
- If  $MIT - 5^\circ\text{C}$  is between 80 and  $90^\circ\text{C}$ , the bed temperature set-point is set to  $MIT - 5^\circ\text{C}$  and is tracked using PI controllers. We therefore impose a constraint on  $T$ . The scenarios shown in this paper concern this case.

Note that all these calculations are inserted within the optimization loop, as the different variables are correlated (temperature, reaction rate, density, etc.).

In order to control the bed temperature, two PI controllers were employed by manipulating the coolant water temperature in the exchanger,  $T_w$ , as well as the fresh gas temperature.[27] Both control variables allow keeping the bed temperature at the desired value.

$$\begin{bmatrix} T_w^{in} \\ T_g^{in} \end{bmatrix} = \begin{bmatrix} k_{p1} \\ k_{p2} \end{bmatrix} (T^{SP} - T) + \begin{bmatrix} k_{i1} \\ k_{i2} \end{bmatrix} \int_0^t (T^{SP} - T) dt \quad (5.5)$$

Where  $k_{pi}$  and  $k_{ii}$  are the proportional and integral tuning parameters,  $T_w^{in}$  and  $T_g^{in}$  are the temperatures of the exchanger water inlet and the fresh gas inlet, and  $T^{SP}$  is the bed set-point temperature.

## 5. Simulation results and discussion

Simulations are done using a bed diameter  $D_{bed}=4.75$  m, bed voidage  $\varepsilon_{bed}=0.7$  and bed height  $h_{nominal}=13.3$  m. The pressure of ethylene (and of ICA if present) is maintained constant during the transition, whereas the comonomer and hydrogen pressures are varied following the optimization results of the flow rates. The bed temperature is kept at its nominal value 90°C except when there is a risk of sticking where it is decreased, using the PI controllers. Like in the chapter 4, the optimization is solved using the `fmincon` solver of Matlab®. In the following sections, arbitrary specifications of grade transitions are implemented from higher to lower polymer density, where the risk of sticking is the highest.

### *Copolymerization of ethylene with 1-butene*

The weighting factors required by the optimization were tuned based on few simulations. The objective was to ensure a rapid convergence of the cumulative properties to the desired set-points (SP), while keeping the instantaneous properties within an acceptable range. The tuning was done with a constant bed temperature, as the weights in the criterion are not affected by the control of  $T$ . One of the weights was fixed at 1 (here  $w_2 = 1$ ), and the others were varied, as only their ratios has a signification in the criterion. It is important at this level to remind that when modifying the

comonomer flow rate to control the density, the melt index is also affected. However, when modifying the hydrogen flow rate, the density is not affected. Moreover, the density converges at a slower rate, as shown in Figure 5.3. Therefore, it is required to attribute higher weights to the density terms than the melt index, especially when using local optimization methods. This ensures the convergences of both properties. In Figure 5.3, the weights attributed to the instantaneous and cumulative density are  $w_3 = w_4 = 3$ . Then, two simulations are compared by varying the weight of the instantaneous melt index,  $w_1 = 1.1$  and  $w_1 = 0.5$ . The figure shows that when lower weights are attributed to cumulative properties, they converge faster but this causes important overshoots in the instantaneous properties. Indeed, the optimization leads to high variations in the flow rates and pressures of hydrogen, which is usually not desirable. The allowable extent of overshoots should be indicated in the process and properties specifications. In the following, the used values are:  $w_1 = 0.5$ ,  $w_2 = 1$ ,  $w_3 = 3$  and  $w_4 = 3$ . The same values were used for both systems. It is to be noted however that when varying importantly the operating conditions, some adjustment of these factors may be required.

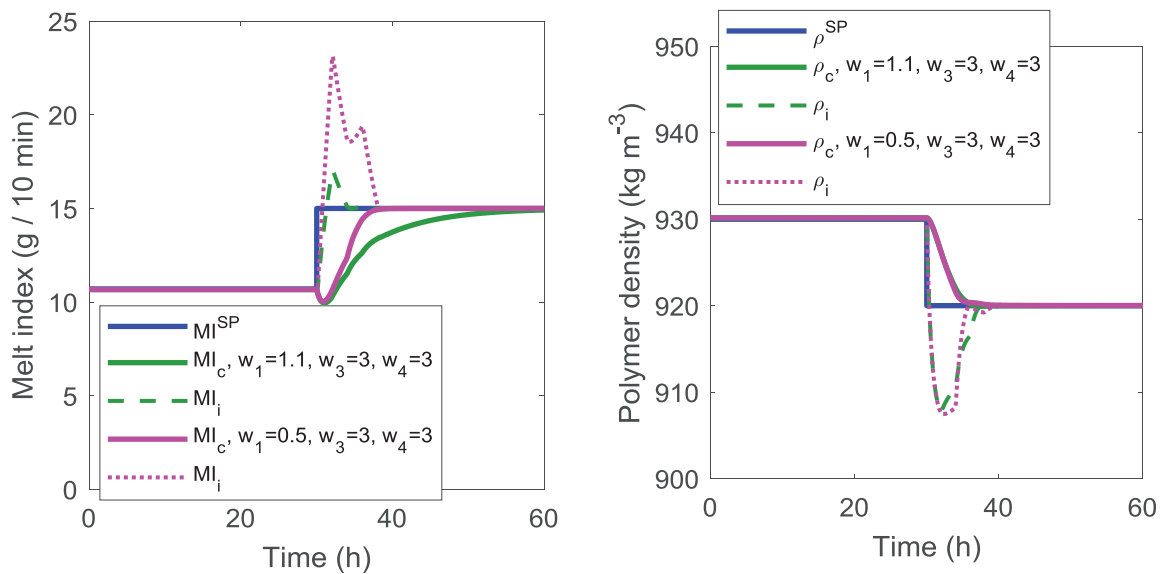


Figure 5.3. Tuning of  $w_1$  during grade transition in ethylene-1-butene copolymerization, without a constraint on T.

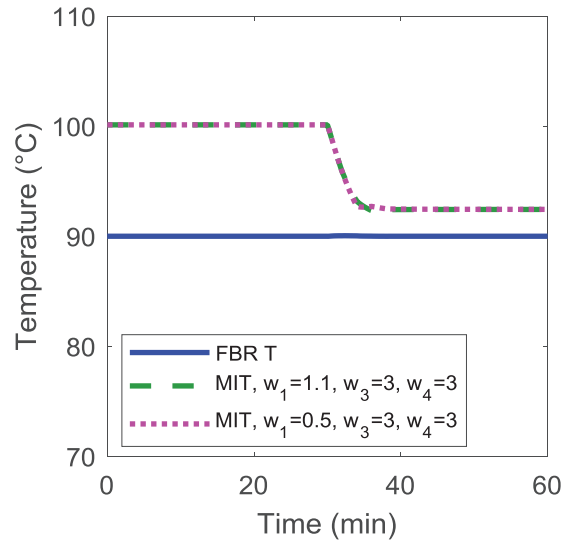


Figure 5.4. Grade transition in ethylene-1-butene copolymerization, without a constraint on  $T$ .

Figure 5.4 shows the evolution of the particle melting temperature obtained with the two options of  $w_i$  tuning, without constraints on the reactor temperature which was kept at its nominal value 90°C. The  $MIT$  was predicted by combining the correlation of Hari et al.[15] and the particle swelling by comonomer predicted by the Flory-Huggins theory. During the transition from the first to the second grade, the reduction in the density and the increase in the swelling by comonomer both lead to a decrease of the  $MIT$ , which gets close to the bed temperature. This might be assumed to be a risky situation as the polymer particles may start sticking and aggregating. Therefore, it is important to consider the time-varying constraint on the bed temperature with the safety margin  $T \leq MIT - 5^\circ\text{C}$ .

The same scenario presented in Figure 5.3 and Figure 5.4 was simulated while adding a temperature constraint with a safety margin  $T \leq MIT - 5^\circ\text{C}$  (Figure 5.5). It can be seen that the reactor temperature starts cooling during the transition and reaches about 86.7°C for the new grade. By this way, the bed temperature is always about 5°C lower than the onset melting temperature. Note also that the time scale for the convergence of density remains more or less the same, with the temperature being constant or reduced, thanks to the optimization of the comonomer flow rate.

Cooling the bed certainly impacts the reaction rates, but this is necessary in order to prevent polymer sticking and agglomeration.

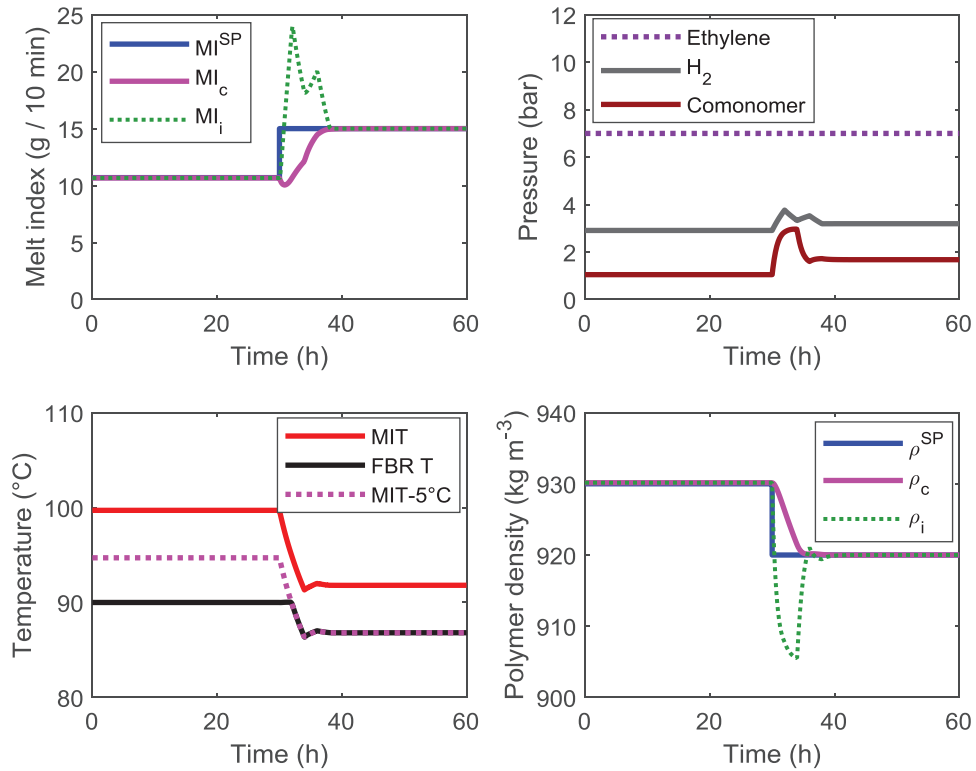


Figure 5.5. Grade transition in ethylene-1-butene copolymerization under the constraint  $T \leq MIT - 5^{\circ}C$ .

### Copolymerization of ethylene with 1-hexene

The proposed methodology was evaluated in the second system: ethylene and 1-hexene copolymerization, first without ICA. Note that not only the comonomer is changed but also the operating conditions: with a much lower amount of comonomer (on the range of 0-1 bar) and ethylene pressure around 10 bar. The choice of set-points was also varied.

Figure 5.6 shows the results of a transition where reducing the polymer density and increasing the melt index are required. The optimization constraint was considered as in the first system,  $T \leq MIT - 5^{\circ}C$ . It can be seen that with the polymer density and penetrant concentration of the first

grade, the *MIT* was about 96°C. Then, during the transition, an injection of comonomer and hydrogen was realized to increase  $MI_i$  and decrease  $\rho_i$ . As a result, for the new grade the *MIT* decreased to about 89.6°C as a lower density is produced and more comonomer swells the particles. In order to avoid particle sticking, the reactor temperature was cooled to 84.6°C. Again, a net decrease in the reaction rate is expected when cooling the bed from 90 to 84.6°C. But, with the closed loop optimization, an adjustment of the properties could be maintained and the sticking constraint was respected. The main observed effect is the slower convergence of the cumulative properties, as less polymer is produced to renew the bed.

It can be noticed that only a small amount of 1-hexene (0-1 bar) can lead to an important decrease of the density of LLDPE and eventual polymer stickiness (compared to the system of 1-butene, with comonomer pressure close to 2 bars for the same density range). This is due to the fact that 1-hexene is more soluble in PE at a given temperature and pressure which leads to a higher reaction rate of the comonomer and so to a lower density. Both the increase in the fraction of diluent in the particles and the decrease in density lead to a faster decrease in the *MIT*.

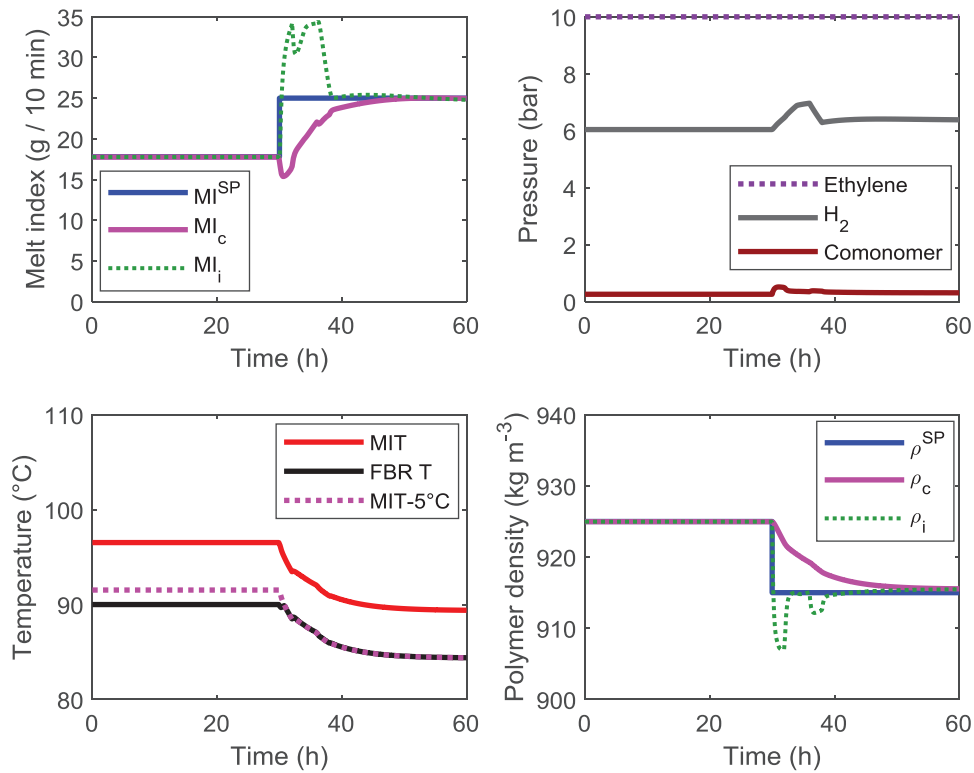


Figure 5.6. Grade transition in ethylene-1-hexene copolymerization under constraint  $T \leq MIT - 5^\circ\text{C}$ .

### *Copolymerization of ethylene with 1-hexene in presence of n-hexane*

In this section, the second system ethylene and 1-hexene copolymerization is considered in presence of ICA n-hexane. Figure 5.7 shows the optimization results of this system, with constraint on the bed temperature. The ICA pressure was 1.2 bar. Adding an ICA to the system affects polymer swelling by ethylene and diluents. This leads to an increase in the reaction rates of monomer and comonomer, which affects the polymer properties. Moreover, due to the higher swelling of the particle with diluents, the  $MIT$  decreases and the risk of sticking increases. In this simulation, it was necessary to reduce the bed temperature to  $82^\circ\text{C}$  in order to avoid sticking. Note

that the set-point of polymer density in the new grade is  $920 \text{ kg m}^{-3}$  in this scenario while it was  $915 \text{ kg m}^{-3}$  in the scenario without ICA (with a similar transition of  $MI$ ). In the presence of this amount of ICA, it is not possible to produce a polymer of low density  $915 \text{ kg m}^{-3}$  at temperature higher than  $80^\circ\text{C}$  without avoiding sticking.

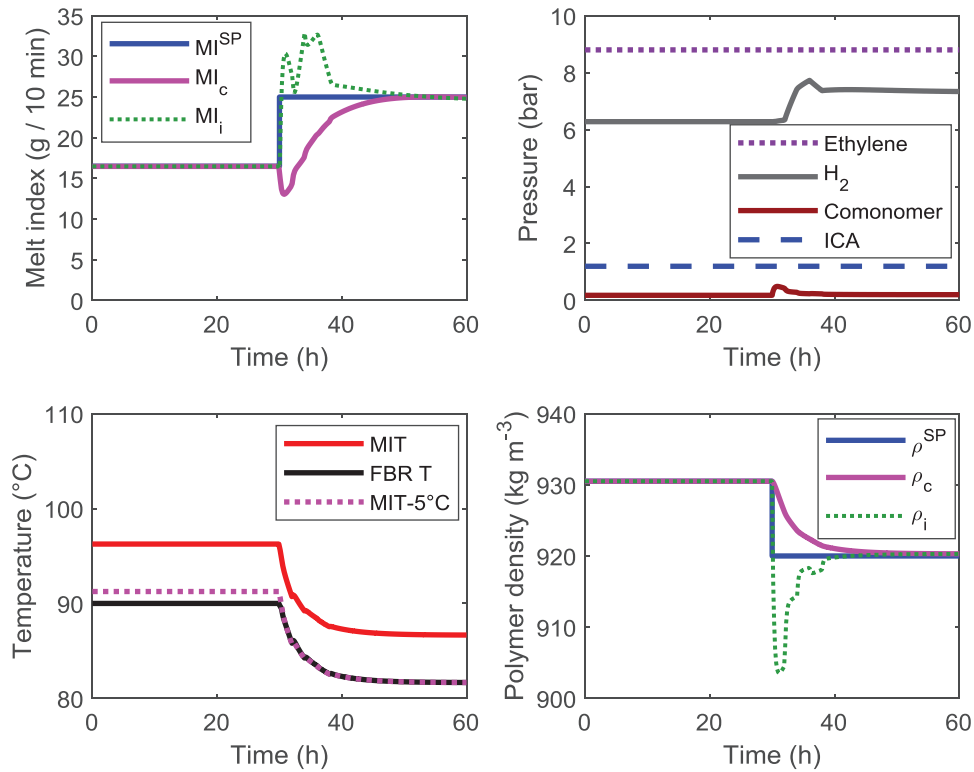


Figure 5.7. Grade transition in ethylene-1-hexene copolymerization, in presence of n-hexane, under constraint  $T \leq MIT - 5^\circ\text{C}$ .

In Figure 5.3, it was shown that a good tuning of the parameters  $w_i$  allows reducing the overshoots in the instantaneous properties  $MI_i$  and  $\rho_i$ . Another efficient way of ensuring these instantaneous properties to remain within a specific range is to consider inequality constraints on the outputs during the optimization. Figure 5.8 shows a scenario of optimization with constraints on the instantaneous properties. Compared to Figure 5.7, it can be seen that the overshoots were decreased and remained within the allowed margin. However, this slowed down the convergence of the

cumulative properties. Also, considering constraints in the optimization increases the computation time. However, in this manner, one may ensure a good control of the instantaneous properties. Indeed, such overshoots lead to wider distributions of the properties (e.g. polymer molecular weight or branches), which are difficult to model and for which the effects on the properties such as the *MIT* are not well-known.

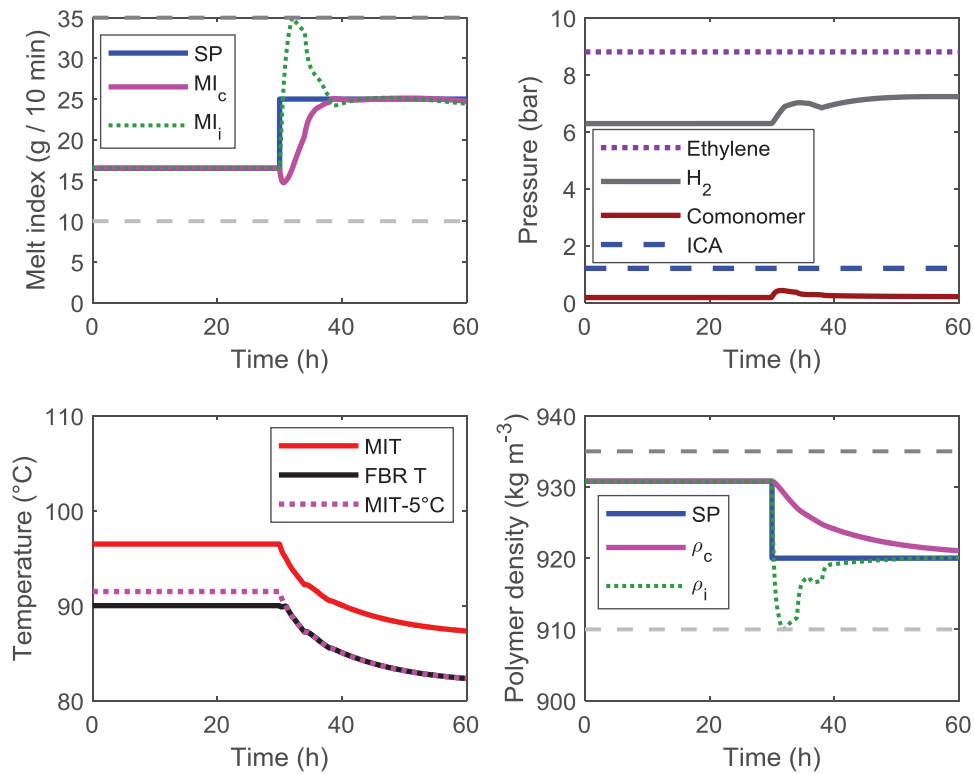


Figure 5.8. Grade transition in ethylene-1-hexene copolymerization, in presence of n-hexane under constraint  $T \leq MIT - 5^{\circ}\text{C}$ , as well as constraints on the outputs  $MI_i$  and  $\rho_i$  (grey dotted lines).

## 6. Conclusion

In this chapter, an additional model based on data collected from the patent literature combined to the Flory-Huggins theory was implemented. This model was used to predict the onset melting temperature of particles in the presence of diluents. A control of the bed temperature is done in a

way to respect the constraint of the *MIT*. The *MIT* is considered to be the most representative of the sticking temperature. Coupled with the offline dynamic optimization developed in chapter 4, this model of PE polymerization allows controlling the end-use properties of polymer grades (melt index and density), while avoiding particle stickiness and agglomeration. This last point appears to be extremely important, especially in case of copolymerization due to the effect of the comonomer as a plasticizer species on the sticking temperature of the polymer. In this purpose, the effect of comonomer on the particle sticking temperature was evaluated by two ways: first, it leads to the creation of more branches in the polymer chain and so to a decrease in the polymer density; second it may plasticize the particle when dissolved in it; both effects lead to a decrease in the *MIT*. Similarly, the presence of ICA leads to a greater swelling by the diluents, which leads to a decrease in the *MIT* and increases the risk of sticking.

Three different copolymerization systems were considered; the copolymerization of ethylene with 1-butene and the copolymerization of ethylene with 1-hexene (in presence or not of n-hexane). Hence, the employment of adapted thermodynamic models (from chapter 2) is also highlighted, since in a ternary system the gases may influence the solubility of each other, which affects the reaction rates of monomer and comonomer, and therefore of the properties (polymer melt index, density and particle sticking temperature). Finally, the simulation results highlight the importance of optimizing the comonomer flow rate, and consequently the density of the polymer which has the most significant effect on the behavior of equilibrium melting temperature of the polymer. The variation of the melting temperature was detected while maintaining the concentration of ethylene constant during the transition, which validates ethylene as no sticking promoter under the employed operating conditions.

# References

- [1] J. B. P. Soares et T. F. L. McKenna, « Polyolefin Reaction Engineering », p. 345.
- [2] S. A. Dadebo, K. B. McAuley, et P. J. McLellan, « INTERACTIONS BETWEEN PRODUCTION RATE OPTIMIZATION AND TEMPERATURE CONTROL IN GAS PHASE POLYETHYLENE REACTORS », in *Dynamics and Control of Chemical Reactors, Distillation Columns and Batch Processes (Dycord'95)*, J. B. Rawlings, Éd. Oxford: Pergamon, 1995, p. 293-298.
- [3] N. M. Ghasem, W. L. Ang, et M. A. Hussain, « Dynamics and stability of ethylene polymerization in multizone circulating reactors », *Korean J. Chem. Eng.*, vol. 26, n° 3, p. 603-611, mai 2009, doi: 10.1007/s11814-009-0102-1.
- [4] C. Chatzidoukas, « Control and Dynamic Optimisation of Polymerization Reaction Processes », University of London, London, 2004.
- [5] S. A. Dadebo, M. L. Bell, P. J. McLellan, et K. B. McAuley, « Temperature control of industrial gas phase polyethylene reactors », *Journal of Process Control*, vol. 7, n° 2, p. 83-95, janv. 1997, doi: 10.1016/S0959-1524(96)00016-9.
- [6] M. R. Rahimpour, J. Fathikalajahi, B. Moghtaderi, et A. N. Farahani, « A Grade Transition Strategy for the Prevention of Melting and Agglomeration of Particles in an Ethylene Polymerization Reactor », *Chem. Eng. Technol.*, vol. 28, n° 7, p. 831-841, juill. 2005, doi: 10.1002/ceat.200500055.
- [7] N. M. Turkistani, « Fluidized bed methods for making polymers », US6759489B1, juill. 06, 2004.
- [8] J. Chmelar, P. Matuska, T. Gregor, M. Bobak, F. Fantinel, et J. Kosek, « Softening of polyethylene powders at reactor conditions », *Chemical Engineering Journal*, vol. 228, p. 907-916, juill. 2013, doi: 10.1016/j.cej.2013.05.069.
- [9] M. L. DeChellis, J. R. Griffin, et M. E. Muhle, « Process for polymerizing monomers in fluidized beds », US5405922A, avr. 11, 1995.
- [10] R. O. Hagerty, K. B. Stavens, M. L. DeChellis, D. B. Fischbuch, et J. M. Farley, « Polymerization process », US7122607B2, oct. 17, 2006.
- [11] D. Singh, S. Hinds, B. Fischbuch, et N. A. Vey, « Gas-phase process », US20050182207A1, août 18, 2005.
- [12] G. G. Hendrickson, « Method for operating a gas phase polymerization reactor », US7531606B2, mai 12, 2009.

- [13] « Exxon Mobile Product Data Sheets, <https://www.exxonmobilchemical.com/en/products/polyethylene>, Product Data Sheets, accessed 12 October 2020. », oct. 2020.
- [14] M. G. Goode, M. W. Blood, et W. G. Sheard, « High condensing mode polyolefin production under turbulent conditions in a fluidized bed », US6391985B1, mai 21, 2002.
- [15] A. S. Hari, B. J. Savatzky, D. M. Glowczwski, et X. Cao, « Controlling a polyolefin reaction », US 9,718,896 B2, 2015.
- [16] M. J. Schneider et R. Mülhaupt, « Influence of indenyl ligand substitution pattern on metallocene-catalyzed propene copolymerization with 1-octene », *Macromolecular Chemistry and Physics*, vol. 198, n° 4, p. 1121-1129, 1997, doi: 10.1002/macp.1997.021980415.
- [17] M. R. Kamal, L. Feng, et T. Huang, « A generalized equation for the prediction of melting temperatures of homopolymers and copolymers », *Can. J. Chem. Eng.*, vol. 80, n° 3, p. 432-442, juin 2002, doi: 10.1002/cjce.5450800312.
- [18] P. J. Flory, « Thermodynamics of Crystallization in High Polymers. IV. A Theory of Crystalline States and Fusion in Polymers, Copolymers, and Their Mixtures with Diluents », *The Journal of Chemical Physics*, vol. 17, n° 3, p. 223-240, mars 1949, doi: 10.1063/1.1747230.
- [19] T. Asano et W. J. L. Noble, « “Void” and “expansion” volume contributions to reaction and activation volumes of nearly nonpolar reactions », *The Review of Physical Chemistry of Japan*, vol. 43, n° 2, p. 82-91, janv. 1974.
- [20] J. R. Fried, *Polymer Science and Technology*, Pertinance Hall. Saddle River, 1995.
- [21] D. N. T. JR et E. J. Markel, « Polymerization reaction monitoring with determination of induced condensing agent concentration for preventing discontinuity events », US7754830B2, juill. 13, 2010.
- [22] A. G. Mikos et N. A. Peppas, « Flory interaction parameter  $\chi$  for hydrophilic copolymers with water », *Biomaterials*, vol. 9, n° 5, p. 419-423, sept. 1988, doi: 10.1016/0142-9612(88)90006-3.
- [23] W. V. Titow, *PVC Technology*, Fourth. London and New York: Elsevier Applied Science Publishers Ltd, 1984.
- [24] P. J. Marsac, T. Li, et L. S. Taylor, « Estimation of Drug–Polymer Miscibility and Solubility in Amorphous Solid Dispersions Using Experimentally Determined Interaction

- Parameters », *Pharm Res*, vol. 26, n° 1, p. 139, sept. 2008, doi: 10.1007/s11095-008-9721-1.
- [25] M. E. Muhle, R. B. Pannell, E. J. Markel, et Robert O. Hagerty, « Systems and methods for monitoring a polymerization reaction », US 8,383,739 B2, 2013.
- [26] K. B. McAuley et J. F. MacGregor, « Optimal grade transitions in a gas phase polyethylene reactor », *AIChE J.*, vol. 38, n° 10, p. 1564-1576, oct. 1992, doi: 10.1002/aic.690381008.
- [27] C. Chatzidoukas, J. D. Perkins, E. N. Pistikopoulos, et C. Kiparissides, « Optimal grade transition and selection of closed-loop controllers in a gas-phase olefin polymerization fluidized bed reactor », *Chemical Engineering Science*, vol. 58, n° 16, p. 3643-3658, août 2003, doi: 10.1016/S0009-2509(03)00223-9.

# General Conclusions-Perspectives

---

## General Conclusions

Gas phase olefin polymerization processes are by far the most widely used to make such products. For the particular case of polyethylene, gas phase polymerization processes within FBR represent the process of choice for PE producers for its several profits, such as being the cleanest process to make PE, the least energy consuming, and the least expensive. However, PE polymerization is highly exothermic, and the reactor can generate enormous amount of heat.[1] The reactor is then forced to operate under condense mode cooling using ICAs to improve the heat transfer. These compounds present an important impact on the thermodynamic equilibrium in the reactor.

While previous research works at C2P2 laboratory, [2]–[4] confirmed the significant impact of ICA on the reaction rate, we have attempted in this PhD work to study the impact of ICAs in grade transition of PE with modeling. This study can be decomposed globally into three major parts

In the first part, a simplified thermodynamic model based on the Sanchez-Lacombe equation of state was developed in the chapter 2. This model allows to account for the co-solubility effect (i.e., co-solvent and antisolvent effects) in presence of ICA (e.g., iso-butane, n-hexane) in a ternary system. The thermodynamic model was extended to pseudo-quaternary systems using some proposed correlations to reduce the calculation time, but mainly due to the lack of thermodynamic data. That was also needed in order to account for the co-solubility effects of not only ICA on ethylene but also comonomers (e.g., 1-hexene, 1-butene). The extended thermodynamic model was afterwards integrated into an FBR reactor model for the catalytic copolymerization of ethylene with either 1-butene or 1-hexene in order to account for the effects of condensable materials on the reaction rate and the polymer properties. This dynamic model of polymerization represents the reaction kinetics of copolymerization coupled with the reactor model (mass and energy balances)

and correlations of the polymer properties during grade transitions. (chapter 3) Moreover, the reactor model is assumed to behave as a stirred tank reactor with one phase. The simulation results demonstrated the importance of the thermodynamic model in the evaluation of the comonomer concentration in a quaternary system, which highly impacts the polymer properties (melt index and density).

In the second part of this work, based on the dynamic model developed (chapters 2+3); an off-line dynamic optimization was implemented to optimize the grade transitions in a fluidized bed reactor of polyethylene. Indeed, the primary focus of this PhD thesis is to explore the impact of the co-solubility effect on grade change optimization. A control scheme that relied on the manipulation of the flow rates of hydrogen and comonomer was used to pilot the end-use properties of the polymer (melt index and density). Using the developed grade transition strategy, both instantaneous and cumulative properties were controlled in a duration shorter than the long residence time of the reactor. Indeed, in the dynamic optimization strategy, the control variables (flow rates of hydrogen and comonomer) were optimized wisely in order to reduce the convergence times of the polymer properties to their new set-points. Furthermore, by only tuning the weighting factors we were able to either control faster the cumulative properties (thus reduce the transition product) or to focus on the instantaneous properties. Finally, we showed the importance of accounting for the effect of the induced condensing agent within grade transition optimization, as it has a direct effect on the polymer properties and the reaction rate.

In the last part of this study, we used a model based on data collected from the patent literature combined to Flory-Huggins in order to estimate the onset melting temperature of particles (and so the sticking temperature) in the presence of diluents. This model was then injected in the developed dynamic polymerization model including a precise thermodynamic-kinetic model and an optimization strategy. Therefore, it allowed controlling the end-use properties of polymer grades

(polymer melt index and density) while avoiding particle stickiness and agglomeration. The control of the bed temperature is done in a way to respect a physically important constraint (the *MIT*), which has never been done before in the open literature. The *MIT* is considered as the most representative of the sticking temperature. We found that particle sticking temperature is a function of the polymer density, which depends on the number and the type of chain branches resulting from the copolymerization (presence of comonomer). The sticking temperature is also affected by the polymer molecular weight and particle swelling by the different additives, such as comonomer and ICAs. Finally, the use of an adequate thermodynamic model was highly recognized here, since the gas species present in the system may impact the solubility of each other, which results in affecting the final properties of the polymer (*MI* and the density and particle softening temperature).

To conclude, the developed polymerization process model in this study; treating multicomponent systems and complex thermodynamic aspects is expected to serve as a powerful tool in the polyolefin industry. Using this model, we tried to approach to real condition problems frequently encountered in industrial gas phase processes (treating multicomponent systems, accounting for condensable materials, polymer sticking issue, etc.); despite the great lack of experimental data. Furthermore, as mentioned before the large scale of polyolefin market means that a huge number of polymer producers around the world will find the result of this study pertinent. Besides, the significance of thermodynamic modeling, often ignored at many levels in the open literature, will be an important aspect for the accuracy of polymer process models that would be developed by academic researchers in the future. Furthermore, the modeling approach in this thesis can be used in other polyolefin processes as the dynamic model covers many aspects of the polymerization process (kinetics of copolymerization coupled with FBR model, thermodynamics and grade transition optimization). Besides, although the optimization methodology and the temperature control procedure in this thesis are presented in the context of a gas phase ethylene

copolymerization, the problems encountered and approaches used to solve them are applicable to many other polymerization systems. The developed strategy can also be used for simple systems (e.g. binary or ternary systems) when using a classical kinetic model of homopolymerization.

## Perspectives

Recalling the results presented in this work about the dominant impact of thermodynamics (condensed operating mode) during grade transition in gas phase ethylene polymerization; and thinking ahead of the future objectives, it becomes that this research serves as an initial reference for further research studies industrially pertinent. In this context, concerning **the modeling part** and as mentioned before the actual developed model does not include description of some extra levels such as hydrodynamics of the bed. It would be desirable to extend the proposed strategy of grade transition and the work done on the reactor temperature control to a multi-compartment model. This more representative reactor model will be needed to allow for temperature gradients and the presence of liquid components, which is not the case of the actual developed model. The optimization strategy can be easily updated when improving simplified kinetics and polymerization models. Therefore, the kinetic model can be extended to multiple site catalysts. In order to improve the morphology and the properties of the final polyethylene product, the catalyst particles used in the polymerization process can also be bi-supported (i.e., a catalyst particle with two kinds of active sites, where one is more sensitive to the comonomer than the other). Moreover, the polymerization model can include a particle model accounting for the reactant diffusion through the polymer phase until reaching the active sites, and the different heat and mass transfer resistances according to the different compositions in the system rather than assuming a thermodynamic equilibrium. This update would allow to improve the precision of the outcome of the optimization strategy.

Another point concerning the modeling future work, the grade transition methodology obtained with dynamic optimization could also be approached afterwards by an optimal or predictive control (MPC), in order to evaluate the differences.

Since, using two reactor cascades is common in commercial processes for bimodal polyethylene, the model can also be extended to this configuration of two successive reactors in series. The developed grade transition strategy in this work can be afterwards integrated and tested in this model. Finally, regarding the thermodynamic model it is necessary to extend SL EoS to treat quaternary and higher order systems; in order to validate the assumptions made and to use SL EoS model instead of simplified polynomial approximations, even if that would make the model heavier to compute. With a modified SL EoS able to treat higher order systems we could represent better the reality of polymerization system in the polyolefin industry nowadays (using numerous condensable materials).

This brings us to the next perspectives concerning **the experimental part**; as the assumptions were also made due to the lack of experimental data (mainly the pseudo-quaternary assumption). Hence, the availability of more thermodynamic data (solubility data) based on extended experimental campaigns for the quaternary systems used in this work could be a good perspective for validation. The results of this study point to the need for more thermodynamic data in multicomponent systems and over a large range of temperatures and pressures; which could be so helpful in our study on the polymer sticking temperature, when evaluating the solubility of species with the change of the bed temperature. Finally, and as it the case of any modeling study; an experimental validation could be very profitable and could perfectly complete this research. However, this is a hard task at the laboratory level as FBR fluidization is not possible to reproduce at small scale in a comparable way as industrially. Validation at industrial level was not possible in this project as it included no industrial partners.

Combining experimental work with the developed model would allow the simulation, under higher fidelity levels and would result in a key tool for the design of intrinsically safer, more efficient reaction modes while ensuring precise polymer quality control.

## References

- [1] J. B. P. Soares et T. F. L. McKenna, « Polyolefin Reaction Engineering », p. 345.
- [2] A. Alizadeh, M. Namkajorn, E. Somsook, et T. F. L. McKenna, « Condensed Mode Cooling for Ethylene Polymerization: Part I. The Effect of Different Induced Condensing Agents on Polymerization Rate », *Macromol. Chem. Phys.*, vol. 216, n° 8, p. 903-913, avr. 2015, doi: 10.1002/macp.201400600.
- [3] A. Alizadeh, M. Namkajorn, E. Somsook, et T. F. L. McKenna, « Condensed Mode Cooling for Ethylene Polymerization: Part II. The Effect of Different Condensable Comonomers and Hydrogen on Polymerization Rate », *Macromol. Chem. Phys.*, vol. 216, n° 9, p. 985-995, mai 2015, doi: 10.1002/macp.201500023.
- [4] M. Namkajorn, A. Alizadeh, D. Romano, S. Rastogi, et T. F. L. McKenna, « Condensed Mode Cooling for Ethylene Polymerization: Part III. The Impact of Induced Condensing Agents on Particle Morphology and Polymer Properties », *Macromol. Chem. Phys.*, vol. 217, n° 13, p. 1521-1528, juill. 2016, doi: 10.1002/macp.201600107.

### Appendix A. Thermodynamic model development

This **Appendix A** summarizes the basis sets of equations used for solving the Sanchez-Lacombe equation of state, and to derive the sorption phenomenon properties for both binary and ternary systems, which was first developed by Alizadeh.[1]

#### A.1. Modeling Binary systems

For a binary system (solvent 1, polymer 2), the subscripts 1, 2 refer to the penetrant component and the polymer component, respectively:

- ✓ Component 1: is the solvent (ethylene, comonomer or ICA). It can penetrate the polymer. So it is partitioned between the polymer phase and in the gaseous phase.
- ✓ Component 2: is the Polyethylene which represents the solid phase of the system.
- ✓ Gas phase: is gathering the gaseous components of the system.
- ✓ Polymer phase: includes the solvent that is included in the polymer matrix and swollen polymer.

In the calculation steps, the sorption is only considered in the amorphous phase, as the crystalline phase is assumed as impenetrable for solute species.

The most important parameters required by the model are the characteristic parameters for both the single solute species and the polymer:  $T_1^*$ ,  $P_1^*$ ,  $\rho_1^*$  and  $T_2^*$ ,  $P_2^*$ , and  $\rho_2^*$ , respectively; and the binary interaction parameter  $k_{1,2}$  that can be determined from experimental solubility data by minimizing the following objective function  $J$ :

$$J = \frac{S_{\text{exp}} - S_{\text{calc}}}{S_{\text{exp}}} \quad (\text{A-1})$$

$S_{\text{exp}}$  and  $S_{\text{calc}}$  represent the experimental solubility and the theoretical solubility calculated with the model, respectively.

And:

$$T^* = \frac{\varepsilon^*}{R} \quad (\text{A-2})$$

$$P^* = \frac{\varepsilon^*}{v^*}$$

$$V^* = N(rv^*) \text{ and } \rho^* = \frac{Mw}{(rv^*)}$$

$\varepsilon^*$  is the mer-mer interaction parameter;  $v^*$  is the closed packed molar volume of the mer;  $Mw$  is the molecular weight;  $N$  is the number of molecules;  $r$  is the number of sites and  $R$  is the gas constant.

The reduced temperature, pressure and density are defined as follows:

$$\bar{T} = \frac{T}{T^*} \quad (\text{A-3})$$

$$\bar{P} = \frac{P}{P^*}$$

$$\bar{\rho} = \frac{\rho}{\rho^*} = \frac{1}{\bar{V}} = \frac{V^*}{V}$$

The SLEOS calculation procedure aims at first to calculate the solubility of component 1 in equilibrium with the polymer at specific temperature and pressure ( $T, P$ ). The details of calculations are summarized in Table A-1.

Table A-1.Subroutines for Binary systems

Followed steps	Description	Equation
Gas phase	The reduced density of the gas phase $\bar{\rho}_1^{\text{gas}} = \frac{\bar{P}_1}{\bar{\rho}_1^{\text{gas}}}$	$\bar{\rho}_1^{\text{gas}^2} + \bar{P}_1 + \bar{T}_1 \left[ \ln(1 - \bar{\rho}_1^{\text{gas}}) + \left(1 - \frac{1}{r_1}\right) \bar{\rho}_1^{\text{gas}} \right] = 0$
	The chemical potential of the solute species 1 in the gas phase, $\mu_1^{\text{gas}}$	$\mu_1^{\text{gas}} = r_1 \left\{ -\bar{\rho}_1^{\text{gas}} \varepsilon_1^* + \frac{RT}{\bar{\rho}_1^{\text{gas}}} \left[ (1 - \bar{\rho}_1^{\text{gas}}) \ln(1 - \bar{\rho}_1^{\text{gas}}) + \frac{\bar{\rho}_1^{\text{gas}}}{r_1} \ln \bar{\rho}_1^{\text{gas}} \right] + \frac{Pv_1^*}{\bar{\rho}_1^{\text{gas}}} \right\}$
Polymer phase	Characteristic parameters for a mixture:	
	The characteristic closed-packed molar volume of a 'mer' of the polymer phase mixture, $v_{\text{mix}}^{\text{pol}}$ assuming $\phi_1^{\text{pol}} + \phi_2^{\text{pol}} = 1$	Where: $\alpha = v_1^* - v_2^*$ $\beta = v_2^*$
	The interaction energy of mixture mers, $\varepsilon_{\text{mix}}^*$	$\varepsilon_{\text{mix}}^{\text{pol}} = \frac{A\phi_1^{\text{pol}^2} + B\phi_1^{\text{pol}} + C}{\alpha\phi_1^{\text{pol}} + \beta}$ Where: $A = \varepsilon_1^*v_1^* + \varepsilon_2^*v_2^* - \varepsilon_{12}^*(v_1^* + v_2^*)\beta = v_2^*$ $B = \varepsilon_{12}^*(v_1^* + v_2^*) - 2\varepsilon_2^*v_2^*$ $C = \varepsilon_2^*v_2^*$
The number of sites (mers) occupied by a molecule of the mixture, $r_{\text{mix}}^{\text{pol}}$ assuming that $r_2 \gg r_1$	$\frac{1}{r_{\text{mix}}^{\text{pol}}} = \frac{\phi_1^{\text{pol}}}{r_1}$	

By combining all equations we get the following equations that are solved for  $\bar{\rho}^{\text{pol}}$  and  $\phi_1^{\text{pol}}$ :

$$\bar{\rho}^{\text{pol}^2} + P \frac{(\alpha\phi_1^{\text{pol}} + \beta)^2}{A\phi_1^{\text{pol}^2} + B\phi_1^{\text{pol}} + C} + RT \frac{\alpha\phi_1^{\text{pol}} + \beta}{A\phi_1^{\text{pol}^2} + B\phi_1^{\text{pol}} + C} \left[ \ln(1 - \bar{\rho}^{\text{pol}}) + \left(1 - \frac{\phi_1^{\text{pol}}}{r_1}\right) \bar{\rho}^{\text{pol}} \right] = 0$$

And

$$\begin{aligned} & RT \left[ \ln\phi_1^{\text{pol}} + 1 - \phi_1^{\text{pol}} \right] \\ & + r_1 \left\{ -\bar{\rho}^{\text{pol}} \left[ \frac{2}{\alpha\phi_1^{\text{pol}} + \beta} \left( (M'\phi_1^{\text{pol}} + N') - \left( \frac{A\phi_1^{\text{pol}^2} + B\phi_1^{\text{pol}} + C}{\alpha\phi_1^{\text{pol}} + \beta} \right) (M''\phi_1^{\text{pol}} + N'') \right) + \left( \frac{A\phi_1^{\text{pol}^2} + B\phi_1^{\text{pol}} + C}{\alpha\phi_1^{\text{pol}} + \beta} \right) \right] \right. \\ & + \frac{RT}{\bar{\rho}^{\text{pol}}} \left[ (1 - \bar{\rho}^{\text{pol}}) \ln(1 - \bar{\rho}^{\text{pol}}) + \frac{\bar{\rho}^{\text{pol}}}{r_1} \ln\bar{\rho}^{\text{pol}} \right] \\ & \left. + \frac{P}{\bar{\rho}^{\text{pol}}} \left( 2(M''\phi_1^{\text{pol}} + N'') - (\alpha\phi_1^{\text{pol}} + \beta) \right) \right\} \\ & - \mu_1^{\text{gas}} = 0 \end{aligned}$$

Where:

$$M' = v_1^* \varepsilon_1^* - v_{12}^* \varepsilon_{12}^*$$

$$N' = v_{12}^* \varepsilon_{12}^*$$

$$M'' = v_1^* - v_{12}^*$$

$$N'' = v_{12}^*$$

Note: The reduced density of the polymer phase,  $\bar{\rho}^{\text{pol}}$ , and the closed-packed volume fraction of the solute species in the polymer phase,  $\phi_1^{\text{pol}}$  are solved simultaneously:

All the rest of the properties of interest are consequently calculated from  $\bar{\rho}^{\text{pol}}$  and  $\phi_1^{\text{pol}}$  as explained below.

Solubility in the polymer	The mass fraction of the penetrating solute in the amorphous phase of the polymer, $w_{1,am}$	$w_{1,am} = \frac{\left(\frac{\phi_1^{pol}}{1 - \phi_1^{pol}}\right)}{\left(\frac{\rho_2^* v_2^*}{\rho_1^* v_1^*}\right) \left(\frac{\phi_1^{pol}}{1 - \phi_1^{pol}}\right)} [=] \frac{\text{g sol. 1}}{\text{g (sol. 1 + am. pol)}}$
	The solubility of component 1 in the amorphous polymer phase, $S_{1,am}$	$S_{1,am} = \frac{w_{1,am}}{1 - w_{1,am}} [=] \frac{\text{g sol. 1}}{\text{g am. pol}}$
	The solubility of component 1 in the total polymer (amorphous phase+ crystalline phase), $S_{1,tot}$	$S_{1,tot} = S_{1,am}(1 - x_i) [=] \frac{\text{g sol. 1}}{\text{g am. pol}}$ <p>Where:  <math>x_i</math>: is the weight-based crystallinity of the polymer particle.</p>
Swelling of polymer	The reduced amorphous polymer density, $\bar{\rho}_2$	$\bar{\rho}_2 = 1 - \exp\left(-\frac{\bar{\rho}_2^2}{\bar{T}_2} - \frac{\bar{P}_2}{\bar{T}_2} - \bar{\rho}_2\right)$

	The characteristic density of the amorphous polymer phase, $\rho^*$	$\rho^* = \frac{1}{\left(\frac{w_{1,am}}{\rho_1^*}\right) + \left(\frac{1-w_{1,am}}{\rho_2^*}\right)}$
	The extent of swelling of the amorphous polymer phase, $SW_{am}$	<p>Where:</p> $SW_{am} = \frac{\bar{\rho}_2 \rho_2^* (1 + S_{1,am})}{\rho^* \bar{\rho}^{pol}} - 1$ $\frac{\bar{\rho}_2 \rho_2^* (1 + S_{1,am})}{\rho^* \bar{\rho}^{pol}} [=] \frac{m^3 (\text{am. pol} + \text{sol. 1})}{m^3 (\text{am. pol})}$
	The extent of total polymer swelling assuming no solubility in the crystalline phase, $SW_{tot}$	<p>Where:</p> $SW_{tot} = \frac{x_i v_c + \frac{(1-x_i)(1+S_{1,am})}{\rho^* \bar{\rho}^{pol}}}{x_i v_c + \frac{(1-x_i)}{\bar{\rho}_2 \rho_2^*}} - 1$ $[=] \frac{\frac{x_i v_c + \frac{(1-x_i)(1+S_{1,am})}{\rho^* \bar{\rho}^{pol}}}{x_i v_c + \frac{(1-x_i)}{\bar{\rho}_2 \rho_2^*}}}{m^3 (\text{am. pol} + \text{crys. pol})} \frac{m^3 (\text{am. pol} + \text{crys. pol} + \text{sol. 1})}{m^3 (\text{am. pol} + \text{crys. pol})}$ <p>With <math>v_c = 0.001 \text{ m}^3/\text{kg}</math> (The specific volume of fully crystalline polymer phase)</p>
Concentration in the polymer	The concentration of the component 1 in the amorphous polymer phase, $C_{1,am}$	<p>Where:</p> $C_{1,am} = \frac{w_{1,am} \rho^* \bar{\rho}^{pol}}{Mw_1} [=] \frac{\text{mol sol. 1}}{m^3 (\text{am. pol} + \text{sol. 1})}$ <p><math>Mw_1</math>: is the molecular weight of component 1 (<math>\text{kg}/\text{mol}</math>).</p>

	<p>The concentration of the component 1 in the whole polymer (amorphous phase+ crystalline phase), <math>C_{1,tot}</math></p>	$C_{1,tot} = C_{1,am} \frac{(1 + SW_{am})}{(1 + SW_{tot})} (1 - x_{iv})$ $[=] \frac{\text{mol sol. 1}}{\text{m}^3 (\text{am. pol} + \text{sol. 1})}$ <p>Where the volume-based crystallinity of polymer can be expressed as:</p> $x_{iv} = \frac{x_i v_c}{x_i v_c + \frac{(1 - x_i)}{\rho_2 \rho_2^*}} [=] \frac{\text{m}^3 \text{ crys. pol}}{\text{m}^3 (\text{crys. pol} + \text{am. pol})}$
--	---	---

## A.2 Modeling Ternary systems

For a ternary system (solvent 1, solvent 2, polymer 3), the subscripts 1, 2 refer to the penetrant components, respectively and 3 refers to the polymer component:

- ✓ Component 1: is the solvent with the lighter molecular weight in the system. It can penetrate the polymer. So it is partitioned between the polymer phase and in the gaseous phase.
- ✓ Component 2: is the solvent with the heavier molecular weight in the system. It can penetrate the polymer, so it can be in the polymer phase or in the gaseous phase.
- ✓ Component 3: is the Polyethylene which represents the solid phase of the system.
- ✓ Gas phase: is gathering the gaseous components of the system.
- ✓ Polymer phase: includes the solvent that is included in the polymer matrix and the swollen polymer.

Here, the calculation procedure aims to calculate the solubility of both components 1 and 2 in equilibrium with the polymer at specific temperature ( $T$ ), when knowing the partial pressures of the penetrant components ( $P_1, P_2$ ) as well as the total pressure ( $P$ ). For that, at first the binary interaction parameters between the solvents and the polymer ( $k_{13}, k_{2,3}$ ) and between the solvents themselves ( $k_{1,2}$ ) are required.

The other important parameters required by the model for ternary systems are the characteristic parameters for both solute species (1 and 2);  $T_1^*$ ,  $P_1^*$ ,  $\rho_1^*$  and  $T_2^*$ ,  $P_2^*$ , and  $\rho_2^*$ , respectively as well as those for the polymer component (3);  $T_3^*$ ,  $P_3^*$ ,  $\rho_3^*$ . In order to calculate the solubility of both solute species in the amorphous polymer, the calculation procedure is resumed in Table A-2.

Table A-2. Subroutines for Ternary systems

Followed steps	Description	Equation
Gas phase Polymer phase	The reduced density of each gas in the gas phase ( $\bar{\rho}_1^{\text{gas}}$ , $\bar{\rho}_2^{\text{gas}}$ ),	$\bar{\rho}_1^{\text{gas}^2} + \bar{P}_1 + \bar{T}_1 \left[ \ln(1 - \bar{\rho}_1^{\text{gas}}) + \left(1 - \frac{1}{r_1}\right) \bar{\rho}_1^{\text{gas}} \right] = 0$ <p>And</p> $\bar{\rho}_2^{\text{gas}^2} + \bar{P}_2 + \bar{T}_2 \left[ \ln(1 - \bar{\rho}_2^{\text{gas}}) + \left(1 - \frac{1}{r_2}\right) \bar{\rho}_2^{\text{gas}} \right] = 0$ <p>With:</p> $\rho_1^{\text{gas}} = \rho_1^* \bar{\rho}_1^{\text{gas}}$ $\rho_2^{\text{gas}} = \rho_2^* \bar{\rho}_2^{\text{gas}}$
	The mass fraction of component 1 and 2 at a given volume of the gas phase mixture	<p>And</p> $\omega_1^{\text{gas}} = \frac{\rho_1^{\text{gas}}}{\rho_1^{\text{gas}} + \rho_2^{\text{gas}}}$ $\omega_2^{\text{gas}} = \frac{\rho_2^{\text{gas}}}{\rho_1^{\text{gas}} + \rho_2^{\text{gas}}}$
	The closed packed volume fraction of components 1 and 2	$\phi_1^{\text{gas}} = \frac{\frac{(\rho_1^{\text{gas}}/\rho_1^{\text{gas}} + \rho_2^{\text{gas}})}{\rho_1^* v_1^*}}{\frac{(\rho_1^{\text{gas}}/\rho_1^{\text{gas}} + \rho_2^{\text{gas}})}{\rho_1^* v_1^*} + \frac{(\rho_2^{\text{gas}}/\rho_1^{\text{gas}} + \rho_2^{\text{gas}})}{\rho_2^* v_2^*}}$ <p>When considering no polymer molecules in the gas phase:</p> $\phi_2^{\text{gas}} = 1 - \phi_1^{\text{gas}}$

<p>The reduced gas phase density, <math>\bar{\rho}^{\text{gas}}</math></p>	$\bar{\rho}^{\text{gas}^2} + \bar{p}^{\text{gas}} + \bar{T}^{\text{gas}} \left[ \ln(1 - \bar{\rho}^{\text{gas}}) + \left(1 - \frac{1}{r_{\text{mix}}^{\text{gas}}}\right) \bar{\rho}^{\text{gas}} \right] = 0$ <p>Where:</p> $\bar{T}^{\text{gas}} = RT \frac{\alpha \phi_1^{\text{gas}} + \beta}{A \phi_1^{\text{gas}^2} + B \phi_1^{\text{gas}} + C}$ $\bar{p}^{\text{gas}} = P \frac{(\alpha \phi_1^{\text{gas}} + \beta)^2}{A \phi_1^{\text{gas}^2} + B \phi_1^{\text{gas}} + C} C = \varepsilon_2^* v_2^*$
<p>The characteristic parameters of the mixture</p>	$\varepsilon_{\text{mix}}^*{}^{\text{gas}} = \frac{A \phi_1^{\text{gas}^2} + B \phi_1^{\text{gas}} + C}{\alpha \phi_1^{\text{gas}} + \beta}$ $v_{\text{mix}}^*{}^{\text{gas}} = \alpha \phi_1^{\text{gas}} + \beta$ <p>And</p> $\frac{1}{r_{\text{mix}}^{\text{gas}}} = \frac{\phi_1^{\text{gas}}}{r_1} + \frac{(1 - \phi_1^{\text{gas}})}{r_2}$
<p>The chemical potential of components 1 and 2</p>	$\mu_1^{\text{gas}} = RT \left[ \ln \phi_1^{\text{gas}} + 1 - \frac{r_1}{r_{\text{mix}}^{\text{gas}}} \right. \\ \left. + r_1 \left\{ -\bar{\rho}^{\text{gas}} \left[ \frac{2}{v_{\text{mix}}^*{}^{\text{gas}}} \left( (\phi_1^{\text{gas}} v_1^* \varepsilon_1^* + \phi_2^{\text{gas}} v_{12}^* \varepsilon_{12}^* \right) - \varepsilon_{\text{mix}}^*{}^{\text{gas}} (\phi_1^{\text{gas}} v_1^* + \phi_2^{\text{gas}} v_{12}^*) \right) + \varepsilon_{\text{mix}}^*{}^{\text{gas}} \right] \right. \\ \left. + \frac{RT}{\bar{\rho}^{\text{gas}}} \left[ (1 - \bar{\rho}^{\text{gas}}) \ln(1 - \bar{\rho}^{\text{gas}}) + \frac{\bar{\rho}^{\text{gas}}}{r_1} \ln \bar{\rho}^{\text{gas}} \right] \right. \\ \left. + \frac{P}{\bar{\rho}^{\text{gas}}} \left[ 2(\phi_1^{\text{gas}} v_1^* + \phi_2^{\text{gas}} v_{12}^*) - v_{\text{mix}}^*{}^{\text{gas}} \right] \right\}$ <p>And</p> $\mu_2^{\text{gas}} = RT \left[ \ln \phi_2^{\text{gas}} + 1 - \frac{r_2}{r_{\text{mix}}^{\text{gas}}} \right. \\ \left. + r_2 \left\{ -\bar{\rho}^{\text{gas}} \left[ \frac{2}{v_{\text{mix}}^*{}^{\text{gas}}} \left( (\phi_1^{\text{gas}} v_{12}^* \varepsilon_{12}^* + \phi_2^{\text{gas}} v_2^* \varepsilon_2^* \right) - \varepsilon_{\text{mix}}^*{}^{\text{gas}} (\phi_1^{\text{gas}} v_{12}^* + \phi_2^{\text{gas}} v_2^*) \right) + \varepsilon_{\text{mix}}^*{}^{\text{gas}} \right] \right. \\ \left. + \frac{RT}{\bar{\rho}^{\text{gas}}} \left[ (1 - \bar{\rho}^{\text{gas}}) \ln(1 - \bar{\rho}^{\text{gas}}) + \frac{\bar{\rho}^{\text{gas}}}{r_2} \ln \bar{\rho}^{\text{gas}} \right] \right. \\ \left. + \frac{P}{\bar{\rho}^{\text{gas}}} \left[ 2(\phi_1^{\text{gas}} v_{12}^* + \phi_2^{\text{gas}} v_2^*) - v_{\text{mix}}^*{}^{\text{gas}} \right] \right\}$

		<p>When considering the equilibrium condition:</p> $\mu_1^{\text{gas}} = \mu_1^{\text{pol}} \text{ and } \mu_2^{\text{gas}} = \mu_2^{\text{pol}}$ <p>And</p> $v^*_{\text{mix}}^{\text{gas}} = \alpha\phi_1^{\text{gas}} + \beta$ $\varepsilon^*_{\text{mix}}^{\text{gas}} = \frac{A\phi_1^{\text{gas}^2} + B\phi_1^{\text{gas}} + C}{\alpha\phi_1^{\text{gas}} + \beta}$
Polymer phase	The Closed packed molar volume of 'mer' polymer phase mixture	<p>Considering this condition to calculate the characteristic parameters of the polymer phase mixture:</p> $\phi_1^{\text{pol}} + \phi_2^{\text{pol}} + \phi_3^{\text{pol}} = 1$
	The characteristic parameters for the mixture	$\varepsilon^*_{\text{mix}}^{\text{pol}} = \frac{A_1\phi_1^{\text{pol}^2} + A_2\phi_2^{\text{pol}^2} + A_{12}\phi_1^{\text{pol}}\phi_2^{\text{pol}} + B_1\phi_1^{\text{pol}} + B_2\phi_2^{\text{pol}} + C_1}{\sigma_1\phi_1^{\text{pol}} + \sigma_2\phi_2^{\text{pol}} + \sigma_3}$ $v^*_{\text{mix}}^{\text{pol}} = \sigma_1\phi_1^{\text{pol}} + \sigma_2\phi_2^{\text{pol}} + \sigma_3$ <p>Where:</p> $\sigma_1 = v_1^* - v_3^*$ $\sigma_2 = v_2^* - v_3^*$ $\sigma_3 = v_3^*$ $A_1 = \varepsilon_1^*v_1^* + \varepsilon_3^*v_3^* - 2\varepsilon_{13}^*v_{13}^*$ $A_2 = \varepsilon_2^*v_2^* + \varepsilon_3^*v_3^* - 2\varepsilon_{23}^*v_{23}^*$ $A_{12} = 2(\varepsilon_{12}^*v_{12}^* - \varepsilon_{13}^*v_{13}^* - 2\varepsilon_{23}^*v_{23}^* + \varepsilon_3^*v_3^*)$ $B_1 = 2\varepsilon_{13}^*v_{13}^* - 2\varepsilon_3^*v_3^*$ $B_2 = 2\varepsilon_{23}^*v_{23}^* - 2\varepsilon_3^*v_3^*$ $C_1 = \varepsilon_3^*v_3^*$ <p>And</p> $\frac{1}{r^{\text{pol}}_{\text{mix}}} = \frac{\phi_1^{\text{pol}}}{r_1} + \frac{\phi_2^{\text{pol}}}{r_2}$
	The reduced density of the polymer phase, $\bar{\rho}^{\text{pol}}$ , and the closed-packed volume fractions of solute species in the polymer phase, $\phi_1^{\text{pol}}$ and $\phi_2^{\text{pol}}$ obtained simultaneously:	$\bar{\rho}^{\text{pol}^2} + P \frac{(\sigma_1\phi_1^{\text{pol}} + \sigma_2\phi_2^{\text{pol}} + \sigma_3)^2}{A_1\phi_1^{\text{pol}^2} + A_2\phi_2^{\text{pol}^2} + A_{12}\phi_1^{\text{pol}}\phi_2^{\text{pol}} + B_1\phi_1^{\text{pol}} + B_2\phi_2^{\text{pol}} + C_1} + RT \frac{\sigma_1\phi_1^{\text{pol}} + \sigma_2\phi_2^{\text{pol}} + \sigma_3}{A_1\phi_1^{\text{pol}^2} + A_2\phi_2^{\text{pol}^2} + A_{12}\phi_1^{\text{pol}}\phi_2^{\text{pol}} + B_1\phi_1^{\text{pol}} + B_2\phi_2^{\text{pol}} + C_1} - \bar{\rho}^{\text{pol}} + \left(1 - \frac{\phi_1^{\text{pol}}}{r_1} - \frac{\phi_2^{\text{pol}}}{r_2}\right) \bar{\rho}^{\text{pol}} = 0$

$$\begin{aligned}
& RT \left[ \ln \phi_1^{\text{pol}} + 1 - r_1 \left( \frac{\phi_1^{\text{pol}}}{r_1} + \frac{\phi_2^{\text{pol}}}{r_2} \right) \right] \\
& + r_1 \left\{ -\bar{\rho}^{\text{pol}} \left[ \frac{2}{\sigma_1 \phi_1^{\text{pol}} + \sigma_2 \phi_2^{\text{pol}} + \sigma_3} \left( (v_1^* \varepsilon_1^* - v_{13}^* \varepsilon_{13}^*) \phi_1^{\text{pol}} + (v_{12}^* \varepsilon_{12}^* - \right. \right. \right. \\
& \left. \left. \left. v_{13}^* \varepsilon_{13}^*) \phi_2^{\text{pol}} + v_{13}^* \varepsilon_{13}^* \right) - \right. \right. \\
& \left. \left. \left( \frac{A_1 \phi_1^{\text{pol}^2} + A_2 \phi_2^{\text{pol}^2} + A_{12} \phi_1^{\text{pol}} \phi_2^{\text{pol}} + B_1 \phi_1^{\text{pol}} + B_2 \phi_2^{\text{pol}} + C_1}{\sigma_1 \phi_1^{\text{pol}} + \sigma_2 \phi_2^{\text{pol}} + \sigma_3} \right) \left( (v_1^* - v_{13}^*) \phi_1^{\text{pol}} + \right. \right. \right. \\
& \left. \left. \left. (v_{12}^* - v_{13}^*) \phi_2^{\text{pol}} + v_{13}^* \right) \right) + \right. \\
& \left. \left( \frac{A_1 \phi_1^{\text{pol}^2} + A_2 \phi_2^{\text{pol}^2} + A_{12} \phi_1^{\text{pol}} \phi_2^{\text{pol}} + B_1 \phi_1^{\text{pol}} + B_2 \phi_2^{\text{pol}} + C_1}{\sigma_1 \phi_1^{\text{pol}} + \sigma_2 \phi_2^{\text{pol}} + \sigma_3} \right) \right] + \frac{R_g T}{\bar{\rho}^{\text{pol}}} \left[ (1 - \right. \\
& \left. \bar{\rho}^{\text{pol}}) \ln(1 - \bar{\rho}^{\text{pol}}) + \frac{\bar{\rho}^{\text{pol}}}{r_1} \ln \bar{\rho}^{\text{pol}} \right] + \frac{P}{\bar{\rho}^{\text{pol}}} \left[ 2 \left( (v_1^* - v_{13}^*) \phi_1^{\text{pol}} + \right. \right. \\
& \left. \left. (v_{12}^* - v_{13}^*) \phi_2^{\text{pol}} + v_{13}^* \right) - \left( \sigma_1 \phi_1^{\text{pol}} + \sigma_2 \phi_2^{\text{pol}} + \sigma_3 \right) \right] \left. \right\} - \mu_1^{\text{gas}} = 0
\end{aligned}$$

In which:

$$\begin{aligned}
G_1 &= v_1^* \varepsilon_1^* - v_{13}^* \varepsilon_{13}^* \\
G_2 &= v_{12}^* \varepsilon_{12}^* - v_{13}^* \varepsilon_{13}^* \\
G_3 &= v_{13}^* \varepsilon_{13}^* \\
g_1 &= v_1^* - v_{13}^* \\
g_2 &= v_{12}^* - v_{13}^* \\
g_3 &= v_{13}^*
\end{aligned}$$

And

$$\begin{aligned}
& RT \left[ \ln \phi_2^{\text{pol}} + 1 - r_2 \left( \frac{\phi_1^{\text{pol}}}{r_1} + \frac{\phi_2^{\text{pol}}}{r_2} \right) \right] \\
& + r_2 \left\{ -\bar{\rho}^{\text{pol}} \left[ \frac{2}{\sigma_1 \phi_1^{\text{pol}} + \sigma_2 \phi_2^{\text{pol}} + \sigma_3} \left( (v_{12}^* \varepsilon_{12}^* - v_{23}^* \varepsilon_{23}^*) \phi_1^{\text{pol}} + (v_2^* \varepsilon_2^* - \right. \right. \right. \\
& \left. \left. \left. v_{23}^* \varepsilon_{23}^*) \phi_2^{\text{pol}} + v_{23}^* \varepsilon_{23}^* \right) - \right. \right. \\
& \left. \left. \left( \frac{A_1 \phi_1^{\text{pol}^2} + A_2 \phi_2^{\text{pol}^2} + A_{12} \phi_1^{\text{pol}} \phi_2^{\text{pol}} + B_1 \phi_1^{\text{pol}} + B_2 \phi_2^{\text{pol}} + C_1}{\sigma_1 \phi_1^{\text{pol}} + \sigma_2 \phi_2^{\text{pol}} + \sigma_3} \right) \left( (v_{12}^* - \right. \right. \right. \\
& \left. \left. \left. v_{23}^*) \phi_1^{\text{pol}} + (v_2^* - v_{23}^*) \phi_2^{\text{pol}} + v_{23}^* \right) \right) + \right. \\
& \left. \left( \frac{A_1 \phi_1^{\text{pol}^2} + A_2 \phi_2^{\text{pol}^2} + A_{12} \phi_1^{\text{pol}} \phi_2^{\text{pol}} + B_1 \phi_1^{\text{pol}} + B_2 \phi_2^{\text{pol}} + C_1}{\sigma_1 \phi_1^{\text{pol}} + \sigma_2 \phi_2^{\text{pol}} + \sigma_3} \right) \right] + \frac{R_g T}{\bar{\rho}^{\text{pol}}} \left[ (1 - \right. \\
& \left. \bar{\rho}^{\text{pol}}) \ln(1 - \bar{\rho}^{\text{pol}}) + \frac{\bar{\rho}^{\text{pol}}}{r_2} \ln \bar{\rho}^{\text{pol}} \right] + \frac{P}{\bar{\rho}^{\text{pol}}} \left[ 2 \left( (v_{12}^* - v_{23}^*) \phi_1^{\text{pol}} + \right. \right. \\
& \left. \left. (v_2^* - v_{23}^*) \phi_2^{\text{pol}} + v_{23}^* \right) - \left( \sigma_1 \phi_1^{\text{pol}} + \sigma_2 \phi_2^{\text{pol}} + \sigma_3 \right) \right] \left. \right\} - \mu_2^{\text{gas}} = 0
\end{aligned}$$

In which:

$$\begin{aligned}
H_1 &= v_{12}^* \varepsilon_{12}^* - v_{23}^* \varepsilon_{23}^* \\
H_2 &= v_2^* \varepsilon_2^* - v_{23}^* \varepsilon_{23}^*
\end{aligned}$$

		$H_3 = v_{23}^* \varepsilon_{23}^*$ $h_1 = v_{12}^* - v_{23}^*$ $h_2 = v_2^* - v_{23}^*$ $h_3 = v_{23}^*$
Solubility of polymer	The mass fraction of solute 1 and 2 in the amorphous phase of the polymer	$\omega_{1,am} = \frac{1}{1 + \left(\frac{\rho_2^* v_2^*}{\rho_1^* v_1^*}\right) \left(\frac{\phi_2^{pol}}{\phi_1^{pol}}\right) + \left(\frac{\rho_3^* v_3^*}{\rho_1^* v_1^*}\right) \left(\frac{1 - \phi_1^{pol} - \phi_2^{pol}}{\phi_1^{pol}}\right)}$ $[=] \left(\frac{\text{g sol. 1}}{\text{g (sol. 1 + sol. 2 + am. pol)}}\right)$ $\omega_{2,am} = \left[\left(\frac{\rho_2^* v_2^*}{\rho_1^* v_1^*}\right) \left(\frac{\phi_2^{pol}}{\phi_1^{pol}}\right)\right] \omega_{1,am}$ $[=] \left(\frac{\text{g sol. 2}}{\text{g (sol. 1 + sol. 2 + am. pol)}}\right)$ $\omega_{3,am} = 1 - \omega_{1,am} - \omega_{2,am} [ = ] \left(\frac{\text{g am. pol}}{\text{g (sol. 1 + sol. 2 + am. pol)}}\right)$
	The solubility	$S_{1,am} = \frac{\omega_{1,am}}{\omega_{3,am}} [ = ] \left(\frac{\text{g sol. 1}}{\text{g am. pol}}\right)$ $S_{2,am} = \frac{\omega_{2,am}}{\omega_{3,am}} [ = ] \left(\frac{\text{g sol. 2}}{\text{g am. pol}}\right)$ $S_{12,am} = \frac{\omega_{1,am} + \omega_{2,am}}{\omega_{3,am}} [ = ] \left(\frac{\text{g (sol. 1 + sol. 2)}}{\text{g am. pol}}\right)$ $S_{12,tot} = S_{12,am} (1 - \chi) [ = ] \left(\frac{\text{g (sol. 1 + sol. 2)}}{\text{g (am. pol + crys pol)}}\right)$
Swelling of polymer	The reduced amorphous polymer density	$\bar{\rho}_3 = 1 - \exp\left(-\frac{\bar{\rho}_3^2}{\bar{T}_3} - \frac{\bar{P}_3}{\bar{T}_3} - \bar{\rho}_3\right)$

	The characteristic density of the amorphous polymer phase	$\rho^* = \frac{1}{\left(\frac{w_{1,am}}{\rho_1^*}\right) + \left(\frac{w_{2,am}}{\rho_2^*}\right) + \left(\frac{w_{3,am}}{\rho_3^*}\right)}$
	The extent of swelling of the amorphous polymer phase, $SW_{12,am}$	$SW_{12,am} = \frac{\bar{\rho}_3 \rho_3^* (1 + S_{1,am} + S_{2,am})}{\rho^* \bar{\rho}^{pol}} - 1$ <p>Where:</p> $\frac{\bar{\rho}_3 \rho_3^* (1 + S_{1,am} + S_{2,am})}{\rho^* \bar{\rho}^{pol}} [=] \frac{\text{m}^3 (\text{am. pol} + \text{sol. 1} + \text{sol. 2})}{\text{m}^3 (\text{am. pol})}$
	The extent of total polymer swelling assuming no solubility in the crystalline phase for both solute species, $SW_{12,tot}$	$SW_{12,tot} = \frac{x_i v_c + \frac{(1 - x_i)(1 + S_{1,am} + S_{2,am})}{\rho^* \bar{\rho}^{pol}}}{\chi v_c + \frac{(1 - \chi)}{\bar{\rho}_3 \rho_3^*}} - 1$ <p>Where:</p> $\frac{x_i v_c + \frac{(1 - x_i)(1 + S_{1,am} + S_{2,am})}{\rho^* \bar{\rho}^{pol}}}{x_i v_c + \frac{(1 - \chi)}{\bar{\rho}_3 \rho_3^*}} [=] \frac{\text{m}^3 (\text{am. pol} + \text{crys. pol} + \text{sol. 1} + \text{sol. 2})}{\text{m}^3 (\text{am. pol} + \text{crys. pol})}$ <p>With <math>v_c = 0.001 \text{ m}^3/\text{kg}</math> (The specific volume of fully crystalline polymer phase)</p>
Concentration in the polymer	The concentration of the component 1 in the amorphous polymer phase, $C_{1,am}$	$C_{1,am} = \frac{w_{1,am} \rho^* \bar{\rho}^{pol}}{Mw_1} [=] \frac{\text{mol sol. 1}}{\text{m}^3 (\text{am. pol} + \text{sol. 1} + \text{sol. 2})}$ <p>Where:</p> <p><math>Mw_1</math>: is the molecular weight of the component 1 (<math>\text{kg}/\text{mol}</math>).</p>

	<p>The concentration of the component 1 in the whole polymer (amorphous phase+ crystalline phase), <math>C_{1,tot}</math></p>	$C_{1,tot} = C_{1,am} \frac{(1 + SW_{12,am})}{(1 + SW_{12,tot})} (1 - x_{i_v})$ $[=] \frac{\text{mol sol. 1}}{\text{m}^3 (\text{am. pol} + \text{crys. pol} + \text{sol. 1} + \text{sol. 2})}$ <p>Where the volume-based crystallinity of polymer can be expressed as:</p> $x_{i_v} = \frac{x_i v_c}{x_i v_c + \frac{(1 - x_i)}{\rho_3 \rho_3^*}} [=] \frac{\text{m}^3 \text{crys. pol}}{\text{m}^3 (\text{crys. pol} + \text{am. pol})}$
--	---	---

## References

- [1] A. Alizadeh, « Study of sorption, heat and mass transfer during condensed mode operation of gas phase ethylene polymerization on supported catalyst », Queen's University, Kingston, Ontario, Canada, 2014.

# Appendix B. Disseminations

## B.1. Publications

1-S. Kardous, T. F. L. McKenna, et N. Sheibat-Othman, « Thermodynamic Effects on Grade Transition of Polyethylene Polymerization in Fluidized Bed Reactors », *Macromolecular Reaction Engineering*, vol. n/a, n° n/a, p. 2000013, doi: 10.1002/mren.202000013

2-S. Kardous, T. F. L. McKenna, et N. Sheibat-Othman, « Optimization of Polyethylene Grade Transitions in Fluidized Bed Reactors with Constraints on the Polymer Sticking Temperature », *Ind. Eng. Chem. Res.*, janv. 2021, doi: 10.1021/acs.iecr.0c05466

## B.2. Oral Presentations

1-Sabrine Kardous, Nida Sheibat-Othman, Timothy F.L. McKenna, “Optimization of grade transition in fluidized-bed reactors accounting for condensed agent effects,” 8<sup>th</sup> PhD Students Workshop on Polymer Reaction Engineering, Hamburg Germany., Jun. 14- 16, 2019

2-Sabrine Kardous, Nida Sheibat-Othman, Timothy F.L. McKenna, “Optimisation de la transition de grade dans la polymérisation de polyéthylène dans un réacteur à lit fluidisé,” Annual Meeting of Chemistry Graduate School, Lyon, France, Avril, 2019

3-Sabrine Kardous, Nida Sheibat-Othman, Timothy F.L. McKenna, “Effets thermodynamiques sur la vitesse dans les réactions de polyoléfines en phase gaz,” Journée Scientifique du CODEGEPRA, Saint Etienne, France, 15 Novembre, 2018

4- Sabrine Kardous, Nida Sheibat-Othman, Timothy F.L. McKenna, “Thermodynamic effects on the reaction rate in gas phase polyolefin reactions,” European Federation of Chemical Engineering 7<sup>th</sup> PhD Students Workshop on Polymer Reaction Engineering, Prague, Gzech Republic., Aug. 31- Sep 02, 2018

## B.3. Posters

1-Sabrine Kardous, Nida Sheibat-Othman, Timothy F.L. McKenna, “Optimization of grade transition in fluidized-bed reactors accounting for condensed agent effects,” DECHEMA International Workshop on Polymer Reaction Engineering, Hamburg, Germany, 11-14 June, 2019

2-Sabrine Kardous, Nida Sheibat-Othman, Timothy F.L. McKenna, “Effets thermodynamiques sur la vitesse dans les reactions de polyoléfines en phase gaz,” Journée Scientifique du CODEGEPRA, Saint Etienne, France, 15 Novembre, 2018

“Now it is not the end. It is not even the beginning. But it  
is, perhaps, the end of the beginning.”

*-Winston Churchill (1959–1964)*